Philosophy in Physiology at UCL.

ProQuest LLC
789 East Eisenhower Parkway
P.O. Box 1346
Ann Arbor, MI 48106-1346

Declaration

I, Ruth Doreen Theresa Taylor, confirm that the work presented in this thesis is my own. Where information has been derived from other sources, I confirm that this has been indicated in the thesis. A part of the experimental portion of this work was submitted for the degree of B.Sc. in Physiology at University College London. Where experimental work has been previously submitted, I confirm that this has been indicated in the thesis.

Abstract

This thesis focuses on the modulation of two Ca^{++} activated K^+ currents, I_{AHP} and sI_{AHP} that underlie part of the medium (mAHP) and the slow afterhyperpolarisation (sAHP) in cortical neurons. The afterhyperpolarisation is a transient hyperpolarisation of the membrane potential following a burst of action potentials.

The aim of the first part of this study was to investigate whether neuronal SK channels, which are known to mediate I_{AHP} in hippocampal neurons, are modulated by the newly characterised compound NS8593. I have characterised the effect of NS8593 on I_{AHP} in mouse hippocampal slices, finding that NS8593 suppresses I_{AHP}.

The second part of my project focused on identifying the signal transduction cascade mediating the sI_{AHP} suppression induced by application of pituitary adenylyl cyclase activating polypeptide (PACAP). PACAP acts via the activation of its own receptors (PAC-1-R) and of vasoactive intestinal peptide (VIP) receptors (V-PAC1, V-PAC2). Previous experiments have shown that the VIP-mediated reduction of sI_{AHP} occurs via a protein kinase A (PKA) dependent mechanism. PACAP was found to suppress sI_{AHP} in a PKA and p38 mitogen-activated protein kinase (MAPK)-dependent manner in rat CA1 pyramidal neurons.

In part three, the involvement of the calcium stimulatable adenylyl cyclases (AC1/AC8), in the modulation of sI_{AHP}/sAHP by the neuromodulators: isoproterenol, serotonin and dopamine was investigated. I found that different monoamines signalled through different adenylyl cyclases (AC) in order to suppress sI_{AHP}/sAHP.

Lastly, the modulation of sAHP by high frequency stimulation of the Schaffer-collateral pathway results in a transient inhibition of sAHP in CA1 pyramidal neurons by a pathway involving N-methyl-D-aspartate receptors (NMDAR) and PKA. My results showed that delivery of high frequency stimulation results in a transient sAHP suppression by a pathway that involves, besides NMDAR and PKA, the activation of AC1/AC8. Additionally, I found that when low frequency

synaptic stimulation was paired with post-synaptic depolarisation, a transient sAHP suppression was elicited in an NMDAR and AC1/AC8 dependent manner.

(313 words)

Table of Contents

List of figures

Chapter 1

Chapter 2

Chapter 3

Chapter 4

Chapter 5

Chapter 6

List of abbreviations

AC	adenylyl cyclase
ACSF	artificial cerebro-spinal fluid
AHP	afterhyperpolarisation
AKAP	A-kinase anchoring protein
AMPAR	α-amino-3-hydroxy-5-methylisoxazole-4-propionic acid receptor
AP5	D-2-amino-phosphopentanoate
Ca^{++}	calcium
CaM	calmodulin
CamBD	clamodulin binding domain
cAMP	3'5'-cyclic adenosine monophosphate
CRF	corticotrophin releasing factor
DARPP-32	dopamine and cyclic adenosine 3'5'-monophosphate regulated phosphoprotein, 32 kilo Daltons
DKO	mice with a double knockout for both AC1 and AC8
dTC	d-tubocurarine
EPAC	exchange factor directly activated by cAMP
EPSC	excitatory post synaptic current
EPSP	excitatory post synaptic potential
fAHP	fast afterhyperpolarisation
GEF	G protein exchange factor
GIRK channels	G protein-coupled inwardly rectifying potassium channels
GΩ	gigaohm
HFS	high frequency synaptic stimulation
Iso	isoproterenol
K^+	potassium
LTP	long term potentiation
MA	monoaminergic neurotransmitter

mAHP	medium afterhyperpolarisation
mGluR	metabotropic glutamate receptor
MPEP	MPEP hydrochloride
NMDAR	N-methyl-D-aspartate receptor
PACAP	pituitary adenylyl cyclase activating polypeptide
PKA	protein kinase A/ cAMP-dependent protein kinase
P38 MAPK	p38 mitogen-activated protein kinase
Rp-cAMPS	Rp-adenosine-3'5'-cyclic monophosphorothioate
sAHP	slow afterhyperpolarisation
SEM	standard error of the mean
SK channels	small conductance calcium activated potassium channels
τ	decay time constant
TEA	tetraethylammonium
Trace EBC	trace eye blink conditioning
TTX	tetrodotoxin
VIP	vasoactive intestinal peptide
WAY	WAY100135
WT	wild-type
5HT	serotonin

Acknowledgements

My primary thanks go to my supervisor Dr. Paola Pedarzani, for her time, help and advice both before and during my PhD. I am also indebted to Dr. Martin Stocker for both critical advice and discussions over the years, and his work in breeding, geno-typing and managing the strains of mice used in this study. I wish to acknowledge both past and present members of the Pedarzani and Stocker Laboratories for the fun, sanity, coffees, advice and scientific discussion over the years. It has been a hard slog, and without them, none of this would have been possible.

Special thanks go to Professor Daniel Storm for his generous gift of the double knockouts used in this study. Additionally I would like to thank Dr. Ethan Lerner for his gift of maxadilan and maxadilan-d-4 used in the second part of this study.

On a personal note I wish to thank my mother Odette, my father Philip, my sister Harriet and my fiancé Andrew Roberts, who have put up with the long hours, grumbles, bad moods and frustrations that are inevitable during a PhD, I am hopeful that this will get better as I grow and improve both personally and professionally.

Chapter 1: Introduction

1.1: The hippocampus and neuromodulation

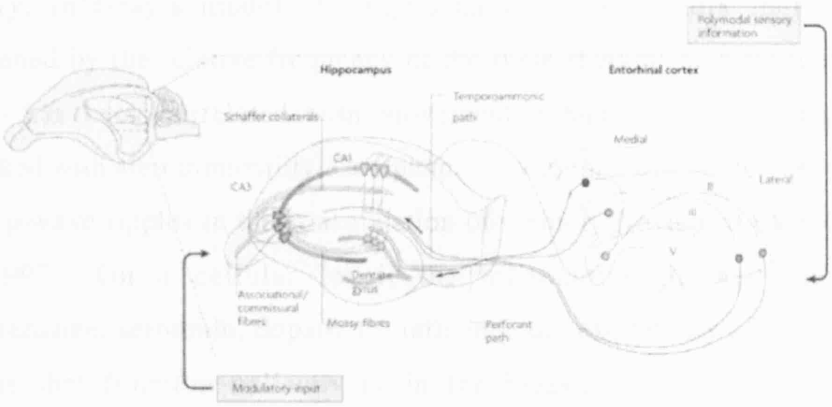

Figure 1: The hippocampal tri-synaptic circuitry

The hippocampus has a tri-synaptic circuitry. The major input to the hippocampus is from layer II of the entorhinal corex along the perforant path. Axons from the perforant path make excitatory connections with the granule cells of the dentate gyrus. The granule cells subsequently project to the proximal apical dendrites of CA3 pyramidal cells (termed the mossy fibre pathway). CA3 neurons project both ipsilaterally to CA1 (the Schaffer collateral pathway), and contralaterally to CA3 and CA1 (the commissural pathway). The main output of the hippocampus is from CA1 pyramidal cells which project to layer V of the entrorhinal cortex. (Figure adapted from Neves *et al.*, 2008)

The hippocampus is a temporal lobe structure that is vital for the encoding and recall of episodic memory (Squire *et al.*, 2004). The hippocampus has various neuronal activity patterns that can be recorded at the level of the neuronal network. The hippocampal theta rhythm is a slow rhythmic pattern of excitatory activity that oscillates at a frequency of between 3-12 Hz. It is recorded *in vivo* during exploratory behaviour and REM sleep. Sharp wave-ripples correspond to irregular neuronal bursts of firing in the CA3 region correlated with high frequency (150-200 Hz) neuronal firing in CA1. Sharp wave-ripples are recorded when an animal is sitting quietly, drinking, eating, face washing, grooming or in deep sleep. The significance of these two hippocampal states in relation to the function of the hippocampus is explained by two complementary theories. In the Gray's theory of Behavioural Inhibition, the hippocampus function is as a

comparator that compares actual stimuli with expected stimuli and therefore determines the entry of behaviourally significant information into long-term memory. In Gray's model, the hippocampal circuits work in two modes determined by the relative frequency of the theta rhythm: high frequency theta rhythm has been correlated with movement, whilst the lower frequency is associated with alert immobility. Complementary to this, Buzsaki argues for a role of sharp-wave ripples in the consolidation of memory (reviewed by Mongeau *et al.*, 1997). On a cellular level, the monoaminergic neuromodulators (noradrenaline, serotonin, dopamine) influence the excitability of the individual neurons that function collectively in the hippocampal network. A single neuromodulator can have both excitatory and/or inhibitory effects on a single neuron's excitability dependent on the receptors, signal transduction cascades and ion channels expressed by that neuron and activated at any one time. This idea is developed further in the following sections.

1.2: Adrenergic modulation of hippocampal neuronal excitability

Noradrenergic axons project to the hippocampus from the locus coeruleus (Lopes da Silva *et al.*, 1990; Andersen, 2007). The major effect of noradrenaline in the CA1 region of the hippocampus is mediated via β adrenoceptors and functions to increase excitability. The effect was first described in the early 1980s when application of noradrenaline to CA1 pyramidal cells was shown to depolarise the membrane potential, increase in input resistance, increase the firing frequency, decrease the spike frequency adaptation and decrease the slow afterhypepolarisation (sAHP) (Madison & Nicoll, 1982; Haas & Konnerth, 1983). The evidence suggesting this combined effect was mediated by β adrenoceptors was pharmacological. The effect was resistant to phentolamine, an α adrenoceptor antagonist, mimicked by isoproterenol, a β adrenoceptor agonist, and inhibited by both timolol and propanolol, β adrenoceptor antagonists (Madison & Nicoll, 1986a).

The effects of noradrenaline on hippocampal neuronal excitability are achieved by the modulation of two neuronal currents I_h/I_Q and sI_{AHP}. I_h (formerly I_Q) is a mixed

sodium (Na^+) and potassium (K^+) conductance activated by hyperpolarisation (Halliwell & Adams, 1982) , whilst sI_{AHP} is a calcium (Ca^{++}) activated K^+ current mediating the sAHP (Alger & Nicoll, 1980; Hotson & Prince, 1980; Schwartzkroin & Stafstrom, 1980; Lancaster & Adams, 1986).

The noradrenergic mediated depolarisation was associated with activation of an inward current. β adrenoceptors are positively coupled to AC in a well-characterised pathway that leads to generation of 3'5'-cyclic adenosine monophosphate (cAMP) and activation of PKA. Therefore it was investigated whether the AC/cAMP/PKA pathway mediated the effect of noradrenaline on the inward current. The results of these experiments indicated that the activation of the inward current was dependent on cAMP but was not mediated by PKA. The pharmacological profile of the inward current indicated it was I_h/I_Q (Pedarzani & Storm, 1995b). A direct, non-PKA mediated modulation of the mixed cationic current (I_f) by cAMP had been demonstrated in the heart (DiFrancesco & Tortora, 1991). Later, cloning of HCN channels demonstrated that these channels are responsible for I_h/I_f. Furthermore the cAMP binding site on the HCN channel has been isolated and the effect of the direct binding of cAMP has been molecularly dissected (Wainger *et al.*, 2001). Furthermore, the expression of HCN1, HCN2, and HCN4, has been demonstrated in CA1 pyramidal cells (Brewster *et al.*, 2007). These experiments are consistent with the idea that the noradrenaline mediated depolarisation is associated with cAMP dependent activation of the HCN channels that mediate I_h.

The indication that the noradrenergic mediated suppression of sI_{AHP} involved the AC-cAMP pathway came from experiments with forskolin, which appeared to mimic the noradrenergic effect (Madison & Nicoll, 1982, 1986b). Further experiments with the AC inhibitor SQ 22,566 and the GTP analogue guanylyl-imido diphosphate, which activates G proteins that in turn can stimulate AC, confirmed the involvement of AC in the signal transduction pathway (Madison & Nicoll, 1986b). The involvement of cAMP was inferred from experiments using the membrane permeant cAMP analogue 8-bromo-cAMP that was found to mimic the effect of noradrenaline on the sAHP and spike frequency adaptation. The role of cAMP was further implicated by experiments with the phosphodiesterase

inhibitors IBMX and Ro20-1724 that suppressed the sAHP and increased the noradrenergic effect (Madison & Nicoll, 1986b).

The role of phosphorylation in the modulation of sI_{AHP} was shown through the intracellular application of the broad-spectrum phosphatase inhibitor microcystin, which resulted in a gradual rundown of the sI_{AHP}, mimicking the effect of isoproterenol (Pedarzani & Storm, 1993). A potential candidate for the kinase involved in the noradrenergic modulation of sI_{AHP} was PKA. Three lines of evidence supported this conclusion. Firstly, the isoproterenol-induced suppression of sI_{AHP} was inhibited by preventing the activation of PKA by cAMP through inclusion of the PKA inhibitor Rp-cAMPS in the patch pipette. Intracellular application of PKI, a pseudo substrate inhibitor that acts by binding to the substrate recognition site of PKA (Cheng *et al.*, 1986), also inhibited the suppression of sI_{AHP} by isoproterenol (Pedarzani & Storm, 1993). Thirdly, the effect of isoproterenol on sI_{AHP} could be mimicked by inclusion of the catalytic subunit of PKA in the recording pipette (Pedarzani & Storm, 1993).

In conclusion the effect of noradrenaline on hippocampal neuronal excitability is mediated by β adrenoceptors and subsequent activation of AC. The rise in cAMP leads on one hand to the direct activation of I_h and membrane depolarisation, and on the other to PKA-mediated phosphorylation resulting in sI_{AHP} suppression.

1.3: Serotonergic modulation of hippocampal neuronal excitability

There are two distinct types of serotonergic projections to the hippocampus, both arising from the raphe nuclei. The thin varicose axon system arises from the dorsal raphe nucleus and innervates the ventral hippocampus. It is a diffuse branching, network with small fusiform boutons. Innervation of the dorsal hippocampus arises from the median raphe nucleus. It is characterised by thick varicose tract fibres with short thin branches and large round boutons (reviewed by Hensler, 2006). The density of serotonergic axons is highest in the CA3 sub region of the hippocampus, with an abrupt reduction at the boundary between CA2 and CA1 (Mamounas *et al.*, 1991). There is a narrow band of thick varicose tract fibres present in the stratum lacunosum of CA1, whilst the stratum oriens and

stratum radiatum are innervated by the thin varicose axon system (Mamounas *et al.*, 1991).

Serotonergic transmission in the hippocampus has been described as volume or paracrine transmission (Descarries & Mechawar, 2000). Consistent with this idea, serotonin receptors are present on CA1 pyramidal cells despite the diffuse innervation. Serotonin has three distinct effects on neuronal excitability in CA1 pyramidal cells. Firstly, application of serotonin results in a striking membrane potential hyperpolarisation; secondly, there is a decrease in the sAHP; and thirdly, over a slower timescale, there can be membrane potential depolarisation. It has been observed that antagonism of the $5HT_{1A}$ and $5HT_4$ subtypes of serotonin receptors abolishes the effect of serotonin on neuronal excitability in CA1 pyramidal cells (Andrade, 1998). Therefore I will concentrate on the effects and signal transduction mechanisms of $5HT_{1A}$ and $5HT_4$ receptors in CA1 pyramidal cells. Both $5HT_{1A}$ (Wright *et al.*, 1995) and $5HT_4$ (Vilaro *et al.*, 1996) are expressed on CA1 pyramidal cells.

It was shown that application of serotonin to CA1 pyramidal cells resulted in a membrane hyperpolarisation due to agonism at $5HT_{1A}$ receptors resulting in activation of a K^+ current (Andrade & Nicoll, 1987; Colino & Halliwell, 1987), The membrane hyperpolarisation on application of serotonin was absent in the GIRK2 knockout mouse (Luscher *et al.*, 1997), indicating that the activation of GIRK channels underlies the membrane hyperpolarisation. GIRK channels are G protein-coupled inwardly rectifying potassium channels. Several lines of evidence had converged on the activation of heterotrimeric G proteins in the signalling cascade linking the $5HT_{1A}$ receptor to membrane hyperpolarisation. Firstly, the GDPβS and GTPγS, a G protein inhibitor and activator, respectively, indicated a role for a G protein in the serotonin mediated membrane hyperpolarisation (Andrade *et al.*, 1986). Secondly, the use of pertussis toxin (Andrade *et al.*, 1986) specifically indicated the role of the G_i/G_o subtype. GIRK channels have been shown to be directly activated by the βγ subunits of G proteins in a membrane-delimited manner in the heart (Logothetis *et al.*, 1987). The above evidence indicates that application of serotonin most likely leads to the activation of GIRK

channels by the βγ subunits released from G_i/G_o proteins resulting in membrane hyperpolarisation in CA1 hippocampal pyramidal neurons.

A second notable effect of serotonin application in CA1 pyramidal neurons is the suppression of the sAHP mediated by $5HT_4$ receptors (see for review Andrade, 1998). The involvement of $5HT_4$ receptors in the serotonin-mediated sAHP suppression was shown in experiments using selective $5HT_4$ receptor antagonists: GR113808, DAU6285, SDZ 205-557 all abolished the effect of serotonin on the sAHP (Torres *et al.*, 1994). The role of the AC-cAMP-PKA pathway, already described for the noradrenergic modulation of sAHP, was confirmed also for the serotonergic suppression of sAHP and sI_{AHP} (Pedarzani & Storm, 1993; Torres *et al.*, 1994). The role of PKA was assessed through the use of the broad-spectrum protein kinase inhibitor staurosporine (Torres *et al.*, 1994), and the selective PKA inhibitor Rp-adenosine-3'5'-cyclic monophosphorothioate (Rp-cAMPS)(Pedarzani & Storm, 1993; Torres *et al.*, 1994). Both of these compounds inhibited the effect of serotonin on sI_{AHP}. Therefore the serotonin-mediated suppression of sAHP and its underlying current sI_{AHP} was shown to be due to activation of $5HT_4$ receptors positively coupled to AC, and activation of PKA as has similarly been shown for the β adrenergic suppression of sAHP.

1.4: Dopaminergic modulation of hippocampal neuronal excitability

The CA1 region of the hippocampus receives dopaminergic input from both the substantia nigra and the ventral tegmental area (Gasbarri *et al.*, 1997). There are two groups of dopamine receptors, classified by their coupling to ACs. Group 1 receptors stimulate AC through $G\alpha_s$ (Kebabian & Calne, 1979) and comprise of the D_1 and D_5 subtypes, both of which are expressed in the pyramidal cells of the CA1 region of the hippocampus (Fremeau *et al.*, 1991; Tiberi *et al.*, 1991; Khan *et al.*, 2000). Dopaminergic type 2 receptors comprise of the D_2, D_3 and D_4 subtypes and are negatively coupled to AC (Kebabian & Calne, 1979). Only the D_4 subtype of the group 2 dopamine receptors subtype is expressed in CA1 pyramidal cells (Khan *et al.*, 1998).

Given the varied distribution of dopamine receptors on CA1 pyramidal cells and the opposing effects on AC, the effect of dopamine on these cells is complex. Consistent with this view, both enhancing effects (Benardo & Prince, 1982b; Haas & Konnerth, 1983) and inhibitory effects (Malenka & Nicoll, 1986; Pedarzani & Storm, 1995a) of dopamine on the sAHP or sI_{AHP} have been described. The involvement of the cAMP pathway has been implicated in both the up-regulation and suppression of the sAHP/sI_{AHP} (Benardo & Prince, 1982b; Pedarzani & Storm, 1995a). There have also been contradictory reports on the receptors involved in the dopamine-induced suppression of the sAHP. While Malenka and Nicoll (1986) reported that the sAHP suppression was a result of cross reactivity of dopamine with β adrenoceptors, Pedarzani and Storm (1995a) demonstrated that the effect of dopamine on both sAHP and sI_{AHP} was still elicited in the presence of the β adrenoceptor antagonists timolol and propanolol. The receptors mediating the dopaminergic effect on sAHP/sI_{AHP} have however proved elusive. The dopaminergic suppression of sAHP persisted in the presence of the broad-spectrum dopamine receptor antagonists fluphenazine and haloperidol (Malenka & Nicoll, 1986; Pedarzani & Storm, 1995a). However, SKF-38393, a selective D1 agonist, suppressed the sAHP in a subset of cells and, consistent with a role of D1 receptors in the dopaminergic sAHP suppression, the D1 antagonist SCH-23390 antagonised the effect of dopamine in a subset of cells (Pedarzani & Storm, 1995a).

A possible explanation for these somewhat contradictory effects of dopamine could be the existence of a sub population of CA1 pyramidal neurons expressing D1 receptors. Consistent with this hypothesis, the effect of dopamine on a subset of cells has been shown for a transient potassium (K^+) current in the dendrites of CA1 pyramidal neurons, responsible for the decremental decrease in action potential amplitude along the dendrites (Hoffman & Johnston, 1999). In particular, it was shown that PKA activation by β adrenoceptors led to an increase in the amplitude of back-propagating dendritic action potentials through downregulation of the transient K^+ channels. However dopamine was only effective in a subset of CA1 neurons (Hoffman & Johnston, 1999).

In addition to its role in modulating transient potassium currents, dopamine has also been shown to suppress voltage gated sodium currents in isolated hippocampal neurons via activation of PKA by D1 like receptors (Cantrell *et al.*, 1997).

In summary noradrenaline, serotonin and dopamine converge on G protein coupled receptors to modulate neuronal excitability. They all have both excitatory and inhibitory effects dependent on the receptors, signal transduction cascades and ion channels expressed by that neuron and activated at any one time. Noradrenaline, serotonin and dopamine all converge on the AC/cAMP/PKA pathway to suppress the calcium (Ca^{++}) activated K^+ current that underlies sAHP. The next sections will investigate the different forms of AHP in CA1 pyramidal cells, the currents that underlie them, and their function in controlling neuronal excitability. Particular emphasis will be placed on the Ca^{++} activated components of the afterhyperpolarisation (AHP) on which this study focuses.

1.5: Afterhyperpolarisation and afterhyperpolarising currents

The term AHP describes the transient hyperpolarisation of the membrane potential that follows the repolarising phase of single or trains of action potentials. The AHP is mediated by the activation of a number of currents and consists of three kinetically distinct phases that are named according to their time courses (Storm, 1990).

The fast AHP (fAHP) is activated immediately after the repolarisation of the action potential and lasts several tens of milliseconds. The macroscopic current that underlies the fAHP is denoted I_C and contributes to the membrane repolarisation following the action potential (Storm, 1987). The current is mediated by K^+ channels of large conductance (BK channels), which open in response to simultaneous membrane depolarisation and the rise in intracellular calcium concentration that occurs via the opening of voltage gated calcium channels during the action potential. The fAHP is elicited after a single action potential and becomes less pronounced during repetitive firing (Lancaster & Nicoll, 1987; Shao *et al.*, 1999). This is in contrast to the the slow AHP (sAHP),

which become more prominent following a burst of action potentials (Lancaster & Nicoll, 1987).

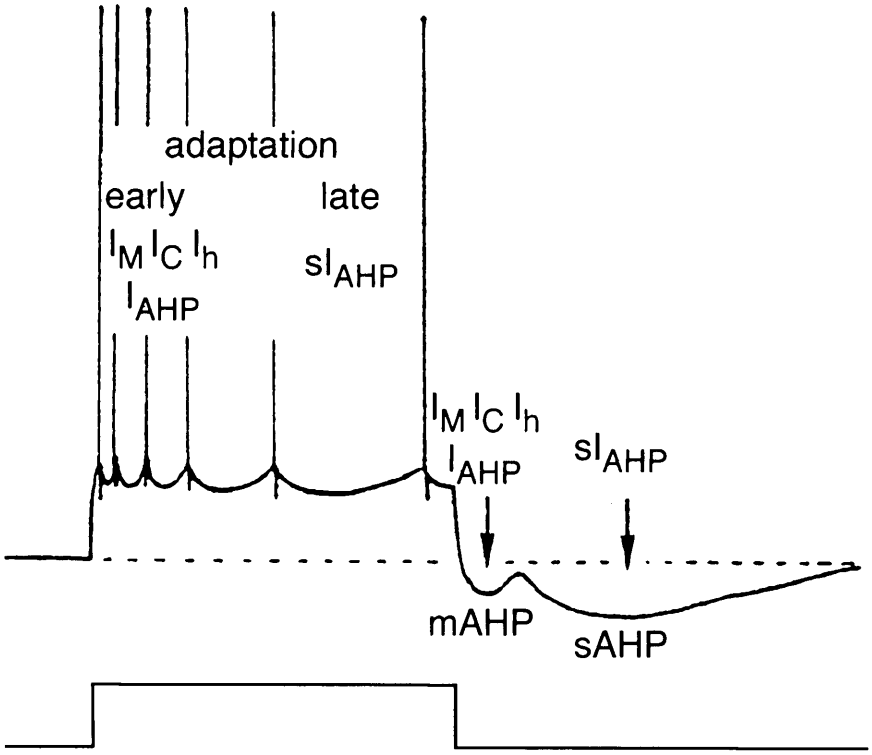

Figure 2: The phases of the AHP and of spike frequency adaptation

Currents underlying the mAHP are responsible for the early phase of adaptation. The current underlying the sAHP, sI_{AHP}, generates the late phase of adaptation. Both AHP are visible after the current injection. The currents that contribute to each phase of adaptation are shown. (Figure adapted fromStorm, 1990.)

The AHP of medium duration (mAHP) follows a train of action potentials and lasts 50-100 ms (Storm, 1989). The mAHP is mediated by the activation of four different currents: the voltage dependent M current I_M (Storm, 1989); the voltage and Ca^{++} dependent I_C (Storm, 1989); the mixed Na^+ and K^+ conductance activated by hyperpolarisation I_h (also known as I_Q) (Storm, 1989); and the Ca^{++} activated K^+ current I_{AHP} (Stocker *et al.*, 1999). The contribution of each current to the mAHP has been assessed pharmacologically in a number of studies and partly depends on the cell's resting potential. For example, when the pyramidal cell is held at a slightly depolarised potential (–60 mV), the major component of the mAHP appears to be mediated by I_M, because the mAHP can be suppressed by the

M channel blocker XE991 (Gu *et al.*, 2005). However at hyperpolarised potentials (-80 mV) the slow re-activation of HCN/h channels generates a mAHP-like waveform. Concordantly, the mAHP elicited at –80 mV is blocked by caesium ions (Storm, 1989) and ZD7288 (Gu *et al.*, 2005), which suppress I_h.

The contribution of I_{AHP} to the mAHP has raised some controversy. Although several groups have reported an I_{AHP}-mediated component of mAHP in CA1 neurons (Stocker *et al.*, 1999; Kramar *et al.*, 2004; Shah *et al.*, 2006; Cai *et al.*, 2007; Kaczorowski *et al.*, 2007), one group has failed to observe it (Gu *et al.*, 2005). The channels underlying I_{AHP} in CA1 pyramidal cells are small conductance Ca^{++} activated K^+ channels (SK channels) (for review see Stocker, 2004). There are several lines of evidence indicating that I_{AHP} contributes to the mAHP. Firstly, the activation of I_{AHP} is dependent on the influx of extracellular Ca^{++} because both cadmium ions and Ca^{++} free medium inhibit I_{AHP} (Stocker *et al.*, 1999). Consistent with a role for a Ca^{++} activated current contributing to the generation of the mAHP, manipulations that reduced Ca^{++} influx have been demonstrated to partially suppress the mAHP (Storm, 1989). Secondly apamin, a selective SK channel blocker, suppresses both I_{AHP} and a component of the mAHP (Stocker *et al.*, 1999; Shah *et al.*, 2006; Kaczorowski *et al.*, 2007). These lines of evidence indicate that SK-mediated I_{AHP} contributes partially to the mAHP. A possible explanation for the lack of effect of apamin on the mAHP seen by Gu (2005) is the apparent frequency dependence of the contribution of I_{AHP} to the mAHP (Shah *et al.*, 2006). For example, it has been reported that apamin has no significant effect on the mAHP when it is elicited by a train of five action potentials or less (Gu *et al.*, 2005; Shah *et al.*, 2006). Conversely, application of apamin increases the number of action potentials in response to a high current injection that elicits at least six action potentials (Shah *et al.*, 2006). This indicates a threshold for the activation of the I_{AHP}. Because I_{AHP} is a voltage insensitive, Ca^{++} activated current; the threshold for activation of the I_{AHP} must be a critical Ca^{++} concentration. Therefore it can be concluded that I_{AHP} contributes to the mAHP in conditions where sufficient Ca^{++} influx occurs to activate SK channels.

The slowly decaying phase of the AHP following a burst or train of action potentials is the sAHP. The sAHP decays over a time course of seconds. The

current that underlies the sAHP, sI_{AHP}, is mediated by a Ca^{++} activated, voltage-independent K^+ conductance (Alger & Nicoll, 1980; Hotson & Prince, 1980; Schwartzkroin & Stafstrom, 1980; Lancaster & Adams, 1986). The molecular identity of the channels underlying sI_{AHP} is as yet unknown (Stocker, 2004). However given the biophysical similarity in the I_{AHP} and sI_{AHP} (they are both voltage insensitive Ca^{++} activated K^+ currents), there has been speculation as to whether the SK channels could mediate sI_{AHP}. The most convincing evidence against the role of SK channels in mediating sI_{AHP} is the selective deletion of I_{AHP} and not sI_{AHP} in SK channel knock out mice (Bond *et al.*, 2004).

1.6: Ca^{++} activated AHP currents modulate neuronal firing frequency and adaptation to synaptic responses

The AHP currents regulate neuronal firing frequency in different ways. The role of the after hyperpolarising currents in regulating neuronal behaviour has been investigated by studying the effects of pharmacological agents that are known to selectively modulate the currents that mediate each phase of the AHP on neuronal firing patterns. Using this approach Lancaster and Nicoll (1987) and Storm (1987) both working in parallel demonstrated that the primary effect of blocking I_C, the current that underlies the fAHP, is action potential broadening. Furthermore, I_C in CA1 pyramidal neurons is a transient current that decays within less than 20 ms during sustained depolarisation (Zbicz & Weight, 1985; Gu *et al.*, 2007). This indicates that the fAHP plays a role in repolarising the membrane potential after a single action potential but will have little effect on a train of action potentials. This was confirmed by experiments that selectively blocked I_C where the neuronal firing frequency of only the first few action potentials increased during a depolarising pulse (Lancaster & Nicoll, 1987). Interestingly it has been suggested that BK channels facilitate high frequency neuronal firing by ensuring rapid repolarisation and narrow action potentials in CA1 pyramidal neurons (Gu *et al.*, 2007). However the inactivation of BK channels would result in action potential broadening (Shao *et al.*, 1999) and thus enhanced Ca^{++} influx through voltage gated Ca^{++} channels that could then accumulate and activate the Ca^{++} dependent components of the mAHP and sAHP. The evidence indicates that the fAHP has a

role in setting the initial firing frequency of a CA1 pyramidal neuron and its inactivation may contribute to the generation of the mAHP and sAHP.

CA1 pyramidal neurons display a phenomenon termed "spike frequency adaptation" in their firing patterns. The effect of spike frequency adaptation is that the neuronal firing frequency reduces with continuing depolarisation (Storm, 1990). The mAHP is thought to underlie the early phase of spike frequency adaptation, whereas the sAHP contributes mainly to the late phase. The Ca^{++} activated K^+ current I_{AHP} contributes to the mAHP and is mediated by the activation SK channels. Suppressing I_{AHP} with apamin in the CA1 region of the hippocampus leads to an increase in the number and initial frequency of action potentials elicited by a current injection but has no effect on the late phase of spike frequency adaptation. Application of apamin to CA1 pyramidal cells shortens the inter-spike interval in a short (100 ms) burst of action potentials (Stocker *et al.*, 1999). Under conditions where the sAHP is suppressed, apamin increases the firing rate of CA1 neurons by affecting the extent of membrane hyperpolarisation during each inter-spike interval (Stocker *et al.*, 1999). This indicates that I_{AHP} controls the instantaneous frequency of action potential firing. More recently, experiments with SK channel enhancers have further indicated the role of SK channels in controlling the tonic firing frequency of hippocampal pyramidal neurons. Application of 1-EBIO in the presence of 8CPT-cAMP resulted in a reduction in the firing frequency of CA1 pyramidal neurons (Pedarzani *et al.*, 2001). Additionally application of NS309, a compound that selectively enhances I_{AHP} but not sI_{AHP} in CA1 pyramidal cells, resulted in a reduction in firing frequency in CA1 pyramidal neurons (Pedarzani *et al.*, 2005). NS309 demonstrates the role of I_{AHP} in controlling firing frequency independently of sI_{AHP}.

The contribution of the sAHP to spike frequency adaptation was investigated in a set of experiments that studied the mechanisms that control repetitive firing. Pharmacological or experimental manipulations that led to a decrease in Ca^{++} influx through voltage-gated Ca^{++} channels or intracellular Ca^{++} rises led to a reduction in the sAHP. This reduction in sAHP was associated with an increase in the number of action potentials fired during a depolarising current injection and a

concomitant decrease in the late phase of spike frequency adaptation (Madison & Nicoll, 1984; Lancaster & Nicoll, 1987).

The current that mediates sAHP, sI_{AHP}, is also involved in the modulation of synaptic responses. Evidence for this came from a study that investigated whether the current can be activated by sub-threshold, excitatory postsynaptic potentials. The finding that sAHP was activated by a train of excitatory post-synaptic potentials (EPSPs) has relevance for the ability of the current to modulate the propagation of synaptic signals from dendrites to the soma (Lancaster *et al.*, 2001). It would be expected that activation of the sAHP would reduce temporal summation of EPSPs because the EPSP would generate Ca^{++} influx, resulting in a sAHP which hyperpolarises the membrane and shunts the next EPSP. This was demonstrated experimentally, EPSPs that were elicited during the peak of sI_{AHP} showed less summation (Lancaster *et al.*, 2001). When sI_{AHP} was suppressed the EPSPs decayed with a slower time course, thereby favouring temporal summation (Lancaster *et al.*, 2001). This illustrates an involvement of sI_{AHP} in the modulation of synaptic responses.

This thesis will explore further the modulation of I_{AHP} and sI_{AHP} in the CA1 region of the hippocampus. Firstly, the inhibition of neuronal I_{AHP} by the negative modulator NS8593 will be tested. The thesis then concentrates on the modulation of sI_{AHP}. I previously demonstrated for my undergraduate project, that application of pituitary adenylate cyclase activating polypeptide (PACAP) results in an increase in neuronal firing rate and a reduction in spike frequency adaptation in CA1 pyramidal cells. Here I will investigate whether this increase in neuronal excitability can be attributed to inhibition of sI_{AHP} and the signal transduction cascade underlying this effect. In the last two sections, I will examine whether there is an involvement of the Ca^{++} stimulatable adenylate cycalses (AC) in the modulation of sI_{AHP} by both monoaminergic neurotransmitters and synaptic transmission.

Chapter 2: Methods

2.1: Preparation of transverse dorsal hippocampal slices in rodents

Rat hippocampal slices were prepared from P21-28 male Sprague Dawley rats and were 350 μm thick. Mouse hippocampal slices were prepared from adult wild type (WT) and DKO (mice with a double knockout for both AC1 and AC8) C57BL/6J mice (20-90 days old) and were 300 μm thick. The dissection and slicing procedure was identical for rat and mouse slices.

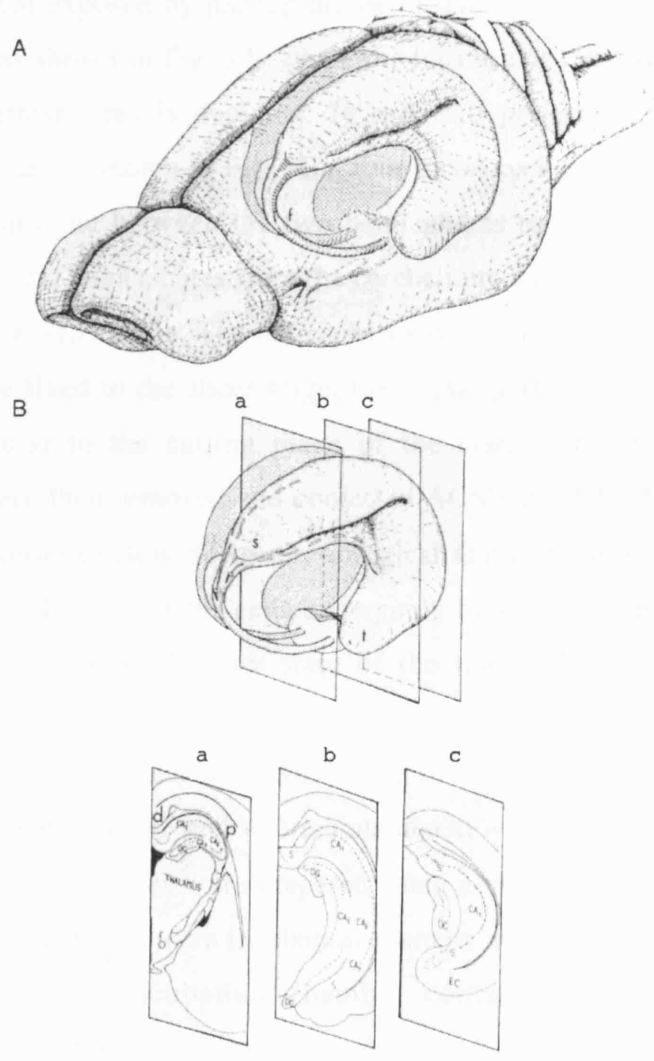

Figure 3: The anatomy of the hippocampus Panel ***A*** depicts the location of the hippocampi within the rat brain. Panel ***B*** shows the transverse hippocampal slices obtained at different levels along the rostro-caudal axis of the hippocampus: ***a***, is a slice through the dorsal hippocampus as used in these experiments; ***b*** and ***c*** are slices obtained

from the more caudal portion of the hippocampus and comprise sections of the ventral hippocampus. Adapted from (Paxinos, 1995).

The animals were anaesthetised with isoflurane and decapitated. Throughout dissection, the head was maintained in a petri dish containing artificial cerebro-spinal fluid (ACSF) at ~4°C. An incision was made running from the nose to the back of the head. The skin was parted in order to expose the cranium, which was subsequently bisected along the middle line using scissors. The cortical hemispheres were exposed by parting the two halves of the cranium. The brain was visualised as shown in Fig. 3A, where the location of the hippocampi inside the cortical hemispheres is depicted. In order to prepare dorsal transverse hippocampal slices as shown in Fig. 3Ba, four incisions were made in the brain, one along the midline between the two hemispheres to separate them, one to separate the cortical hemispheres from the cerebellum, and two at the level of the frontal lobes at a ~15° angle. The hemispheres were cut at a ~15° angle so that when they were fixed to the slicer stage, the dorsal portions of the hippocampi lied perpendicular to the cutting plane of the blade. The trimmed cortical hemispheres were then removed and cooled in ACSF at ~4°C. The preparation was cooled in order to slow down physiological and metabolic processes, thus decreasing the probability of the cells undergoing hypoxic/ischemic damage and therefore maintaining the healthy state of the tissue. The trimmed cortical hemispheres were then glued to the slicer plate using a small amount of cyanoacrylate glue. The plate was fixed to the slicer stage. The slicing chamber contained oxygenated ACSF and was maintained at ~4°C throughout the slicing procedure. Transverse slices were prepared using a vibroslicer Leica VT1000S. The slices were transferred to an incubation chamber using a cut and fire polished Pasteur pipette. The incubation chamber contained ACSF, which was continuously bubbled with 95% oxygen and 5% carbon dioxide. The slices were left to recover from the slicing procedure for one hour before use in the incubation chamber at room temperature (20-25 °C), and could be kept in good condition for up to nine hours.

2.2: Whole cell patch clamp recording

Slices were transferred from the incubation chamber to the recording chamber at the microscope where they were held in position by a platinum harp placed on top of them. The slices were continuously perfused with oxygenated ACSF at a rate of 2-3 ml/min at room temperature. Unless otherwise stated, all drugs were added to the bath. Whole cell patch clamp recording was conducted using a HEKA EPC9 amplifier.

Patch pipettes were made from borosilicate glass capillary tubes in a two-stage vertical puller (Narishige PP-830) and had a resistance of 4.5-7.5 MΩ. Cells were patched blind by positioning the patch pipette over the CA1 region of the hippocampus using a 10X magnification objective. Positive pressure was applied to the patch pipette in order to prevent its fine tip from becoming blocked during its approach to the cell. The pipette was slowly lowered onto the tissue whilst the resistance of the electrode was monitored. An increase in electrode resistance of ~ 0.4 MΩ was taken as an indication of a cell being in close proximity to the patch pipette. The positive pressure was then released, and gentle suction applied to the patch pipette interior in order to favour the formation of a high resistance seal (gigaseal) between the cell membrane and the tip of the pipette. In addition the membrane potential was simultaneously depolarised in order to favour the formation of a gigaseal. Once a gigaohm (GΩ) seal been formed the pipette is said to be in the on cell configuration. The whole cell configuration was achieved through the simultaneous application of short suction to the patch pipette and a short high voltage pulse (zap; 400 mV for 7 ms). Access to the interior was then further improved by applying either gentle suction or pressure until the desired access resistance was achieved. In order to increase the probability of patching a healthy pyramidal cell, cells were taken from beneath the first layer. The advantage of blind patching is that cells do not have to be taken from the first layer of cells, which have a higher probability of their processes being damaged by the slicing procedure (Blanton *et al.*, 1989).

2.3.0: Voltage clamp protocol

The primary aim of the experiments conducted in voltage clamp was to isolate the afterhyperpolarising Ca^{2+}-activated K^+ currents of interest: I_{AHP} and sI_{AHP}. In order to elicit these afterhyperpolarising currents, pyramidal cells were clamped at a membrane holding potential of –50 mV, depolarised to +10 mV for 100 ms, and then stepped back to –50 mV for 12 s during which both I_{AHP} and sI_{AHP} were visualised as Ca^{++} activated tail currents. The voltage clamp protocol is shown in Fig. 4A.

The membrane potential was clamped at –50 mV because both afterhyperpolarising currents are outward K^+ currents. The resting potential of pyramidal neurons is relatively close to the equilibrium potential for K^+ determined by the Nernst equation. (In the ionic conditions used in these experiments the value of E_K predicted by the Nernst Equation is - 102.4-104.3 mV at room temperature.) Therefore if the cell were clamped close to its resting membrane potential the K^+ current elicited by the protocol would be relatively small. By clamping the membrane at the slightly depolarised potential of –50 mV, the driving force for K^+ is increased and both sI_{AHP} and I_{AHP} display larger amplitudes.

sI_{AHP} and I_{AHP} are Ca^{++} activated K^+ currents. In order to elevate the intracellular Ca^{++} concentration, the cell was depolarised to +10 mV for 100 ms. This depolarisation was sufficient to activate voltage gated Ca^{++} channels resulting in Ca^{++} influx that activated the Ca^{++} -activated K^+ channels that underlie both I_{AHP} and sI_{AHP}. The Ca^{++} current was visualised during the step depolarisation as an unclamped "Ca^{++} spike" as shown in Fig. 4B. The Ca^{++} spike amplitude and shape were monitored during the course of experiments because, although unclamped, changes may indicate changes in Ca^{++} influx, possibly due to changes in the voltage gated Ca^{++} currents or in access resistance. The membrane potential was then stepped back to –50 mV and sI_{AHP} and I_{AHP} were visualised as a tail current following the step depolarisation (Fig. 4C). In some experiments where the sI_{AHP} had a small amplitude, the depolarising step was increased to +30 mV for 200 ms to further enhance Ca^{++} influx and thus the magnitude of sI_{AHP}.

In standard voltage clamp experiments, voltage gated sodium channels and some voltage gated potassium channels were blocked using 0.5 μM tetrodotoxin (TTX) and 1 mM tetraethylammonium (TEA), respectively. Under these conditions I_{AHP} and sI_{AHP} displayed larger amplitudes because the required Ca^{++} influx was enhanced. Enhanced calcium influx occurred because voltage gated sodium channels and some voltage and Ca^{++} activated K^+ channels were blocked by TTX and TEA, respectively. Therefore the electrical gradient is maintained in favour or positive ions entering the cell. Consequently , more Ca^{++} enters the cell to balance the electrical gradient.

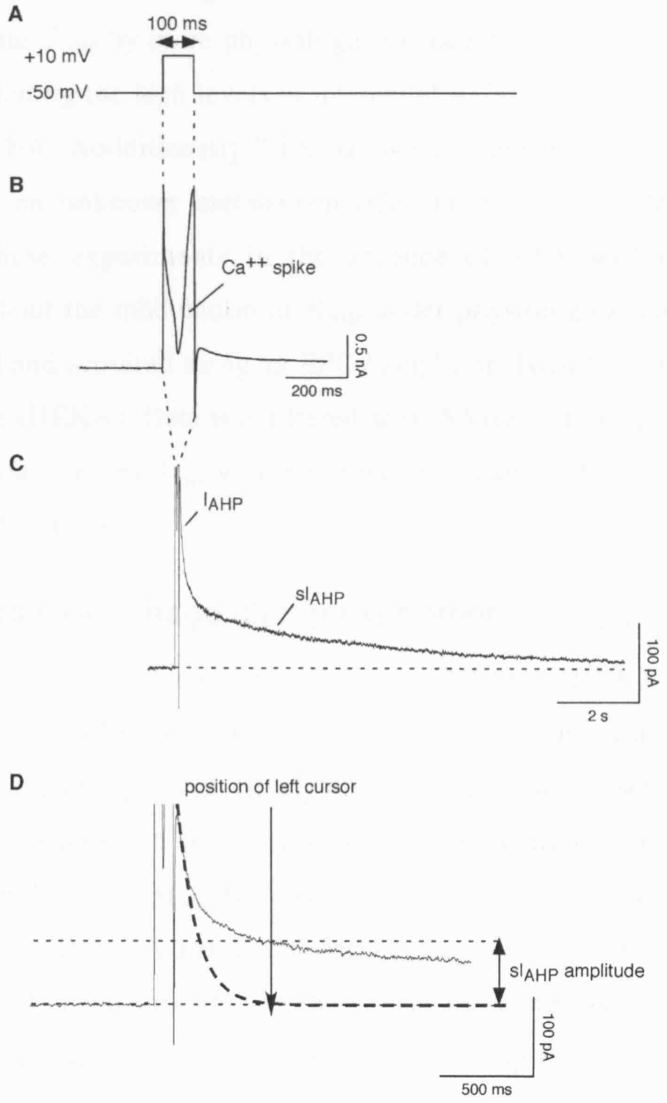

Figure 4: Recording and analysing sI_{AHP} Panel ***A*** shows the voltage clamp protocol used to elicit afterhyperpolarising currents. The cell is depolarised from a holding

potential of –50 mV to +10 mV for 100 ms. This step depolarisation is sufficient to activate voltage gated calcium channels resulting in the calcium influx depicted as an unclamped "calcium spike" in panel ***B***. The afterhyperpolarising currents sI_{AHP} and I_{AHP} are visualised as tail currents following the step depolarisation in ***C***. Panel ***D*** is a demonstration of the positioning of the left cursor used to calculate the amplitude of sI_{AHP}. In order to prevent contamination of I_{AHP} in the measurement of the amplitude of sI_{AHP}, a single exponential function was fit to I_{AHP} as shown by the heavy dotted line in ***D***. The function used was: $y_0+Aexp^{(-invtau*\chi)}$. The left cursor is positioned at χ when $y_o = 0$. This is the time point at which sI_{AHP} is measured in isolation from I_{AHP}.

Some voltage clamp recordings were made in the absence of TTX and TEA in order to activate sI_{AHP} by more physiological concentrations of intracellular Ca^{++} i.e. without eliciting the high levels of intracellular Ca^{++} achieved in the presence of TTX and TEA. Addditionally TTX has been demonstrated to suppress sI_{AHP} amplitude by an unknown mechanism (Constanti & Sim, 1987). Therefore conducting these experiments in the absence of TTX will confer further information about the modulation of sI_{AHP} under physiological conditions. Data was generated and acquired using an EPC9 amplifier (HEKA, Germany) and the software Pulse (HEKA). Data was filtered at 0.25 kHz and sampled at 1 kHz. In some experiments, where I_{AHP} was measured in isolation, data was filtered at 1 kHz and sampled at 4 kHz.

2.3.1: Analysis of voltage clamp experiments - sI_{AHP}

Analysis was conducted using the software PulseFit (HEKA) and IgorPro (WaveMetric). As illustrated in Fig. 4C, a tail current consisiting of two components, I_{AHP} and sI_{AHP}, with clearly different time courses (see also Stocker *et al.*, 1999) were elicited in response to the voltage clamp paradigm described above. The amplitude of sI_{AHP} for any given trace was calculated by fitting an exponential between two cursors and determining the amplitude and the decay time constant (τ) of the current. The charge was calculated as the integral of the waveform between the two cursors. It was therefore important when analysing the sI_{AHP} that the left cursor was positioned so that there was as little "contamination" as possible by I_{AHP}. The right cursor was positioned at the end of the sweep where

the current had returned to baseline. Fig. 4D is an example of how the position of the left cursor was determined. A single exponential function was fit to the portion of the current corresponding to I_{AHP}. Where $y_0 = 0$ for the exponential function, χ corresponds to the first time point where the amplitude of sI_{AHP} could be determined in isolation.

Control data was taken as the arithmetic mean of the three traces immediately prior to drug application. The maximal drug effect was calculated by selecting three traces when at least five minutes of stabilisation had occurred after drug application. The arithmetic mean of these three traces was calculated.

2.3.2: Analysis of voltage clamp experiments - I_{AHP}

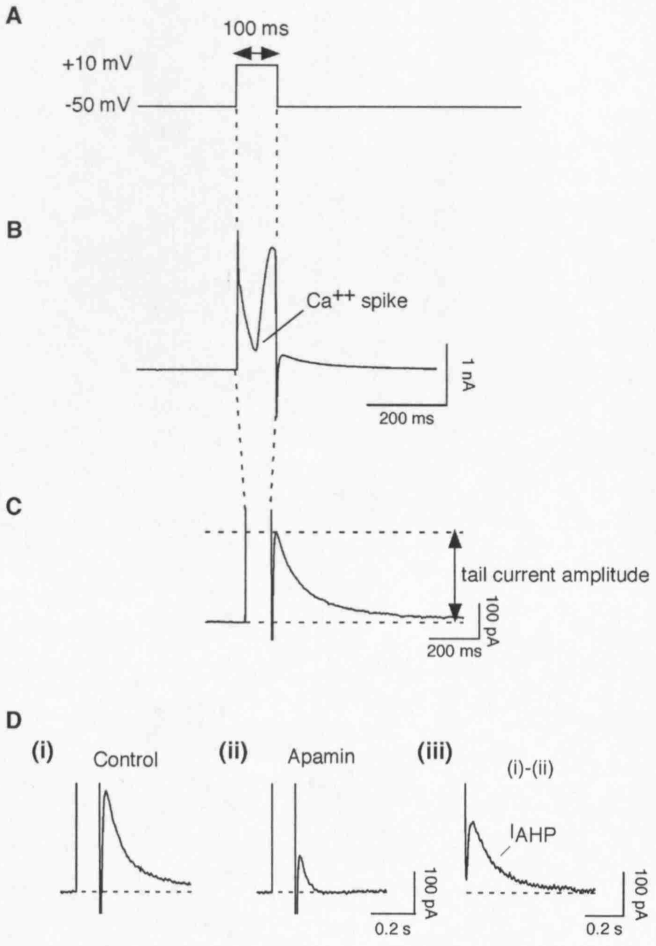

Figure 5: Recording and analysing I_{AHP} I_{AHP} is a calcium activated potassium current that is mediated by SK channels. It can be elicited by the voltage clamp protocol shown in panel ***A***. In order to record I_{AHP} in isolation from sI_{AHP}, recordings were conducted in the presence of 50 μM 8CPT-cAMP. All experiments were conducted in the presence of

0.5 μM TTX and 1 mM TEA in order to block voltage gated sodium channels and some voltage- and calcium- activated potassium channels, respectively. Under these conditions the "calcium spike" (***B***) and tail current (***C***) could be visualised clearly. The tail current in panel ***C*** was mostly, but not completely inhibited by the selective SK channel blocker apamin (***Dii***). Panel ***D*** illustrates how the SK-mediated I_{AHP} could be obtained from the tail current. Apamin (50 nM) was routinely applied at the end of the experiment. The apamin insensitive component (***Dii***) was subtracted from the control tail current (***Di***). This subtraction revealed the apamin sensitive I_{AHP} (***Diii***), whose peak amplitude and charge could then be determined. Experiments were conducted in hippocampal slices from mouse.

In order to record I_{AHP} in isolation from sI_{AHP}, experiments were conducted with 50 μM 8CPT-cAMP in the recording pipette, as previously described by Stocker et al. (1999). As shown in Fig. 5, under these conditions a single tail current could be elicited in response to the voltage paradigm described above. However, in mouse CA1 pyramidal neurons this tail current was composed of both apamin-sensitive (I_{AHP}) and apamin-insensitive (mainly I_M) components. In order to determine the effect of drugs on the apamin-sensitive I_{AHP}, apamin (50 nM) was routinely applied at the end of the experiment. The apamin insensitive component left after apamin application (Fig. 5Dii) was then subtracted from the control (Fig. 5Di) and drug traces in Igor Pro, so that the amplitude and charge of I_{AHP} (Fig. 5Diii) could be determined.

2.3.3: Analysis of voltage clamp experiments: time of effect

To calculate the time of effect of a drug's action, the time course of the change in sI_{AHP} amplitude was plotted against time. Then two cursors were positioned on the timecourse of the experiment. The first cursor was positioned at last timepoint where the sI_{AHP} amplitude was maximal. The second cursor was positioned where the effect of the drug on the sI_{AHP} amplitude had reached stabilisation. The sI_{AHP} amplitude change with time was fit by a monoexponential equation with which the tau of effect could be calculated. The tau is defined as the time to 63 % of a drug's maximal effect. In experiments where the effect of the drug was not

immediate i.e. where there was a lag between the addition of the drug to the bath, and the effect on the sI_{AHP} amplitude, the time of the lag was calculated and added to the time of effect.

2.4.0: Current clamp protocols

Current clamp experiments were conducted with two aims: to monitor the effect of a drug on spike frequency adaptation and/or to monitor the effect of a drug on the sAHP. Therefore neurons were subjected to two protocols in current clamp: a "burst" protocol was used to monitor the sAHP, while a "family of spike trains" protocol was used to evaluate spike frequency adaptation. Current clamp experiments were conducted in the absence of TTX and TEA in order to visualise the action potentials elicited by somatic injection of square pulses of current.

2.4.1: Burst protocol

In order to monitor the sAHP following a burst of action potentials, current was injected for 400 ms to stimulate a short train of action potentials. Data was filtered at 0.4 kHz and sampled at 1.6 kHz.

2.4.2: Spike train protocol

In order to monitor the spike frequency adaptation, 800 ms-long current pulses were injected into the cell and repeated sequentially with a stepwise increase of current of 50-100 pA in order to elicit an increasing number of action potentials. Data was filtered at 3.3 kHz and sampled at 13.3 kHz.

2.4.3: Experimental design

The experimental design of current clamp experiments was as follows. In order to ensure stable recording conditions, the sI_{AHP} was first monitored in voltage clamp. This was because the sI_{AHP} that underlies sAHP shows a 'run up' phenomenon. Fig. 6 gives an example of the sI_{AHP} 'run up'. Typically, the sI_{AHP} has a very small amplitude (<10 pA) when recording is commenced. Over the first 10 – 20 minutes of recording, the sI_{AHP} increases in amplitude and then stabilises. Once sI_{AHP} had reached stable amplitude in voltage clamp, the amplifier was switched to the current clamp mode. The lowest current injection that elicited a single action

potential was identified. A family of pulses eliciting spike trains was then run with incremental current injections. Secondly the lowest current injection to elicit a maximal sAHP in a burst protocol was identified. This burst protocol was then repeated five times. Returning back into voltage clamp mode, the sI_{AHP} was re-assessed for stability, and then the drug was applied. Once the full effect of the drug on the sI_{AHP} had been visualised in voltage clamp, the burst and spike train protocols were run again in current clamp. The membrane potential was monitored before and after drug application. If the membrane potential changed after the drug application, DC current was injected to return the membrane potential back to its control value.

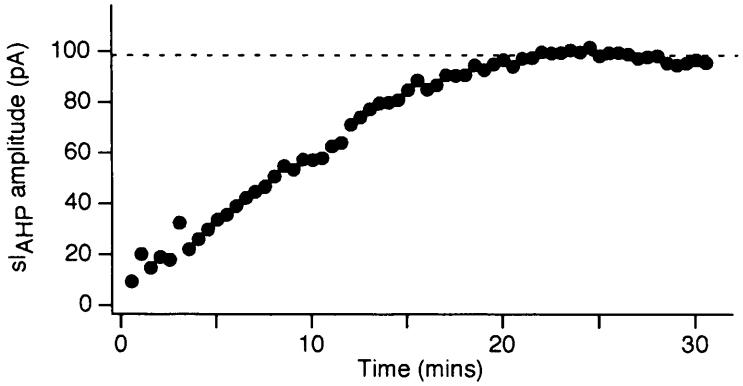

Figure 6: The sI_{AHP} displays a "run-up" phenomenon An example of a typical sI_{AHP} "run-up". When recording is commenced (at time = 0) the sI_{AHP} has an initial amplitude of ~ 10 pA. As recording continues, the sI_{AHP} amplitude gradually increases in amplitude until stability is reached. The dashed line indicates the maximal sI_{AHP} amplitude achieved in this cell (~ 100 pA). Once the sI_{AHP} "run-up" is completed the sI_{AHP} amplitude remains constant for the duration of the experiment.

2.4.4: Analysis of current clamp experiments

In mouse CA1 pyramidal neurons, current clamp experiments were conducted to compare the effect of monoamines in slices from DKO and WT animals. The main aim of the current clamp experiments was to assess changes in amplitude of the sAHP in response to the application of monoamines. The amplitude of the sAHP before and after drug application was determined as the mean between two cursors that were 100 ms apart and placed 1 s after the end of the current injection. Five consecutive sweeps were averaged for each data point. Experiments in which the burst protocol only elicited one action potential were

excluded. The number of action potentials the burst protocol elicited was also monitored. Application of monoamines led to an increase in action potential number and a decrease in sAHP. Cells were excluded in which the action potential number in response to the burst protocol decreased.

2.5.0: Series resistance

In voltage clamp recordings, current is injected through the pipette in order to clamp the membrane at a specific voltage. Current in the pipette flows first through a resistance in series with the cell membrane, this is termed the series resistance. Because of the series resistance the membrane voltage does not mirror exactly the pipette voltage, i.e. a voltage error occurs so that there is a delay between the onset of the command and the actual voltage of the clamped cell membrane.

In whole-cell patch-clamp recording, the electrode acts as a point source of current located at the tip of the voltage recording microelectrode. For a cell to be uniformly voltage-clamped i.e. for the membrane voltage to mirror the command voltage in all portions of the membrane, each portion of the cell membrane should be separated from the tip by equal access resistance. Therefore a small, spherical cell can be uniformly voltage clamped and therefore is 'space clamped'. However, neurons have extended dendritic processes. A single neuronal process can be modelled as a single 'cable' where the voltage change in response to a given current injection decays exponentially with distance from the point source of current. For a simple neuron, consisting of a soma and single dendrite that is voltage-clamped by an electrode at the soma, the change in voltage with respect to the current injection will decay with distance from the soma. Consequently a second voltage error is introduced in voltage clamp recording from neurons, that is due to inadequate 'space clamp.'

No series resistance compensation was used in these experiments for several reasons. First, the afterhyperpolarising currents are calcium activated and not voltage sensitive: it is therefore not necessary to achieve fast and accurate membrane voltage to activate these currents, since their amplitude will mainly depend on the amount of intracellular calcium. Second, both I_{AHP} and sI_{AHP} are

slow tail currents with a rise time of greater than 5 ms (Sah & Faber, 2002) and ~650 ms (Gerlach *et al.*, 2004) for I_{AHP} and sI_{AHP} respectively in rat CA1 pyramidal neurons. The membrane time constant was extrapolated as 4.1±0.2 ms (n=7) which is shorter than the time-to-peak of these currents. Finally, pyramidal neurons have many long dendritic processes with complex shapes. This results in multiple exponential components of the transient corresponding to the charging of the slow membrane capacitance (Llano *et al.*, 1991). Amplifier circuits for the compensation of the slow membrane capacitance and series resistance compensate at best one of the exponentials, thereby not providing a very satisfactory compensation in complex cells.

In order to monitor the series resistance, a dedicated protocol was run at various points during the experiment. After compensating the fast capacitative transients due to the pipette, a 200 ms-long hyperpolarising step from –50 mV to –55 mV (Fig. 7A) generated a current response (Fig. 7B). The relatively fast transients observed were mainly due to the passive properties of the membrane. After fully charging the membrane capacitance, current flowed (I_{input}) through leak channels open at –55 mV. In the whole cell configuration, the access resistance is caused by the aperture in the disrupted patch of membrane under the pipette. The series resistance can be calculated from series current (I_{series}) according to Ohm's law (Fig. 7C). Data acquired from the protocol used to monitor series resistance was filtered at 5 kHz and sampled at 20 kHz.

2.5.1: Analysis of series resistance

Series resistance was monitored throughout the experiment and maintained at ≤30 MΩ. Experiments were discarded if the series resistance changed ≥25% over the drug application or period of stimulation-induced sAHP depression. Series resistance was analysed as shown in Fig. 7B and calculated from the series current according to Ohm's law (Fig. 7C).

Changes in input resistance were monitored in voltage clamp or in current clamp recordings. Analysis of input resistance in voltage clamp was conducted as shown in Fig. 7B and calculated from the I_{input} according to the equation in Fig. 7D. Input resistance can be measured in current clamp by calculating the change in steady

state voltage in response to a small current injection (Fig. 7E). The current injection should not elicit an active membrane response e.g. action potential. For a cell with a stable series resistance, any change in the amplitude of the steady state voltage response can be attributed to a change in input resistance. The input resistance can then be approximated using the equation shown in Fig. 7D. Analysis of input resistance in current clamp was conducted in synaptic experiments in order to calculate any change due to the stimulation paradigm.

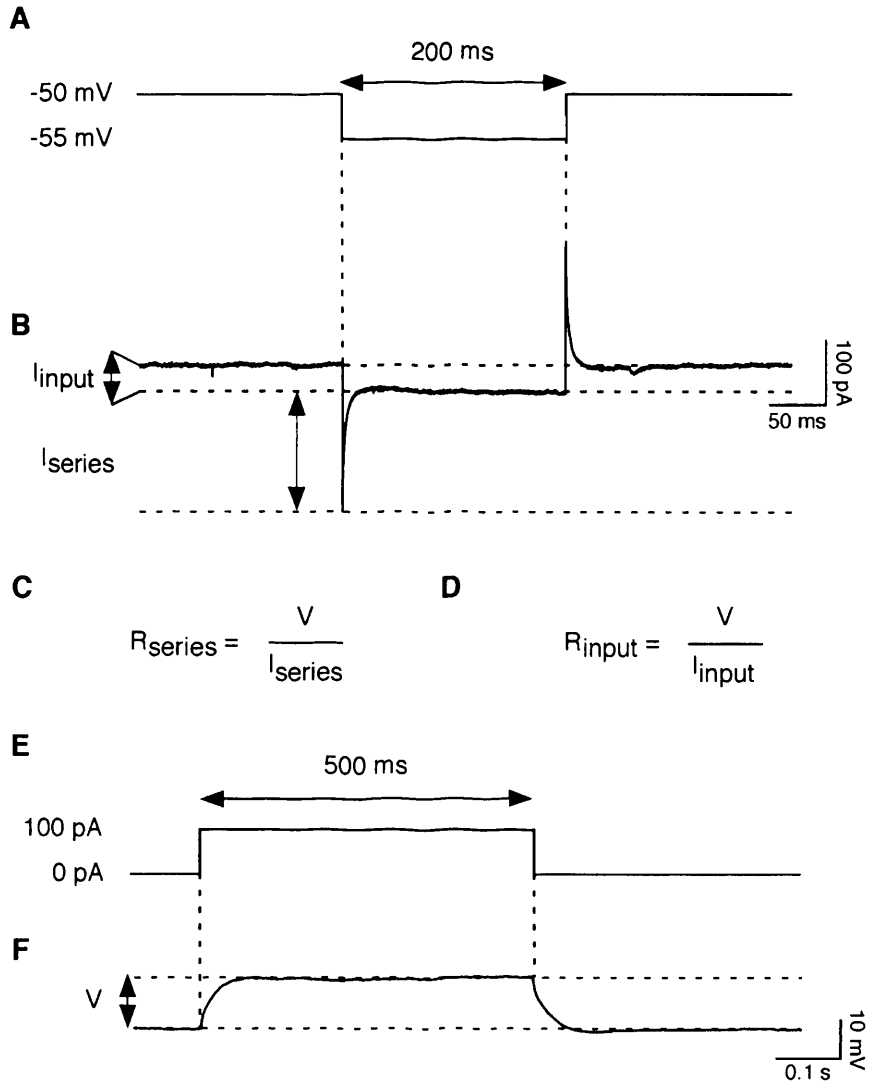

Figure 7: Recording and analysing passive membrane properties Panel ***A*** shows the voltage protocol used to determine the series (R_{series}) and input (R_{input}) resistances of CA1 pyramidal cells in whole cell voltage clamp experiments. After compensation of the fast capacitative transients, a 200 ms hyperpolarising step from a holding potential of –50 mV to –55 mV generated the current response shown in ***B***. The current response was translated into resistance measurements using the equations shown in ***C*** and ***D*** (Ohm's

law). The series resistance was calculated in current clamp at –60 mV by injecting a 500 ms depolarising pulse that did not elicit action potentials (***E***). The potential difference measured in response to a 100 pA depolarising pulse is shown in ***F***. This potential difference was translated into the input resistance using the equation shown in ***D***.

2.6.0: Synaptic stimulation experiments

In synaptic stimulation experiments, the ACSF used for dissection and slice incubation had the composition of ACSF3. Recordings were performed in a submerged chamber with a constant perfusion of oxygenated ACSF4 (2 ml/min) at 30 °C. Once the whole cell configuration had been established, the slice was perfused with 50 μM picrotoxin in order to minimise stimulus-induced plasticity of inhibitory transmission mediated by $GABA_A$ receptors. A cut was made in each slice between areas CA3 and CA1 in order to prevent epileptiform activity.

Giga-seal whole cell recordings were obtained as described earlier from the somata of CA1 pyramidal cells. Stimulating pipettes were pulled from borosilicate glass capillary tubes in a two stage vertical puller and subsequently broken to a resistance of ~ 1-2 MΩ and filled with ACSF4. Stimulating pipettes were positioned in the stratum radiatum of CA1 in order to stimulate the Schaffer collaterals.

2.6.1: High frequency synaptic stimulation (HFS)

Approximately five minutes after establishing the whole cell configuration, once the membrane potential of the cell had stabilised, the depolarising current injection used to monitor the sAHP was ascertained. The criterion for selecting the depolarising step was the minimum current injection that elicited the maximum number of action potentials for each cell. The protocol used involved a set of 500 ms-long current pulses with current injections increasing in steps of 100 pA. The sAHP was elicited every 20 s from a membrane potential of –60 mV. Sufficient DC current was injected to maintain the membrane potential at –60 mV for the duration of the experiment. In order to monitor the sAHP data was filtered at 615 Hz and sampled at 3.08 kHz.

Intracellular EPSPs were measured at a membrane potential of –80 mV. The EPSPs were elicited by a series of test pulses (1000 μs, 3 pulses at 0.05 Hz) given every 5 – 10 min. The EPSPs were filtered at 250 Hz and sampled at 1 kHz.

High frequency stimulation (HFS) was delivered at least 30 min after achieving the whole-cell configuration, when the basal EPSP amplitude had stabilised at ≥ 20 mV for at least 10 min. HFS was delivered at –60 mV as three trains of 100 pulses at 100Hz, separated by 3 min. After HFS, the number of action potentials elicited by the sAHP protocol was monitored and maintained as the pre-HFS action potential number ± 1 by adjusting the current injection eliciting the sAHP.

2.6.2: Synaptic stimulation by pairing protocol

The membrane potential of the cell was monitored in current clamp until it became stable and a family of action potential trains was recorded (500 ms-long current injections every 20 s, 100 pA increments). The criterion used for selecting the current injection for monitoring the sAHP was a current injection that gave an intermediate number of action potentials. Subsequently, the sAHP was elicited every 20 s from a membrane potential of –60 mV. Sufficient DC current was injected to maintain the membrane potential at –60 mV for the duration of the experiment. In order to monitor the sAHP data was filtered at 615 Hz and sampled at 3.08 kHz.

After the sAHP had been stable for ≥ 10 min, (~ 30 min after achieving the whole cell configuration), the intensity of the synaptic stimulation was determined as follows. The postsynaptic cell was clamped at – 60 mV and an input-output relationship was established by plotting stimulus intensity vs excitatory postsynaptic current amplitude (EPSC). The stimulus intensity was then selected to give an EPSC that was half of the maximal EPSC amplitude. The sAHP was subsequently monitored for a further 15 min. Prior to applying the pairing protocol, a family of 500 ms-long action potential trains was obtained (every 20 s, 200 pA increment).

The cell was then stimulated by clamping it at 0 mV, and simultaneously delivering to the Schaffer collaterals a train of 200 stimuli at 5 Hz. Subsequent to stimulation, the cell was kept for ~2 min in current clamp allowing its membrane

potential to re-stabilise. Sufficient DC current was injected to maintain the membrane potential at –60 mV and a third family of action potential trains was elicited (500 ms-long current injections, every 20 s, 200 pA increment) in order to identify the current injection giving a similar action potential number (± 1) to that used to monitor the sAHP before stimulation. This current injection was subsequently used to monitor the sAHP. The number of action potentials evoked by the current injection was continuously monitored and maintained as the pre-stimulation action potential number ± 1 by adjusting the current injection eliciting the sAHP.

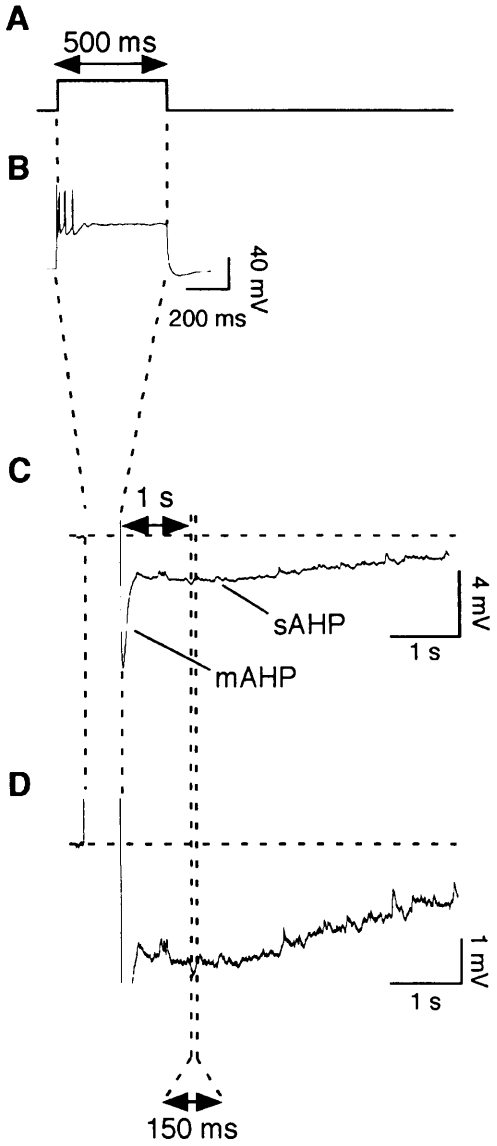

Figure 8: Recording and analysing mAHP and sAHP in synaptic stimulation experiments The mAHP and sAHP were elicited by triggering spike trains by 500 ms-long current injections from a membrane potential kept at –60 mV by DC current

injection (***A***). The current injection chosen was sufficient to trigger a maximal number of action potentials (***B***). The mAHP and sAHP were visualised as hyperpolarising shifts in the membrane potential following the end of the current injection (***C***). The amplitude of the sAHP was determined as the mean between two cursors placed 150 ms apart (***D***), 1 s after the end of the current injection (***C***).

2.6.3: Analysis of synaptic stimulation experiments

The sAHP was elicited every 20 seconds, and its amplitude was determined every minute by the following procedure. Three consecutive sweeps were averaged for each data point in Pulsefit and exported into IgorPro. The amplitude of the sAHP was determined as the mean amplitude of the averaged trace between 1.0 – 1.15 s after the end of the current injection used to elicit the sAHP. This time boundary is marked as dashed lines on Fig. 8C and in the enlargement shown (Fig. 8D). As can be seen in Fig. 8D, at this time boundary there was no overlap between the mAHP and sAHP.

As a baseline before stimulation, the sAHP amplitude was monitored for either 6 min (HFS) or 10 min (pairing protocol). In order to quantify the change in sAHP after stimulation obtained in different experiments, data was normalised to the arithmetic mean of the baseline data.

The mAHP was recorded simultaneously with the sAHP, (Fig. 8C). In order to detect changes in the mAHP following HFS, the amplitude of the mAHP was determined by placing cursors around the mAHP and measuring the maximal hyperpolarisation.

Time-plots were generated from several experiments by calculating the arithmetic mean of the normalised data at each time-point.

2.7: Statistics

The standard error of the mean (SEM) was calculated using the equation:

$SEM = SD/\sqrt{(n-1)}$

Significance was assessed using several different statistical tests. In all cases data was assessed for normality using the Kolmogorov and Smirnov test. If data was normally distributed with equal standard deviations, then significance was

assessed by paired t tests (for matched data), and unpaired t tests (to compare groups). An unpaired t test with Welch correction was performed on normally distributed data that had significantly different standard deviations. If the data did not follow a Gaussian distribution, then paired data was assessed by a Wilcoxon matched-pairs signed-ranks test. Mann Whitney tests were used to compare independent groups. In synaptic experiments, one-way repeated measures ANOVA were used to analyse the significance of the time course for a given condition i.e. to test whether the stimulation was effective. Where there was not a large enough sample size to assess whether the data followed a Gaussian distribution, a non-parametric repeated measures ANOVA (Friedman test) was conducted. The statistical test used in each case is included in parenthesis with the significance level ascertained. Significance was determined as $p<0.05$.

2.8.0: Materials

2.8.1: Equipment

TYPE OF EQUIPMENT	MODEL/TYPE	BRAND AND SOURCE
Anti-vibration table	9102-11-00	Physik Instrumente, Germany
Chart recorder	WR7900	Graphtec
Microelectrode Puller	PP-830	Narishige
Micromanipulator	SM1	Luigs & Neumann
Microscope	Axioscope	Zeiss
Osmometer	Vapor 5520	Wescor
Patch-clamp amplifier	EPC9	Heka
Peristaltic pump	Not applicable	Made in laboratory
pH meter	766 Calimatic	Knick
Scale	30TD	Oertling
Scale	LA120	Sartorius
Stimulator	DS2	Digitimer Ltd.
Stimulator timer	D4030	Digitimer Ltd.
Temperature control system	TC-324B	Warner Instrument
Vacuum pump	Dymax30	Charles Austen Pumps
Vibroslicer	VT1000S	Leica

2.8.2: Toxins and drugs

Drug	Source	Solubility
8CPT-cAMP	Sigma	
Albumin	Sigma	
Apamin	Latoxan	Toxin buffer
DL-AP5	TOCRIS	50mM NaOH
Dopamine hydrochloride	Research Biochemicals International	
D-tubocurarine	Sigma	
Isoproterenol hydrochloride	Research Biochemicals International	
Maxadilan	Dr Ethan Lerner, Harvard University	
Maxadilan-d-4	Dr Ethan Lerner, Harvard University	
MPEP hydrochloride	TOCRIS	
Noradrenaline	Research Biochemicals International	
NS8593	NeuroSearch, Denmark	DMSO
PACAP-27	Calbiochem	
PACAP-38	Peninsula Laboratories Europe	
PACAP-6-38	BACHEM/ Peptide Institute	
PD98059	Calbiochem	DMSO
Picrotoxin	TOCRIS	DMSO

PKI-6-22-amide	Calbiochem	
Rp-cAMPS	Biolog- Life Science Institute	
SB203580	Calbiochem	DMSO
Serotonin hydrochloride	Research Biochemicals International	
Tetraethylammonium	Sigma	
Tetrodotoxin	Latoxan	PH 4-5 with HCl
UO126	Calbiochem	DMSO
WAY 100135	TOCRIS	
XE991 hydrochloride	TOCRIS	

2.8.3: Salts and other chemicals

Compound	Source
$CaCl_2$	Fluka
Glucose	Anachem
HEPES	VWR International Ltd
Isoflurane	Curamed Pharma GmbH
KCl	Merck and Anachem
Kgluconate	Sigma
KH_2PO_4	Merck and Anachem
$KmeSO_4$	ICN Biomedicals Inc.
KOH	Merck
$MgCl_2$	Merck and Anachem
Na_2-ATP	Sigma
Na_3-GTP	Fluka
NaCl	Merck and Anachem
$NaHCO_3$	Merck and Anachem

2.9.0: Solutions

2.9.1: Toxin buffer

Compound	Concentration (mM)
NaCl	100
HEPES	20

pH to 7.4 with KOH

2.9.2: Extracellular solutions: ACSF1 (dissection and incubation)

Compound	Concentration (mM)
NaCl	125
KCl	1.25
$MgCl_2$	1.5
$CaCl_2$	1
KH_2PO_4	1.25
$NaHCO_3$	24
Glucose	16

2.9.3: Extracellular solutions: ACSF2 (recording)

Compound	Concentration (mM)
NaCl	125
KCl	1.25
$MgCl_2$	1.5
$CaCl_2$	2.5
KH_2PO_4	1.25
$NaHCO_3$	24
Glucose	16

2.9.4: Extracellular solutions: ACSF3 (synaptic stimulation experiments – dissection and incubation)

Compound	Concentration (mM)
NaCl	119
KCl	2.25
$MgCl_2$	1.3
$CaCl_2$	1
KH_2PO_4	1.25
$NaHCO_3$	25
Glucose	16

2.9.5: Extracellular solutions: ACSF4 (synaptic stimulation experiments - recording)

Compound	Concentration (mM)
NaCl	119
KCl	2.25
$MgCl_2$	1.3
$CaCl_2$	3.5
KH_2PO_4	1.25
$NaHCO_3$	25
Glucose	16

2.9.6: Intracellular solution: 1 (rat CA1 neurons)

Compound	Concentration (mM)
Kgluconate	135
KCl	10
HEPES	10
$MgCl_2$	1
Na_2-ATP	2
Na_3-GTP	0.4

2.9.7: Intracellular Solution: 2 (mouse CA1 neurons)

Compound	Concentration (mM)
$KMeSO_4$	135
KCl	10
HEPES	10
$MgCl_2$	1
Na_2-ATP	2
Na_3-GTP	0.4

pH 7.2-7.3 with KOH, osmolarity 290-300 mosmols.

2.9.8: Selection of intracellular solution

It has been reported that gluconate based intracellular solutions cause a reduction in the sI_{AHP} amplitude (Zhang *et al.*, 1994). Because the amplitude of sI_{AHP} appears qualitatively reduced in mouse compared to rat CA1 neurons, it was decided to replace gluconate with methylsulphate in the intracellular solution when recording from mouse CA1 neurons. The amplitude of sI_{AHP} in methylsulphate solution is larger than in gluconate based solution (Zhang *et al.*, 1994).

Chapter 3: Inhibition of neuronal I_{AHP} by the SK channel modulator NS8593

3.1.0: Introduction

The aim of this study is to investigate whether NS8593 is an effective modulator of neuronal SK channels. In this section, the literature on the involvement of SK channels in mediating I_{AHP} in CA1 pyramidal neurons will be reviewed. The present model of SK channel gating is presented and the Ca^{++} dependent negative modulator NS8593 is introduced.

3.1.1: The activation of SK channels underlies I_{AHP}

In 1996 the genes encoding small conductance Ca^{2+}-activated K^+ (SK) channels were cloned and expressed in Xenopus oocytes (Kohler *et al.*). The SK channel genes were found to encode channels whose single channel activity increased with increasing Ca^{++} concentration, but did not respond to voltage(Kohler *et al.*, 1996) . SK channels were half maximally activated by intracellular Ca^{++} concentrations of between 300-700 nM (Kohler *et al.*, 1996; Hirschberg *et al.*, 1998).

Recombinant SK channels were found to be sensitive to the bee-venom toxin apamin and the plant alkaloid d-tubocurarine to varying degrees (Kohler *et al.*, 1996). Four SK channel subunits have been cloned: SK1, SK2, SK3 and SK4. SK4 (also known as IK) is only expressed in the periphery (reviewed by Stocker, 2004) and so will not be discussed further. SK channel subunits can be distinguished on the basis of their apamin sensitivity so that SK1<SK3<SK2 with SK2 being the most sensitive (reviewed by Stocker *et al.*, 2004). Initially it was thought that SK2 and SK3 were the only apamin sensitive SK channel subunits (Kohler *et al.*, 1996; Ishii *et al.*, 1997). However it has later been demonstrated that SK1 is also blocked by apamin in expression systems (Shah & Haylett, 2000; Strobaek *et al.*, 2000). I_{AHP} currents that are inhibited to various extents by apamin and d-tubocurarine have been characterised in a number of central and peripheral neurons (for review see Stocker *et al.*, 2004), including CA1 pyramidal cells (Stocker *et al.*, 1999). Thus the pharmacological profile of the recombinant SK channels seemed to be similar to that of neuronal I_{AHP}. A further line of evidence supporting a role for SK channels in mediating neuronal I_{AHP} is the correlation between the regional distribution of SK channel mRNA and protein

3.1.0: Introduction

The aim of this study is to investigate whether NS8593 is an effective modulator of neuronal SK channels. In this section, the literature on the involvement of SK channels in mediating I_{AHP} in CA1 pyramidal neurons will be reviewed. The present model of SK channel gating is presented and the Ca^{++} dependent negative modulator NS8593 is introduced.

3.1.1: The activation of SK channels underlies I_{AHP}

In 1996 the genes encoding small conductance Ca^{2+}-activated K^+ (SK) channels were cloned and expressed in Xenopus oocytes (Kohler *et al.*). The SK channel genes were found to encode channels whose single channel activity increased with increasing Ca^{++} concentration, but did not respond to voltage(Kohler *et al.*, 1996) . SK channels were half maximally activated by intracellular Ca^{++} concentrations of between 300-700 nM (Kohler *et al.*, 1996; Hirschberg *et al.*, 1998).

Recombinant SK channels were found to be sensitive to the bee-venom toxin apamin and the plant alkaloid d-tubocurarine to varying degrees (Kohler *et al.*, 1996). Four SK channel subunits have been cloned: SK1, SK2, SK3 and SK4. SK4 (also known as IK) is only expressed in the periphery (reviewed by Stocker, 2004) and so will not be discussed further. SK channel subunits can be distinguished on the basis of their apamin sensitivity so that SK1<SK3<SK2 with SK2 being the most sensitive (reviewed by Stocker *et al.*, 2004). Initially it was thought that SK2 and SK3 were the only apamin sensitive SK channel subunits (Kohler *et al.*, 1996; Ishii *et al.*, 1997). However it has later been demonstrated that SK1 is also blocked by apamin in expression systems (Shah & Haylett, 2000; Strobaek *et al.*, 2000). I_{AHP} currents that are inhibited to various extents by apamin and d-tubocurarine have been characterised in a number of central and peripheral neurons (for review see Stocker *et al.*, 2004), including CA1 pyramidal cells (Stocker *et al.*, 1999). Thus the pharmacological profile of the recombinant SK channels seemed to be similar to that of neuronal I_{AHP}. A further line of evidence supporting a role for SK channels in mediating neuronal I_{AHP} is the correlation between the regional distribution of SK channel mRNA and protein

and the expression of a current corresponding to I_{AHP} (Stocker & Pedarzani, 2000; Sailer *et al.*, 2002).

In CA1 pyramidal cells, SK1 and SK2 subunit mRNA and protein are expressed (Stocker & Pedarzani, 2000; Sailer *et al.*, 2002). This indicates that either the SK1 or SK2 subunit mediates I_{AHP} in CA1 neurons. The apamin sensitivity reported for I_{AHP} in CA1 pyramidal cells has an IC_{50} ~ 480 pM (Stocker *et al.*, 1999). This is lower than the apamin sensitivity of SK2 homomultimers expressed in mammalian cell lines, which have an IC_{50} ~ 83 pM (Strobaek *et al.*, 2000) and higher than the apamin sensitivity of SK1 homomultimers expressed in mammalian cell lines which have an IC_{50} ~ 3.3 nM (Strobaek *et al.*, 2000). Two explanations have been suggested to account for the difference in sensitivity between neuronal I_{AHP} in the CA1 region of the hippocampus, and recombinant SK channels expressed in mammalian cell lines. Firstly, it is possible that problems of toxin diffusion and penetration in brain slices might reduce the effective concentration of apamin at the channels. The second explanation suggests the possibility that SK1 and SK2 form heteromultimeric channels and this may lead to the reduced apamin sensitivity of I_{AHP} in CA1 pyramidal cells (Stocker *et al.*, 1999; Stocker & Pedarzani, 2000). The formation of heteromultimeric SK1/SK2 channels in heterologous expression systems has been demonstrated and it was shown that these channels display an intermediate apamin sensitivity compared with the homomultimeric SK1 and SK2 channels (Benton *et al.*, 2003). However to date, expression of heteromultimeric SK1, SK2 channels has not been demonstrated in native systems. Lastly it has been reported that the apamin sensitive I_{AHP} in CA1 pyramidal neurons is abolished in mice lacking the SK2 subunit, but present in SK1 knock out mice (Bond *et al.*, 2004). Therefore it seems likely that I_{AHP} in CA1 neurons is mainly mediated by SK2 channel subunits.

3.1.2: The model of SK channel gating

SK channels are tetrameric with a membrane topology for each subunit similar to that of *Shaker*-like voltage gated K^+ channels with six putative transmembrane segments (S1-S6) and a pore loop between S5 and S6 (Kohler *et al.*, 1996; Stocker, 2004). The current model for SK channel gating occurs in three steps. In

the closed channel state i.e. in the absence of Ca^{++}, calmodulin is constitutively bound to each SK channel subunit by a calmodulin binding domain (CamBD) located at the intracellular C terminal region of the SK channel subunit (Xia *et al.*, 1998; Keen *et al.*, 1999; Schumacher *et al.*, 2001; Schumacher *et al.*, 2004).

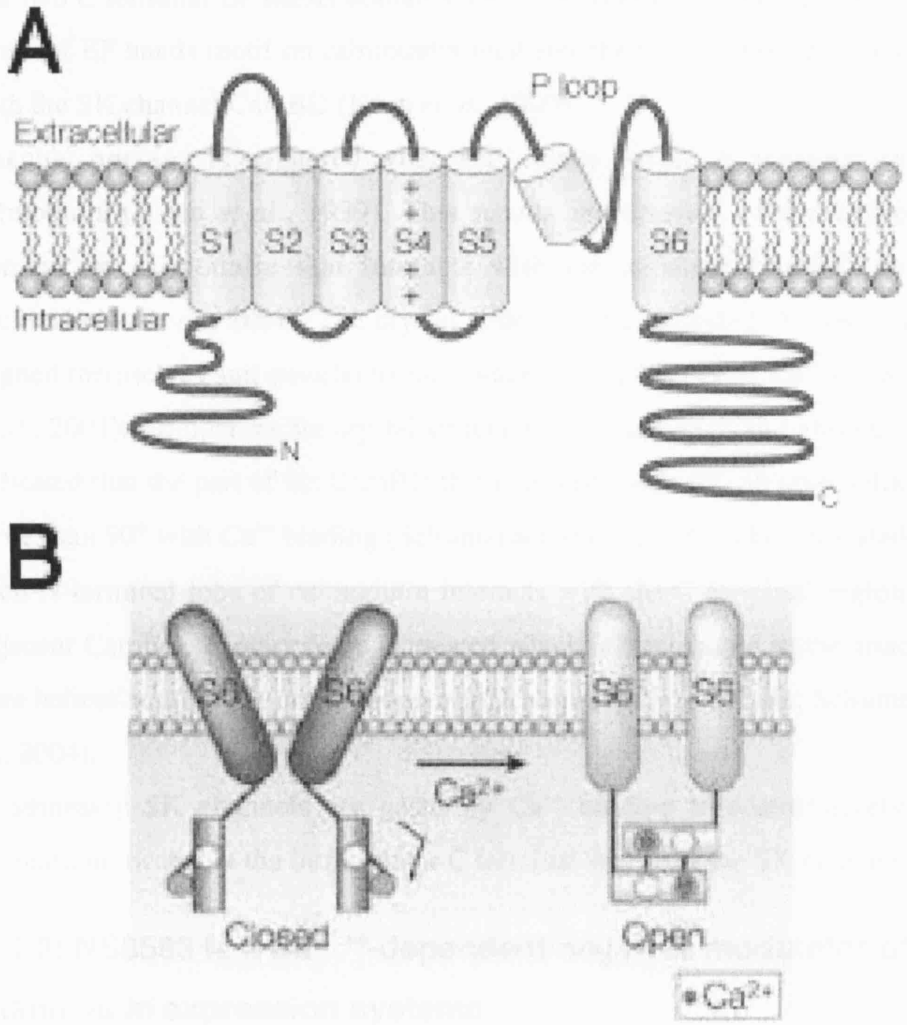

Figure 9: Membrane topology of SK channels

A, Schematic illustrating the membrane topology of SK channels (adapted from Flynn *et al.*, 2001).

B, Diagramatic representation of the Ca^{++} gating of SK channels. Ca^{++} binding to the constitutively bound Calmodulin molecules on the SK channel results in a conformational change and channel opening. (Adapted from Stocker, 2004.)

Initial experiments indicated that Ca^{++} gating of the SK channel is through Ca^{++} binding to the constitutively bound calmodulin. It was hypothesised that Ca^{++} binding results in conformational changes in the calmodulin molecule translating to the SK channel subunits (Xia *et al.*, 1998). Calmodulin contains two N terminal and two C terminal EF hands domains, i.e. it has four Ca^{++} binding motifs. The C terminal EF hands motif on calmodulin mediates the Ca^{++} independent interaction with the SK channel CamBD (Keen *et al.*, 1999).

Channel opening is triggered when Ca^{++} binds to the N terminal lobes on calmodulin (Keen *et al.*, 1999). This results in exposure of the hydrophobic domain on calmodulin that interacts with the adjacent CamBD monomer (Schumacher *et al.*, 2001). The crystal structure had indicated that two CamBDs aligned themselves anti-parallel to each other in the presence of Ca^{++} (Schumacher *et al.*, 2001). Comparing the crystal structure in the presence and absence of Ca^{++} indicated that the part of the CamBD that is linked to the SK S6 pore helix rotates more than 90° with Ca^{++} binding (Schumacher *et al.*, 2004). This indicated that as each N terminal lobe of calmodulin interacts with the C terminal region on the adjacent CamBD, a rotary force is created which is transmitted to the attached S6 pore helices resulting in channel opening(Schumacher *et al.*, 2001; Schumacher *et al.*, 2004).

In summary SK channels are gated by Ca^{++} binding to constitutively bound calmodulin located at the intracellular C terminal region of the SK channel.

3.1.3: NS8593 is a Ca^{++}-dependent negative modulator of SK channels in expression systems

NS8593 is a small, uncharged lipophilic compound that shows no structural or physiochemical resemblance to any known SK channel inhibitor. The NS8593-mediated inhibition of SK currents in expression systems decreased with increasing Ca^{++} concentration, indicating that the affinity of NS8593 for SK channels is Ca^{++} dependent and its inhibitory action takes place by reducing their apparent sensitivity to Ca^{++} (Strobaek *et al.*, 2006). By contrast, 1-EBIO (Pedarzani *et al.*, 2001) and NS309 (Pedarzani *et al.*, 2005) have been identified as SK channel enhancers or positive gating modulators that act by increasing the

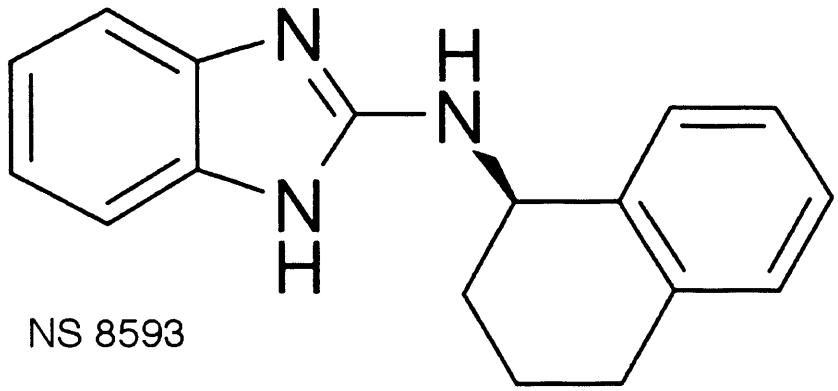

Figure 10: Chemical structure of NS 8593 (Figure reproduced fromStrobaek *et al.*, 2006)

apparent calcium sensitivity of SK channels. These compounds are especially interesting because they appear to modulate the Ca^{++} sensitivity of the SK channel from the intracellular side of the membrane. Additionally, it has been proposed that the positive modulators, 1-EBIO and NS309, may share their binding site with NS8593 because high concentrations of NS309 can prevent NS8593 mediated inhibition of SK channels (Strobaek *et al.*, 2006). However, a common binding site between the positive modulators and NS8593 is questionable because of the different selectivity towards SK4 shown by the different compounds. NS8593 is selective for the SK1/SK2/SK3 channel subunits over SK4 (Strobaek *et al.*, 2006), whilst 1-EBIO and NS309 are more potent at SK4 (Strobaek *et al.*, 2004). Although a shared physical binding site between NS8593 and NS309/1-EBIO is uncertain, there is evidence that they may share a common mechanism of action. The C terminus of the SK channel is the locus for the Ca^{++} gating machinery (Keen *et al.*, 1999) and has been shown to be important for the mechanism of action of 1-EBIO (Pedarzani *et al.*, 2001). This indicates that the mechanism of action of 1-EBIO may centre on the Ca^{++} gating mechanism of SK channels.

An intracellular locus for the mechanism of action of NS8593 contrasts with the mechanism of action of apamin. Apamin acts extra-cellularly by a mechanism involving pore blockade (Strong, 1990; Ishii *et al.*, 1997). Recently, it has been

shown that the action of apamin involves its binding to a region outside the pore, in the extracellular loop between the S3 and S4 segments (Nolting *et al.*, 2007) in addition to its binding to residues in the pore region (Ishii *et al.*, 1997). Consistent with apamin displaying a contrasting mechanism of action to NS8593, apamin binding studies showed that NS8593 does not displace apamin binding either in HEK293 cells expressing recombinant SK3 channels, or in striatal membranes (Strobaek *et al.*, 2006).

3.2: Aims and objectives

The primary aim of this part of the study was to investigate whether NS8593 was an effective inhibitor of neuronal SK channels. To this aim we conducted whole cell patch clamp recordings of CA1 pyramidal cells in mouse hippocampal slices and tested the effect of NS8593 on the SK-mediated current I_{AHP}.

3.3.0: Results

3.3.1: The effect of NS8593 on the SK-mediated I_{AHP}

To study the effect of NS8593 on neuronal I_{AHP}, whole cell voltage clamp experiments were obtained from CA1 pyramidal cells in acute mouse hippocampal slices. Experiments were conducted in the presence of tetrodotoxin (TTX, 0.5 μM) and tetraethylammonium (TEA, 1 mM) to block voltage gated sodium channels and calcium and voltage dependent potassium (BK) channels, respectively. To study the I_{AHP} in isolation from the sI_{AHP}, 8CPT-cAMP (50 μM) was included in the pipette solution. 8CPT-cAMP is a membrane permeable, non-hydrolysable cAMP analogue. Under these conditions, 100 ms-long depolarising pulses yielded tail currents that were partially sensitive to NS8593. In this section, statistical significance was assessed using one-sample t tests and unpaired t tests. Application of 10 μM NS8593 significantly suppressed the tail current (% tail current inhibition amplitude: 55.3±4.8 %; n=6; $p<0.0001$; % charge transfer: 67.8±4.4 %; n=6; $p<0.0001$, Fig. 11B, C, E). Subsequent application of the SK channel blocker d-tubocurarine (50 μM) on the NS8593-insensitive current had no further significant effect (% inhibition of tail current amplitude by d-tubocurarine: 16.2±8.6 %; n=6; $p>0.1$; % inhibition of tail current charge transfer by d-tubocurarine: 28.1±14.2 %; n=6; $p>0.1$, Fig. 11B), indicating that 10 μM NS8593 had almost completely suppressed the SK mediated current I_{AHP}. The time of effect of NS8593 was defined as the time to 63 % of the maximal effect of the drug. NS8593 (10 μM) had a time of effect on I_{AHP} of 24.4±7.1 min (n=6).

Control currents were recorded in DMSO at the same final concentration used for the application of 10 μM NS8593 (0.1%). DMSO had no significant effect on the amplitude and time course of the recorded currents (amplitude: 100.0±6.0%; n=12; $p>0.9$; charge transfer: 93.6±6.1%; n=12; $p>0.3$). Fig. 11C shows the effect of DMSO (0.1%) on the tail current amplitude in time-matched controls.

In order to compare the effect of NS8593 (10 μM) with the effect of the known SK channel blocker apamin, further experiments were conducted in which apamin (50 nM) was directly applied to the tail current. Application of apamin (50 nM)

significantly reduced the tail current (amplitude of tail current left: 57.1±12.1%: n=7: $p<0.05$, charge transfer of I_{AHP} left: 44.9±10.0 %: n=7: $p<0.01$, Fig. 11D). There was no significant difference between the effect of apamin (50 nM) and NS8593 (10 μM) on I_{AHP} amplitude or charge transfer ($p>0.1$). This indicates that the effect of NS8593 (10 μM) is comparable with the effect of apamin (50 nM) in mouse hippocampal pyramidal neurons and that the NS8593 sensitive component of the tail current corresponds to I_{AHP}.

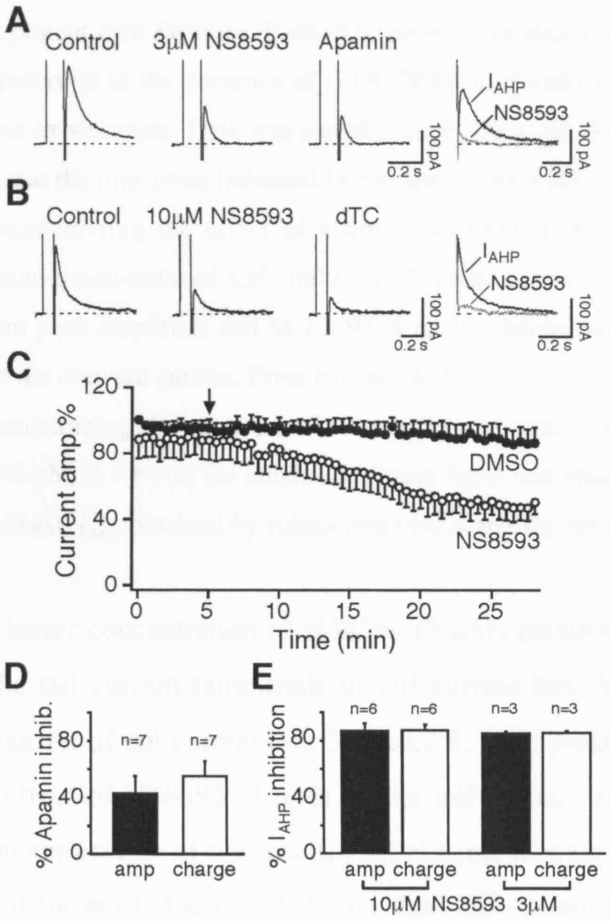

Figure 11: Effect of NS8593 on the SK-mediated I_{AHP} in CA1 pyramidal neurons

A, In mouse CA1 pyramidal neurons, 100 ms-long depolarizing pulses eliciting a Ca^{2+} current were followed by a tail current that was partly inhibited by 3 μM NS8593. The remaining current was slightly, but significantly further reduced by the SK channel blocker apamin (50 nM). Right panel: the SK-mediated component of the tail current, I_{AHP}, was obtained by subtracting the current trace obtained in the presence of apamin from the control and NS8593 traces. NS8593 (3 μM) strongly reduced the apamin sensitive I_{AHP}.

B, 10 μM NS8593 reduced the tail current following a depolarization-induced Ca^{2+} influx in CA1 neurons. The SK channel blocker d-tubocurarine (dTC, 50 μM) did not significantly affect the residual current left after the application of 10 μM NS8593. Right panel: I_{AHP} was obtained by subtracting the current trace obtained in the presence of dTC from the control and NS8593 traces (see also ***A***). NS8593 (10 μM) largely suppressed the dTC-sensitive I_{AHP}.

C, Time course of the effect of 10 μM NS8593 on the normalized amplitude of the total tail current (open circles), comprising the SK-mediated I_{AHP} and a Ca^{2+}-independent, TEA-sensitive component (see Results). Each data point is the mean of six experiments. Control data was recorded in the presence of 0.1% DMSO (closed circles). Data points are the mean of four experiments. Data was sampled every 30 s. 10 μM NS8593 or 0.1% DMSO were applied at the time point indicated by the arrow. Error bars represent SEM.

D, Bar diagram summarizing the effect of apamin (50 nM) on the total tail current following the depolarization-induced Ca^{2+} influx. In 7 cells, apamin suppressed 42.9 ± 12.1% of the current peak amplitude and 55.1 ± 9.9% of the charge transfer, measured as the area underneath the outward current. Error bars are SEM.

E, Bar diagram summarizing the maximal effect of different concentrations of NS8593 (3 μM, n = 3 and 10 μM, n = 6) on the amplitude (black bars) and charge transfer (white bars) of the SK-mediated I_{AHP} obtained by subtraction (see ***A*** and ***B***). Error bars are SEM.

Application of a lower concentration of NS8593 (3 μM) resulted in a significant suppression of the tail current (amplitude of tail current left: 50.1±6.0%; n=3; $p<0.02$, charge transfer of tail current left: 32.2±9.2%; n=3; $p<0.02$, Fig. 11A, E). The time of the effect of NS8593 (3 μM) on the tail current was 32.8±8.3 min (n=3). Subsequent application of the specific SK channel blocker apamin (50 nM) resulted in a slight further reduction of the residual tail current (% inhibition by apamin on the amplitude of tail current: 18.4±2.9%; n=3; $p<0.03$; % inhibition by apamin on the charge transfer of tail current: 44.8±15.8%; n=3; $p>0.1$, Fig. 11A). The further effect of apamin on the residual tail current indicates that 3 μM NS8593 did not completely inhibit the SK-mediated current and provides an indication of the concentration dependence of the drug action on neuronal SK channels.

3.3.2: I_M contributes to the tail current in mouse

A residual current remained after suppression of I_{AHP} by NS8593 (3-10 μM) and specific SK channel blockers (d-tubocurarine, apamin) (Fig. 11A and B). In order to investigate the calcium dependence of the residual current, ACSF in which magnesium was substituted for calcium (calcium free ACSF) was applied to the residual current after application of apamin (50 nM). On application of calcium free ACSF to the residual current there was a significant increase in the residual current (% change of residual current amplitude in calcium free ACSF: 145.7±13.7%; n=4; $p<0.05$: % change of residual current charge transfer: 168.9±34.4%; n=4; $p>0.1$, data not shown) indicating the residual current was not calcium dependent.

To investigate whether the residual current left after SK channels inhibition was mediated by voltage dependent K^+ channels, 5 mM TEA was applied after application of NS8593 and specific SK channel blockers. 5 mM TEA further suppressed the residual current (% inhibition of residual current amplitude by 5 mM TEA: 74.0±9.7%; n=7; $p<0.01$; % inhibition of residual current charge transfer by 5 mM TEA: 96.6±3.4%; n=7; $p<0.0001$). This indicates that the residual current is mediated by a voltage gated K^+ channel. A possible candidate for the voltage dependent K^+ current is I_M. I_M is a non inactivating voltage dependent K^+ current that is mediated by KCNQ channels. The KCNQ 2/3 hetermultimer, whose TEA sensitivity closesly matches I_M, has an IC_{50} for TEA of 3.8 mM (Hadley *et al.*, 2000). This suggests that the TEA sensitive residual current may be in part I_M.

To specifically test whether the residual current was I_M, and therefore indicate whether the NS8593-mediated inhibition of I_{AHP} was complete, experiments were conducted with the specific Kv7/KCNQ/M channel blocker XE991. Fig. 12 shows the effect of NS8593 in the presence of XE991 (5 μM) (Fig. 12A, B and C). Application of 10 μM NS8593 to the XE991 insensitive tail current component, i.e. the current left after application of 5 μM XE991, resulted in 100 % inhibition of I_{AHP} amplitude and 98.4±1.6% charge transfer inhibition (n=3). Administration of 5 μM XE991 to the apamin insensitive residual current, i.e. the current left after application of 50 nM apamin, resulted in 90.5±5.9 % tail current amplitude

suppression (% tail current charge inhibition: 80.5±7.6 %, n=4, p<0.005). Taken together, these results indicate that 10 μM NS8593 is sufficient to suppress I_{AHP} and the residual apamin/NS8593 insensitive current is I_M.

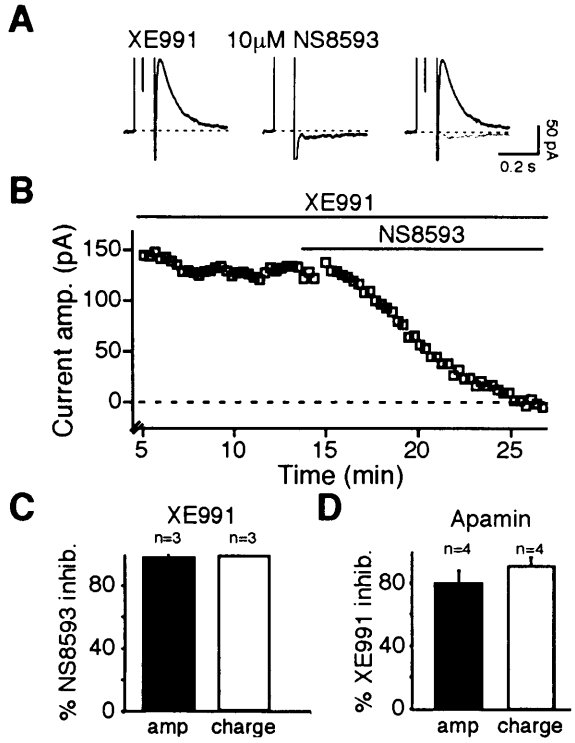

Figure 12: Suppressing M current reveals the NS8593-mediated effect on the SK-mediated I_{AHP} in isolation in CA1 pyramidal neurons

A, 100 ms-long depolarising pulses recorded in the presence of 5 μM XE991, 1 mM TEA and 0.5 μM TTX yielded a tail current that was suppressed by 10 μM NS8593.

B, Time course of the effect of 10 μM NS8593 in the presence of XE991 in a representative cell. The XE991 resistant tail current was completely inhibited by NS8593.

C, Bar diagram summarising the significant effect of 10 μM NS8593 in the presence of XE991. In three cells, 10 μM NS8593 suppressed the XE991 resistant tail current by 100 % and charge transfer by 98.4±1.6 %. Bars depict the mean, error bars represent SEM.

D, Bar diagram illustrating the effect of XE991 on the apamin resistant tail current. Apamin was applied at 50 nM. Subsequent application of 5 μM XE991 resulted in 90.5±5.9 % tail current amplitude suppression and 80.5±7.6 % charge transfer inhibition (n=4).

3.4.0: Discussion

The aim of this set of experiments was to investigate whether NS8593 is an effective inhibitor of neuronal SK channels and of the corresponding current I_{AHP}. Application of 3 μM and 10 μM NS8393 resulted in suppression of the tail current corresponding to I_{AHP} in mouse CA1 pyramidal neurons. In addition, this study showed that, after application of SK inhibitors (apamin, d-tubocurarine, NS8593), there was some residual outward tail current remaining. This residual tail current was shown to be M current because of its inhibition by the KCNQ channel blocker XE991. This study furthers that of Strobaek et al (2006), which described NS8593 as a modulator of recombinant SK channels by demonstrating the effectiveness of NS8593 in slices. In this section, the possible uses of NS8593 compared with apamin as a therapeutic cognitive enhancer and a tool for investigating neuronal firing patterns is explored.

3.4.1: Modulating SK channels to enhance cognition

An emerging role of SK channels in CA1 pyramidal neurons is in their modulation of synaptic function. Transfection of dissociated cultures of hippocampal pyramidal neurons with GFP-tagged SK2 has shown that SK channels are positioned in the dendritic spines and within clusters in the dendritic shafts and soma (Ngo-Anh *et al.*, 2005). This places SK channels in the ideal place to modulate synaptic function.

The role of SK channels in regulating the induction of synaptic plasticity in CA1 pyramidal cells has been demonstrated by comparing long term potentiation (LTP) induction paradigms in the presence and absence of apamin. Using a single stimulus frequency it was shown that the magnitude of LTP induced in the CA1 region was increased by the extracellular application of apamin (Behnisch & Reymann, 1998; Norris *et al.*, 1998). Comparison of the threshold for induction of synaptic modification (i.e. induction of LTP/long term depression) in the presence and absence of apamin revealed that apamin shifted the threshold for induction of LTP/LTD to lower synaptic stimulation frequencies in an NMDAR dependent manner (Behnisch & Reymann, 1998; Norris *et al.*, 1998; Stackman *et al.*, 2002).

The locus of this effect was postsynaptic because apamin had no effect on paired pulse facilitation (Stackman *et al.*, 2002). The mechanism by which SK channels could regulate hippocampal synaptic plasticity was proposed as a negative feedback loop between the voltage changes mediated by the currents produced by NMDARs and SK channels. In their model, Ngo-Anh et al (2005) proposed that Ca^{++} influx through the NMDARs mediating part of the EPSP would activate SK channels. The ensuing hyperpolarisation would facilitate the magnesium block of the NMDARs and thus limit their contribution to the EPSP and prevent synaptic plasticity in CA1 pyramidal neurons (Ngo-Anh *et al.*, 2005). Thus SK channels play important roles in the regulation of synaptic plasticity in CA1 pyramidal neurons. Consistent with the facilitatory effect of apamin on synaptic plasticity, and the proposed role of synaptic plasticity in learning and memory (Bliss & Collingridge, 1993), apamin has been shown to increase the cognitive performance of mice in the Morris water maze, the object recognition test (Stackman *et al.*, 2002), and the Y maze (Deschaux & Bizot, 2005). Therefore, SK channel inhibitors, such as apamin, could have a potential therapeutic use as a cognitive enhancer.

However, apamin is a very toxic compound with a narrow therapeutic window (van der Staay *et al.*, 1999), making it of limited clinical use. In addition, when the effects of apamin on behaviour are tested, the narrow therapeutic window means that the adverse effects of apamin e.g. tremor and clonic convulsions, can overlap with the effect of interest (van der Staay *et al.*, 1999). Therefore, the *in vivo* investigation of the functional role of SK channels is complicated by the toxicity of apamin. It has been suggested that the toxicity of apamin is due to its mechanism of action as a pore blocker (Strobaek *et al.*, 2006) This is because a pore blocker will bind to its target channel indiscriminately of the state of the neuron leading to uncontrolled neuronal firing i.e. a neuron's activity state will not regulate the binding of a pore blocker to the channel. Conversely, NS8593 has been shown to bind to a site on SK channels other than the apamin binding site (Strobaek *et al.*, 2006). Although NS8593 binds to all three SK channel subtypes (Strobaek *et al.*, 2006), the inhibitory action of NS8593 has been shown to be calcium dependent and this might confer reduced toxicity. The SK channel

inhibition mediated by NS8593 decreases with increasing intracellular Ca^{++} concentration, additionally closed SK channel inhibition can be reversed by high Ca^{++} (Strobaek *et al.*, 2006). This provides a mechanism for preventing uncontrolled neuronal firing. The increased intracellular Ca^{++} concentration resulting from increased neuronal firing will serve to feedback and relieve the SK channel inhibition by NS8593. The Ca^{++} activated SK channels will reopen and the ensuing K^+ current will hyperpolarise the membrane thus terminating neuronal firing. Therefore the mechanism of action of NS8593 may render it a less toxic compound than apamin. Given that inhibition of SK channels facilitates the induction of LTP and improves cognitive performance, NS8593 may prove a useful compound with which to study the functional role of SK channels *in vivo*.

3.4.2: Avenues for further study: NS8593 and neuronal firing patterns

The Ca^{++} dependency of inhibitory gating modulation of SK channels by NS8593 could be effective in subtly changing firing patterns. If it is assumed that (i) the total Ca^{++} influx per action potential remains approximately constant, as has been indicated by Ca^{++} imaging studies (Schiller *et al.*, 1995; Helmchen *et al.*, 1996), and (ii) that Ca^{++} extrusion processes are slow so that the intraceullar Ca^{++} concentration is increased proportionately to the Ca^{++} influx (Traub *et al.*, 1991), then it would be expected that NS8593 is likely to be more effective in inhibiting SK channels in neurons with a low firing frequency, where the intracellular Ca^{++} concentration remains lower than in neurons with a high firing frequency. Further experiments are needed in order to characterise the effects of NS8593 on the firing properties of central neurons. This could be interesting both in the hippocampus, where SK channels contribute to setting the early firing frequency (Stocker *et al.*, 1999), and in midbrain dopaminergic neurons, where SK channels have been shown to switch firing patterns from a pace-making pattern, where neurons fire with rhythmical precision, to burst mode in which a neuron fires an irregular, phasic discharge which consists of two or more action potentials (Ji & Shepard, 2006).

Chapter 4: Modulation of sI_{AHP} by Pituitary Adenylyl Cyclase Activating Polypeptide (PACAP)

4.1.0: Introduction

The hypothalamic hormones are synthesised by neurones in the hypothalamus and include, among others, corticotrophin releasing factor (CRF), vasoactive intestinal peptide (VIP) and pituitary adenylyl cyclase activating peptide (PACAP) (Vaudry *et al.*, 2000). CRF and VIP have been shown to suppress the sAHP in hippocampal neurons and consequently decrease the spike frequency adaptation (Aldenhoff *et al.*, 1983; Haas & Gahwiler, 1992). The CRF- and VIP-mediated effects on sI_{AHP} were inhibited by PKA inhibitors in CA1 pyramidal neurons (Haug & Storm, 2000). This indicated that these neuropeptides modulate sI_{AHP} by a PKA-dependent mechanism. PACAP is a member of the VIP-glucagon-GRF-secretin super-family of structurally related proteins and shows 68 % homology to VIP (Campbell & Scanes, 1992). PACAP is physiologically available in two isoforms comprising of 38 and 27 amino acids respectively (Kimura *et al.*, 1990). The primary aim of this study was to investigate whether PACAP modulates the Ca^{++} activated K^+ current sI_{AHP} in CA1 pyramidal cells.

4.1.1: PACAP receptors and their expression in the hippocampus

PACAP receptors fall into two categories, depending on whether or not they are activated by VIP. Type 1 PACAP receptors (PAC-1-R) exhibit a high selectivity for PACAP and are coupled to both adenylyl cyclase and phospholipase C (Spengler *et al.*, 1993). Type 2 PACAP receptors can be activated by PACAP and VIP and are solely coupled to AC (Ishihara *et al.*, 1992). They can be further subdivided into two subtypes that are distinguished through their different affinities for the neuropeptides: PACAP-38, PACAP-27 and VIP have equal potency at V-PAC2 receptors, whilst V-PAC1 receptors have a higher affinity for PACAP than for VIP (Vaudry *et al.*, 2000).

Schaffer collateral afferents from CA3 pyramidal cells synapse to CA1 pyramidal cells. Other synaptic inputs on CA1 pyramidal cells come from interneurons. Using immunocytochemistry and in situ hybridisation, it has been shown that the

CA3 pyramidal cells express PACAP, while the interneurons are free of PACAP gene expression in the hippocampus (Hannibal, 2002).

Hashimoto et al. (1996) used in situ hybridisation to demonstrate V-PAC1 and V-PAC2 receptor mRNA expression in CA1, CA2 and CA3 pyramidal cells. Additionally, using immunocytochemistry and in situ hybridization, it has been shown that PAC-1 receptors are localised on the hippocampal pyramidal cells (Shioda *et al.*, 1997). Thus PACAP is expressed in the CA3 pyramidal cells of the hippocampus that synapse onto CA1 pyramidal cells, which express PAC-1, V-PAC1 and V-PAC-2 receptors.

4.1.2: The effect of PACAP on neuronal excitability

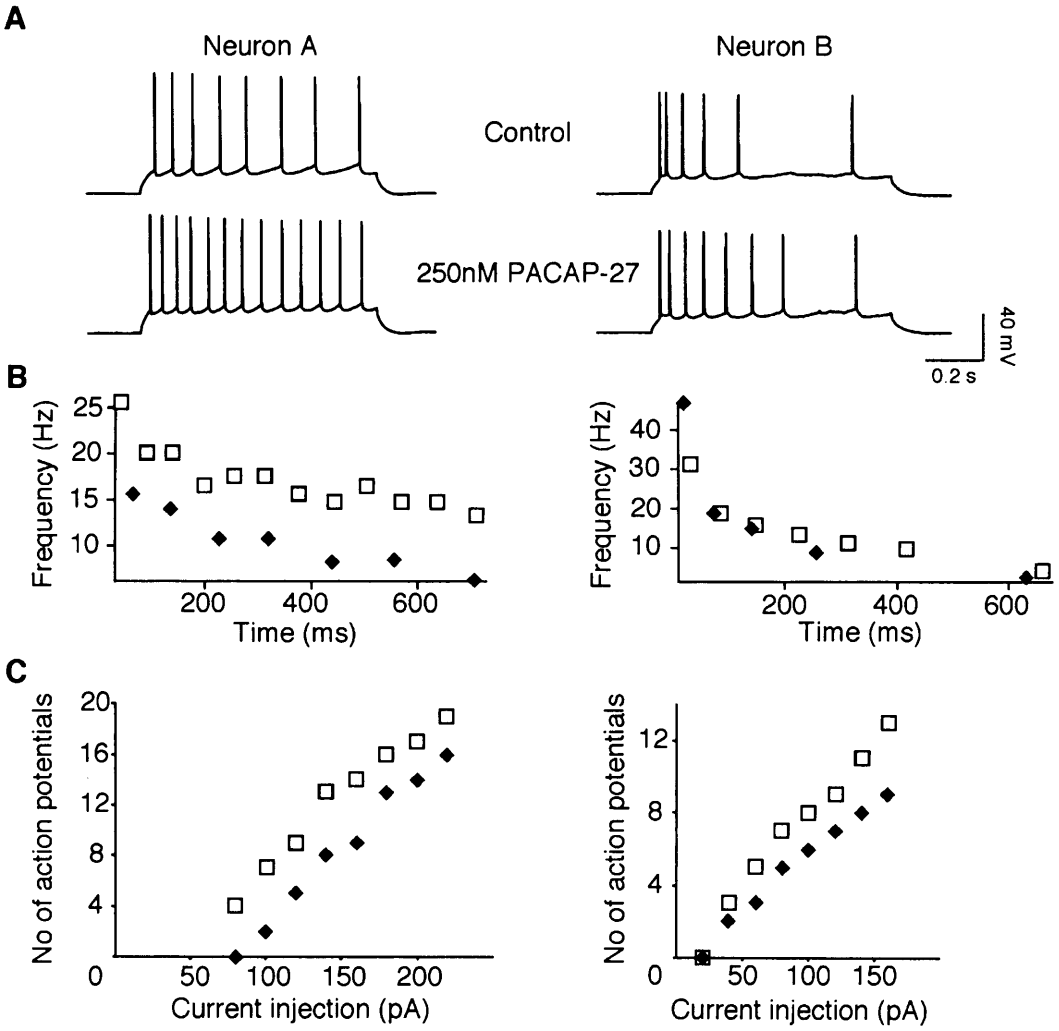

Figure 13: The effect of PACAP-27 on spike frequency adaptation and firing rate in CA1 pyramidal cells (reproduced from Taylor, 2003)

A, Voltage response of two different neurons to an 800 ms-long depolarising pulse before (control) and after application of 250 nM PACAP-27. The current injection was 140 pA for neuron A and 100 pA for neuron B.

B, Graphs depicting the frequency of action potential firing against time for the two neurons shown in *A*. Solid diamonds represent the neuronal response before PACAP-27 (control), whilst unfilled squares illustrate the response after PACAP-27 application. The reciprocal of the interspike interval between pairs of action potentials is equivalent to the action potential frequency. The time (ms) at which the frequency of action potentials has been determined is defined as the time (ms) of the second action potential of the pair used to calculate the interspike interval. Time = 0 ms at the point when the first action potential in response to the current injection is fired.

C, Graph illustrating the variation in the number of action potentials fired with increasing depolarising pulses. Unfilled squares indicate after PACAP-27 application. Solid diamonds indicate the control situation.

PACAP has been shown to affect neuronal excitability in different types of neurons, both through the modulation of identified ion channels, Ca^{++} currents and neuronal firing rate and membrane potential. PACAP application leads to an increase in intracellular Ca^{++} both through the mobilisation of Ca^{++} from intracellular stores (Tatsuno *et al.*, 1992) and the modulation of Ca^{++} influx in a store-independent manner (Tompkins *et al.*, 2006). In thalamocortical neurons, application of PACAP has been shown to lead to membrane potential depolarisation with an associated decrease in membrane resistance. This was shown to be due to a cAMP-mediated activation of I_h (Sun *et al.*, 2003). Application of PACAP-27 to individual cardiac ganglion neurons also resulted in membrane depolarisation (Braas *et al.*, 1998). In the same preparation, application of PACAP-27 resulted in an increase in the number of action potentials fired in response to a current pulse, indicating an increase in neuronal excitability (Braas *et al.*, 1998). In superior cervical ganglion sympathetic neurons, PACAP-27 application similarly results in a membrane depolarisation due to both (i) activation of a sodium conductance and (ii) inhibition of a potassium conductance (Beaudet *et al.*, 2000). In hippocampal CA1 pyramidal cells, application of PACAP-38 results in an increase in firing rate (Di Mauro *et al.*, 2003). We have

previously shown, in work presented for my undergraduate examination, that application of both PACAP-27 and PACAP-38 (250 nM) results in an increase in firing rate and a decrease in the spike frequency adaptation of CA1 pyramidal neurons(Taylor, 2003).

As already discussed, the sAHP is responsible for the late phase of spike frequency adaptation. The sAHP is mediated by the Ca^{++} activated K^{+} current, sI_{AHP}. Therefore we hypothesise that PACAP exerts its effect on neuronal excitability of CA1 pyramidal cells by suppressing sI_{AHP}.

4.2: Aims and Objectives

It had previously been reported that hypophysiotropic neurohormones such as VIP and CRF suppress the sAHP in hippocampal neurons and consequently decrease spike frequency adaptation (Aldenhoff *et al.*, 1983; Haas & Gahwiler, 1992). In 2000, Haug and Storm conducted a set of experiments to investigate the modulation of sI_{AHP} by neuropeptides. They reported that 400 nM VIP significantly reduced the amplitude of sI_{AHP} (Haug & Storm, 2000). Given the sequence homology between PACAP and VIP (Campbell & Scanes, 1992), and the knowledge that PACAP and VIP have identical K_d values and therefore similar affinity for VPAC-1 and VPAC-2 receptors (Lam *et al.*, 1990), it was decided to test whether PACAP affects sI_{AHP} in CA1 pyramidal neurones. The first aim of these experiments was to replicate and extend preliminary experiments already conducted in Dr Pedarzani's laboratory by Dr Michael Krause that had indicated that 500nM PACAP-38 suppressed sI_{AHP} (n=3). The further aim of this study was to elucidate the signal transduction cascade that underlies the PACAP mediated effect in CA1 pyramidal neurons.

4.3.0: Results

4.3.1: Effect of the neuropeptide PACAP on sI_{AHP} in CA1 pyramidal neurons

Several precautions were undertaken in the experimental procedure to increase the accuracy of the results. A run up phenomenon of unknown mechanism has been described for the sI_{AHP} (Borde *et al.*, 2000, see Fig. 6), therefore after addition of TTX and TEA, the amplitude of the sI_{AHP} was allowed to stabilise in order to establish a clear baseline, against which the effect of drugs could be measured. 25 μg/ml albumin was added to the ACSF for ten minutes prior to the application of PACAP to prevent binding of the peptide to any non specific protein binding sites, thereby increasing the bioavailability of the protein at the receptor. Again the amplitude of the sI_{AHP} was allowed to stabilise for at least five minutes after the application of albumin. PACAP was applied to the slice for ten minutes. During and following this application, the amplitude of the sI_{AHP} was monitored and recording was continued until stabilisation. Prior to albumin application the sI_{AHP} had a peak amplitude of 62.7±6.9 pA and charge of 150.1±16.8 pC (n=21). The ten-minute application of 25 μg/ml albumin did not significantly alter the peak amplitude or charge of sI_{AHP} compared with the sI_{AHP} prior to albumin application (peak sI_{AHP} amplitude after 10 minute application of albumin = 58.9±7.5 pA, n=21, p=0.39, Wilcoxon matched-pairs signed-ranks test; charge = 143.4±18.6, n=21, p=0.22, Wilcoxon matched-pairs signed-ranks test). To confirm that albumin did not affect the sI_{AHP}, further experiments were conducted in which the effect of albumin on sI_{AHP} was evaluated over a longer timescale. In general, the time of effect of PACAP was 17.6±5.6 minutes. In 6 cells, albumin did not significantly change the sI_{AHP} peak amplitude (% inhibition: 9.5±12.5 %, p=0.44, Wilcoxon matched-pairs signed-ranks test) or charge (% inhibition: 6.5±13.7 %, p>0.99, Wilcoxon matched-pairs signed-ranks test) in this timeframe.

Fig. 14A illustrates the effect of PACAP on sI_{AHP}. PACAP reduced both the peak amplitude and charge transfer of sI_{AHP}. The effect of PACAP-38 (500 nM) on the

sI_{AHP} took 17.6±5.6 minutes to develop (Fig. 14B). This is in contrast to the effect

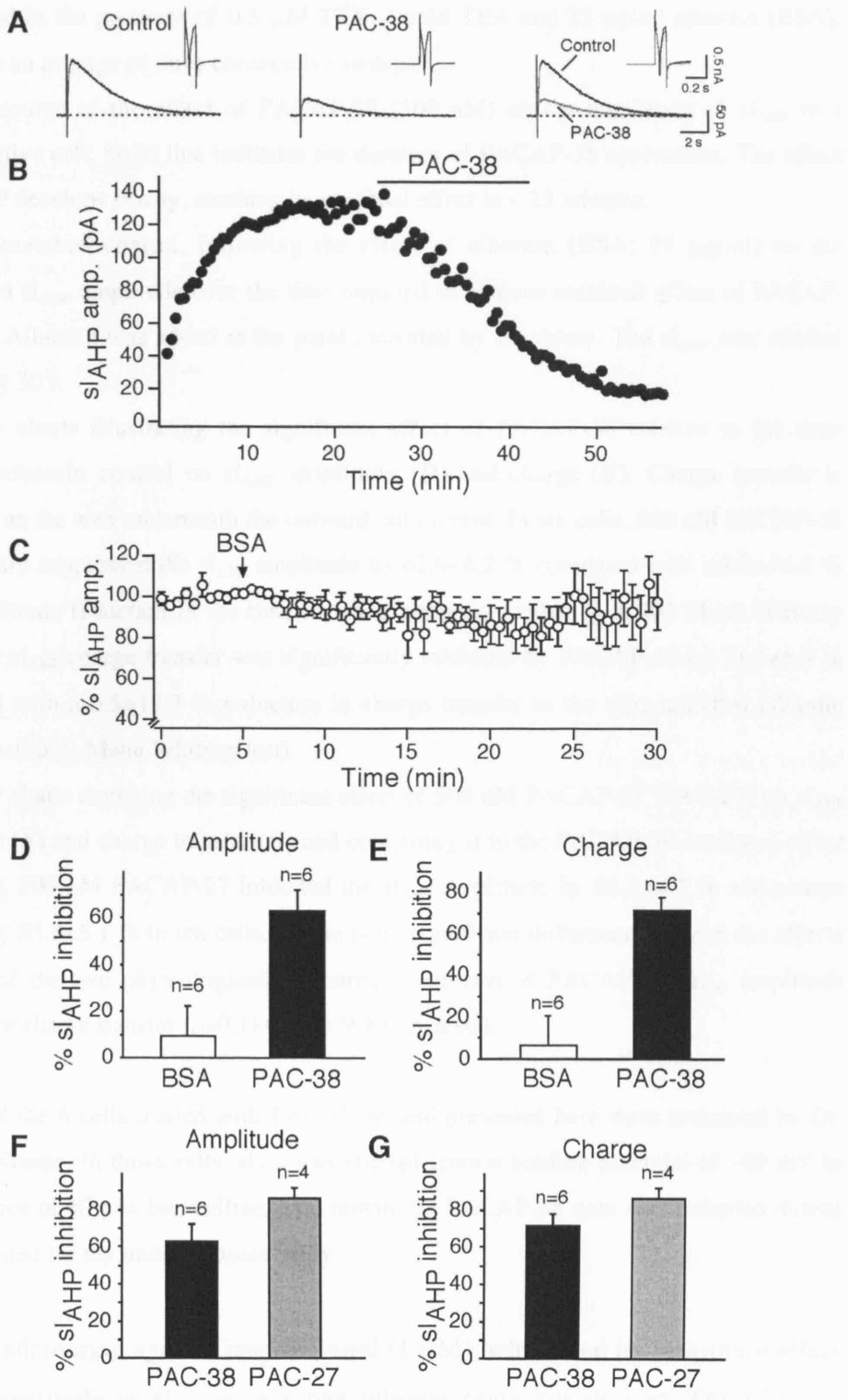

Figure 14: PACAP-38 suppresses sI_{AHP}

A, 100 ms-long depolarising pulses eliciting calcium influx were followed by a sI_{AHP} in rat CA1 pyramidal neurons. 500 nM PACAP-38 (PAC-38) suppressed sI_{AHP} with little

effect on the amplitude of the unclamped calcium spike (inset panels). The control trace is recorded in the presence of 0.5 μM TTX, 1 mM TEA and 25 μg/ml albumin (BSA). Traces are an average of three consecutive sweeps.

B, Time course of the effect of PACAP-38 (500 nM) on the amplitude of sI_{AHP} in a representative cell. Solid line indicates the duration of PACAP-38 application. The effect of PACAP develops slowly, reaching its maximal effect in ~ 25 minutes.

C, Time-matched control, following the effect of albumin (BSA; 25 μg/ml) on the normalised sI_{AHP} amplitude over the time required to achieve maximal effect of PACAP-38 (n=7). Albumin was added at the point indicated by the arrow. The sI_{AHP} was elicited once every 30 s.

D, E, Bar charts illustrating the significant effect of PACAP-38 relative to the time matched albumin control on sI_{AHP} amplitude (***D***) and charge (***E***). Charge transfer is measured as the area underneath the outward tail current. In six cells, 500 nM PACAP-38 significantly suppressed the sI_{AHP} amplitude by 62.9±8.2 % compared with a 9.5±12.5 % sI_{AHP} amplitude reduction in the time matched albumin control ($p<0.005$ Mann Whitney test). The sI_{AHP} charge transfer was significantly inhibited by PACAP-38 by 71.6±5.5 % compared with a 6.5±13.7 % reduction in charge transfer in the time matched albumin control ($p<0.005$, Mann Whitney test).

F, G, Bar charts depicting the significant effect of 500 nM PACAP-27 (PAC-27) on sI_{AHP} amplitude (***F***) and charge transfer (***G***) and comparing it to the PACAP-38-mediated effect (PAC-38). 500 nM PACAP-27 inhibited the sI_{AHP} amplitude by 86.1±4.7 % and charge transfer by 85.8±5.1 % in ten cells. There is no significant difference between the effects on sI_{AHP} of the two physiologically occurring isoforms of PACAP on sI_{AHP} amplitude ($p>0.06$) or charge transfer ($p>0.1$) (Mann Whitney tests).

Note: 3 of the 6 cells treated with PACAP-38 and presented here were measured by Dr. Michael Krause. In those cells, sI_{AHP} was elicited from a holding potential of –60 mV in the presence of 10 μM bicuculline. The remaining PACAP-38 data was recorded during and presented for my undergraduate study.

of the β-adrenergic agonist isoproterenol (1 μM), which had its maximum effect on the amplitude of sI_{AHP} within two minutes (data not shown). The effect is quantified in Fig. 14D and E. Over a time of ~25 minutes, 500 nM PACAP-38 suppressed the amplitude of the sI_{AHP} by 62.9±8.2% (n=6, $p<0.001$, one sample t

test) and the charge by 71.6±5.5 % (n=6, p<0.0001, one sample t test). The Ca^{++} spike showed no significant change over the course of the experiments, indicating that approximately the same amount of Ca^{++} entered the cells before and during PACAP application (Fig. 14A inset panels). There was no significant change in series resistance over the course of the experiments; therefore, the suppression of the sI_{AHP} cannot be attributed to this. In several cases the experiment was continued post PACAP application for at least ten minutes in order to determine the reversibility of the PACAP effct. The PACAP mediated inhibition of the sI_{AHP} did not reverse over this timescale.

4.3.2: Both PACAP isoforms suppress sI_{AHP}

PACAP occurs in nature in two isoforms comprising of 38 and 27 amino acids respectively (Kimura *et al.*, 1990). The 27 amino acid isoform (PACAP-27) is generated from the same PACAP precursor as the 38 amino acid isoform and is cleaved at an internal cleavage-amidation site eleven amino acids from the amino terminal (Chartrel *et al.*, 1991). The next stage in this study was to determine whether there was any difference in the action of the two naturally occurring isoforms of PACAP. Application of 500 nM PACAP-27 resulted in inhibition of sI_{AHP} with little effect on the calcium spike (Fig. 15A). The time to effect of PACAP-27 was 12.3±3.6 min (n=4) (Fig. 15B), similar to 17.6±5.6 mins (n=6) for PACAP-38 (p=0.76, Mann Whitney test). 500 nM PACAP-27 significantly reduced sI_{AHP} amplitude from 68.1±11.4 pA to 9.8±3.6 pA (86.1±4.7 % sI_{AHP} inhibition, n=4, p<0.01, paired t test) and charge from 169.8±23.4 pC to 24.7±9.7 pC (85.8±5.1 % sI_{AHP} inhibition, n=4, p<0.01, paired t test) (Fig. 15C). There was no significant difference revealed by Mann Whitney tests between the extent of the effect of the same concentration of PACAP-38 (n=6) and PACAP-27 (n=4) in CA1 pyramidal cells on sI_{AHP} amplitude (p=0.06) or charge (p=0.11) (Fig. 14F and G). Due to the similarity in the effect of the two PACAP variants, it was decided to conduct further experiments with PACAP-27.

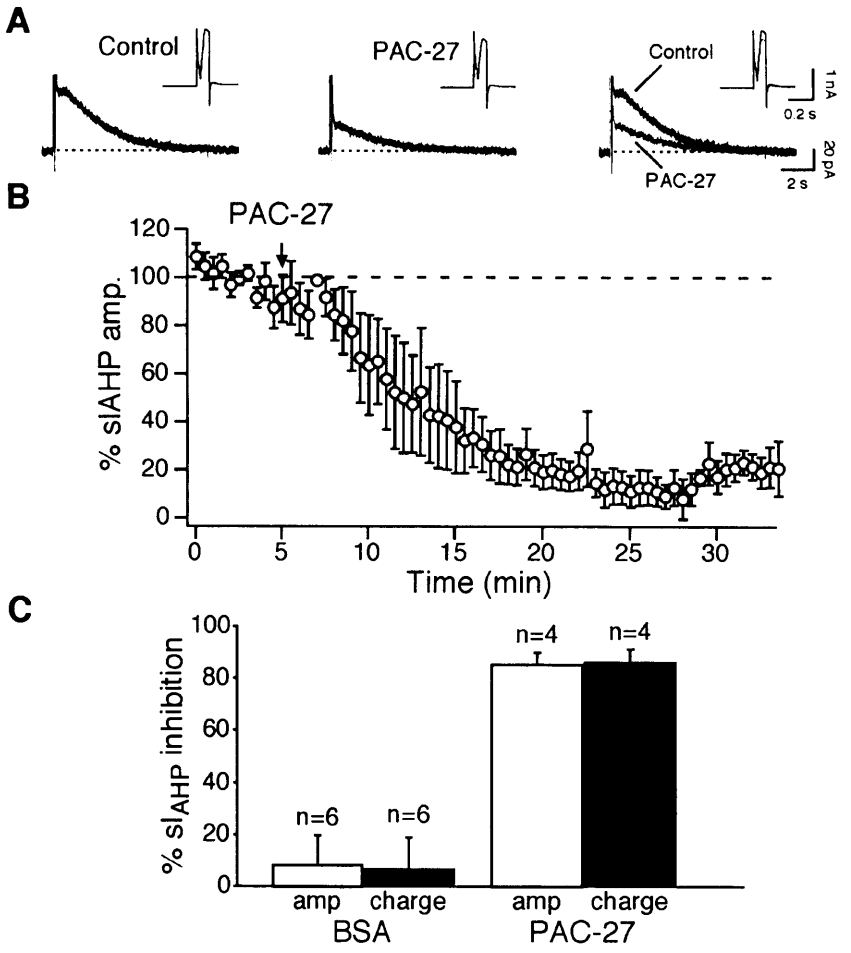

Figure 15: PACAP-27- mediated effect on neuronal sI_{AHP}

A, 500 nM PACAP-27 (PAC-27) suppresses sI_{AHP} with little effect on the amplitude of the "Ca^{++} spike" (insets).

B, Time-course of the effect of PACAP-27 (500 nM) on the normalised sI_{AHP} amplitude. The arrow represents the beginning of PACAP-27 application. PACAP-27 was applied for 12.1±0.8 mins (n=4). Each data point represents the average of four cells with the error bars depicting the SEM

C, Bar chart illustrating the significant effect of PACAP-27 on sI_{AHP} amplitude ($p<0.01$, paired t test) and charge transfer ($p<0.01$, paired t test) compared with the non-significant effect of albumin (BSA; 25 μg/ml; sI_{AHP} amplitude: $p=0.44$, Wilcoxon matched-pairs signed-ranks test; sI_{AHP} charge transfer: $p>0.99$, Wilcoxon matched-pairs signed-ranks test) in time-matched controls. Application of 500 nM PACAP-27 suppressed the sI_{AHP} amplitude by 86.1±4.7 % and charge transfer by 85.8±5.1 %. The effect of albumin was measured at 20 minutes post start of application, in this timeframe the sI_{AHP} had reduced in amplitude by 9.5±12.5 % and charge transfer by 6.5±13.7 %. There was significant difference in the effect of PACAP-27 compared with the effect of albumin on sI_{AHP}

amplitude ($p<0.01$, Mann Whitney test) and charge transfer ($p<0.01$, Mann Whitney test). The effect of PACAP was measured at its maximum.

Note: The four cells treated with PACAP-27 were recorded and presented in my undergraduate study.

4.3.3: The PACAP effect is specific for sI_{AHP} over I_{AHP}

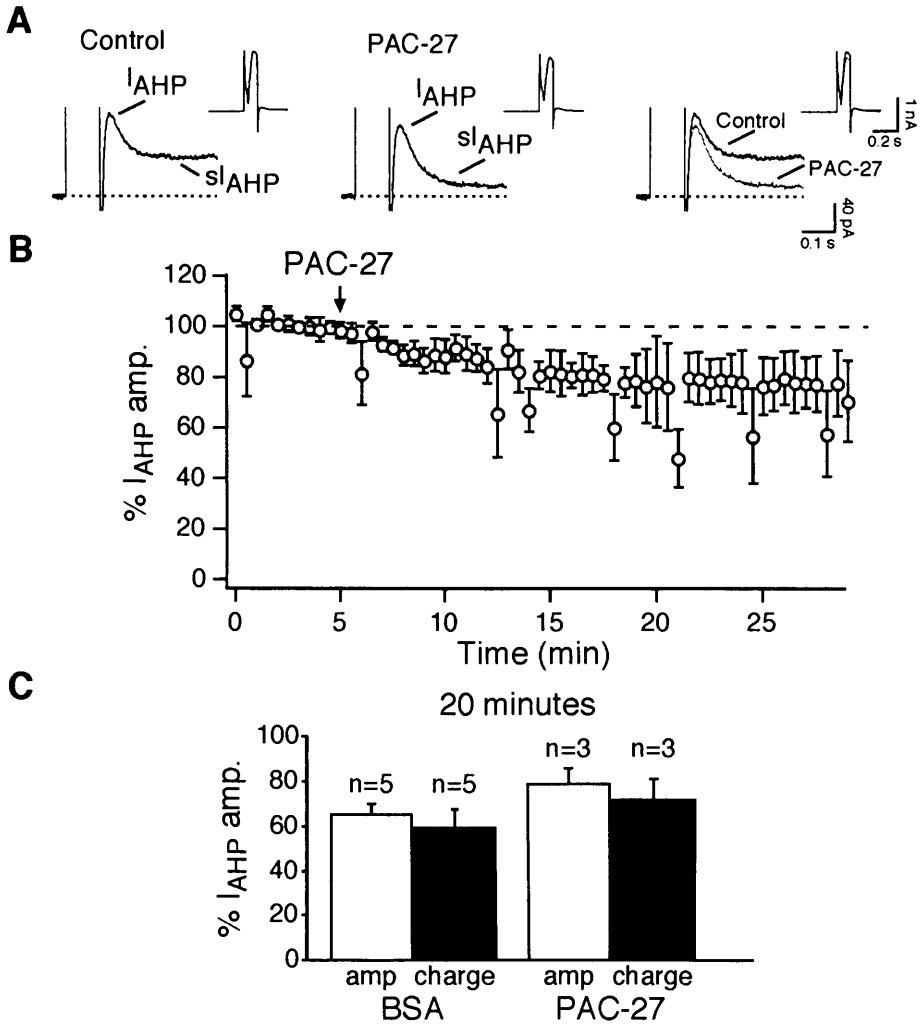

Figure 16: The effect of PACAP-27 on the SK-mediated I_{AHP}

A, 100 ms–long depolarising pulses elicited I_{AHP} followed by sI_{AHP}. I_{AHP} was measured in the same cells as sI_{AHP}. PACAP-27 (PAC-27; 500 nM) had a weak effect on I_{AHP}, while suppressing sI_{AHP}. The unclamped calcium currents (displayed as insets) were largely unchanged by PACAP-27 application.

B, C, PACAP-27 (PAC-27; 500 nM) did not significantly affect I_{AHP} amplitude (***B***, ***C***) or charge transfer (***C***). There was no significant difference between the effect of PACAP-27 and albumin (BSA) on I_{AHP} amplitude (% I_{AHP} left: BSA, 65.3±4.8 %; PAC-27, 78.5±7.1 %; p=0.07; Mann Whitney test) or charge transfer (% I_{AHP} left: BSA, 59.2±8.6 %; PAC-27, 72.0±8.6; p=0.79; Mann Whitney test). The effect of the two compounds was measured twenty minutes after commencement of application, when the effect of PACAP-27 on sI_{AHP} was maximal. Each data point in (***B***) is an average of three experiments.

In Fig. 16A, two distinct tail currents can be visualised: sI_{AHP} and I_{AHP}. To determine whether PACAP-27 affects both sI_{AHP} and I_{AHP}, the effect of PACAP-27 on I_{AHP} was elucidated. The effect of 500 nM PACAP-27 on I_{AHP} was quantified at both ten and twenty minutes after commencement of PACAP application. This was because PACAP-27 was seen to have its full effect on sI_{AHP} in ~ 20 minutes, and was seen to have significant effects at 10 minutes (Fig. 15B). In Fig. 16A, the I_{AHP} is visualised on an expanded time scale, and part of sI_{AHP} is visible. Fig. 16B follows the timecourse of PACAP-27 (500 nM; PAC-27) application on the I_{AHP} amplitude. The effect of PACAP-27 on the I_{AHP} amplitude and charge transfer is quantified in Fig. 16C. In three cells in which PACAP-27 suppressed sI_{AHP}, there was little effect on I_{AHP} compared to intercalated time-matched albumin controls. Twenty minutes after commencement of drug application, I_{AHP} amplitude and charge were not significantly different from vehicle control (% I_{AHP} amplitude left in albumin: 65.3±4.8%, n=5; PACAP: 78.5±7.1, n=3; p=0.07, Mann Whitney test) (% I_{AHP} charge transfer left in albumin: 59.2±8.6 %, n=5; PACAP: 72.0±8.6, n=3; p=0.79, Mann Whitney test). The 30-35 % reduction of the I_{AHP} amplitude and charge transfer observed during the application of drug and vehicle control is most likely due to run-down of this current, and not an effect of the drug.

4.3.4: The effect of PACAP-27 is concentration dependent

The next stage was to determine whether the effect of PACAP-27 on sI_{AHP} was concentration dependent in order to find the ideal concentration of PACAP-27 to conduct further experiments. The ideal concentration of the neuropeptide was

defined as the lowest concentration of PACAP-27 that gave a consistent, close to maximal effect. Fig. 17C shows the effect of varying PACAP-27 concentration on both sI_{AHP} amplitude and charge. 100 nM PACAP-27 did not significantly reduce the amplitude of the sI_{AHP} (% inhibition: 29.9±10.6%, n=4, p=0.06, paired t test). The effect of 100 nM PACAP on sI_{AHP} charge was consistent with its effect on sI_{AHP} amplitude (% inhibition: 32.7±11.5, n=4, p=0.06, paired t test). Application of 250 nM PACAP-27 resulted in significant suppression of sI_{AHP} (% sI_{AHP} inhibition: amplitude 70.2±7.3, n=10, p<0.0001; charge 59.3±11.4, n=10, p<0.0005, paired t test). From figure 17C it can be seen that, in spite of the few data points, the steep part of the concentration response curve seems to lie between 100 nM and 250 nM. There is no significant evidence of change in the effect between 250 nM and 500 nM (maximum amplitude inhibition: 86.1±4.7 % 500 nM PACAP-27 (n=4): 70.5±7.3 % 250nM PACAP-27 (n=10); p=0.35, Mann Whitney test), indicating that 500 nM is close to the concentration giving the maximal effect of PACAP. Given the strong and consistent effect observed and illustrated in Fig. 17A, B and C, it was decided to conduct further experiments with 250 nM PACAP-27.

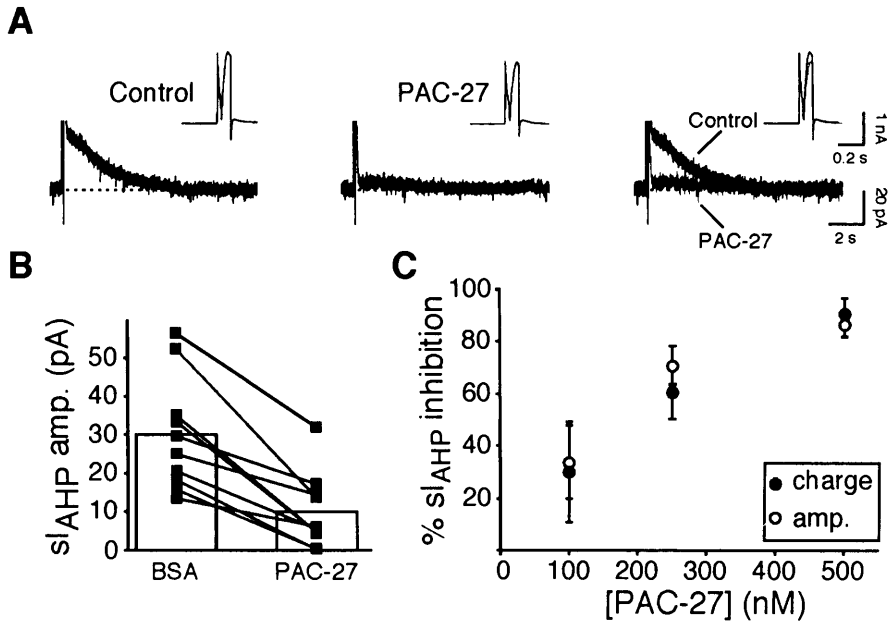

Figure 17: The effect of PACAP-27 on sI_{AHP} is concentration dependent

A, Application of PACAP-27 (PAC-27; 250 nM) resulted in a strong inhibition of sI_{AHP} with little effect on the amplitude of the unclamped calcium current (insets).

B, The effect of PACAP-27 (250 nM) on the amplitude of sI_{AHP}. Square symbols represent individual cells. Each pair of symbols represents the sI_{AHP} amplitude prior to PACAP-27 application (in 25 μg/ml albumin; BSA) matched to the sI_{AHP} amplitude at the maximal effect of PACAP-27. Bars represent the averaged data. 250 nM PACAP-27 significantly suppressed sI_{AHP} amplitude by 70.5±7.3 % (n=10, $p<0.05$).

C, The effect of PACAP-27 on sI_{AHP} is concentration dependent. PACAP-27 significantly suppressed sI_{AHP} amplitude (open circles) and charge transfer (solid circles) at both 250 nM (n=10) and 500 nM (n=4). Although 100 nM PACAP-27 partially inhibited sI_{AHP}, the effect was not significant (n=4).

Note: All cells, except for five with 250 nM PACAP-27, were presented in my undergraduate study.

4.3.5: Activation of PAC-1-R partially mimics the PACAP effect

PACAP receptors are distinguished by their relative activation by VIP. PACAP type 1 receptors (PAC-1-R) are selective for PACAP and couple to both AC and phospholipase C. PACAP type 2 receptors (V-PAC1-R and V-PAC2-R) fall into two subtypes based on their relative selectivity for PACAP and VIP and couple mainly to AC (Vaudry *et al.*, 2000). Experiments using *in situ* hybridisation have shown mRNA expression for all three PACAP receptor subtypes in CA1 hippocampal cells (Hashimoto *et al.*, 1996; Shioda *et al.*, 1997). To elucidate whether activation of PAC1-R is responsible for the PACAP-mediated sI_{AHP} suppression in CA1 pyramidal cells, experiments were conducted with the PAC-1-R selective agonist maxadilan (Moro & Lerner, 1997).

Maxadilan is a peptide originally isolated from the saliva of the sandfly (Lerner *et al.*, 1991). Maxadilan is structurally unrelated to PACAP; however, it acts as a selective agonist at PAC-1-R, whilst it has no activity at VIP receptors (Moro & Lerner, 1997). It was decided to use the same concentration of maxadilan as PACAP-27 because maxadilan has a similar affinity to PAC-1-R as PACAP in rat brain (Moro *et al.*, 1996). Fig. 18 illustrates the effect of 250 nM maxadilan on sI_{AHP}. In five cells, maxadilan (250 nM) suppressed the sI_{AHP} amplitude from 31.2±6.9 pA to 20.67±4.29 pA over 14.2±4.6 min ($p<0.05$, paired t test, Fig. 18A,

C and D). The maxadilan mediated suppression occurred over a similar timescale to the PACAP mediated suppression (time to effect of 250 nM PACAP-27: 15.7±2.6 min). In Fig. 18F it can be seen that 250 nM maxadilan suppressed sI_{AHP} to a lesser extent than 250 nM PACAP-27. 250 nM maxadilan inhibited sI_{AHP} amplitude by 32.6±4.3 % and charge by 24.4±5.3 %. The difference between the PACAP mediated sI_{AHP} amplitude suppression and the inhibition induced by maxadilan is significant ($p<0.005$; unpaired t test). This indicates that only part of the PACAP induced suppression of sI_{AHP} is mediated by PAC-1-R.

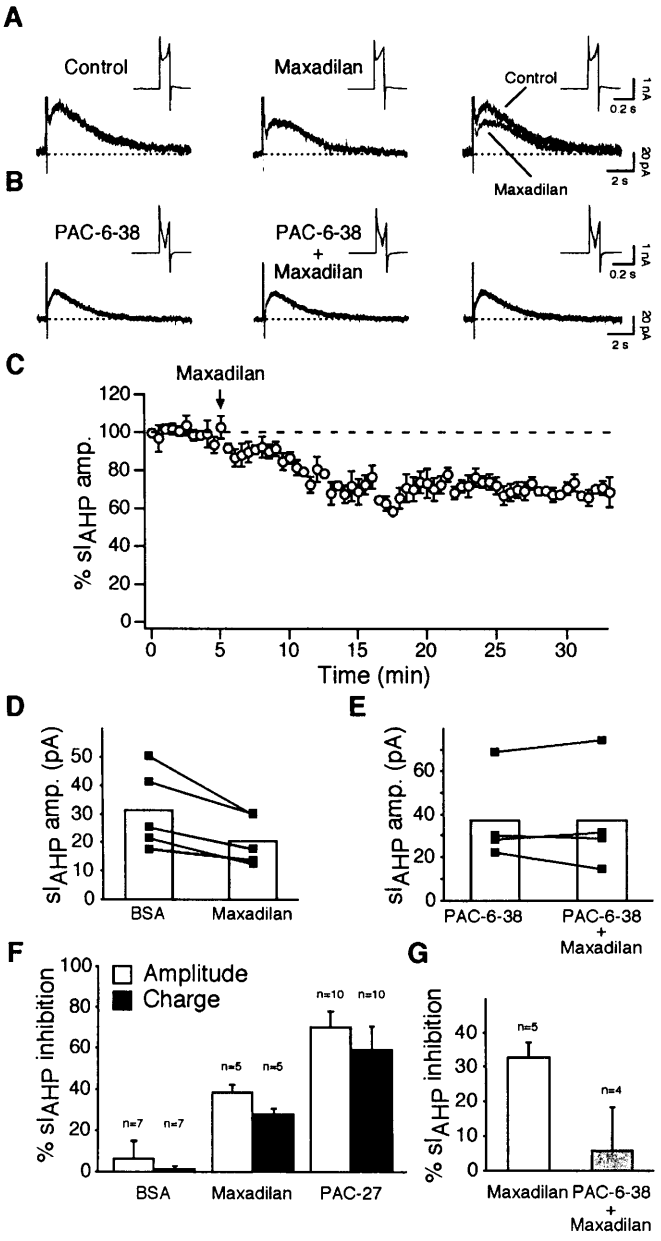

Figure 18: Activation of PAC-1-R leads to suppression of sI_{AHP}

A, The effect of 250 nM maxadilan on sI_{AHP}. Maxadilan is a selective agonist at PAC-1-R.250 nM maxadilan caused a partial suppression of sI_{AHP} with little effect on the unclamped Ca^{++} current.

B, The PAC-1-R antagonist PACAP-6-38 (PAC-6-38; 500 nM) inhibited the PAC-1-R mediated suppression of sI_{AHP}. PACAP-6-38 is a truncated form of PACAP-38 that is a selective antagonist at PAC-1-R and VPAC2-R. The slices were pre-incubated with PACAP-6-38 (500 nM) for at least ten minutes prior to co-application of maxadilan (250 nM) for ~ 20 min.

C, Time-course of the effect of maxadilan (250 nM) on the amplitude of sI_{AHP}. Each point is an average of five experiments, error bars represent the SEM. Maxadilan, which was applied at the time point indicated by the arrow, had a time of effect of 14.2±4.6 mins and reached its maximum effect in ~20 mins. The dotted line indicates the amplitude of sI_{AHP} prior to maxadilan application.

D, Graph depicting the effect of 250 nM maxadilan in individual experiments on sI_{AHP} amplitude (matched squares). In 5 cells, maxadilan significantly reduced sI_{AHP} amplitude from 31.1±6.9 pA to 20.7±4.3 pA ($p<0.05$). Bars represent averaged data.

E, Graph illustrating the effect of 250 nM maxadilan co-applied with PACAP-6-38 in 4 individual cells (matched squares). Pre-incubation with PACAP-6-38 antagonises the effect of maxadilan. Bars represent averaged data.

F, Bar chart comparing the effect of 250 nM maxadilan with the same concentration of PACAP-27 (PAC-27), and time matched albumin controls (BSA; 25 μg/ml). 250 nM maxadilan significantly suppressed sI_{AHP} amplitude by 32.6±4.3 % ($p<0.05$, paired t test). sI_{AHP} charge transfer was suppressed by 24.4±5.3 % ($p=0.08$, paired t test). Application of PACAP-27 (250 nM) resulted in 70.2±7.3 % sI_{AHP} amplitude and 59.3±11.4 % sI_{AHP} charge transfer inhibition. There is significant difference between the maxadilan mediated and PACAP-27 mediated suppression of sI_{AHP} amplitude ($p<0.005$, unpaired t test). Black bars represent the effect on charge transfer, whilst white bars indicate the effect on sI_{AHP} amplitude. Error bars are SEM.

G, Bar chart illustrating the difference between the effect of maxadilan on the amplitude of sI_{AHP} when applied alone (% sI_{AHP} amplitude inhibition: 32.6±4.3 %), and when co-applied with PACAP-6-38 (% sI_{AHP} amplitude suppression 5.6±12.4 %; $p=0.11$; Mann Whitney test). Error bars are SEM.

Note: Experiments with sole application of maxadilan (n=5) were recorded during and previously presented in my undergraduate study.

The next step was to investigate whether the suppression of sI_{AHP} mediated by maxadilan, an agonist at PAC-1-R, could be prevented by antagonism at PACAP receptors. PACAP-6-38 is a truncated form of PACAP-38 that lacks the first six amino acids from the amino terminus. It is a selective antagonist at PAC-1-R and V-PAC2-R (Robberecht et al., 1992). In experiments with PACAP-6-38, slices were pre-incubated with 500 nM PACAP-6-38 for at least ten minutes prior to application of maxadilan. In four cells recorded under these conditions, the mean sI_{AHP} amplitude was 37.3±12.2 pA and charge was 91.8±33.4 pC. Subsequent application of maxadilan (250 nM) did not result in significant changes in sI_{AHP} amplitude (sI_{AHP} mean amplitude after maxadilan application: 37.0±14.9 pA, n=4, $p>0.99$, Wilcoxon matched-pairs signed-ranks test) or charge transfer (sI_{AHP} mean charge transfer after maxadilan application: 102.1±48.9, n=4, p=0.63 Wilcoxon matched-pairs signed-ranks test) (Fig. 18E and G). These results suggest that activation of PAC-1-R is involved in the PACAP-mediated regulation of sI_{AHP} because the effect of a specific PAC-1-R agonist (maxadilan) is inhibited by antagonism of these receptors.

To further investigate the receptors involved in the PACAP-mediated sI_{AHP} suppression, experiments were conducted in which PACAP-27 was applied after pre-incubation with PACAP-6-38. In these cells, pre-incubation in 500 nM PACAP-6-38 slightly decreased the amplitude of sI_{AHP} from 53.4±9.7 pA to 46.3±9.1 pA (n=5, $p<0.01$, paired t test). Addition of PACAP-27 (250 nM), further reduced the sI_{AHP} amplitude to 8.6±4.7 pA (n=5, $p<0.05$, paired t test). There was no significant difference between the effect of PACAP-27 on the control current in the presence and absence (% sI_{AHP} amplitude inhibition by PACAP-27 in PACAP-6-38: 79.2±12.6, n=5; % sI_{AHP} amplitude by PACAP-27: 70.5±7.3 %, n=10; p=0.52; unpaired t test) of PACAP-6-38 (data not shown). This indicates that the effect of PACAP-27 was not antagonised by PACAP-6-38, suggesting the activation of more than one receptor subtype in the PACAP-27 mediated inhibition of sI_{AHP}.

Maxadilan-d-4 is a form of maxadilan that has had the nineteen amino acids between positions 24 and 42 deleted. It is a selective PAC-1-R antagonist that is

more potent than PACAP-6-38 (Moro *et al.*, 1999). Application of 500 nM maxadilan-d-4 resulted in a slight membrane depolarisation and a significant reduction of amplitude of the calcium spike, although the sI_{AHP} remained constant (n=4; % sI_{AHP} amplitude left in maxadilan-d-4: 86.0±11.4 %, p=0.34, paired t test; % sI_{AHP} charge left in maxadilan-d-4: 78.9±10.6, p=0.11, paired t test). Prior application of 500 nM maxadilan-d-4, followed by co-application of maxadilan-d-4 and 250 nM PACAP-27 resulted in a significant inhibition of sI_{AHP} amplitude from 42.6±11.8 pA to 14.3±7.7 pA (n=4, p>0.05, paired t test) and charge from 139.6±37.1 pC to 40.6±29.9 pC (n=4, p<0.05, paired t test). The difference in the mean sI_{AHP} inhibition between the application of 250 nM PACAP-27 (n=10) and 250 nM PACAP-27 after application of 500 nM maxadilan-d-4 (n=4; % amplitude inhibition: 69.8±10.8 %, p=0.94, Mann Whitney test; % charge inhibition: 74.5±7.3 %, p=0.64 Mann Whitney test) is not statistically significant, further indicating that antagonism of PAC-1-R is not sufficient to antagonize the PACAP-27 mediated effect. This suggests that the PACAP-27 effect on sI_{AHP} is due to agonism at more than just PAC-1-R, although the selective activation of PAC-1-R is sufficient to mimic partially the PACAP-27 effect.

4.3.6: Signal transduction mechanism: is the PACAP effect PKA dependent?

PACAP receptors, PAC-1-R, V-PAC1-R, and V-PAC2-R, are positively coupled to adenylyl cyclase in a variety of cell types (Vaudry *et al.*, 2000). To test the hypothesis that the PACAP mediated suppression of sI_{AHP} occurs via cAMP and PKA, experiments were conducted with Rp-cAMPS, a competitive inhibitor of PKA that binds to the cAMP binding sites on the regulatory subunits of PKA, thereby preventing activation of the catalytic subunits (Botelho *et al.*, 1988). Rp-cAMPS (500 μM) was added to the patch pipette solution, and in order to allow optimal diffusion of Rp-cAMPS into the cell, R_{series} was maintained ≤ 20 MΩ for 30 minutes before application of PACAP-27. Under these conditions, Rp-cAMPS significantly reduced the noradrenergic effect on the amplitude of sI_{AHP} (% inhibition by noradrenaline in controls: 83.7±18.8 %, n=4; % inhibition by

noradrenaline in the presence of Rp-cAMPS: 33.3±7.0 %, n=6; p<0.05, Mann Whitney test).

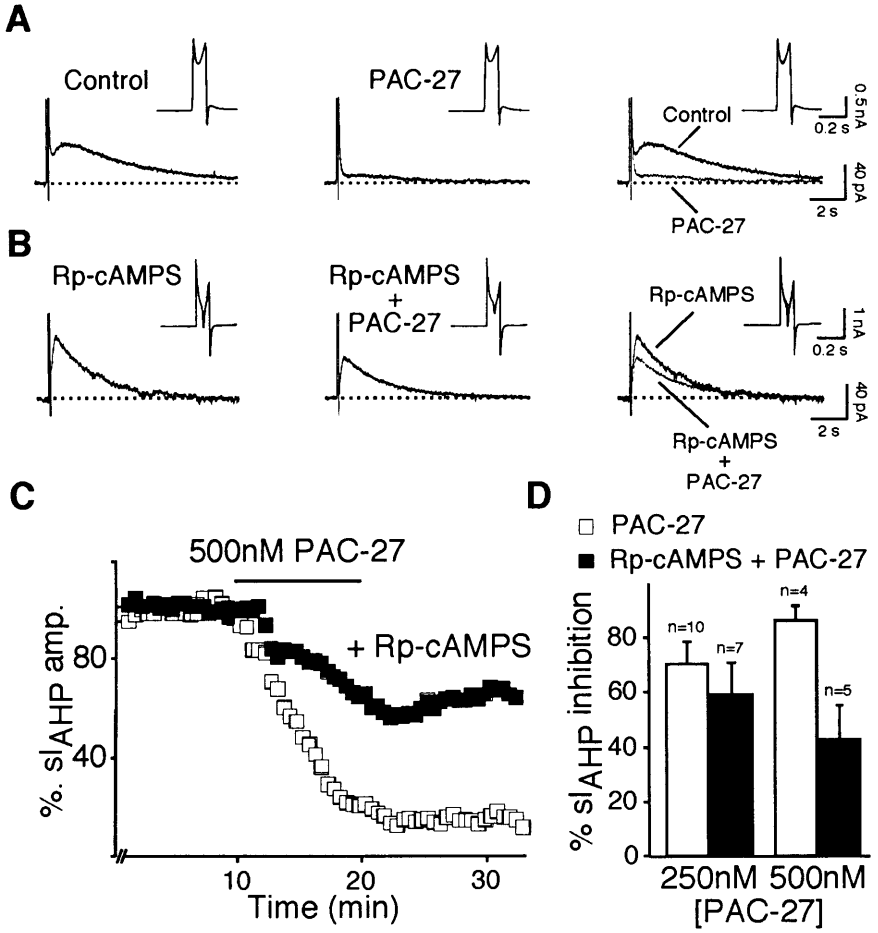

Figure 19: The PACAP effect on sI_{AHP} is partially PKA dependent

A, The effect of 500 nM PACAP-27 on the sI_{AHP}. Application of PACAP-27 (PAC-27; 500 nM) results in a strong suppression of sI_{AHP} with little effect on the amplitude of the unclamped Ca^{++} current (insets).

B, Inclusion of 500 μM Rp-cAMPS in the patch pipette partially suppresses the effect of PACAP-27 (500 nM) on sI_{AHP}. In this cell there is a small reduction in the amplitude of the Ca^{++} spike.

C, Timecourse of sI_{AHP} inhibition by 500 nM PACAP-27 in two representative cells. sI_{AHP} amplitude was normalised to the amplitude of the current prior to PACAP-27 application. 500 nM PACAP was applied as indicated by the solid line in the absence (open squares) or presence (closed squares) of 500 μM Rp-cAMPS.

D, Bar chart illustrating the result of inclusion of 500 μM Rp-cAMPS in the patch pipette on the effect of PACAP-27 on sI_{AHP} amplitude at 250nM and 500 nM PACAP. Application of 250 nM PACAP-27 inhibits sI_{AHP} amplitude by 70.5±7.3 %, whilst in the

presence of Rp-cAMPS, PACAP-27 (250 nM) results in 59.3±10.3 % sI_{AHP} amplitude suppression (p=0.37; unpaired t test). Inclusion of Rp-cAMPS in the patch pipette results in a suppression of the effect of PACAP-27 on sI_{AHP} at 500 nM from 86.1±4.7 % sI_{AHP} amplitude inhibition in the absence of Rp-cAMPS to 42.7±11.1 % sI_{AHP} amplitude inhibition in its presence. Error bars are SEM.

This indicated that Rp-cAMPS was effective at inhibiting PKA-dependent signalling at this concentration and under these conditions.

Application of 250 nM PACAP-27 significantly suppressed sI_{AHP} amplitude from 35.4±9.5pA to 14.1±5.2 pA (n=7, p<0.05, Wilcoxon matched-pairs signed-ranks test) and charge from 97.0±28.7 pC to 39.5±15.6 pC (n=7, p<0.05, Wilcoxon matched-pairs signed-ranks rest) in the presence of 500 mM Rp-cAMPS. Fig. 19D compares the effect of PACAP-27 (250nM; PAC-27) on sI_{AHP} in the presence (% sI_{AHP} inhibition: 59.3±10.3 %, n=7) and absence (% sI_{AHP} suppression: 70.5±7.3 %, n=10) of Rp-cAMPS (p=0.37; unpaired t test). In particular, in 5 out of the 7 cells in which Rp-cAMPS was included in the patch pipette, the sI_{AHP} inhibition by 250 nM PACAP-27 was suppressed (% sI_{AHP} inhibition in Rp-cAMPS: 44.8±6.1 %, n=5) compared with cells in which PACAP-27 was applied alone (p<0.05, unpaired t test).

The sI_{AHP} amplitude was inhibited by 42.7±12.4 % by 500 nM PACAP-27 in Rp-cAMPS (n=5, p<0.01, paired t test) (Fig. 19D). There was no significant difference between the maximal effect of PACAP-27 (500 nM) on sI_{AHP} amplitude in the presence (% sI_{AHP} inhibition: 42.7±12.4 %; n=5) and absence (% sI_{AHP} inhibition: 86.1±4.7 %, n=4) of Rp-cAMPS (p=0.06; Mann Whitney test). Fig. 19B, gives an example of a cell where inclusion of Rp-cAMPS in the patch pipette clearly inhibited the PACAP effect. There was variability in the data. In 1 out of 5 cells recorded in the presence of Rp-cAMPS, the PACAP effect on sI_{AHP} was intact, whilst in the remaining 4 cells the PACAP effect on sI_{AHP} was significantly suppressed (% sI_{AHP} inhibition in Rp-cAMPS: 32.7±6.2 %, n=4, p<0.05, Mann Whitney test).

These results indicate that the suppression of sI_{AHP} mediated by PACAP involves the activation of PKA. Possible reasons for the lack of effect of Rp-cAMPS in some cells (n=4) will be discussed in the discussion.

4.3.7: Signal transduction mechanism: do MAPKs mediate the PACAP effect?

PACAP has been shown to induce neuronal differentiation of PC12 cells by activating mitogen-activated protein kinases (MAPKs). To investigate whether the PACAP effect on sI_{AHP} was mediated by MAPKs in CA1 neurons, experiments were conducted including the MAPK inhibitors PD98059 and UO126 in the patch pipette solution. Control experiments were intercalated and conducted including 0.13% DMSO in the patch pipette. The difference in the PACAP-27 mediated suppression of the sI_{AHP} when 0.13% DMSO was included in the intracellular solution (250 nM: 63.1±7.7 %, n = 6; 500 nM: 96.4±4.0 %, n=6) compared to standard intracellular solution (250 nM: 70.5±7.8 %, n = 10; 500 nM: 86.1±5.4 %, n=4) is not statistically significant (250 nM: $p>0.51$, unpaired t test; 500 nM: $p=0.27$, Mann Whitney test).

PD98059 is an inhibitor that prevents the activation of MEK, a kinase one step upstream from ERK, by the small GTPase, Raf (Alessi *et al.*, 1995). The difference in the PACAP-27 (250 nM) mediated suppression of sI_{AHP} in cells where PD98059 was included in the intracellular solution (75.8±7.3%, n = 5) and where it was not (63.1±7.7%; n=6), was not statistically significant ($p=0.22$, unpaired t test). However, the inclusion of 100 μM PD98059 in the patch pipette for 30 minutes prior to PACAP application resulted in a profound reduction in the amplitude of the calcium spike, indicating adequate diffusion of PD98059 in the cells. A reduction in the amplitude of the unclamped calcium spike may be an indication that PD98059 affects voltage gated calcium channels. PD98059 has been shown to prevent calcium action potentials in *Urechis* oocytes (Gould & Stephano, 2000). Further studies have also shown a possible link between PD98059 and inhibition of calcium channels (Lagaud *et al.*, 1999; Aoki *et al.*, 2000). Therefore, it was decided to try another inhibitor of the Raf/MEK/ERK

pathway, to elucidate whether this pathway is involved in the modulation of sI_{AHP} by PACAP-27.

UO126 is a specific inhibitor of MEK (Favata *et al.*, 1998; Davies *et al.*, 2000). The inclusion of 40 μM UO126 in the patch pipette solution for 30 minutes prior to 500 nM PACAP-27 application had no significant effect on the PACAP mediated reduction in sI_{AHP} (90.2±4.8%, n=6) compared with the control conditions (0.13% DMSO in the intracellular solution; 96.4±4.0 %, n =6) (p=0.16, Mann-Whitney test). The effect of 250 nM PACAP-27 was also not inhibited by UO126 (% sI_{AHP} amplitude inhibition in DMSO: 63.1±7.7, n=6; in UO126: 58.5±9.3, n=8; p=0.66 Mann-Whitney test). Therefore, the Raf/MEK/ERK pathway does not appear to be involved in the PACAP-27 mediated inhibition of sI_{AHP}.

4.3.8: The PACAP effect involves the activation of p38 MAPK

The activation of p38 MAPK by PACAP has been reported in PC12 cells (Sakai *et al.*, 2001). This information, together with the fact that CA1 pyramidal cells show a high level of expression for two isoforms of p38 MAPK (Lee *et al.*, 2000), led us to test the hypothesis of an involvement of p38 MAPK in the PACAP mediated reduction of sI_{AHP}. SB203580 binds to a residue in the ATP binding site of p38 MAPK and therefore inhibits its enzymatic activity (Eyers *et al.*, 1998). Inclusion of 20 μM SB203580 in the patch pipette solution for 30 minutes prior to addition of 250 nM PACAP-27 resulted in a statistically significant inhibition of the PACAP mediated suppression of sI_{AHP} amplitude (63.1±7.8%, n=6, in 0.13% DMSO; 31.3±12.1%, n=7, in SB203580; $p<0.05$, unpaired t test) (Fig. 20A, B and C). These experiments were replicated with an increased concentration of 500 nM PACAP-27. Inclusion of 20 μM SB203580 did not result in significant inhibition of the PACAP mediated reduction of sI_{AHP} amplitude (70.4±13.0 %, n=5) compared with control conditions (96.4±4.0%, n=6; $p>0.06$, Mann Whitney test, Fig. 20D). These results indicate that the PACAP mediated reduction in the amplitude of sI_{AHP} is partly achieved via activation of p38 MAPK.

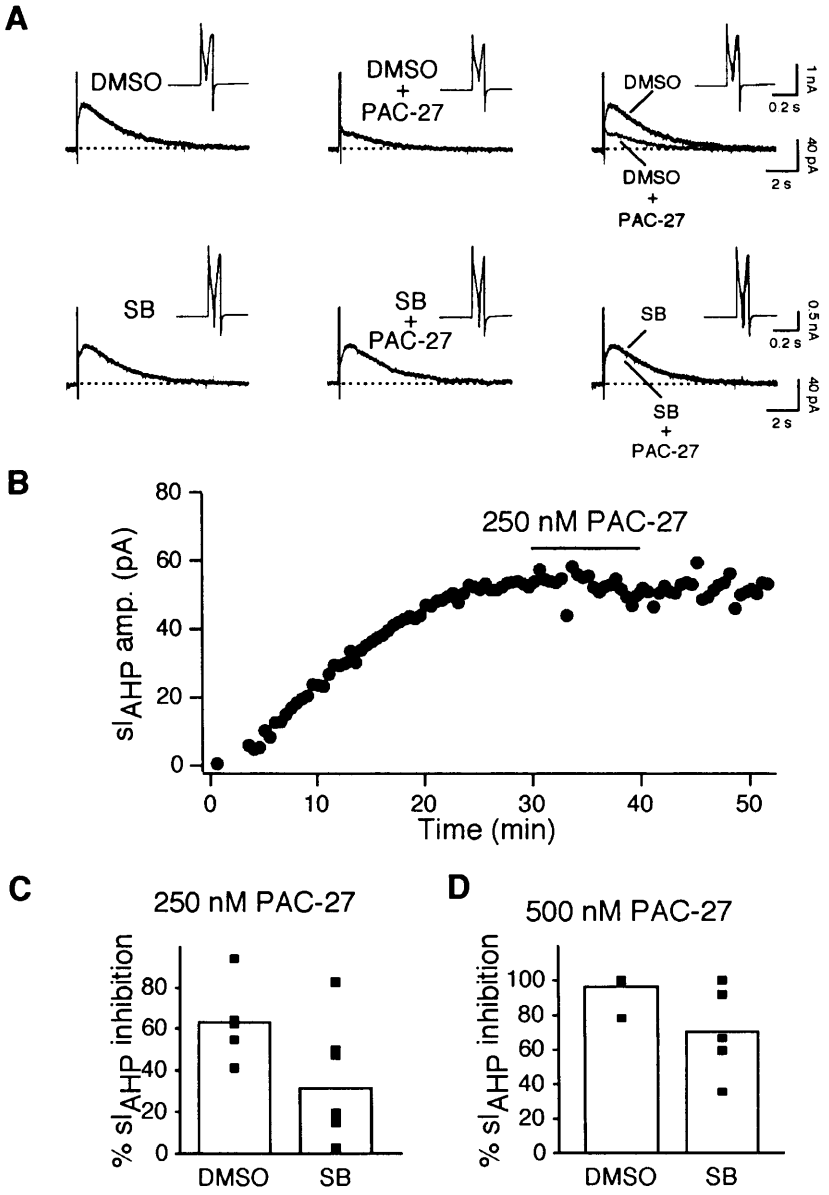

Figure 20: The PACAP effect on sI_{AHP} is p38 MAPK dependent

A, p38 MAPK was inhibited by inclusion of 20 μM SB203580 in the patch pipette. Panel A compares representative traces of the effect of 250 nM PACAP-27 (PAC-27) recorded with 0.13 % DMSO (DMSO) and 20 μM SB203580 in the patch pipette (SB). The final concentration of DMSO in experiments with SB203580 was 0.025%. The unclamped Ca^{++} current (shown as insets) remained approximately the same amplitude over the application of PACAP-27.

B, Time-course of the effect of 250 nM PACAP-27 on sI_{AHP} amplitude in a cell pre-incubated with SB203580. Same cell as in ***A***. PACAP-27 was applied for 10 minutes. The sI_{AHP} was elicited once every 30 seconds.

C, D, Both panels illustrate the PACAP-mediated inhibition of sI_{AHP} comparing the control situation (DMSO) with cells recorded in the presence of SB203580. Each point corresponds to a single cell. Bars indicate the averaged data, whilst panel D, shows the results for application of 500 nM PACAP-27. Application of 250 nM PACAP-27 suppressed sI_{AHP} amplitude by 31.3±12.1 % (n=7) in cells pre-incubated with SB203580, compared with 63.1±7.7 % (n=6) sI_{AHP} amplitude suppression in DMSO controls ($p<0.05$, unpaired t test, *C*). Panel *D* illustrates that the sI_{AHP} amplitude was inhibited by 96.4±4.0 % (n=6) by PACAP-27 (500 nM) in DMSO controls. When cells were pre-incubated with SB203580, the sI_{AHP} amplitude was inhibited by 70.4±13.0 % (n=5) by 500 nM PACAP-27 (p=0.06 Mann Whitney test).

4.3.9: The PACAP effect includes an inward shift in holding current

In addition to suppressing sI_{AHP}, PACAP-27 induced an inward shift in the holding current that reversed on washout of the peptide within minutes. Application of 500 nM PACAP-27 resulted in a decrease in holding current from 61.1±20.8 pA to 37.6±22.8 pA (n=4; $p<0.05$; paired t test). A smaller decrease in holding current was seen with application of 250 nM PACAP-27 (mean holding current in albumin: 62.5±7.4 pA; mean holding current in 250 nM PACAP-27: 52.5±6.7 pA; n=10; $p<0.005$; paired t test). Addition of maxadilan (250 nM) did not result in a significant change in holding current (mean holding current in albumin: 34.3±4.8 pA; mean holding current in maxadilan: 30.8±3.9 pA; n=5; p=0.12; paired t test). These results indicated that the inward shift in holding current is due to activation of either V-PAC1-R, or V-PAC2-R.

The inward shift in the holding current in response to PACAP application, was suppressed when the PKA inhibitor Rp-cAMPS was included in the patch pipette prior to PACAP application. Application of 500 nM PACAP-27 in the presence of Rp-cAMPS did not result in a significant shift in holding current (mean holding current in albumin: –25.4±24.1 pA; mean holding current in PACAP-27: –31.6±24.5 pA; n=5; p=0.58, paired t test). Similarly, the effect of 250 nM PACAP-27 on the holding current was not significant in the presence of Rp-

cAMPS (n=7; p=0.15). This result indicates that the effect of PACAP-27 on the holding current involves the activation of the cAMP-PKA pathway.

The results described above suggest that the PACAP mediated inhibition of sI_{AHP} involves the activation of p38 MAPK. Experiments with the p38 MAPK inhibitor SB203580 were conducted in the presence of DMSO (0.025%). Application of 500 nM PACAP-27 in the presence of DMSO (0.13%) resulted in a significant inward shift in the holding current from 45.1±11.2 pA to 33.8±12.4 pA (n=5; $p<0.05$; paired t test). When 20 μM SB203580 was included in the patch pipette, application of PACAP-27 (500 nM) did not result in a significant change in the holding current (mean holding current in control: 29.7±6.0 pA; mean holding current in PACAP-27: 24.3±4.7 pA; n=5; p=0.20; paired t test). However, there was no significant difference between the mean change in the holding current elicited by PACAP-27 in DMSO (11.3±3.3 pA; n=6) and SB203580 (5.4±3.5 pA; n=5; p=0.26; unpaired t test). This was replicated by experiments conducted with 250 nM PACAP-27 (mean inward shift in holding current in DMSO: 7.2±4.4 pA; n=6; mean inward shift in holding current in SB203580: 4.8±2.9 pA; n=7; p=0.64; unpaired t test). These results suggest that the inward shift in the holding current does not involve the activation of p38 MAPK.

The results presented above indicate that the PACAP effect involves an inward shift in the holding current that is mediated through the activation of V-PAC1-R or V-PAC2-R and dependent on the cAMP/PKA pathway. An inward shift in holding current can be due to the activation of an inward current (i.e. sodium mediated) or the inhibition of an outward current (K^+ mediated) or a combination of both. A preliminary indication of whether the shift is due to channels opening or closing can come from measuring changes in input resistance. This is because membrane conductance is inversely related to membrane/input resistance. Therefore to gain information on the type of channel mediating the inward shift in holding current, the change in input resistance was determined over the period of the PACAP-27 effect on holding current. Application of 500 nM PACAP-27 did not result in a significant change in input resistance ove the application of PACAP-27 (mean input resistance in albumin: 164.3±8.9 MΩ; mean input resistance in PACAP-27: 173.8±10.7 MΩ; n=4; p=0.15; paired t test). However,

there was a significant increase in input resistance upon application of 250 nM PACAP-27. The mean input resistance measured in albumin (25 μg/ml) was 151.4±10.0 MΩ compared with 157.3±9.9 MΩ in the presence of 250 nM PACAP-27 ($n=10$; $p<0.05$; paired t test). Therefore, application of PACAP-27 resulted in an increase in input resistance, suggesting that channels are closed in response to PACAP-27. Taken together the results suggest that application of PACAP-27 leads to channel closing resulting in an inward shift in holding current.

4.4.0: Discussion

4.4.1: Which receptor is responsible for the effect of PACAP on sI_{AHP}?

There are two classes of PACAP receptors that are distinguished through different affinities for the neuropeptides. PAC-1 receptors have a thousand fold higher affinity for PACAP over VIP. Both PACAP and VIP activate VIP receptors. PACAP-38, PACAP-27 and VIP have equal potency at V-PAC2 receptors, whilst PACAP-38 has a higher affinity at V-PAC1 receptors (Vaudry *et al.*, 2000).

Radioligand binding studies have shown that PACAP binding sites are dense in the pyramidal cell layer of the hippocampus (Masuo *et al.*, 1992). Using immunohistochemistry and *in situ* hybridization, it has been shown that PAC-1 receptors are expressed in hippocampal pyramidal cells (Shioda *et al.*, 1997), as well as V-PAC1 and V-PAC2 receptors (Hashimoto *et al.*, 1996). This evidence supports the experimental findings of this study. Maxadilan reduced the amplitude of the sI_{AHP} indicating that selective stimulation of PAC-1 receptors is sufficient to modulate this current. The suppression of sI_{AHP} mediated by maxadilan could be antagonised by pre-incubation with PACAP-6-38, an antagonist at V-PAC2 and PAC-1 receptors, suggesting that the PACAP effect might be at least partly mediated by PAC-1 receptors. However, the effect of comparable concentration of maxadilan was significantly less than of PACAP-27, despite the affinity of the two peptides for PAC-1 receptors being similar in the rat brain (Moro *et al.*, 1996). Maxadilan and PACAP-27 also have similar potency for cAMP production following activation of PAC-1 receptors (Dickson *et al.*, 2006). Taken together, these results suggest that the PACAP effect on sI_{AHP} is only partially mediated via PAC-1 receptors.

It can be argued that if PACAP is acting partially via PAC-1 receptors, then antagonizing these receptors with maxadilan-d-4, a PAC-1 selective antagonist, should significantly reduce the effect of PACAP. This prediction is not borne out by the experimental results because pre-incubation with maxadilan-d-4 (500 nM), did not antagonise the effect of 250 nM PACAP-27 on sI_{AHP}. Competitive binding

data for 50 pM ^{125}-I-PACAP-27 in rat brain crude membranes indicated that the affinity (IC_{50}) of maxadilan-d-4 for PACAP receptors was ~ 6 nM compared with ~ 10 nM for PACAP-27 (Moro *et al.*, 1999). The available data on relative affinities for the PAC-1 receptor indicates that the concentration of maxadilan-d-4 used in this study (500 nM) should have been sufficient to antagonise 250 nM PACAP-27. However it has also been reported that ~300 nM maxadilan-d-4 was required to inhibit cAMP production induced by 1 nM PACAP-38 by 50 % in COS cells transfected with PAC-1 receptors (Moro *et al.*, 1999). This raises the possibility that the concentration of maxadilan-d-4 used in this study was not sufficient to antagonise PAC-1 receptors. Therefore, there are two possible explanations that can be offered to explain the fact that pre-incubation with maxadilan-d-4 did not antagonise, at least partly, the effect of PACAP-27. Firstly, it could be concluded that the PACAP effect on sI_{AHP} is mainly elicited by receptors other than PAC-1. A second possibility is that the concentration of max-d-4 was not sufficient to antagonise PAC-1 receptors. In order to distinguish between these two possibilities a further experimental approach could be to investigate whether the effect of maxadilan (250 nM) on sI_{AHP} can be inhibited by (500 nM) maxadilan-d-4. This experiment was not performed in this study due to the limited supply of maxadilan and maxadilan-d-4 that was kindly provided by Dr Ethan Lerner of Harvard University. As already discussed above, maxadilan and PACAP-27 have similar affinities for PAC-1 receptors in rat brain (Moro *et al.*, 1996; Dickson *et al.*, 2006). Therefore if the effect of a similar concentration of maxadilan on sI_{AHP} can be inhibited by 500 nM maxadilan-d-4, then it could be concluded that the PACAP-27 mediated suppression of sI_{AHP} occurs through agonism at receptors other than PAC-1.

PACAP-6-38 is an antagonist at PAC-1 and V-PAC2 receptors. Pre-incubation with PACAP-6-38 (500 nM) did not antagonise the effect of PACAP-27 (250 nM). The IC_{50} for PACAP-6-38 in displacing 50 pM ^{125}-I-PACAP-27 in rat brain crude membranes has been determined as ~ 40 nM (Moro *et al.*, 1999). This indicates that PACAP-6-38 is ~6 fold less potent than maxadilan-d-4. Therefore, the lack of antagonism of PACAP-27 with PACAP-6-38 is consistent with the result obtained with maxadilan-d-4. However, the application of PACAP-6-38

was effective in preventing the suppression of the sI_{AHP} by maxadilan. This indicates that the antagonist PACAP-6-38 was effective at PAC-1 receptors in this system, and that the PACAP effect on sI_{AHP} is likely to be mediated also by receptors other than PAC-1.

These results, taken together, suggest that the PACAP effect on sI_{AHP} is likely to be due to agonism at more than just PAC-1 receptors, although the selective activation of PAC-1 receptors is sufficient to partially mimic the effect of PACAP-27.

VIP was shown to significantly reduce the amplitude of sI_{AHP} in hippocampal pyramidal cells (Haas & Gahwiler, 1992; Haug & Storm, 2000): this indicates that stimulation of VIP receptors is sufficient to suppress sI_{AHP}. PACAP is also known to stimulate VIP receptors. Therefore, there are two populations of different receptors that can be stimulated by PACAP that have similar effects on the sI_{AHP}. It could therefore be expected that antagonizing one population of receptors e.g. PAC-1, could result in the effect being mediated fully via the other population of receptors, V-PAC1 and V-PAC2 receptors. PACAP-6-38 is an antagonist at PAC-1 and V-PAC2 receptors and this study has shown that pre-incubation with PACAP-6-38 does not antagonise the suppression of sI_{AHP} by PACAP-27. This indicates that agonism at just V-PAC1 receptors by PACAP is sufficient to elicit suppression of sI_{AHP}. Additionally, the application of maxadilan, an agonist at PAC-1 receptors, is sufficient to partially suppress the sI_{AHP}, indicating that activation of PAC-1 receptors leads to sI_{AHP} suppression. Therefore, this study concludes that sI_{AHP} suppression by PACAP-27 can be elicited through agonism at PAC-1 and most likely at V-PAC1 receptors. Further study is needed to understand whether the PACAP mediated effect on sI_{AHP} can be elicited through activation of V-PAC2 receptors.

4.4.2: Signal transduction mechanism

Intracellular application of the protein kinase A inhibitor Rp-cAMPS resulted in a partial suppression of the PACAP-mediated inhibition of sI_{AHP} in some cells (in 4 out of 5 cells Rp-cAMPS suppressed the effect of 500 nM PACAP-27; the effect of 250 nM PACAP-27 was suppressed by the presence of Rp-cAMPS in 5 out of

7 cells), suggesting that the PACAP effect might be partly mediated by the activation of the cAMP-PKA pathway. Intracellular application of the MEK inhibitors UO126 and PD98059 had no effect on the PACAP-mediated suppression of sI_{AHP}. By contrast, inclusion of SB203580, a p38 MAPK inhibitor, largely prevented the effect of PACAP on sI_{AHP}. This suggests an involvement of p38 MAPK, but not of the Raf/-MEK/-ERK pathway, in the PACAP-mediated suppression of sI_{AHP}.

CRF, VIP and CGRP have been shown to suppress sI_{AHP} by a mechanism that is dependent on cAMP and is inhibited by the PKA inhibitor Rp-cAMPS (Haug & Storm, 2000). The monoamine transmitters have also been demonstrated to suppress sI_{AHP} via the same mechanism (Pedarzani & Storm, 1993). Maxadilan and PACAP-27 induced a slight depolarization of the membrane potential of the cell. Pedarzani and Storm (1995b) showed that the increase in cAMP associated with activation of adenylyl cyclase by monoamine transmitters resulted in depolarization of the CA1 pyramidal neurons through an enhancement of I_h. Therefore, the depolarization induced by PACAP-27 and maxadilan may be indicative of an increase in cAMP within the cell due to direct activation of I_h. However inclusion of Rp-cAMPS resulted in suppression of the inward shift in holding current mediated by PACAP. The HCN channels that mediate I_h are directly activated by cAMP (Wainger *et al.*, 2001). Activation of I_h has been demonstrated to be independent of PKA (Pedarzani & Storm, 1995b). This argues against the PACAP induced depolarisation of CA1 pyramidal cells being mediated by activation of I_h. Additionally, the PACAP mediated depolarisation is accompanied by a decrease in conductance therefore it is unlikely that activation of I_h is responsible. However in order to experimentally confirm that the activation of I_h is not responsible for the PACAP-mediated depolarisation, further experiments conducted in the presence of ZD 7288 should be performed. The PKA mediated depolarisation could be due to either activation of an inward current or closure of an outward current that contributes to the resting membrane potential of the cell. Analayis of the change in input resistance over the time-course of the PACAP-27 effect on holding current indicated that channels close in response to PACAP-27 application. This indicates that the inward shift in holding

current is due to inhibition of an outward current. However in order to establish which channels mediate the inward shift in holding current, ion substitution experiments and.pharmacology are needed.

PAC-1, VPAC-1 and VPAC-2 are positively coupled to adenylyl cyclase (Vaudry *et al.*, 2000). However, the addition of Rp-cAMPS resulted in a suppression of the effect of PACAP on sI_{AHP} only in some cells. There was large variability in the data because in 1 out of the 5 cells recorded in the presence of Rp-cAMPS, the effect of 500 nM PACAP-27 remained intact. Similarly in 2 out of the 7 cells recorded with 500 nM PACAP-27 in the presence of Rp-cAMPS, the sI_{AHP} suppression remained intact. The experimental procedure utilized in experiments with Rp-cAMPS was to include Rp-cAMPS in the patch pipette solution. The presence of drugs in the patch pipette solution can sometimes hinder the formation of tight gigaohm seals between pyramidal cells and the patch pipette. Therefore, to allow adequate seal formation, the tips of the patch pipette were filled with ordinary intracellular solution. The back of the patch pipette was then filled with intracellular solution containing Rp-cAMPS. This experimental procedure could explain the variable results with Rp-cAMPS. There is a possibility that Rp-cAMPS did not always adequately diffuse into the cell and remained in the patch pipette. This would explain why, in some cells, the PACAP-mediated sI_{AHP} suppression was intact, whereas in other cases, Rp-cAMPS clearly inhibited the PACAP effect. To demonstrate that Rp-cAMPS adequately diffused into the cell and inhibited PKA, positive controls for the effect of PKA should have been conducted in the same cell by applying a neurotransmitter known to suppress sI_{AHP} through the cAMP-PKA pathway (e.g. noradrenaline or isoproterenol) after the application of PACAP. In this way, cells in which the neurotransmitter action on sI_{AHP} was not inhibited could be excluded due to lack of PKA inhibition, probably linked to an inadequate diffusion of Rp-cAMPS.

Recently, Rehmann et al. (2003) showed that Rp-cAMPS acts as an inhibitor of the cAMP guanine nucleotide exchange factors (GEFs). These have been termed EPACs, which is an acronym for: exchange factor directly activated by cAMP. EPACs are directly activated by cAMP in a manner that is independent of PKA (de Rooij *et al.*, 1998; Kawasaki *et al.*, 1998). Both members of the EPAC family

(EPAC1, EPAC2) are expressed in the adult hippocampus (Ster *et al.*, 2007). PACAP-38 mediated activation of EPACs has been demonstrated both in cerebellar neurons (Ster *et al.*, 2007) and PC12 cells (Shi *et al.*, 2006). Experiments with Rp-cAMPS cannot distinguish between a PKA-mediated or an EPAC-mediated suppression of the sI_{AHP} by PACAP-27. Further experiments need to be conducted to distinguish between these two possibilities. To test the involvement of PKA, experiments should be conducted with the PKA inhibitor: Walsh peptide/PKI_{6-22}. The difference in the specificity of the two PKA inhibitors lies in their mechanism of action. PKA is an holoenzyme consisting of two regulatory and two catalytic subunits. In the presence of cAMP, each regulatory subunit binds two molecules of cAMP and the haloenzyme dissociates into a regulatory dimer and two monomeric catalytic subunits. Walsh peptide/PKI_{6-22} is a pseudosubstrate inhibitor of PKA; it acts by binding to the substrate recognition sequence on the free catalytic subunits of PKA (Cheng *et al.*, 1986). This prevents the binding and phosphorylation of the regulatory subunits of PKA. Because Walsh peptide/PKI_{6-22} binds to the substrate recognition site on PKA, it is specific for peptides containing this sequence. Rp-cAMPS is a cAMP analogue that binds to the cAMP binding sites on the regulatory dimer of PKA preventing activation of the catalytic subunits (Botelho *et al.*, 1988). It is therefore a competitive inhibitor of the cAMP-binding site, therefore other peptides which share the binding pocket for cAMP, have the potential for inhibition by Rp-cAMPS. In the continuing absence of a specific EPAC inhibitor, further experiments should also be conducted with the selective EPAC activator 8-pCPT-2'-O-Me-cAMP to elucidate whether the activation of EPAC leads to an inhibition of sI_{AHP}. If 8-pCPT-2'-O-Me-cAMP was found to suppress sI_{AHP} this may provide some preliminary evidence for the involvement of activation of EPACs in the PACAP mediated suppression of sI_{AHP}.

In 1995, Zhong showed that in Drosophila, whilst PACAP-38 could activate adenylyl cyclase to produce cAMP resulting in an enhancement of potassium currents, the full PACAP effect was achieved only via concomitant activation of cAMP and of the Ras/Raf-mediated pathway (Zhong, 1995). In our study, the inhibition of p38 MAPK by SB203580 resulted in a suppression of the effect of

PACAP on sI_{AHP}, suggesting the involvement of p38 MAPK in the PACAP mediated response. The involvement of p38 MAPK in PACAP-mediated actions has been demonstrated in PC12 cells where activation of p38 MAPK by PACAP occurred via the activation of EPAC and the small GTPase Rit (Shi *et al.*, 2006). In cerebellar neurons, the regulation of the BK subgroup of K^+ channels by PACAP involved the activation of EPAC, a small Ras-like GTPase (Rap), and p38 MAPK (Ster *et al.*, 2007). Both these studies demonstrated a role for PKA independent p38 MAPK activation. In cardiac myocytes, there is evidence that agonism at β adrenoceptor leads to PKA-dependent p38 MAPK activation (Zheng *et al.*, 2000). Activation of PKA could enhance p38 MAPK activity by direct phosphorylation of PP1, or phosphorylation of phosphatase inhibitor 1 thus down-regulating the activity of PP1 (Gupta *et al.*, 1996). Alternatively, PKA could phosphorylate protein tyrosine phosphatases, thus inhibiting their interaction with p38 MAPK and enhancing the activity of p38 MAPK (Saxena *et al.*, 1999a; Saxena *et al.*, 1999b). Therefore, there are two independent pathways by which agonism at PACAP receptors could activate p38 MAPK. The results of this study indicate an involvement for PKA and p38 MAPK in the suppression of sI_{AHP} elicited by PACAP. However, it is not clear from the experiments presented here, whether p38 MAPK is activated downstream of PKA, or through a parallel pathway.

4.4.3: Functional role of PACAP

In Drosophila, a specific memory mutant, *amnesiac*, was first isolated in a screen of mutant flies that were produced through random insertions of P elements (Feany & Quinn, 1995). The team found that flies that had mutations in their *amnesiac* gene showed poor performance in one hour memory testing. The signal peptide that was encoded by the gene *amnesiac* in Drosophila was homologous to the neuropeptide PACAP (Feany & Quinn, 1995). Further study of the amnesiac gene product in Drosophila has revealed that it is expressed in the dorsal paired medial cells. These cells project onto the mushroom bodies, which are the key components in Drosophila olfactory learning. Transgenic flies, which are defective in vesicle recycling in the dorsal paired medial cells, show undetectable

memory that can be rescued through expression of the amnesiac gene product in the dorsal paired medial cells (Waddell *et al.*, 2000). This study suggests that the product of the amnesiac gene modulates information processing in the mushroom bodies. The finding that PAC-1 receptor deficient mice show a deficit in associative learning and mossy fibre long-term potentiation extends and strengthens the link between PACAP and learning in vertebrates (Otto *et al.*, 2001b). In the hippocampus, PACAP has been demonstrated to facilitate synaptic transmission (Roberto & Brunelli, 2000). Additionally, PACAP causes membrane potential depolarisation and an increase in cell firing rate in hippocampal pyramidal cells (Di Mauro *et al.*, 2003). The effect of PACAP receptor activation on the activity of specific subtypes of K^+ channels has begun to be studied in the cerebellum, where PACAP inhibits delayed rectifier K^+ channels (Mei *et al.*, 2004) and activates Ca^{++} dependent K^+ channels of the BK subtype (Ster *et al.*, 2007). Our study shows that PACAP modulates sI_{AHP} in CA1 pyramidal cells and therefore PACAP also modulates neuronal firing in the CA1 region of the hippocampus in rats. This poses the question of the functional role of PACAP in the hippocampus, the site of spatial memory in mammals (Shapiro & Eichenbaum, 1999; Moser & Paulsen, 2001). I suggest that PACAP, released from CA3 onto CA1 pyramidal cells, modulates the firing of CA1 pyramidal cells primarily by suppressing sI_{AHP}, the current that underlies sAHP. Zelcer and colleagues (2006) have shown that rule learning in an olfactory discrimination task is accompanied by reduced sAHP amplitude and enhanced excitability. Furthermore, once sAHP suppression was elicited in CA1 pyramidal neurons, rats displayed an enhanced learning capability in the Morris Water maze, a novel task (Zelcer *et al.*, 2006). These results indicate that rule learning is associated with sI_{AHP}/sAHP suppression. Therefore, it could be predicted that neuromodulators that inhibit sI_{AHP}/sAHP and thus increase neuronal excitability, would have an impact on the plastic processes underlying learning and memory. The suppressive effect of muscarinic agonists on hippocampal sI_{AHP} (Benardo & Prince, 1982a; Cole & Nicoll, 1983, 1984; Charpak *et al.*, 1990) has been shown to be mediated by activation of M_3 receptors (Rouse *et al.*, 2000b) signalling to $G\alpha_q$ (Krause *et al.*, 2002). Interestingly, behavioural paradigms associated with an increase in

acetylcholine release in the hippocampus such as eyeblink conditioning (Meyer *et al.*, 1996) are also associated with a reduced post-burst AHP (Moyer *et al.*, 1996). Noradrenaline has been demonstrated to inhibit sAHP (Madison & Nicoll, 1982; Haas & Konnerth, 1983) through activation of β adrenoceptors. Activation of β adrenoceptors has also been shown to facilitate the induction of LTP (Thomas *et al.*, 1996). LTP has been proposed as a possible cellular correlate to learning and memory (Bliss & Collingridge, 1993). Therefore, PACAP release from CA3 pyramidal cells, leading to suppression of sI_{AHP} in CA1 pyramidal cells, may be involved in the process of hippocampal learning and memory formation in rats.

Chapter 5: Does a signalling domain underlie the monoaminergic modulation of sI_{AHP}?

5.1.0: Introduction

5.1.1: A kinase-phosphatase balance modulates sI_{AHP}

The inhibition of the sI_{AHP}/sAHP, by monoaminergic neurotransmitters, such as noradrenaline, serotonin, and dopamine, is known to be mediated by a pathway involving the activation of PKA (Pedarzani & Storm, 1993, 1995a). However, it was noticed that in the absence of exogenous application of neurotransmitters or synaptic stimulation, inhibiting phosphatases in CA1 pyramidal cells resulted in a gradual reduction in amplitude of the sI_{AHP} (Pedarzani & Storm, 1993; Pedarzani *et al.*, 1998). This indicates that phosphorylation/dephosphorylation regulates the amplitude of the sI_{AHP} in the absence of neurotransmitters/synaptic stimulation. Co-application of a kinase and a phosphatase inhibitor prevented the rundown of the sI_{AHP} seen with sole application of the phosphatase inhibitor (Pedarzani *et al.*, 1998). This indicated that the sI_{AHP} was regulated by the tonic activity of a kinase and a phosphatase under basal conditions (i.e. in the absence of neurotransmitters/synaptic stimulation). Through use of the selective PKA inhibitor, Rp-cAMPS, the kinase responsible for the basal modulation of sI_{AHP} was identified as PKA (Pedarzani *et al.*, 1998). Further experiments demonstrated tonic activation of an AC and cAMP-phosphodiesterase type 1V (Pedarzani *et al.*, 1998). Thus a balance between basally active AC/cAMP/PKA pathway and protein phosphatases exists in CA1 pyramidal neurons and is responsible for setting the amplitude and modulating the sI_{AHP}. This indicates that the signalling components that modulate sI_{AHP} might lie in close proximity to each other and thus a signalling complex may underlie the modulation of sI_{AHP}.

5.1.2: A β_2 adrenoceptor signalling complex in neurons

There is evidence that a localised signalling complex underlies β_2 adrenoceptor signalling in hippocampal neurons. The signalling complex consists of a β_2 adrenoceptor, an unidentified AC, PKA, voltage gated L type Ca^{++} channel (Cav 1.2), and a protein phosphatase (PP2A) (Davare *et al.*, 2000; Davare *et al.*, 2001). The functional co-localisation of the β_2 adrenoceptor complex was demonstrated in primary hippocampal cultures. An increase in L type voltage gated Ca^{++}

channel activity was visualised in cell-attached patches when a β_2 agonist was included in the pipette solution (Davare *et al.*, 2001). Thus all components of the β_2 adrenoceptor signalling cascade are brought in close proximity to the receptor allowing highly localised signal transduction. This was one of the first demonstrations that highly localised signal transduction triggered by G-protein-coupled receptors through a signalling domain occurred in neurons.

5.1.3: Is there specificity in the modulation of sI_{AHP} by the different monoaminergic neurotransmitters?

The monoaminergic neurotransmitters (MAs) noradrenaline, dopamine and serotonin all suppress the $sI_{AHP,}$ resulting in an increase in neuronal excitability. The MAs converge on the sI_{AHP} through a similar signal transduction pathway, the cAMP/AC/PKA pathway. This triggered the question as to whether different MAs act in a specific manner by using signalling domains with different sub-cellular locations and molecular compositions in CA1 pyramidal neurons. This could be investigated in several different ways. The signal transduction cascade underlying the MA modulation of the sI_{AHP} has several steps. Each step has the possibility to confer specificity to the signal transduction cascade.

In step 1, the MA binds to its receptor on the CA1 pyramidal cell membrane. The sI_{AHP} is modulated by agonism at several MA receptors with different subcellular distributions. For example, the $5HT_4R$ (Torres *et al.*, 1994) and $5HT_7R$ (Tokarski *et al.*, 2003) are both known to suppress sI_{AHP} and are both expressed at the soma of CA1 pyramidal cells (Bickmeyer *et al.*, 2002). Meanwhile, the group 1 dopamine receptors D_1 and D_5 show a mainly dendritic expression in the pyramidal cells of the hippocampus (Bergson *et al.*, 1995). D_1 receptors are preferentially expressed in the dendritic spines whilst the dendritic shafts express mainly D_5 receptors (Bergson *et al.*, 1995). Therefore the sub-cellular distribution of the receptors relative to the sAHP channel could confer the specificity in the signal transduction pathway of the different MA neurotransmitters.

The second step in the MA inhibition of sI_{AHP} involves the activation of AC (Madison & Nicoll, 1982, 1986b). There are nine membrane bound ACs to date, with five AC isoforms expressed in the CA1 region of the hippocampus: AC1,

AC2, AC4, AC8 and AC9 (Matsuoka *et al.*, 1997; Baker *et al.*, 1999; Muglia *et al.*, 1999). All ACs are stimulated by the G protein: $G\alpha_s$, in expression systems. However, each AC has different regulatory properties and expression patterns (for review see Hanoune & Defer, 2001). For example, AC4 is expressed post-synaptically along the apical dendrite and cell bodies in CA1 pyramidal neurons and is synergistically stimulated by the G protein $\beta\gamma$ subunits released by activation of G_i coupled receptors (Baker *et al.*, 1999), whereas AC1 and AC8 are stimulated by an increase in intracellular Ca^{++} (Choi *et al.*, 1992; Nielsen *et al.*, 1996) and are expressed in the synaptic spines of hippocampal pyramidal neurons (Wang *et al.*, 2003; Conti *et al.*, 2007). Therefore because the MA receptors and the different isoforms of AC show different subcellular expression patterns, it is possible that the molecular identity of the AC could confer specificity to the inhibition of sI_{AHP} by different MAs. It would be expected that MAs whose receptors show a mainly somatic expression pattern e.g. 5HT receptors, would couple to ACs with a somatic expression e.g. AC2/AC4, whilst receptors with a dendritic expression pattern e.g. dopamine receptors, would couple to ACs with a dendritic expression pattern e.g. AC1, AC8.

5.1.4: The Ca^{++} stimulatable ACs

AC1 and AC8 are stimulated by Ca^{++} in a calmodulin (CaM) dependent manner. AC1 is stimulated by Ca^{++}/CaM in intact cells with a half maximal stimulation at ~ 150-200 nM (Choi *et al.*, 1992). AC8 has a half maximal activation by Ca^{++} at ~ 800 nM (Nielsen *et al.*, 1996). The resting cytosolic Ca^{++} concentration is ~ 100 nM and rises to 0.8-1 μM upon triggering of Ca^{++} elevation mechanisms (Willoughby & Cooper, 2007). Therefore, AC1 is activated just above resting Ca^{++} in neurons and is, therefore, a high affinity Ca^{++} sensor, whilst it is predicted that AC8 will only be activated when high Ca^{++} concentrations are achieved.

5.1.5: Distribution and subcellular localisation of AC1 and AC8 in the CA1 region of the hippocampus

In situ hybridisation techniques have demonstrated expression of both AC1 and AC8 in the CA1 region of the adult mouse hippocampus (Xia *et al.*, 1991; Cali *et*

al., 1994; Nicol *et al.*, 2005; Visel *et al.*, 2006). Experimenters have found difficulty in studying AC protein expression until recently. This is because the available antibodies were not sensitive or specific enough to allow finer descriptions of protein expression (Willoughby & Cooper, 2007). However, it has been demonstrated that AC1 and AC8 proteins are both expressed in the CA1 region of the hippocampus. Initial evidence that ACs were expressed in dendritic spines came from a study that utilised an antibody that recognised all AC isoforms (Mons *et al.*, 1995). Since then, it has been demonstrated that, using a tagged construct expressed in hippocampal primary cell cultures, AC8 is directed both to the axons and dendrites and is enriched in synapses in hippocampal neurons (Wang *et al.*, 2003). Co-localisation between AC1 and PSD-95 in the CA1 region (Conti *et al.*, 2007) indicates that AC1 is also localised in the dendritic spines in the CA1 neurons.

5.1.6: The role of the Ca^{++} stimulatable ACs in learning and memory

The drosophila mutant rutabaga has a deficit in associative learning and lacks calcium stimulatable adenylate cyclase activity (Dudai & Zvi, 1984, 1985). To investigate the role of the Ca^{++} stimulatable ACs in learning and memory in mammals, both single mouse knockouts and a double knockout (DKO) have been generated for AC1 and AC8. AC1 and AC8 single knockout mice each show a 50% reduction in Ca^{++} stimulatable AC activity (Wu *et al.*, 1995), whilst no Ca^{++}/CaM stimulatable AC activity is detectable in the DKO brain.

AC1 KO mice show no apparent differences in the gross morphology of the hippocampus (Villacres *et al.*, 1995). AC1 KO mice show normal perforant path LTP, early phase LTP at the Schaffer collateral-CA1 synapse and normal paired pulse facilitation (Villacres *et al.*, 1998). However, mossy fibre LTP is substantially reduced in AC1 KO mice (Villacres *et al.*, 1998). Although AC1 KO mice showed normal learning ability to find a hidden platform compared with WT, there was significant difference in the transfer test conducted at the end of training. In the transfer test when the hidden platform was removed, while WT swam directly to the target quadrant containing the hidden platform, AC1 KO

mice spent less time in the target quadrant (Wu *et al.*, 1995). This suggests that the AC1 KO mice show a deficit in spatial memory.

AC8 KO mice display normal hippocampal morphology. Although basal synaptic transmission is intact, AC8 KO mice showed impaired paired pulse facilitation and mossy fibre LTP at the mossy fibre synapse. In contrast, AC8 KO mice displayed normal perforant path LTP (Wang *et al.*, 2003) and Schaffer collateral-CA1 LTP (Wong *et al.*, 1999). AC8 KO mice display normal passive avoidance and contextual learning (Wong *et al.*, 1999).

The double KO of AC1 and AC8 (DKO) shows no obvious gross abnormalities in the hippocampal morphology. However the DKO shows a severe impairment in the form of LTP that requires *de novo* gene expression (L-LTP) at the Schaffer collateral-CA1 synapse that can be rescued through application of forskolin, an AC activator (Wong *et al.*, 1999). Behaviourally, DKO mice show a memory deficit in passive avoidance tests and contextual learning. Normal passive avoidance learning could be restored through direct administration of forskolin (through a cannula) to area CA1 in vivo (Wong *et al.*, 1999).

5.1.7: Is there a role for the sI_{AHP} suppression in hippocampus dependent learning?

Various pharmacological manipulations known to suppress $sI_{AHP,}$ also faciliatate the induction of LTP by weak stimuli (Sah & Clements, 1999). For example, activation of β adrenoceptors facilitates LTP induction in a stimulation paradigm that does not normally induce LTP in the absence of β receptor agonists (Katsuki *et al.*, 1997). Concomitantly, activation of β adrenoceptors is also known to suppress sI_{AHP} leading to an increase in excitability (Madison & Nicoll, 1986a), which may underlie the facilitation of LTP. Furthermore, training-induced suppression of sAHP has been demonstrated in hippocampal dependent learning paradigms e.g. spatial learning (Oh *et al.*, 2003), odour discrimination tasks (Zelcer *et al.*, 2006) and trace eye blink conditioning (Disterhoft *et al.*, 1986). Taken together, these results suggest a possible role for the cAMP/AC/PKA pathway in hippocampal dependent learning tasks.

In contextual fear conditioning, subjects learn to fear a context e.g. a training cage, because of its temporal association with an aversive stimulus e.g. a foot shock. When the subject is exposed again to the same context, it exhibits a fear response e.g. freezing. This indicates that the context is a cue for fear memory retrieval. Contextual fear conditioning is thought to be a hippocampal dependent process that may become hippocampal independent with time (Kim & Fanselow, 1992). The role of the β-adrenergic pathway leading to activation of PKA in the retrieval of contextual fear conditioning has been demonstrated in the hippocampus (Abel *et al.*, 1997; Murchison *et al.*, 2004). There is evidence that the genetic manipulations that affect contextual fear conditioning, also result in a suppression of L-LTP (Abel *et al.*, 1997; Murchison *et al.*, 2004). Furthermore, contextual fear retrieval and L-LTP are also disrupted in the AC1/AC8 DKO (Wong *et al.*, 1999).

5.2: Aims and objectives

Hippocampal dependent learning paradigms and application of β-adrenergic agonists cause sI_{AHP}/sAHP suppression. The cAMP/AC/PKA pathway is implicated in the signal transduction cascades that mediate both contextual fear conditioning and the β-adreneragic modulation of sI_{AHP}/sAHP. Given that the pathway mediating contextual fear conditioning is disrupted in the double knockout for AC1 and AC8 (DKO) and the role of β adrenoceptors has been demonstrated in contextual fear conditioning in the hippocampus, it was decided to investigate the involvement of AC1/AC8 in the modulation of sI_{AHP} by the β-adrenergic agonist isoproterenol. In order to address this, the inhibition of sI_{AHP} by isoproterenol was compared in DKO and wild type (WT) mice.

The second question of whether all monoamines couple to the same isoform of AC, resulting in suppression of the $sI_{AHP,}$ arose because isoproterenol, dopamine and 5HT all suppress the sI_{AHP}/sAHP in a PKA dependent manner. A possible locus for the specificity of the cascades used by the different neurotransmitters is at the level of the molecular identity of the AC. A first step in addressing this question was to determine if the inhibition of sI_{AHP} by serotonin or dopamine also involved the activation of AC1/AC8.

5.3.0: Results

In order to investigate the role of Ca^{2+}-sensitive ACs in mediating the monoaminergic suppression of sI_{AHP}, the monoaminergic modulation of sI_{AHP} between DKO and WT mice has been compared. The effect of isoproterenol on sI_{AHP} has been reported to be reversible depending on the length of drug application, so that a prolonged exposure to isoproterenol (~10 mins) does not result in recovery (Grabauskas *et al.*, 2007). In the experiments presented here, the amplitude of the sI_{AHP} was allowed to stabilise after the maximal effect on the sI_{AHP} for at least three minutes to ensure a steady state had been reached. Therefore no recovery information was obtained in these experiments.

5.3.1: Monoamines (MAs) suppress sI_{AHP} in a concentration dependent manner in mouse CA1 neurons

In order to investigate the role of AC1 and 8 in the modulation of the sI_{AHP} by MAs, the modulation of the sI_{AHP} by MAs needed to be characterised first in mice. Whole cell patch clamp recordings were obtained from CA1 pyramidal cells. Recordings were obtained in the presence of TTX and TEA in order to block voltage-gated sodium channels and voltage and calcium activated (BK) potassium channels, thus promoting the generation of a calcium spike during the depolarising step. In some cells, the depolarising step was increased from +10 mV for 100 ms, to +30 mV for 200 ms. Under these conditions, 200 ms long depolarising pulses elicited a sI_{AHP} with a mean amplitude of 74.9±10.9 pA (n=22). In most cells measured, the apamin sensitive I_{AHP} coexisted and in some cases partially overlapped with the rising phase of sI_{AHP} (Fig. 21A, left panel). In order to distinguish the peak of the sI_{AHP}, apamin (50 nM) was included in the bath solution in some experiments (Fig. 21A, right panel).

Concentration response curves were obtained for the effect of the β-adrenoceptor agonist isoproterenol and serotonin on the sI_{AHP}. 1 μM isoproterenol was shown to be sufficient to completely inhibit the sI_{AHP} in rat CA1 neurons (Pedarzani & Storm, 1993). However, in mouse, 1 μM isoproterenol led to a 70.1±5.6 % inhibition of sI_{AHP} (n=5, $p<0.0005$, paired t test) (Fig. 21B and C). The effect of

isoproterenol on sI_{AHP} was significant and concentration dependent between 10 nM and 5 μM (Fig 21D). Isoproterenol has been reported to enhance voltage-gated Ca^{++} channel activity in hippocampal neurons (Gray & Johnston, 1987). However at the concentrations used in this study, isoproterenol has been reported to lead to sI_{AHP} suppression without affecting the concomitant Ca^{++} transients or the steady state intracellular Ca^{++} concentration (Knopfel *et al.*, 1990). Therefore the effect of isoproterenol on the sI_{AHP} cannot be attributed to an indirect effect of isoproterenol on Ca^{++} influx.

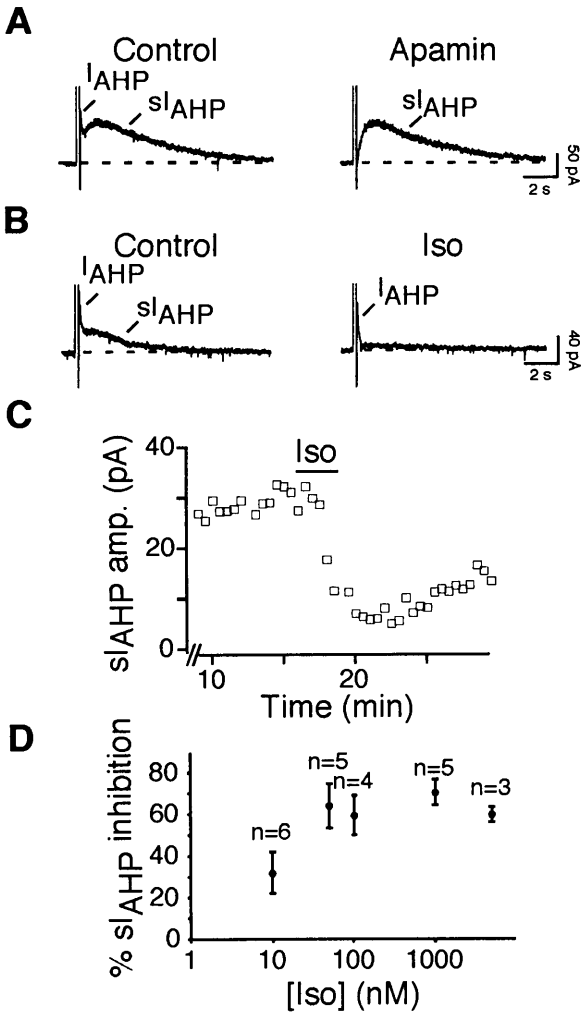

Figure 21: Effect of the β-adrenergic agonist isoproterenol on neuronal sI_{AHP} in mouse CA1 pyramidal neurons

A, I_{AHP} and sI_{AHP} were measured in CA1 pyramidal neurons in response to 200 ms-long depolarising pulses activating calcium influx through voltage-gated calcium channels (left panel). I_{AHP} was blocked by the SK-channel blocker apamin (50 nM) leaving the

remaining, unaffected sI_{AHP} (right panel). Recordings were performed in the presence of 1 mM TEA and 0.5 μM TTX.

B, sI_{AHP} is inhibited by isoproterenol (1 μM; Iso) leaving the remaining I_{AHP} (right panel).

C, Time course of the action of isoproterenol (1 μM) on the amplitude of sI_{AHP}. Data sampled once every 30s. Solid bar depicts isoproterenol application. Same cell as in B.

D, Graph showing the concentration dependent action of isoproterenol. Each concentration of isoproterenol resulted in significant inhibition of sI_{AHP} (5 μM; 59.7±2.9 %, n=3: 1 μM; 70.1±5.6 %, n=5: 100 nM; 59.3±8.1 %, n=4: 50 nM; 66.0±8.1 %, n=5: 10 nM; 31.8±9.0 %, n=6). Data points represent mean±SEM; n denotes the number of experiments for each concentration. Statistical significance was determined as $p<0.05$.

Serotonin activates different receptors in CA1 pyramidal cells. The serotonin-mediated inhibition of sI_{AHP} occurs via activation of $5HT_4$ receptors (Andrade & Chaput, 1991; Torres *et al.*, 1994) and $5HT_7$ receptors (Tokarski *et al.*, 2003). Fig. 22A shows the inhibition of sI_{AHP} by serotonin in mouse CA1 pyramidal cells. Application of 5 μM serotonin results in a 73.5±11.2 % inhibition of sI_{AHP} (n=4; $p<0.005$; one sample t test). However, serotonin also activates GIRK channels through agonism at $5HT_{1A}$ receptors. Fig 22B shows the effect of 5 μM serotonin on the holding current of CA1 pyramidal neurons. Application of serotonin (5 μM) results in an outward (hyperpolarising) shift in holding current from 69.8±11.0 pA to 112.5±34.9 pA (n=4) that is caused by the opening of GIRK channels. The activation of GIRK channels has a shunting effect on the voltage clamp circuit i.e. it provides a low resistance connection between the current sink and current source, thus forming an alternative pathway for a portion of current flow. This results in inefficient voltage clamping, so that the actual voltage achieved across the cell membrane does not reach the command voltage from the amplifier. Therefore, the voltage dependent calcium influx, which activates sI_{AHP}, is reduced and this results in a reduction of sI_{AHP}. In order to prevent the activation of GIRK channels, further experiments with serotonin were conducted in the presence of 1 μM WAY 100135, a $5HT_{1A}$ receptor antagonist (Cliffe *et al.*, 1993; Routledge, 1996). Fig. 22D shows that in experiments with serotonin in the presence of WAY 100135 there was little change in holding current. In contrast to Fig. 22B where the application of serotonin resulted in an outward

(hyperpolarising) shift in holding current, in the presence of WAY 100135, there was an inward (depolarising) shift from 88.9±22.4 pA to 69.5±12.9 pA (n=3). This inward shift in holding current in the presence of WAY 100135 could be attributed to a direct effect of cAMP on the HCN channels that underlie I_h leading

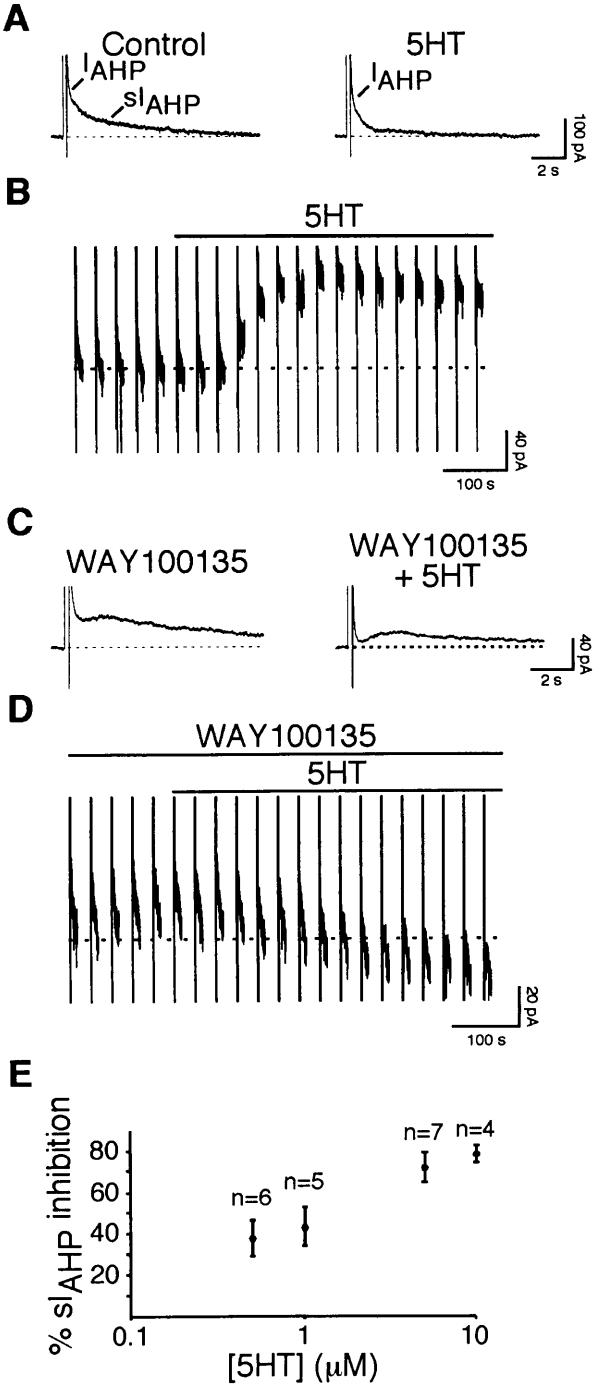

Figure 22: Effect of serotonin on $5HT_{1A}$ and $5HT_4$ receptors in CA1 pyramidal cells

A, sI_{AHP} is inhibited by serotonin (5 μM; 5HT) leaving the SK-mediated I_{AHP}.

B, Voltage-clamp recording of the outward current underlying the hyperpolarising response to 5HT (5 μM) mediated by activation of $5HT_{1A}$ receptors in CA1 pyramidal. The *vertical lines* correspond to depolarizing pulses used to elicit sI_{AHP} once every 30 sec. The *dotted line* represents the baseline holding current before the application of 5HT. The solid bar represents the 5HT application. Same cell as in ***A***.

C, Effect of 5HT (5 μM) on the sI_{AHP} in the presence of the $5HT_{1A}$ receptor antagonist WAY 100135 (1 μM).

D, The $5HT_{1A}$ receptor antagonist WAY 100135 inhibits the outward current elicited by 5HT through activation of GIRK channels and unmasks an inward current. *Vertical lines* and *dotted line* as in ***B***; the solid bars show the application of WAY100135 and 5HT. The cell that was used in ***C*** has also been used in ***D***.

E, Graph showing the concentration dependent effect of 5HT on sI_{AHP} in CA1 pyramidal cells in the presence of WAY 100135. Each concentration of 5HT resulted in significant inhibition of sI_{AHP} (10 μM; 78.4±4.1 %, n=4: 5 μM; 71.4±7.2 %, n=7: 1 μM; 43.0±9.2, n=5: 0.5 μM; 37.6±8.6 %, n=6). Data points represent mean±SEM; n denotes the number of experiments for each concentration. Statistical significance was determined as $p<0.01$.

to greater HCN channel activation. Application of 5 μM serotonin in the presence of WAY 100135 resulted in 81.3±2.5 % inhibition of sI_{AHP} (n=2; $p<0.05$; one sample t test; Fig. 22C) that is not significantly different from the sI_{AHP} inhibition elicited by sole application of serotonin ($p=0.86$; Mann Whitney test). Figure 22E illustrates the dose dependence of the effect of serotonin on the amplitude of the sI_{AHP}.

Application of serotonin results in a reduction in Ca^{++} influx associated with the action potential in hippocampal neurons (Sandler & Ross, 1999). A reduction in Ca^{++} influx may partially explain the sI_{AHP} suppression by serotonin seen in this study. However, in neocortical pyramidal neurons, the serotonergic suppression of high voltage-activated Ca^{++} channel currents has been attributed to the activation of the $5HT_{1A}$ receptor (Foehring, 1996). The suppression of sI_{AHP} persists in the presence of the $5HT_{1A}$ receptor antagonist: WAY 100135, at a concentration that was sufficient to block the GIRK channel activation that is also associated with $5HT_{1A}$ receptor activation. Therefore, the effect of serotonin on sI_{AHP} in the

presence of WAY 100135 cannot be explained by serotonergic modulation of voltage-gated Ca^{++} channels.

5.3.2: Electrical characteristics of cells recorded from WT and DKO

The primary aim of this part of the study was to investigate the role of the Ca^{++} stimulatable AC in the monoaminergic modulation of sI_{AHP}. To achieve this aim, C57BL/6J wild-type mice (WT) were compared with double knock out mice lacking both AC1 and AC8 (DKO). The next step of this investigation was to establish whether there was a difference in the electrical characteristics of DKO CA1 pyramidal neurons compared to WT.

Whole cell patch clamp recordings of sI_{AHP} were obtained from both DKO and WT adult mice under two different conditions. These conditions were (i) TTX (0.5μM) and TEA (1 mM) applied in the bath and (ii) standard ACSF. In TTX and TEA, a 200 ms long depolarising step generated a sI_{AHP} of 74.9±10.6 pA (n=20) in WT cells and 51.2±4.6 pA (n=11) in DKO cells. The mean sI_{AHP} amplitudes did not differ significantly between DKO and WT cells in TTX and TEA ($p=0.05$, unpaired t test with Welch correction; Fig. 23A). A 100-ms long depolarising pulse in standard ACSF resulted in a sI_{AHP} with mean amplitude of 23.2±2.7 pA (n=23) in WT cells, which was significantly different compared to DKO cells (30.8±2.9 pA, n=27, $p<0.05$, Mann Whitney test; Fig. 23B). The increased sI_{AHP} amplitude in DKO compared with WT could be attributed to differing basal concentrations of cAMP within the two groups. It has been demonstrated that there is basal modulation of the sI_{AHP} in hippocampal neurons (Pedarzani *et al.*, 1998). If it is assumed that there is basal production of cAMP in resting conditions, and some of this cAMP is produced by AC1/AC8, then it could be concluded that there is a reduced level of cAMP at rest in the DKO. Because sI_{AHP} is suppressed by cAMP-dependent PKA activation in hippocampal neurons (Pedarzani & Storm, 1993), a reduction in the basal concentration of cAMP could result in a sI_{AHP} of increased amplitude.

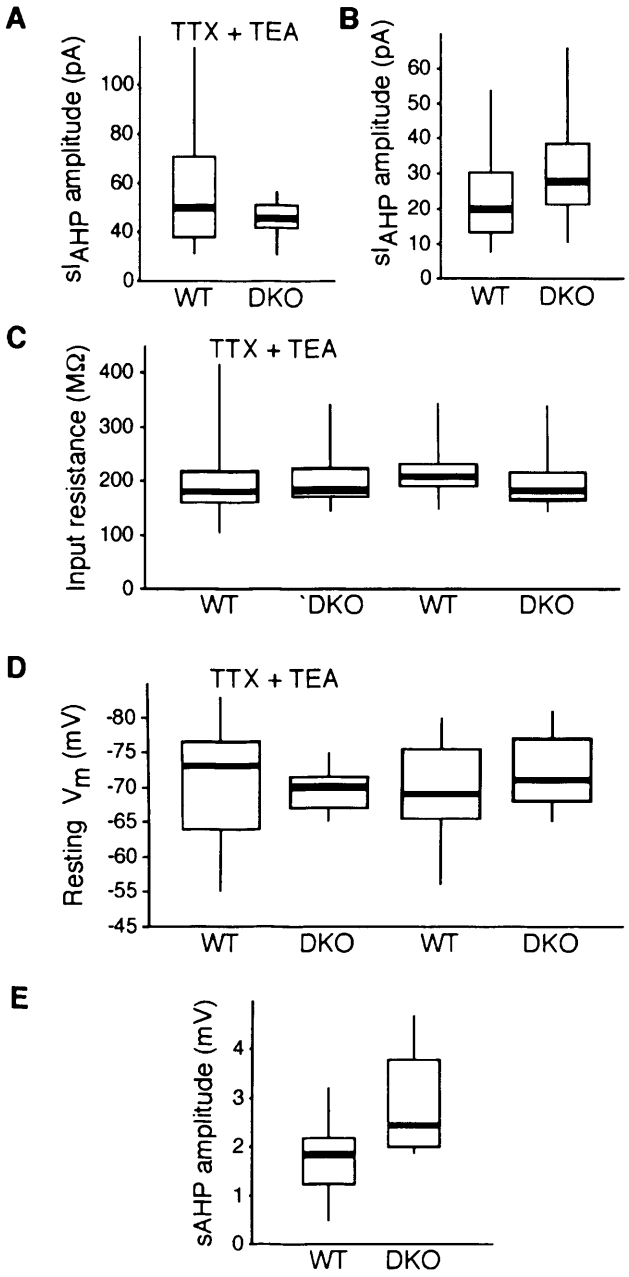

Figure 23: Comparison of the electrical characteristics of CA1 pyramidal neurons recorded from WT and DKO mice

A, Box plot depicting range of sI_{AHP} amplitudes recorded in WT and DKO in the presence of 0.5 μM TTX and 1 mM TEA in response to 200 ms-long depolarising pulses. The box represents the inter-quartile range, whilst the median is depicted as a solid line. The whiskers indicate the entire range of amplitudes. There is no significant difference between the sI_{AHP} amplitude recorded from WT (mean sI_{AHP} amplitude: 74.9±10.6 pA; n=20) and DKO CA1 pyramidal cells (mean sI_{AHP} amplitude: 51.2±4.6 pA; n=11; p=0.05; unpaired t test with Welch correction).

B, The sI_{AHP} was elicited by 100 ms-long depolarising pulses in standard ACSF. Under these conditions, the mean sI_{AHP} amplitude recorded from WT CA1 pyramidal neurons was 23.2±2.7 pA (n=23). The difference between the sI_{AHP} amplitudes recorded from WT and DKO (mean sI_{AHP} amplitude recorded from DKO cells: 30.8±2.9 pA; n=27) CA1 pyramidal neurons was significant ($p<0.05$; Mann Whitney test).

C, The input resistance was determined at the beginning of the experiment by 100 ms-long hyperpolarising steps from –50 mV to –55 mV. In the presence of 0.5 μM TTX and 1 mM TEA there was no significant difference between the input resistance measured from WT (mean input resistance: 193.2±15.8 MΩ; n=20) and DKO CA1 pyramidal neurons (204.1±16.9 MΩ; n=11; p=0.66;unpaired t test). The mean input resistance, measured from WT CA1 pyramidal neurons in standard ACSF, was 215.8±10.2 MΩ (n=23) compared with 197.5±9.5 MΩ (n=27; p=0.07; Mann Whitney test).

D, The resting membrane potential (V_m) was determined at the beginning of the experiment. The resting membrane potential recorded from WT CA1 pyramidal neurons (-65.6±1.8 mV; n=19) was similar to that recorded in neurons from DKO mice (-64.3±1.0 mV; n=11; p=0.52; unpaired t test with Welch correction) in the presence of TTX (0.5 μM) and TEA (1 mM). There was no significant difference between the resting membrane potential in WT (-64.7±1.5 mV; n=23) and DKO CA1 pyramidal neurons (-66.7±1.0 mV; n=27; p=0.41; Mann Whitney test) recorded in standard ACSF.

E, The sAHP was elicited by 400 ms-long depolarising current injections eliciting trains of action potentials. The mean sAHP amplitude in WT CA1 pyramidal neurons was 1.8±0.3 mV (n=9). This was significantly less that the mean SAHP amplitude recorded from DKO CA1 neurons (2.9±0.4 mV (n=7; $p<0.05$; unpaired t test).

Fig. 23C compares the range of input resistance recorded from WT and DKO CA1 pyramidal cells. The input resistance was measured by the administration of a 100 ms-long hyperpolarising step from –50 mV to –55 mV and was determined at the start of the experiment. The current flowing after complete charging of the membrane capacitance is a measure of the channels open at –55 mV, which is below the activation threshold of most voltage-gated channels. Therefore, most of the current flowing at –55 mV can be attributed to leak channels and used to calculate the input resistance according to Ohm's law. When recorded in the presence 1mM TEA and 0.5 μM TTX, the mean input resistance in WT cells was 193.2±15.8 MΩ (n=20) compared to 204.1±16.9 MΩ (n=11) in DKO cells. There

was no significant difference between the input resistance measured in WT and DKO animals ($p>0.6$, unpaired t test). Experiments were also conducted in standard ACSF to record the sI_{AHP} elicited by more physiological levels of calcium influx. Under these conditions, there was no significant difference between the mean input resistance recorded in WT cells (215.3±10.2 MΩ, n=23) and DKO cells (197.5±9.5 MΩ, n=27, p=0.07, Mann-Whitney test).

The resting membrane potential of each cell was determined at the beginning of the recording, immediately after achieving the whole cell configuration. The range of resting membrane potentials recorded from WT and DKO CA1 pyramidal neurons are depicted in Fig. 23D. In TTX and TEA, the mean resting membrane potential of WT cells was -65.6±1.8 mV (n=19). This was not significantly different to the membrane potential recorded in DKO cells (-64.3±1.0 mV, n=11, $p>0.5$, unpaired t test with Welch correction). There was no significant difference between the membrane potentials of DKO and WT mice measured in standard ACSF (Vm in WT: -64.7±1.5 mV, n=23; Vm in DKO: -66.7±1.0 mV, n=27; $p>0.4$; Mann-Whitney test).

To investigate the firing properties and after-potentials of WT and DKO CA1 neurons, short (400 ms-long) depolarising current injections, eliciting trains of action potentials, were delivered and followed by hyperpolarising potentials on termination of the current injection. The afterhyperpolarisation (AHP) consisted of two distinct phases: mAHP and sAHP. The mean amplitude of the sAHP in WT animals was 1.8±0.3 mV (n=9), and in KO animals 2.9±0.4 mV (n=7). There was significant difference between the amplitude of sAHP in WT and KO animals ($p>0.05$; Fig. 23E). The increase in sAHP in DKO, compared to WT cells, is consistent with the larger sI_{AHP} in DKO neurons in standard ACSF (Fig. 23B).

5.3.3: β-adrenergic modulation of sI_{AHP} in WT and KO animals

The primary aim of this section of the experiments was to investigate whether the activation of AC1/AC8 was responsible for the β adrenoceptor mediated suppression of sI_{AHP}. With this aim, the modulation of sI_{AHP} by isoproeternol was compared in WT and DKO cells. In order to avoid desensitisation of the β-adrenergic effect and operate in the optimal dynamic range, it was decided to

proceed with 50 nM isoproterenol, which gave a 66.0±8.1 % inhibition of sI_{AHP} in TTX and TEA (Fig. 21D).

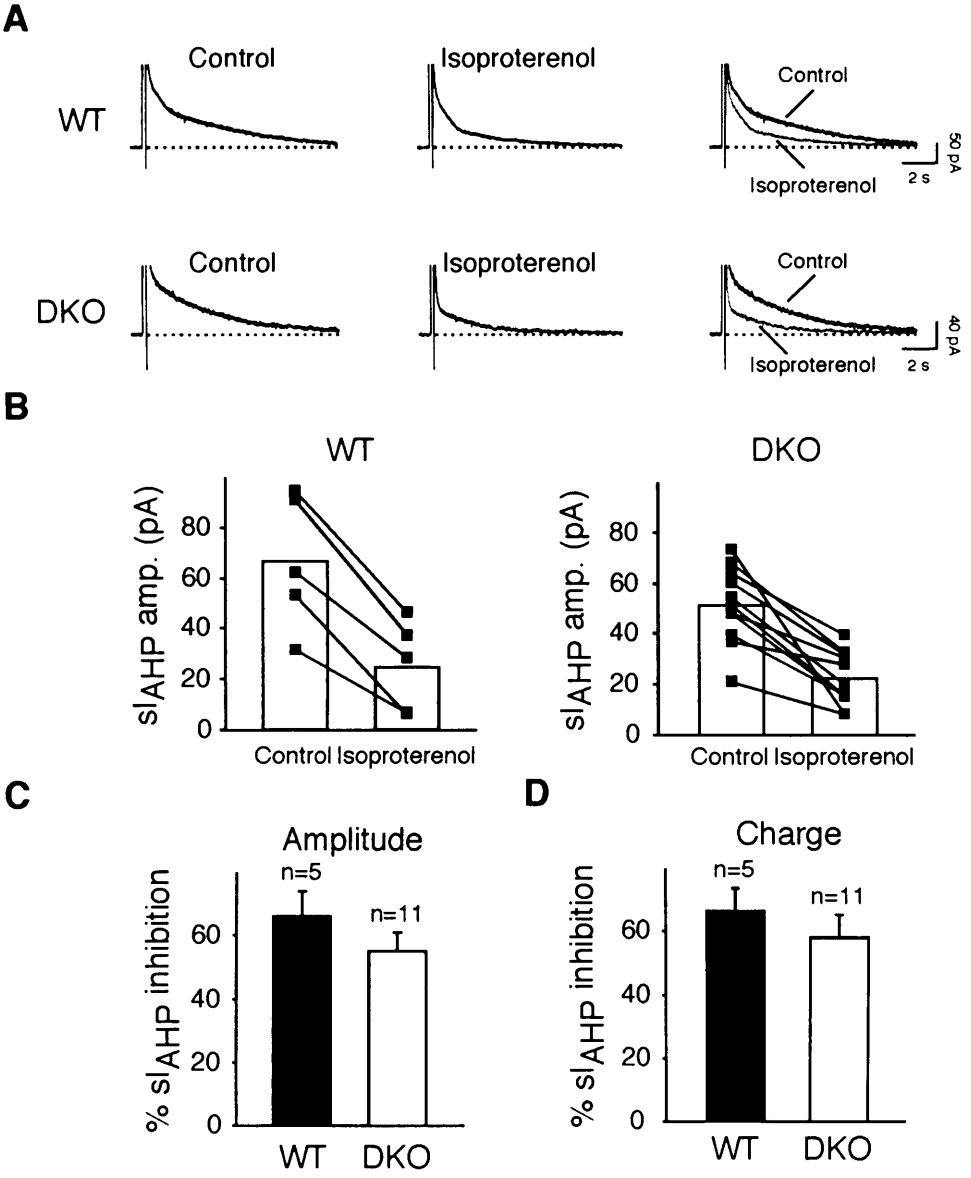

Figure 24: Modulation of sI_{AHP} by isoproterenol in DKO and WT animals

A, sI_{AHP} is inhibited by isoproterenol (50 nM) in wild-type (WT; top panel) and DKO mice (bottom panel). Experiments were conducted in the presence of 1 mM TEA and 0.5 μM TTX. Middle panels represent the effect of isoproterenol on sI_{AHP} at steady state in CA1 neurons from wild-type (upper middle panel) and DKO mice (lower middle panel). Control and isoproterenol traces are overlaid in the right panels to illustrate the isoproterenol-mediated sI_{AHP} suppression. Traces are averages of three consecutive sweeps, each sweep was elicited once every 30 s.

B, Graph showing the effect of 50 nM isoproterenol on the sI_{AHP} amplitude. Symbols represent the amplitude of sI_{AHP} in each single cell before and after the application of

isoproterenol WT (left panel) and DKO (right panel) mice. Bars represent the averaged data.

C, Isoproterenol (50 nM) produced a significant inhibition of sI_{AHP} amplitude in both WT and DKO CA1 neurons. (WT: 66.0±8.1 %, n= 5; DKO: 54.9±5.8, n=11). Bars and error bars represent mean±SEM. There was no significant difference between the effect of isoproterenol in WT and DKO CA1 pyramidal cells (p=0.25).

D, Application of 50 nM isoproterenol resulted in a significant inhibition of sI_{AHP} charge transfer in both WT and DKO CA1 neurons. (WT: 66.3±7.1 %, n=5; DKO: 58.1±6.6 %, n=11). Consistent with the effect of isoproterenol on sI_{AHP} amplitude, there was no significant difference between the isoproterenol mediated charge transfer inhibition between the two groups of animals (p=0.4). Bars and error bars represent mean±SEM.

Fig. 24A illustrates that delivery of a 200 ms long voltage step to +30 mV, resulted in an isoproterenol sensitive sI_{AHP}. The effect of 50 nM isoproterenol on sI_{AHP} in representative cells from WT (top panel) and DKO mice (bottom panel) is shown. In 5 WT cells, the mean sI_{AHP} amplitude was 66.4±13.1 pA (Fig. 24B, left panel). Application of 50 nM isoproterenol resulted in a significant inhibition of sI_{AHP} amplitude by 66.0±8.1 % (sI_{AHP} amplitude post isoproterenol application: 25.2±9.1 pA, p<0.005, paired t test) (Fig. 24B, and C). Fig. 24B (right panel) shows that the mean sI_{AHP} amplitude of DKO cells was 51.2±4.8 pA (n=11), and significantly reduced to 22.4±3.4 pA (n=11) on application of 50 nM isoproterenol (p<0.0001, paired t test). There was no significant difference between the effect of 50 nM isoproterenol in DKO and WT cells on sI_{AHP} amplitude (% sI_{AHP} inhibition in WT: 66.0±8.1 %, n=5; in DKO: 54.9±5.8 %, n=11, p=0.25; Fig. 24C) or charge (% sI_{AHP} inhibition in WT: 66.3±7.1 %, n=5; in DKO: 58.1±6.6 %, n=11, p=0.4; Fig. 24D) (unpaired t tests).

It could be argued that, due to the large variability in the data obtained with 50 nM isoproterenol, any potential difference between the effect of 50 nM isoproterenol in WT and DKO would be obscured. A low concentration of neurotransmitter could lead to variability in the data obtained because of the limitations of the practical technique employed. The neurotransmitter is added to the perfusion medium and the blind patch clamp technique offers little resolution about the depth of the cell being recorded from. Therefore, the actual

concentration of neurotransmitter applied to the cell is unknown and could vary with cell depth in the slice. It was decided to increase the concentration of isoproterenol in an attempt to reduce the variability. Additionally, these experiments would provide information on the involvement of AC1/AC8 in mediating the effect of saturating concentrations of β-adrenergic receptor agonist on the sI_{AHP}. Finally, these experiments were not conducted in the presence of TTX and TEA in order to gain information about the modulation of sI_{AHP} elicited by more physiological concentrations of Ca^{++}.

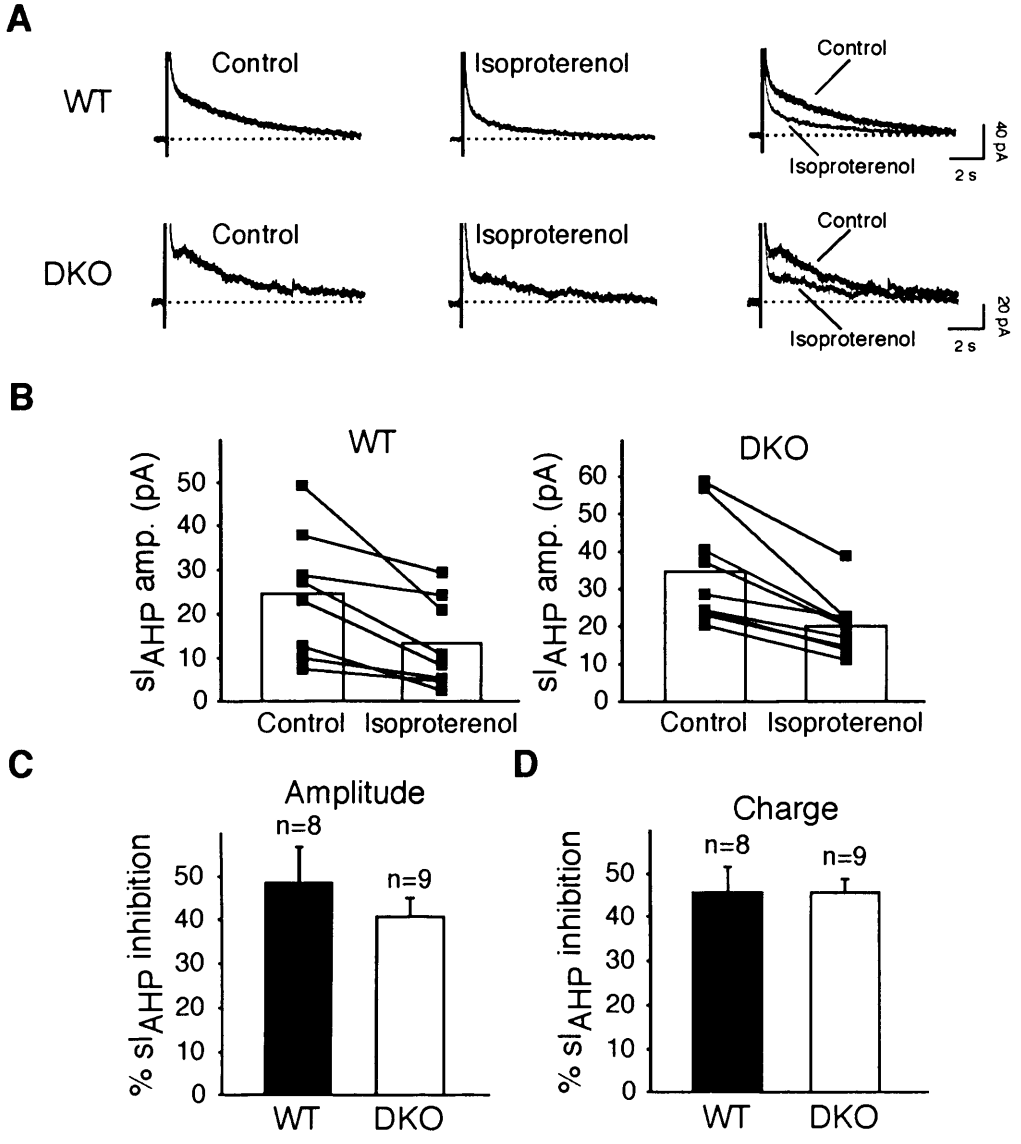

Figure 25: Isoproterenol mediated sI_{AHP} suppression is intact in DKO CA1 neurons

A, 100 ms-long depolarising pulses elicit a sI_{AHP} partly inhibited by isoproterenol (2 μM) in both WT (upper row) and DKO (lower row) cells. Recordings were conducted in standard ACSF, i.e. in the absence of TTX and TEA.

B, C, D The application of 2 μM isoproterenol results in a significant suppression of sI_{AHP} in both WT and DKO cells. In ***B***, symbols represent individual CA1 neurons from WT (left panel) and DKO mice (right panel); bars are averaged data. There was no significant difference between the effect of isoproterenol in WT and DKO on either sI_{AHP} amplitude (***C***, % inhibition WT: 48.4±7.7 %, n=8; DKO: 40.6±3.9, n=9; p=0.36, unpaired t test) or charge transfer (***D***, % inhibition WT: 45.8±5.0 %, n=8; DKO: 45.6±2.9 %, n=9; p=0.97, unpaired t test).

Application of 2 μM isoproterenol resulted in significant sI_{AHP} suppression in both WT and DKO cells. The mean sI_{AHP} amplitude in WT cells was 24.4±5.1 pA (n=8) prior to isoproterenol application. Isoproterenol inhibited the sI_{AHP} amplitude in WT cells by 48.4±7.7 % (n=8, $p<0.01$, paired t test) and charge transfer by 45.8±5.0 % (n=8, $p<0.01$, Wilcoxon matched-pairs signed-ranks test). In DKO cells, isoproterenol significantly suppressed the mean sI_{AHP} amplitude from 34.72±4.83 pA to 20.0±2.7 pA (n=9, $p<0.005$, paired t test). This corresponded to an inhibition of sI_{AHP} amplitude by 40.6±3.9 % (n=9) which was not significantly different from that in WT cells (p=0.36, unpaired t test, data not shown). Therefore, the modulation of sI_{AHP} in CA1 pyramidal cells by β-adrenergic receptor agonists appears to be intact in DKO mice. This implies that the β-adrenergic modulation of sI_{AHP} does not require the activation of AC1/AC8 in CA1 neurons.

5.3.4: Other MAs also modulate sI_{AHP}

The results presented here indicate that the β adrenergic-mediated sI_{AHP} suppression does not involve activation of AC1/AC8. However, other monoaminergic neurotransmitters, e.g. serotonin and dopamine, also converge on the cAMP-PKA pathway to inhibit sI_{AHP} (Pedarzani & Storm, 1993, 1995a). To test whether different monoaminergic neurotransmitters modulate the sI_{AHP} via different ACs, we compared their effects in WT and DKO animals. These experiments were not conducted in the presence of TTX and TEA. Monoamine concentrations were chosen that gave a near maximal effect on sI_{AHP}.

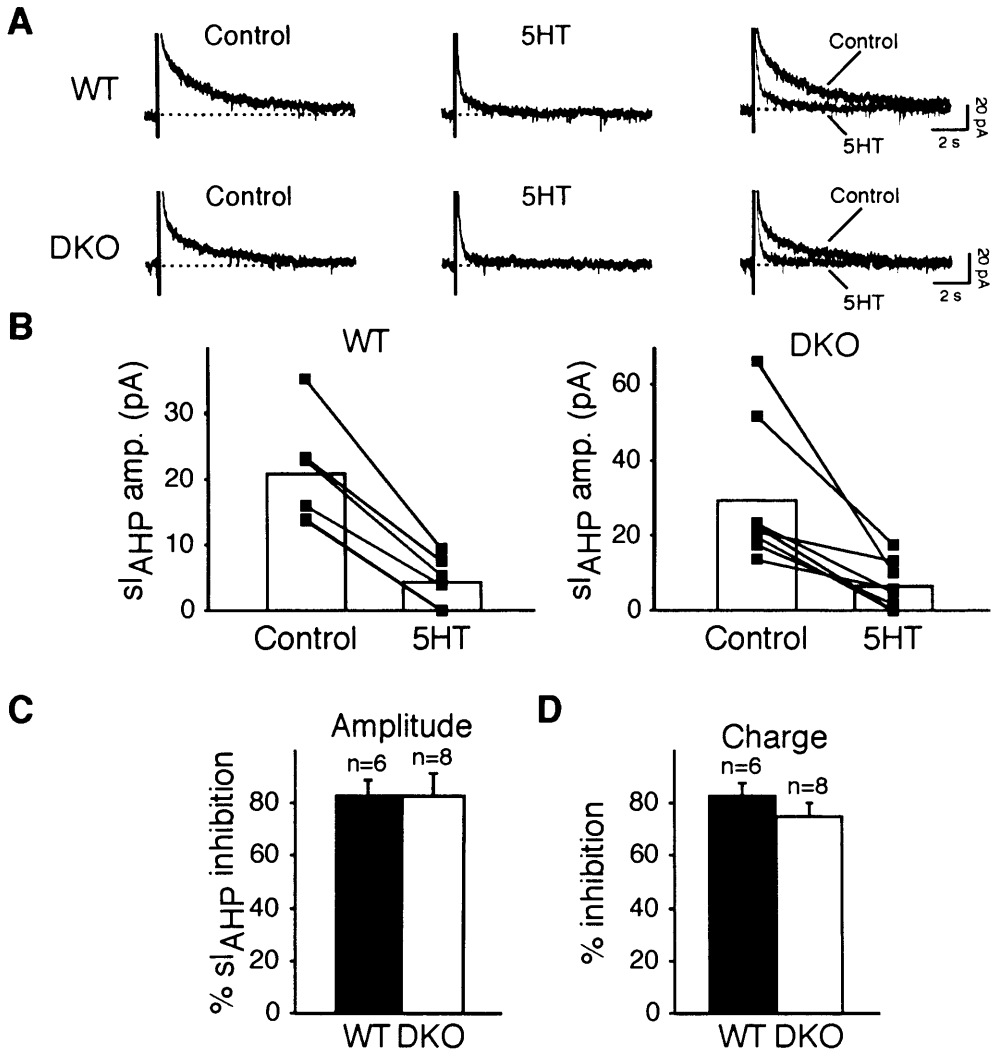

Figure 26: Modulation of sI_{AHP} by serotonin in DKO and WT animals

A, The sI_{AHP} recorded in standard ACSF is inhibited by 10 μM serotonin (5HT). The sI_{AHP} was elicited as previously described.

B, Graphs depicting the sI_{AHP} amplitude before and after application of serotonin (10 μM, 5HT) in WT (left panel) and DKO (right panel). Symbols represent individual CA1 neurons from WT (left panel) and DKO mice (right panel); bars are averaged data.

C, D, Bar diagrams showing the effect of serotonin on sI_{AHP} amplitude (***C***) and charge transfer (***D***). In WT cells, serotonin inhibited 82.1±5.8 % sI_{AHP} amplitude, and 82.2±4.6 % sI_{AHP} charge (n=6). This compares with 76.7±7.9 % inhibition of sI_{AHP} amplitude and 74.7±4.82% sI_{AHP} charge inhibition in DKO cells (n=8). There was no significant difference between the effect of serotonin on sI_{AHP} amplitude (p=0.53) or charge transfer (p=0.30) in WT and DKO cells (unpaired t tests).

A first set of experiments was conducted comparing the effect of 10 μM 5HT in cells from WT and DKO mice. There was no significant difference between the degree of suppression mediated by 10 μM serotonin on sI_{AHP} amplitude or charge in WT and DKO mice (% sI_{AHP} amplitude inhibition in WT: 82.1±5.8 %, n=6; in DKO: 76.7±7.9 %, n=8, p>0.6, unpaired t test; % sI_{AHP} charge inhibition in WT: 82.2±4.6 %, n=6; in DKO: 74.7±4.8 %, n=8, p>0.3, unpaired t test) (Fig. 26).

As previously mentioned, serotonin activates both 5-HT_4 (Torres *et al.*, 1994), $5HT_7$ (Tokarski *et al.*, 2003) and $5HT_{1A}$ (Andrade & Nicoll, 1987; Colino & Halliwell, 1987) receptors in CA1 pyramidal cells. The effect of serotonin on sI_{AHP} occurs through the activation of $5HT_4$ and $5HT_7$ receptors (Torres *et al.*, 1994; Tokarski *et al.*, 2003). In order to minimise the membrane potential hyperpolarisation caused by agonism at $5HT_{1A}$ receptors (Andrade & Nicoll, 1987; Colino & Halliwell, 1987) and resulting in GIRK channel activation (Luscher *et al.*, 1997), a second set of experiments was conducted in the presence of the $5HT_{1A}$ receptor antagonist WAY 100135. In all experiments, 1 μM WAY 100135 was applied to the bath at least fifteen minutes prior to 5HT application. Fig. 27 illustrates that application of 10 μM 5HT in the presence of 1 μM WAY 100135 results in sI_{AHP} suppression in cells from both WT and DKO. Panel A shows traces from representative cells before and after 5HT application when the sI_{AHP} has reached a steady state. In seven WT cells the mean sI_{AHP} amplitude significantly reduced from 22.6±4.4 pA to 12.8±3.2 pA (p<0.005, paired t test, Fig. 27B). This corresponded to 44.4±5.0 % sI_{AHP} amplitude inhibition (Fig. 27C) and 44.7±6.2 % sI_{AHP} charge inhibition (Fig. 27D). Application of 10 μM 5HT to ten DKO cells resulted in significant sI_{AHP} suppression from 32.1±3.5 pA to 20.0±3.2 pA (p<0.0001, paired t test, Fig. 27B). Statistical analysis revealed that there was no significant difference between the degree of serotonin-mediated sI_{AHP} inhibition in WT and DKO cells (% sI_{AHP} amplitude inhibition in DKO: 40.6±4.9 %, p>0.6, Fig. 27C; % sI_{AHP} charge inhibition in DKO: 37.7±4.3 %, p>0.3, Fig. 27D). These results indicate that there is no functional coupling between the $5HT_4$ and $5HT_7$ receptor and AC1/AC8.

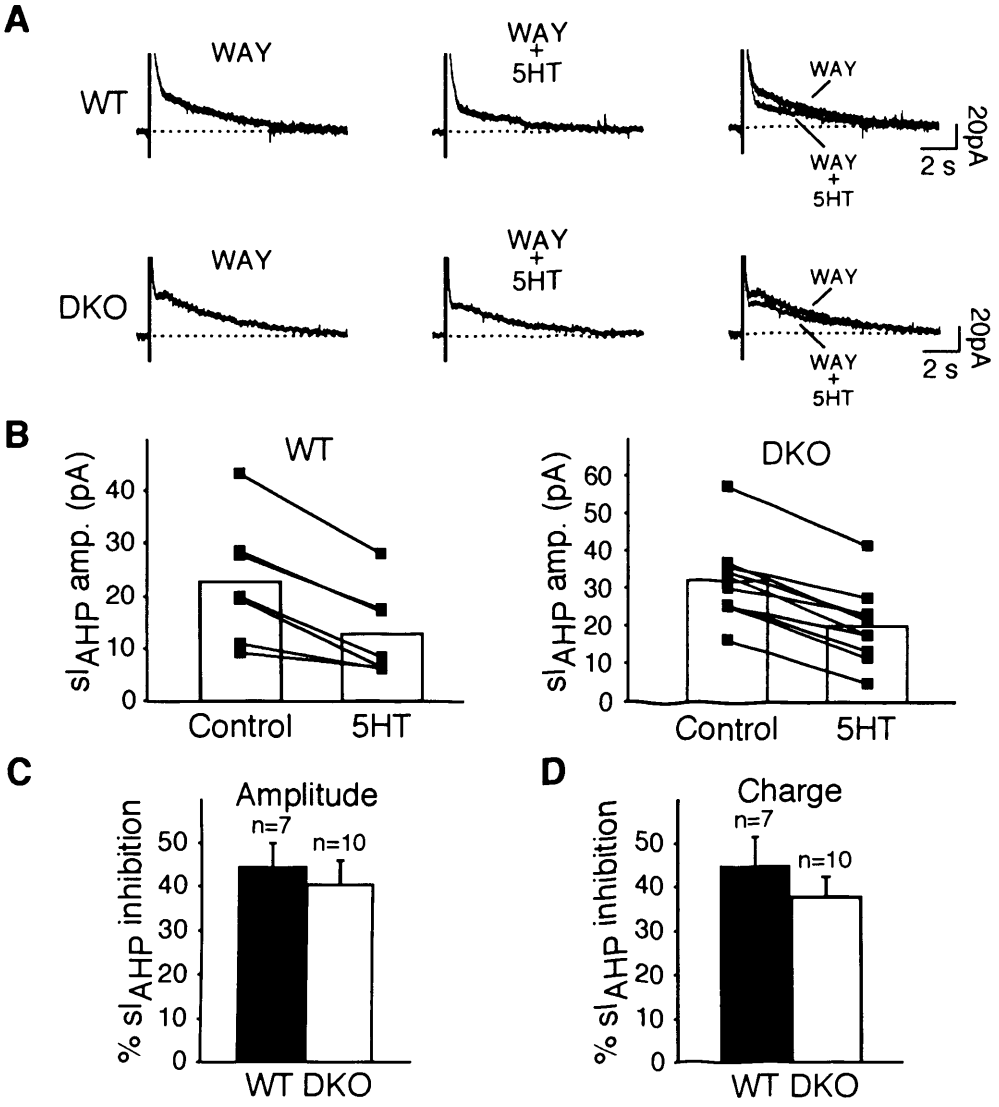

Figure 27: sI_{AHP} suppression by $5HT_4$ and $5HT_7$ receptors in DKO and WT animals

A, The effect of serotonin (5HT; 10 μM) on the sI_{AHP} in the presence of the $5HT_{1A}$ receptor antagonist WAY 100135 (WAY; 1 μM). Application of serotonin suppressed sI_{AHP} in both WT (upper row) and DKO cells (lower row). The sI_{AHP} was elicited as previously described.

B, Agonism at both $5HT_4$ and $5HT_7$ receptors leads to significant suppression of sI_{AHP} in both WT and DKO cells. Graphs illustrate the effect of serotonin on the sI_{AHP} amplitude. Symbols represent individual CA1 neurons before and after the application of serotonin in WT (left panel) and DKO cells (right panel). Bars represent averaged data.

C, D, The application of 10 μM serotonin in the presence of 1 μM WAY 100135 results in a significant suppression of sI_{AHP} in both WT and DKO cells. There was no significant difference between the effect of serotonin in WT and DKO on either sI_{AHP} amplitude (*C*, % inhibition WT: 44.4±5.0 %, n=7; DKO: 40.6±4.9 %, n=10; p=0.60) or charge transfer

(***D***, % inhibition WT: 44.7±6.2 %, n=7; DKO: 37.7±4.3 % n=10; p=0.35)(unpaired t tests).

In a third set of experiments, we tested dopamine, which was previously shown to cause sI_{AHP} and sAHP suppression in a cAMP and PKA-dependent manner in CA1 pyramidal neurons (Pedarzani & Storm, 1995a). To this date, no effect of dopamine on voltage-activated Ca^{++} channels in the hippocampus has been reported. However it has been reported that the dopaminergic suppression of the sAHP occurs independently of a change in the associated Ca^{++} potential (Malenka & Nicoll, 1986). It is therefore unlikely that the suppression of sI_{AHP} reported here can be attributed to a reduction in the amplitude of the Ca^{++} currents that activate sI_{AHP}. The effect of application of 30 μM dopamine in cells from WT and DKO was compared. Addition of 30 μM dopamine to WT mice resulted in significant suppression of sI_{AHP} (% sI_{AHP} amplitude inhibition: 47.7±4.5 %, n=9, $p<0.005$, paired t test, Fig. 28A, B and C; % sI_{AHP} charge inhibition: 58.0±2.9 %, n=9, $p<0.005$, paired t test, Fig. 28A and D). This is in agreement with previous studies conducted in rat (Malenka & Nicoll, 1986; Pedarzani & Storm, 1995a). The mean amplitude of sI_{AHP} in ten DKO cells prior to dopamine application was 28.5±3.9 pA compared to 20.2±3.0 pA post application (Fig. 28A and B). This sI_{AHP} suppression was significant in a paired t test ($p<0.0001$; Fig. 28C). However, there was a significant difference between the inhibition of sI_{AHP} amplitude induced by dopamine in CA1 neurons from WT and DKO mice (% sI_{AHP} amplitude inhibition in WT: 47.7±4.5 %, n=9; in DKO: 30.7±2.3 %, n=10, $p<0.005$; unpaired t test; Fig. 28C). Similarly, in WT cells dopamine inhibited sI_{AHP} charge by 58.0±2.9 % (n=9), compared with 36.6±4.0 % (n=10) in DKO cells ($p<0.001$, unpaired t test, Fig 28D).

These results indicate that activation of AC1/AC8 may contribute to the dopaminergic modulation of sI_{AHP}. Thus, there may be a level of specificity in the monoaminergic modulation of sI_{AHP}, in which different neurotransmitters couple to different ACs to mediate similar effects on sI_{AHP}.

So far the modulation of sI_{AHP} by MAs has been investigated. In the next section the modulation of the potential sAHP by MA will be investigated.

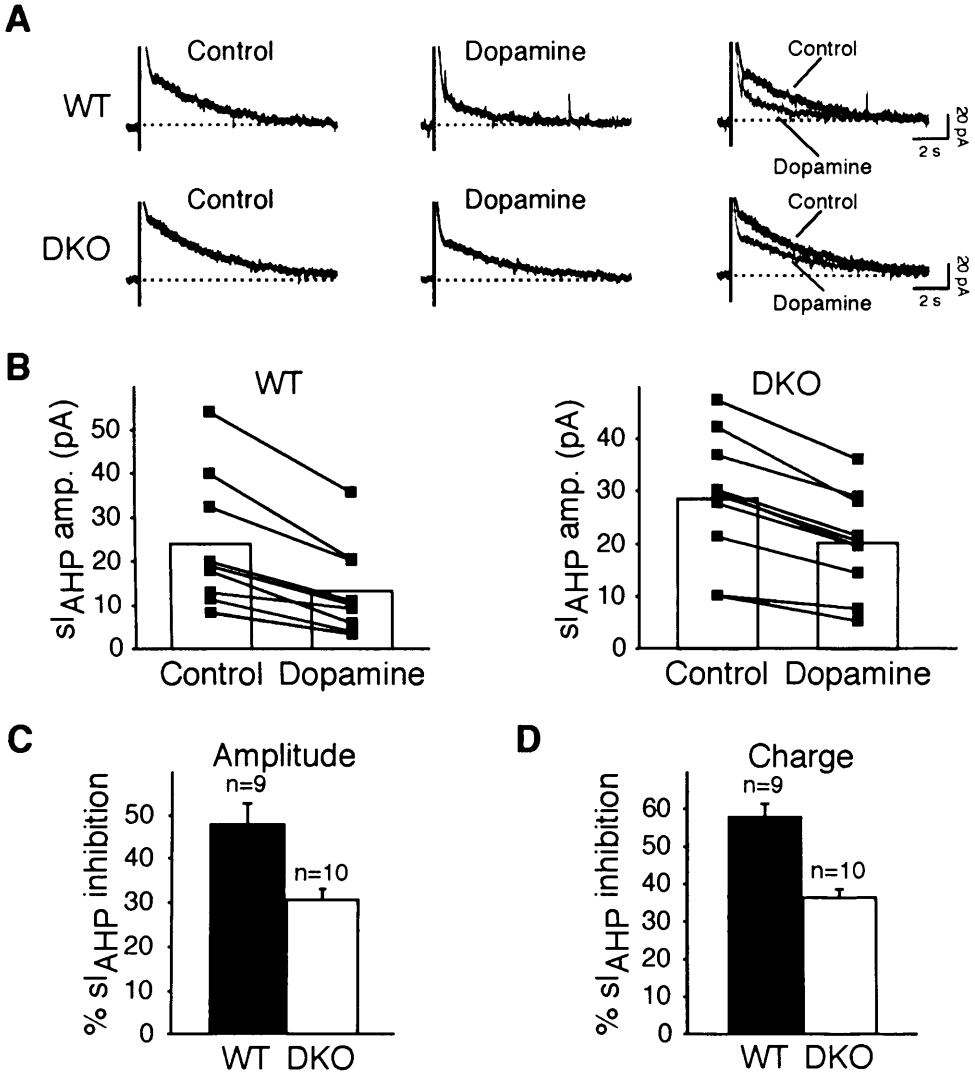

Figure 28: Dopaminergic modulation of sI_{AHP} is partially mediated by AC1/AC8

A, Application of dopamine (30 μM) resulted in a significant inhibition of sI_{AHP} in WT (top row) and DKO CA1 neurons (bottom row). Left panels depict sI_{AHP} prior to dopamine application whilst the middle panels correspond to the sI_{AHP} in the presence of dopamine.

B, Graphs illustrate the effect of dopamine on the sI_{AHP} amplitude. Symbols represent individual cells before and after the application of dopamine. Bars represent averaged data. Data from WT cells is on the left panel, and from DKO cells on the right panel.

C, D, Application of dopamine (30 μM) resulted in significant inhibition of sIAHP in WT cells (% sIAHP amplitude inhibition: 47.7±4.5 %, **C**; % charge transfer inhibition: 58.0±2.9 %, **D**; n=9), and in partial sIAHP suppression in DKO cells (% sIAHP amplitude inhibition: 30.7±2.3 %, **C**; % charge transfer inhibition; 36.6±4.0 % **D**; n=10). There was significant difference between the dopamine mediated sIAHP suppression of

amplitude ($p<0.005$) and charge transfer ($p<0.001$) in WT and DKO cells (unpaired t test). Bars indicate mean±SEM.

5.3.5: Modulation of sAHP by isoproterenol, serotonin and dopamine

The aim of this section of experiments was to investigate to which extent different monoaminergic neurotransmitters modulate sAHP in CA1 neurons from WT and DKO mice. There were several underlying reasons for investigating the effect of the MAs on sAHP in addition to the effect on the underlying current sI_{AHP}. Firstly it was hoped that results obtained on the MA modulation of sAHP would confirm those obtained on the underlying current, sI_{AHP}. Secondly, by monitoring the MA modulation of sAHP in current clamp, information can be inferred about the role of Ca^{++} stimulatable ACs in modulating other currents that are activated/inhibited by MA signalling. Potential candidates identified in this way can then be the focus of further experiments. This information is not easily gleaned from voltage clamp experiments that isolate a current of interest because the membrane potential is clamped at the desired holding potential.

In the case of the β adrenergic pathway, we did not observe any significant difference between the suppression of sAHP by 2 μM isoproterenol in WT compared with DKO cells (% sAHP inhibition in WT cells: 36.8±2.8 %, n=5; in DKO cells: 42.4±11.8 % n=3, $p>0.75$, Mann Whitney test; Fig. 29A, B). This is consistent with previous voltage-clamp experiments, indicating that activation of AC1/AC8 does not contribute to the isoproterenol-mediated suppression of sI_{AHP}.

Addition of 10 μM 5HT in the presence of 1 μM WAY 100135 resulted in significant suppression of sAHP in both WT and DKO. Fig. 29C shows representative AHP traces before (black line) and after 5HT (grey line) application in both WT (left panel) and DKO neurons (right panel). Each trace is an average of five consecutive sweeps.

The effect of 10 μM of 5HT on the sAHP is quantified in Fig. 29D. Application of 10 μM 5HT led to a 45.7±10.3 % suppression of sAHP in WT cells (n=4). The sAHP suppression associated with 5HT application in DKO cells was 17.3±7.4%

(n=6). There was significant difference between the sAHP suppression achieved in WT and DKO cells ($p<0.05$; Mann Whitney test). The number of action potentials fired in response to the 400 ms-long depolarising pulse increased from 7.6±1.2 to 9.2±1.5 with addition of 10 μM 5HT in WT cells, compared with 4.2±0.3 to 5.8±0.8 in DKO cells.

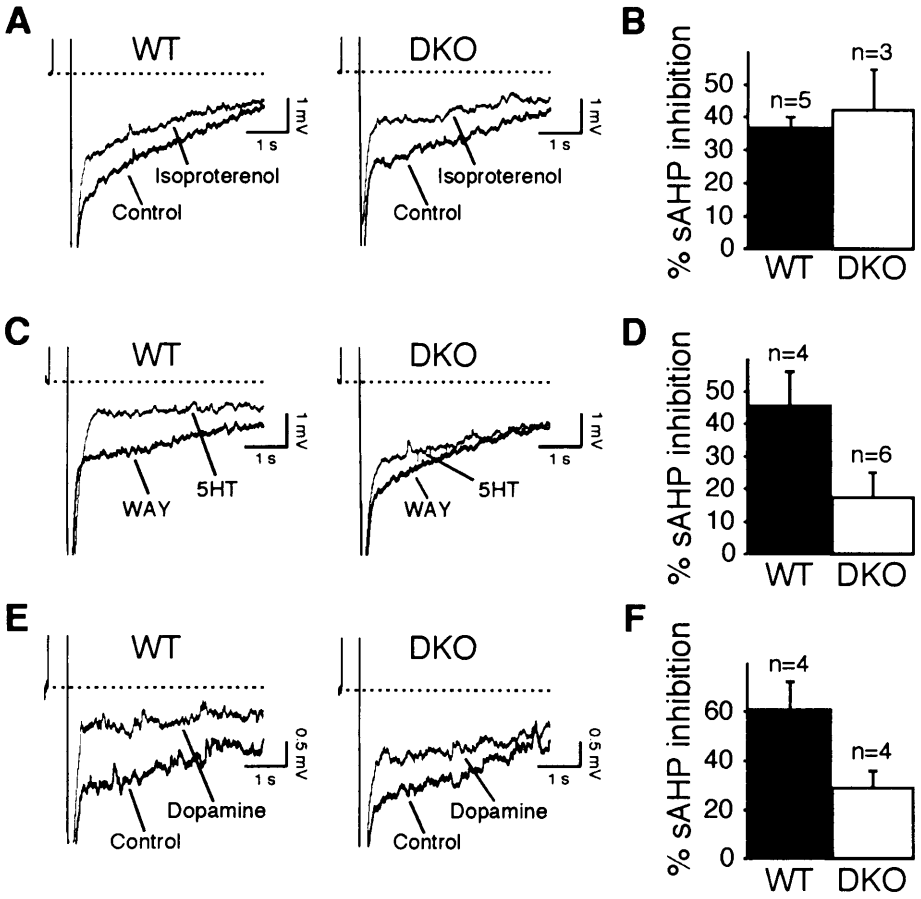

Figure 29: Modulation of sAHP by isoproterenol, serotonin and dopamine

A, Inhibition of the sAHP by isoproterenol in WT (left panel) and DKO CA1 neurons (right panel). The sAHP was elicited by a 400 ms-long current injection. The amplitude of the current injection was determined as the minimum current injection that elicited a maximal number of action potentials. Each trace is an average of five consecutive sweeps, elicited every 20s.

B, Bar graph depicting the significant inhibition of sAHP by isoproterenol in WT and DKO CA1 neurons (% inhibition of sAHP amplitude, WT: 36.8±2.8 %, n=5; DKO: 42.4±11.8 %, n=3). Bars and error bars represent mean±SEM. There was no significant difference between the effect of isoproterenol on sAHP in WT and DKO cells ($p=0.79$, Mann Whitney test).

C, In the presence of 1 μM WAY 100135, application of serotonin (10 μM) results in inhibition of sAHP in WT (left panel) and DKO cells (right panel).

D, The sAHP was inhibited by 45.7±10.3 % (n=4) by 10 μM serotonin in WT cells and by 17.3±7.4 % (n=6) in DKO cells. There was significant difference between the effect of serotonin on WT and DKO cells ($p<0.05$; Mann Whitney test).

E, Application of dopamine results in sAHP inhibition in WT (left panel) and DKO CA1 neurons (right panel). Black traces represent the sAHP elicited in response to a 400 ms long current injection. Grey superimposed traces represent the effect of dopamine (30 μM).

F, Bar chart comparing the effect of dopamine on sAHP in WT (inhibition of sAHP amplitude: 60.7±11.4 %, n=4) and DKO CA1 neurons (inhibition of sAHP amplitude: 29.0±6.6 % n=4). There was no significant difference between the effect of dopamine on sAHP in WT and DKO CA1 neurons ($p=0.0571$; Mann Whitney test).

Fig. 29E and F illustrate the effect of 30 μM dopamine on the sAHP. Panel E compares the effect of dopamine on the sAHP in WT (left panel) and DKO CA1 neurons (right panel) and panel F quantifies the effect. In WT cells, application of 30 μM dopamine resulted in 60.7±11.4 % inhibition of sAHP (n=4). There was no significant difference between the sAHP inhibition achieved in WT and DKO CA1 neurons (% sAHP inhibition DKO: 29.0±6.6, n=4; $p=0.0571$, Mann Whitney test). This is in contrast to the effect of dopamine on sI_{AHP}, the current that underlies sAHP. Although application of 30 μM dopamine resulted in a significantly different inhibition of sI_{AHP} in WT compared with DKO CA1 neurons (see Fig. 28), there was no significant difference between the extent of the sAHP inhibition in WT and DKO cells. It would be expected that a trend seen in the sI_{AHP} data would also be seen in the sAHP data. Possible reasons for this discrepancy between the voltage- and current-clamp data will be discussed in the discussion part of this section.

5.3.6: Comparison of the degree of MA modulation achieved in voltage clamp and current clamp recordings

The aforementioned voltage clamp and current clamp data was collected from experiments in which both the voltage clamp and current clamp results were

obtained within the same cells. The experimental paradigm followed was as follows: the sI_{AHP} was monitored in voltage clamp until sI_{AHP} amplitude had been stable for at least five minutes. Then the amplitude of the sAHP was determined in current clamp in response to a given current injection and the membrane potential was noted. The sAHP amplitude determined at this point corresponded to the control sAHP amplitude. The cell was then monitored in voltage clamp to ensure sI_{AHP} amplitude stability prior to MA application. The last three traces prior to MA application were determined as the amplitude of sI_{AHP} in the control situation. The sI_{AHP} amplitude was monitored in voltage clamp throughout the drug application until it had reached a steady amplitude for ~ 3 mins. The last three traces recorded in voltage clamp were determined to be the sI_{AHP} amplitude in the presence of the MA. Following this, the sAHP amplitude was then determined in current clamp to obtain the change in sAHP amplitude due to MA application.

Data on the degree of inhibition of the sI_{AHP} and sAHP was not achieved from every cell. Fig. 30 directly compares the data obtained in voltage clamp and current clamp from cells in which both sets of data were achieved. Fig. 30A compares the effect of isoproterenol (2 μM) on the sI_{AHP} and sAHP in both WT and DKO. Application of isoproterenol resulted in 60.7±6.5 % inhibition of sI_{AHP} and 36.8±2.8 % inhibition of sAHP in WT mice (n=5; $p<0.05$; paired t test). However there was no significant difference between the degree of inhibition of sI_{AHP} (% sI_{AHP} inhibition: 48.6±7.1 %) and sAHP (% sAHP inhibition 42.4±11.8 %) in DKO (n=3; p=0.5; Wilcoxon matched-pairs signed-ranks test).

The effect of serotonin (5HT; 10 μM) in the presence of WAY 100135 (1 μM) on sI_{AHP} and sAHP in WT and DKO is compared in Fig. 30B. There was no significant difference between the serotonergic effect on sI_{AHP} and sAHP in either WT (% sI_{AHP} inhibition: 41.3±6.0 %; % sAHP inhibition: 45.7±8.9 %; n=4; p=0.87; Wilcoxon matched-pairs signed-ranks test) or DKO (% sI_{AHP} inhibition: 30.5±3.0; % sAHP inhibition: 18.9±5.5 %; n=6; p=0.06; paired t test).

The comparison of the suppression of both sI_{AHP} and sAHP in WT and DKO cells is depicted in Fig. 30C. In the four WT cells in which the effect of dopamine (30 μM) was examined in both voltage clamp (% sI_{AHP} inhibition: 46.8±7.3 %) and

current clamp (% sAHP inhibition: 60.6±8.1 %), there was no significant difference between the degree of dopaminergic inhibition elicited (p=0.25; Wilcoxon matched-pairs signed-ranks test). In DKO cells the inhibition mediated by dopamine was similar (n=4; p=0.25; Wilcoxon matched-pairs signed-ranks test) in both voltage clamp (% sI_{AHP} inhibition: 30.4±2.3 %) and current clamp (% sAHP inhibition: 29.0±5.7 %).

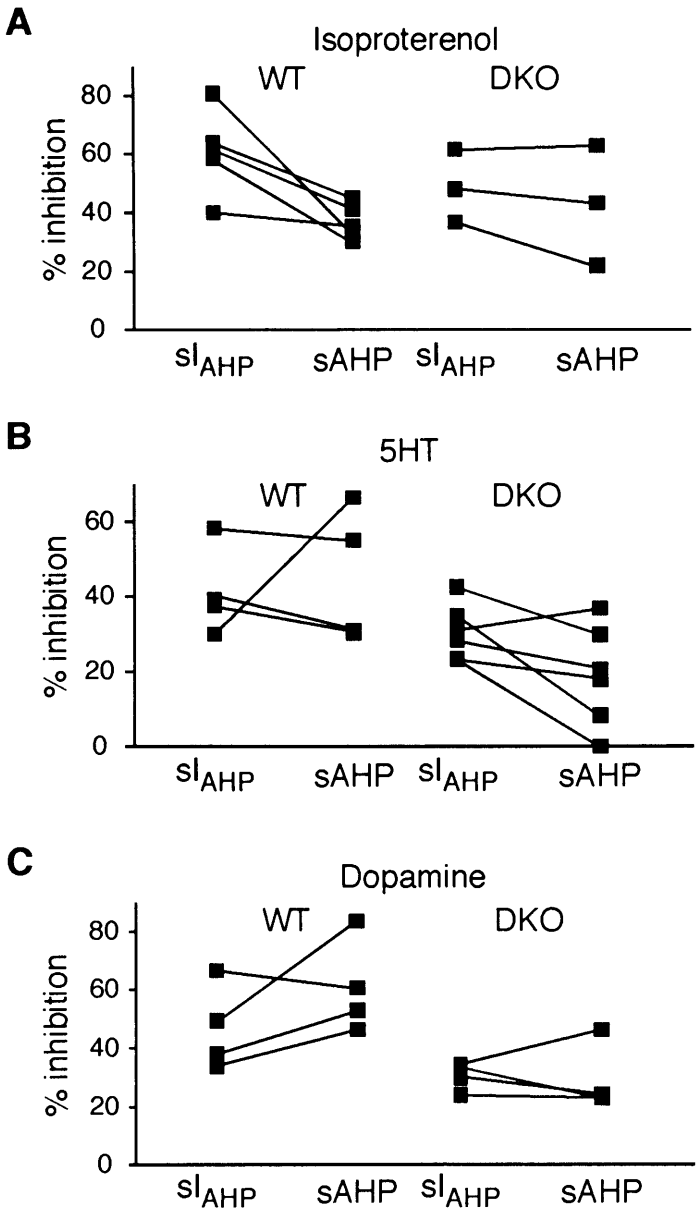

Figure 30: Comparison of the MA effect on sI_{AHP} and sAHP within the same cell

The inhibition of sI_{AHP} by 2 μMisoproterenol *(A)*, 10 μM serotonin in the presence of 1 μM WAY 100135 *(B)* and 30 μM dopamine *(C)* is directly compared with the inhibition of the sAHP recorded in the same cell.

The similarity between the degree of inhibition achieved by the MA neurotransmitters between the data obtained from voltage clamp and current clamp recordings in the same cell indicates that the experimental paradigm did not skew results obtained in a particular recording mode.

5.4.0: Discussion

The primary aim of this set of experiments was to investigate the role of the Ca^{++} stimulatable ACs in mediating the monoaminergic suppression of sI_{AHP}. Before proceeding to the detailed analysis of the effects of monoamine transmitters on the sI_{AHP} in CA1 pyramidal neurons from DKO mice, the effect of isoproterenol and 5HT was characterised in WT mice and shown to be concentration dependent. Then the passive membrane properties (resting membrane potential and input resistance) of cells obtained from WT and DKO animals were compared and did not differ significantly.

5.4.1: The differences in recording in voltage and current clamp

The 5HT-mediated suppression of sI_{AHP} was intact in CA1 neurons from DKO mice. However, there was significant reduction of the 5HT-mediated suppression of the sAHP following bursts of action potentials in CA1 neurons from DKO mice, indicating a possible role for the Ca^{++} stimulatable ACs. These results are conflicting. Meanwhile, the dopaminergic suppression of sAHP was intact in CA1 neurons from DKO mice, whilst there was significant difference between the modulation of sI_{AHP} by dopamine in WT and DKO CA1 neurons. Finally the effect of the β-adrenergic agonist isoproterenol on sI_{AHP} was similar in WT and DKO in all conditions used. Therefore the question addressed in this section of the discussion is: what are the reasons for the apparently contradictory results described in current and voltage clamp upon application of serotonin and dopamine?

There was a significant difference between the dopaminergic modulation of the sI_{AHP} in CA1 neurons from DKO and WT mice. The effect of dopamine on sI_{AHP} was significantly reduced in cells from the DKO compared with WT mice. However, there was no difference in the modulation of the sAHP following bursts of action potentials between WT and DKO. The lack of a significant difference in the current clamp experiments might be linked to the small sample size. Therefore, further experiments investigating the modulation of the sAHP by dopamine are required.

The apparent dichotomy in the results presented here is that AC1/AC8 appear to be involved in the serotonin mediated suppression of sAHP, and yet the modulation of the corresponding current, sI_{AHP}, remains intact in CA1 neurons from DKO mice. A possible explanation for the apparently contradictory results in voltage clamp and current clamp is the difference in the two recording techniques. When the current being measured is generated at a remote site from the voltage clamp electrode, there is inadequate voltage control at the remote site, so that the actual current entry at a synapse is less that it would be if the cell was under ideal space clamp (Spruston *et al.*, 1993). The sI_{AHP} is a voltage independent current, activated by Ca^{++} entry through voltage gated Ca^{++} channels (Alger & Nicoll, 1980; Hotson & Prince, 1980; Schwartzkroin & Stafstrom, 1980; Lancaster & Adams, 1986). Therefore, the consequence of space clamp errors, at a site remote from the voltage clamp electrode, is that the depolarising step used to elicit Ca^{++} influx is attenuated, resulting in the generation of a sI_{AHP} of reduced amplitude. Furthermore, if the sI_{AHP} is generated at a remote site from the voltage clamp electrode, then it is also subject to attenuation as it propagates passively to the soma, therefore, the sI_{AHP} recorded at the soma will be smaller than the actual sI_{AHP} at the remote site. The channel underlying the sI_{AHP} has been inferred to have a somatic (Lancaster & Zucker, 1994; Lima & Marrion, 2007), apical dendritic (Sah & Bekkers, 1996) and basal dendritic (Bekkers, 2000) location. However, in the absence of the molecular identity of the channel underlying sI_{AHP} and the ensuing expression studies, the issue surrounding the location of the channel remains unresolved. If it is assumed that there are two populations of sI_{AHP} channels (i) somatic sI_{AHP} channels that are not functionally coupled to AC1/AC8 and (ii) dendritic sI_{AHP} channels that are modulated by cAMP produced by AC1/AC8, then, when the sI_{AHP} is recorded in voltage clamp, only the somatic and proximal dendritic sI_{AHP} channels are measured whilst the remaining dendritic sI_{AHP} is filtered due to space clamp errors. In current clamp, the current injected in the soma will also electrotonically decay along the membrane. However if it is enough to elicit regenerative events, such as action potentials or Ca^{++} spikes in the dendrites, which are self-sustaining and will propagate for some length, therefore

a sAHP in the dendrites could be generated and may contribute to the sAHP recorded at the soma.

If the discrepency between the data obtained from voltage clamp and current clamp recrodings is purely attributable to poor space clamp than the situation could be improved by repeating the experiments in Barium ions. However there is an alternative explanation for the discrepancy. When the sAHP is recorded in current clamp, the ampltiude of the potential of interest (sAHP) can also be modulated by the activation/deactivation of other currents that are modulated by serotonin. Because in voltage clamp the membrane potential is clamped, there is better control over the number of conductances activated. Whilst in current clamp, channels are able to open and close thus contributing to fluctuations in membrane potential. The experiments presented here were conducted in the presence of WAY 100135, therefore it is unlikely that the activation of GIRK channels contributed to changes in membrane potential. However there are four other scenarios in which the activation of hyperpolarising/depolarising currents by serotonin may contribute to an apparent change in the sAHP. 1) application of serotonin results in the activation of a slow Na^+ or Ca^{++} current which masks the sAHP causing it to appear of smaller ampltiude. 2) serotonin application results in the activation of a fast Na^+ or Ca^{++} current resulting in greater depolarisation during the depolarising step leading to enhanced Ca^{++} influx and activation of more sI_{AHP} channels. The net effect would be a sAHP of larger ampltiude. 3) similarly, if serotonin application results in activation of a fast K^+ or Cl^- current, then the depolarisation associated with the current injection would be reduced resulting in a sAHP of smaller amplitude. 4) Finally activation of a slow K^+ current by serotonin would also mask the amplitude of the sAHP causing it to appear greater.

The effect of serotonin on the activation of neuronal currents could be a result of a direct effect on ionotropic serotonin receptors (e.g. the $5HT_3R$). However the effect of serotonin on the sAHP recorded in current clamp data is different in data from the DKO for AC1 and AC8 from the WT. Therefore it seems probable that a channel that is modulated by changes in cAMP concentrations is activated by serotonin in WT mice and the activation of this channel contaminates the sAHP

causing the sAHP amplitude to appear larger than can be attributed to the channels underlying sI_{AHP}. Therefore it is proposed that the modulation of sI_{AHP}/sAHP by serotonin is not mediated by activation of AC1/AC8.

5.4.2: ACs involved in the β adrenergic modulation of sI_{AHP}

The effect of the β-adrenergic agonist isoproterenol on sI_{AHP} was similar in WT and DKO under all conditions investigated. Accordingly, there was no difference in the modulation of the sAHP following trains of action potentials by isoproterenol when comparing WT and DKO. These results indicate that AC1/AC8 do not mediate the suppression of sAHP/sI_{AHP} induced by isoproterenol. These experiments were conducted with the β-adrenoceptor agonist isoproterenol, instead of the neurotransmitter noradrenaline, because noradrenaline activates both α- and β-adrenoceptors and we addressed the question of the specific involvement of AC1/AC8 in the signal transduction pathway solely activated by the β-adrenoceptors. However, the physiological effect of noradrenaline is most likely mediated by the concomitant activation of α- and β-adrenoceptors. In particular, the suppression of the sI_{AHP} has been demonstrated to be mediated by the activation of β-adrenoceptors, but synergistically enhanced by the concomitant activation of α-adrenoceptors (Pedarzani & Storm, 1996b). It has been postulated that synergism between α- and β-adrenoceptors occurs at the level of the AC, whose activity would be enhanced by the release of βγ subunits from G_i/G_o linked α adrenoceptors (Pedarzani & Storm, 1996b). Type 2 ACs, AC2/AC4, are known to be co-stimulated by G-protein βγ subunits in the mouse hippocampus (Baker *et al.*, 1999). This may suggest that the AC responsible for the physiological noradrenergic effect is a group 2 AC. If AC2/AC4 are responsible for the noradrenergic modulation of sI_{AHP}/sAHP, then the corresponding signalling domain would consist of α- and β-adrenoceptors, AC2/AC4, PKA and the sAHP channel. In support of this hypothesis, it has been shown that AC2 and AC4 are expressed both in the apical dendrites and in the cell bodies of CA1 pyramidal cells of the mouse hippocampus (Baker *et al.*, 1999). Further studies are needed to investigate whether AC2/AC4 are responsible for the effect of noradrenaline on sI_{AHP}/sAHP. In the absence of an AC2/AC4 knockout mouse, a possible

experimental approach could involve the intracellular delivery or expression of βγ subunit scavengers (Rishal *et al.*, 2005) in hippocampal neurons. The modulation of sI_{AHP}/sAHP by noradrenaline could then be compared in control and treated cells from the same animal.

5.4.3: Possible presynaptic effects of β-adrenergic and serotonergic agonists

Some of the experiments presented in this thesis were not conducted in the presence of TTX and TEA, in order to monitor the modulation of an sI_{AHP} elicited by a more physiological Ca^{++} concentration. Under these conditions, there is the possibility that pre-synaptic effects of isoproterenol may lead to changes in the spontaneous release of neurotransmitters. It has been shown that, at the CA3-CA1 synapse, application of isoproterenol results in an increase in glutamatergic miniature excitatory post-synaptic currents (EPSCs) (Gereau & Conn, 1994). This indicates that isoproterenol facilitates glutamate release from CA3 pyramidal neurons. Glutamate application results in sI_{AHP} suppression in CA1 pyramidal neurons through a mechanism that involves metabotropic glutamate receptors (Charpak *et al.*, 1990; Mannaioni *et al.*, 2001) and the pertussis sensitive G-protein $G\alpha_q$ (Krause *et al.*, 2002). Therefore, it is possible that the application of isoproterenol could lead to the suppression of sI_{AHP}/sAHP through an enhancement of spontaneous glutamate release, acting through a pathway that does not involve AC-cAMP-PKA. This, in turn, would explain the observation that the modulation of sAHP/$sI_{AHP,}$ by isoproterenol, is intact in hippocampal neurons from DKO mice. If this were the case, it would be expected that there would be an increase in the frequency of mEPSCs on application of isoproterenol. Further analysis is needed to quantify the effect of isoproterenol on mEPSCs in order to test this possibility. An alternative strategy would be to repeat the experiments conducted with a β_2 agonist e.g. salbutamol, in order to exclude the possible pre-synaptic effects associated β_1 receptor activation.

In vivo microdialysis of serotonergic receptor agonists have shown that activation of the $5HT_{1A}$(Koyama *et al.*, 1999), $5HT_2$ and $5HT_4$ (Nair & Gudelsky, 2004) receptor subtypes leads to facilitation of the release of acetylcholine in the

hippocampus. Muscarinic agonists e.g. carbachol been shown to act on muscarinic receptors to suppress sAHP in the CA1 pyramidal cells (Benardo & Prince, 1982a; Cole & Nicoll, 1983, 1984) through agonism at M_3 receptors (Rouse *et al.*, 2000a) and subsequent activation of $G\alpha_q$ (Krause *et al.*, 2002). Therefore, similar to the possible pre-synaptic effect of isoproterenol facilitating glutamate release, the facilitation of acetylcholine release by serotonin could result in sAHP suppression through a pathway that does not involve the activation of the AC/cAMP/PKA pathway.

However, the effect of both serotonin and β-adrenergic agonists on sI_{AHP}/sAHP is most likely a postsynaptic effect rather than facilitation of neurotransmitter release. Through the use of Rp-cAMPS and Walsh peptide/PKI_{6-22}, the role for PKA in mediating the effect of both serotonin and β-adrenergic agonists has been demonstrated in CA1 pyramidal cells (Pedarzani & Storm, 1993). Additionally Walsh peptide/PKI_{6-22} is membrane impermeant, and was delivered to the neuron through an intracellular pipette. As a result, post-synaptic inhibition of PKA suppressed the effect of serotonin and β-adrenergic agonists. Furthermore, it has been shown that both the cholinergic and glutamatergic inhibition of sI_{AHP}/sAHP occurs independently of activation of PKA (Pedarzani & Storm, 1996a). Therefore, the suppression of sI_{AHP}/sAHP by serotonin and β-adrenergic agonists is most likely due to agonism at post-synaptic receptors leading to activation of PKA.

5.4.4: ACs involved in the dopaminergic suppression of sI_{AHP}/sAHP

Although the results with dopamine are only partially supporting a role of AC1/AC8 in the signal transduction pathway leading to the suppression of sI_{AHP}, there is some indirect evidence that suggests a functional coupling between dopaminergic receptors and Ca^{++} stimulatable ACs (Yang, 2000). D1/D5 dopamine receptors are known to positively couple to AC (Kebabian & Calne, 1979; Kimura *et al.*, 1995). In the CA1 region of the hippocampus, activation of D1/D5 dopamine receptors has been demonstrated to result in an increase in both α-amino-3-hydoxy-5-methylisoxazole-4-propionic acid receptor- (AMPAR) and

NMDAR mediated EPSCs (Yang, 2000). The dopaminergic potentiation of AMPAR-mediated currents was not dependent on the activation of NMDARs, however, the requirement for postsynaptic Ca^{++} was demonstrated through inclusion of the Ca^{++} chelator BAPTA (Yang, 2000). The source of increased Ca^{++} in this study remained undetermined. The missing link in this study was that it was not demonstrated that the modulation of the glutamatergic EPSCs by dopamine was cAMP/PKA dependent. However it is assumed that the mechanisms underlying the dopaminergic potentiation of EPSCs requires cAMP and PKA similar to LTP then a role for Ca^{++} stimulatable ACs is implicated. This is an avenue for further study.

The experimental evidence demonstrating the role of D1/D5 receptors in the modulation of sI_{AHP}/sAHP has proved elusive (see Introduction). In this study, the inhibition of sI_{AHP} by dopamine was suppressed in DKO CA1 pyramidal cells. This indicates that Ca^{++} stimulatable ACs are activated in the dopaminergic inhibition of sI_{AHP}. It has been shown that the sI_{AHP} modulation by dopamine occurs through activation of PKA (Pedarzani & Storm, 1995a). The D1/D5 receptor positively couples to AC (Kebabian & Calne, 1979; Kimura *et al.*, 1995). Additionally, the D1/D5 receptor has been shown to activate PKA in hippocampal pyramidal neurons (Cantrell *et al.*, 1997). Although Group 2 dopaminergic receptors are negatively coupled to AC (Kebabian & Calne, 1979), the group 2 dopamine receptor, subtype D2, have also been shown to activate PKA in a manner that was dependent on a pertussis sensitive G protein and the release of free $\beta\gamma$ subunits leading to generation of cAMP (Yao *et al.*, 2002). The dependence on free $\beta\gamma$ subunits and pertussis sensitive G proteins implicates AC2/AC4 in the D2- mediated activation of PKA. Therefore, the dependence on AC1/AC8 and PKA indicates that the D1/D5 receptor is a probable candidate for the inhibition of sI_{AHP} by dopamine.

5.4.5: ACs mediating the suppression of sI_{AHP}/sAHP by serotonin

The effect of serotonin on CA1 pyramidal cell excitability is mediated by the activation of different types of receptors. $5HT_7$ receptors are expressed on CA1

pyramidal cells (Gustafson *et al.*, 1996) and have been demonstrated to increase CA1 pyramidal cell excitability and suppress sAHP (Tokarski *et al.*, 2003). $5HT_7$ receptors positively couple to AC (Ruat *et al.*, 1993). A synergistic potentiation of AC activation is achieved through co-activation of $5HT_{1A}$ and $5HT_7$ receptors in biochemical assays on hippocampal membrane preparations (Thomas *et al.*, 1999). $5HT_{1A}$ receptors have been shown to couple to G_i/G_o and the release of G-protein βγ subunits leads to the activation of GIRK channels (Andrade *et al.*, 1986; Andrade & Nicoll, 1987; Colino & Halliwell, 1987; Logothetis *et al.*, 1987; Luscher *et al.*, 1997). The synergistic activation of AC by $5HT_7$ (positively coupled to AC) and $5HT_{1A}$ receptors suggests that the AC involved might be a group 2 AC, AC2 or AC4, both of which display an enhanced response to co-activation by $G\alpha_s$ and βγ subunits. Therefore, it would be expected that, if $5HT_7$ receptors were the main receptors responsible for the suppression of the sI_{AHP}/sAHP, with or without $5HT_{1A}$ contribution, its modulation by serotonin would be intact in neurons lacking AC1/AC8. However, in HEK 293 cells $5HT_7$ receptors have been demonstrated to activate AC1 and AC8 by increasing intracellular Ca^{++} (Baker *et al.*, 1998). Furthermore, application of serotonin or a $5HT_7$ receptor agonist to hippocampal cultures led to an increase in intracellular Ca^{++} (Baker *et al.*, 1998). This indicates a possibility that $5HT_7$ receptors may couple to AC1/AC8 in the hippocampus. Furthermore, $5HT_4$ receptors are also expressed in CA1 pyramidal cells (Vilaro *et al.*, 1996), and have been demonstrated to suppress sI_{AHP}/sAHP by a cAMP/AC/PKA mediated mechanism (Pedarzani & Storm, 1993; Torres *et al.*, 1994). In order to determine the serotonin receptor subtype responsible for the modulation of sI_{AHP}/sAHP in CA1 pyramidal cells, further experiments need to be conducted with selective $5HT_4$ and $5HT_7$ receptor agonists and antagonists.

5.4.6: Signalling domains underlie the modulation of sI_{AHP} by cAMP/PKA

The basal modulation of sI_{AHP} by a phosphatase-kinase balance, in the absence of neurotransmitters or neuromodulators, shown in CA1 pyramidal neurons (Pedarzani *et al.*, 1998) suggests that a signalling domain comprising receptors,

G-proteins, second messengers and effectors might underlie the modulation of the sI_{AHP} channel by PKA. The existence of signalling complexes centred on the β_2 adrenoceptor (Davare *et al.*, 2001) and D1-like dopaminergic receptor (Cantrell *et al.*, 1997) has been demonstrated in CA1 pyramidal neurons. The specificity of the PKA signalling domains described in these studies were conferred by A-kinase anchoring proteins (AKAPs). The results of this study suggest that different neurotransmitters, that seemingly converge on a common signal transduction pathway, the cAMP/PKA pathway, may be coupled to different ACs. For example, the modulation of sI_{AHP}/sAHP by dopamine is mediated by AC1/AC8 but the activation of β adrenoceptors does not involve AC1/AC8. This could be the first step in the elucidation of different signalling domains converging on common second messengers (cAMP), effectors (PKA) and targets (sI_{AHP}), whilst specificity is maintained through involvement of different receptors coupling to different ACs that are regulated by different co-factors.

Chapter 6: Glutamatergic modulation of sAHP: modulation of sAHP by synaptic stimulation

6.1.0: Introduction

In this part of the study, the role of the Ca^{++} stimulatable ACs in mediating the suppression of the sAHP elicited by synaptic stimulation paradigms is investigated. The aim of this section is to examine the evidence indicating that AC1/AC8 could be involved in the modulation of sAHP by synaptic stimulation.

6.1.1: Stimulation of glutamatergic synapses can lead to NMDAR dependent Ca^{++} influx

It was initially reported that the release of glutamate activates NMDAR at the CA3-CA1 synapse (Collingridge *et al.*, 1983a, b). Post-synaptic stimulation leads to activation of an EPSP that in turn results in post-synaptic Ca^{++} elevation. This could be due to synaptic activation of NMDAR or Ca^{++} influx through voltage-gated Ca^{++} channels opened by the post-synaptic depolarisation. The evidence that part of the post-synaptic Ca^{++} elevation is due to the activation of NMDAR comes from pharmacological and imaging studies. Initially it was shown by Muller (1991) that weak presynaptic stimulation of pyramidal neurons led to Ca^{++} accumulation in the post synaptic spines that could be blocked by application of D-2-amino-phosphopentanoate (AP5), an NMDAR antagonist. Three studies independently visualised small hotspots of Ca^{++} elevation at the site of active synapses and demonstrated that this Ca^{++} influx was due to activation of NMDAR (Alford *et al.*, 1993; Perkel *et al.*, 1993; Malinow *et al.*, 1994). Therefore, activation of NMDAR can lead to post synaptic Ca^{++} elevation.

6.1.2: NMDAR activation can result in generation of cAMP in CA1 region of the hippocampus

Blitzer et al (1995) postulated that Ca^{++} influx through NMDAR could activate Ca^{++} stimulatable ACs that, in turn, could produce a local rise in cAMP resulting in PKA activation and transient sAHP suppression. Experimentally, it was shown that high frequency synaptic stimulation (HFS) of the Schaffer collateral pathway resulted in a transient sAHP suppression that was dependent on the activation of NMDAR (Blitzer *et al.*, 1995). Activation of NMDAR through LTP-inducing HFS paradigms had already been shown increase cAMP in the CA1 area of the

hippocampus (Chetkovich *et al.*, 1991). Chetkovich and Sweatt (1993) argued that the NMDA receptor mediated increase in cAMP was likely to occur through the activation of Ca^{++} stimulatable ACs because AC activity in membranes prepared from the CA1 area of the hippocampus was stimulated by Ca^{++} in a CaM dependent manner. The involvement of CaM in HFS induced cAMP production has been further demonstrated in biochemical and electrophysiological experiments (Chetkovich & Sweatt, 1993; Blitzer *et al.*, 1995). The CaM dependence of cAMP production by HFS further indicated a role for the Ca^{++} stimulatable ACs in the suppression of sAHP because both AC1 and AC8 stimulation is CaM dependent (Cali *et al.*, 1994; Fagan *et al.*, 1996).

The results obtained by Blitzer et al. (1995) and Chetkovich and Sweatt (1993) rely on the expression of Ca^{++} stimulatable ACs (AC1, AC8) in CA1 neurons. The experiments of Visel et al. (2006) and Conti et al. (2007) indicate that both AC1 and AC8 are expressed in adult mice. The co-localisation of AC1 with PSD-95 (Conti *et al.*, 2007) indicates that AC1 is expressed in the spines of CA1 pyramidal neurons. Furthermore, Wang et al. (2003) showed that AC8 co-localised with PSD-95 in hippocampal neuronal primary cultures. Taken together, the experimental evidence of others presented so far indicates that AC1 and AC8 are both present in the spines of hippocampal neurons where they are ideally located to generate a cAMP signal stimulated by Ca^{++} influx through NMDAR.

6.1.3: High frequency synaptic stimulation (HFS) causes activation of PKA

Blitzer et al. (1995) postulated that HFS would lead to activation of PKA culminating in sAHP suppression. This hypothesis is dependent on whether PKA can be activated by HFS. The evidence that repetitive tetanic (100 Hz) stimulation leads to activation of PKA comes from biochemical, pharmacological and genetic manipulations that seek to understand the mechanisms underlying LTP. Roberson and Sweatt (1996) used biochemistry to assay changes in PKA activity in response to tetanic stimulation, and demonstrated that it was increased two minutes after tetanic stimulation. The activation was NMDAR dependent because it was inhibited by AP5. Abel et al. (1997) generated transgenic mice that

expressed a dominant negative form of the regulatory subunit of PKA in the hippocampus. The late phase of LTP i.e. that is dependent on *de novo* gene transcription, induced by repetitive trains of high frequency synaptic stimulation was significantly reduced in the transgenic mice compared to the controls. Initial pharmacological manipulations utilised membrane permeant cAMP analogues to modulate the activity of PKA. Sp-cAMPS, an activator of PKA, was shown to elicit mild synaptic facilitation, whilst Rp-cAMPS, an inhibitor of PKA, blocks LTP in the Schaffer collateral pathway (Blitzer *et al.*, 1995). However, both of these compounds are membrane permeant, and so a presynaptic locus for PKA could not be excluded. Therefore, experiments using Walsh peptide, a membrane impermeant peptide inhibitor of PKA, have been conducted to illustrate both that PKA is activated by high frequency synaptic stimulation, and that the locus for this effect if post-synaptic. Duffy and Nguyen (2003) were the first to show, using whole cell patch clamp recordings, that intracellular injection of PKI_{6-22} (a fragment of the heat stable PKA inhibitor derived from the active portion of the peptide) inhibited the expression of LTP in response to tetanic stimulation. Therefore, many lines of evidence converge on the idea that repetitive synaptic stimulation at 100 Hz leads to activation of PKA and this is an essential step for the induction of LTP.

6.2: Aims and objectives

High frequency synaptic stimulation of the Schaffer Collateral pathway has been shown to transiently suppress the sAHP in rat CA1 pyramidal cells (Blitzer *et al.*, 1995). The main objective of this set of experiments was to determine whether AC1/AC8 were involved in the suppression of sAHP by stimulation protocols normally used for the induction of LTP in an NMDAR dependent manner. The first aim was to characterise the effect of HFS on sAHP in WT and DKO mice. The second aim was to investigate whether a more physiological LTP inducing pairing protocol could similarly produce sAHP suppression in a NMDAR dependent manner.

6.3.0: Results

6.3.1: Glutamatergic modulation of sAHP: modulation of sAHP by HFS

The sAHP has been shown to be modulated (i.e. transiently suppressed) by glutamate through the activation of NMDAR activated by high frequency stimulation of the Schaffer collateral pathway (Blitzer *et al.*, 1995). The NMDAR-dependent sAHP suppression was dependent on the activation of PKA and calmodulin (Blitzer *et al.*, 1995), and it was postulated that high frequency synaptic stimulation would lead to activation of NMDAR, subsequent Ca^{++} influx and possible activation of a Ca^{++} stimulatable ACs. This, in turn, would lead to production of cAMP, activation of PKA and phosphorylation of the sAHP channel, culminating in sAHP suppression (Blitzer *et al.*, 1995).

The primary aim of these experiments was to test the hypothesis put forward by Blitzer et al (1995) that high frequency synaptic stimulation leads to sAHP suppression via the NMDAR-dependent activation of Ca^{++} stimulatable ACs. The experimental strategy used to test this hypothesis was to compare the effect of high frequency synaptic stimulation on the sAHP in WT and DKO mice.

The first step was to characterise the high frequency synaptic stimulation induced suppression of sAHP in WT mice. The recording electrode was in the whole cell configuration and was positioned at the soma of the CA1 pyramidal neurons. The stimulating electrode was positioned in the stratum radiatum to stimulate the Schaffer collateral pathway. Recordings were conducted at 30°C in the presence of 50 μM picrotoxin. The stimulation paradigm used to induce sAHP suppression was three trains of 100 pulses at 100 Hz separated by a three-minute interval. Whole-cell patch-clamp recordings were obtained from 18 CA1 pyramidal neurons in WT mouse hippocampal slices. Neurons had an average resting membrane potential of -61.7±1.0 mV, and DC current was injected throughout the experiment to maintain the membrane potential at –60 mV. Delivery of high frequency synaptic stimulation resulted in suppression of the sAHP. Fig. 31A

shows the sAHP in a representative cell one minute prior to (left panel) and six minutes post (middle panel) high frequency synaptic stimulation. The third trace

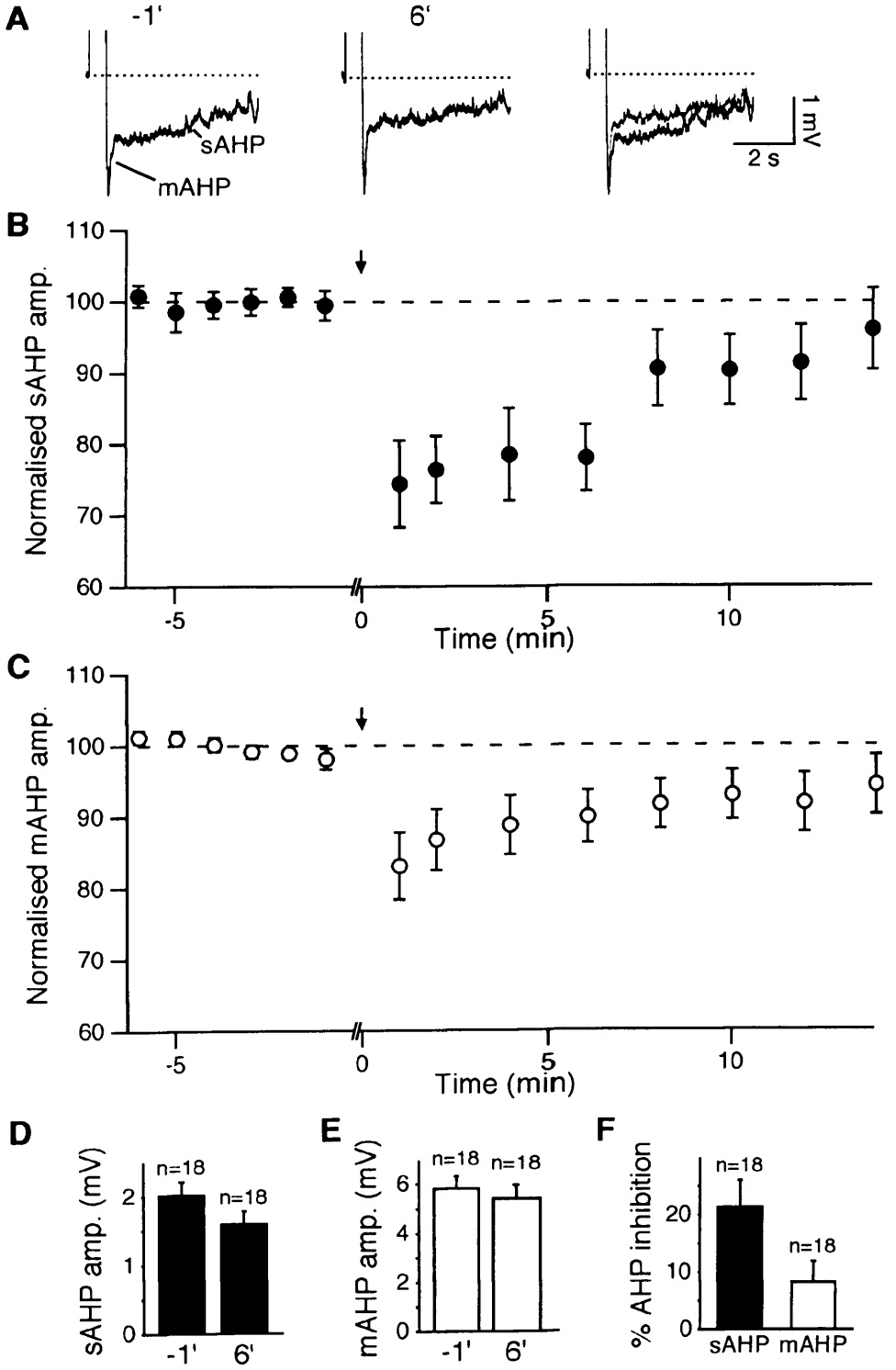

Figure 31: HFS of the Schaffer collaterals suppresses the sAHP in mouse CA1 pyramidal neurons.

A, Representative traces of the sAHP one minute prior to (-1') and six minutes post stimulation (6'). Each trace is an average of three consecutive sweeps, elicited every 20 seconds. The sAHP was elicited by 500 ms-long current injections that elicited trains of action potentials. The membrane potential of the cell was held at –60 mV for the duration of the experiment by constant current injection. The step current injection was adjusted to maintain the number of action potentials constant ± 1 before and after stimulation. HFS (100 Hz for 1 second, repeated three times at a three minute interval) was delivered to the Schaffer collateral pathway. Experiments were conducted in the presence of 50 μM picrotoxin. In order to prevent epileptiform activity in the presence of picrotoxin, a cut was positioned between regions CA3 and CA1 in the slice.

B, Time-course of the HFS-induced reduction in sAHP. Arrow indicates the end of high frequency stimulation. The sAHP was normalised to its pre-stimulation amplitude as indicated by the dashed line. Each point corresponds to the mean±SEM of 14 – 18 experiments.

C, Time course of the effect of HFS on the mAHP. Each point is an average of 14 – 18 experiments. Points are mean, error bars are SEM.

D, Bar chart comparing the amplitude of sAHP at one minute prior to HFS (-1'; mean sAHP amplitude: 2.0±0.2 mV; n=18) with six minutes post stimulation (6'; mean sAHP amplitude: 1.6±0.2 mV; n=18). Bars are mean, error bars are SEM. The sAHP amplitude is significantly suppressed by HFS of the Schaffer collateral pathway ($p<0.0001$, paired t test).

E, Bar chart illustrating the effect of HFS on mAHP amplitude. One minute prior to HFS the mAHP amplitude was 5.8±0.5 mV (n=18). Six minutes post stimulation the mAHP amplitude was 5.4±0.5 mV (n=18). There was significant difference between the mAHP amplitude at one minute prior to and six minutes post stimulation ($p<0.05$; Wilcoxon matched-pairs signed-ranks test).

F. Bar chart illustrating the significant difference between the sAHP suppression induced by HFS at six minutes following stimulation (sAHP; % inhibition: 21.4±4.6 %, n=18) and mAHP suppression (mAHP; % inhibition: 8.2±3.5 %, n=18; $p<0.05$; Mann Whitney test).

is an overlay of the two traces (pre-stimulation: black; post-stimulation: grey), whereby the sAHP reduction following stimulation can be seen clearly. The reduction in the sAHP was transient as it returned to baseline within 15 minutes (Fig. 31B). Repeated measures ANOVA revealed that there was significant

suppression in the sAHP post stimulation (n=12, $p<0.0001$). The reduction of sAHP amplitude between the last minute prior to stimulation and the sixth minute post stimulation is quantified in the bar chart in Fig. 31D. Six minutes post stimulation there was a 21.4±4.6% reduction in sAHP when compared to the last minute prior to stimulation (Fig. 31F; n=18). This sAHP suppression was statistically significant when analysed using a paired t test ($p<0.0001$). In a subset of cells, we investigated whether there was a change in input resistance immediately after stimulation compared with immediately prior to stimulation. In a paired t test, there was no significant change in input resistance over the course of high frequency synaptic stimulation (% change in input resistance: 104.2±3.8 %, n=4, p=0.32).

As shown in Fig. 31A, the two kinetically distinct phases of the AHP that follows a train of action potentials, mAHP and sAHP, can be distinguished. The mAHP is mediated by, among others, at least two currents that have been shown to be modulated either directly by cAMP (I_h; (DiFrancesco & Tortora, 1991; Pedarzani & Storm, 1995b)) or via PKA (SK channels mediating IAHP; (Ren *et al.*, 2006)). We therefore wondered whether the high frequency synaptic stimulation affected the mAHP in WT CA1 pyramidal neurons. Fig. 31C illustrates the change in the peak amplitude of the mAHP over time after stimulation. There was a significant reduction in the mAHP in a repeated measure one way ANOVA (n=13, $p<0.0001$). A post hoc Dunnett multiple comparison test revealed that the mAHP suppression was significant for the first two minutes post stimulation (the control was determined as the mAHP amplitude one minute prior to stimulation). Fig. 31E illustrates the reduction in mAHP amplitude at six minutes following stimulation compared with one minute prior to stimulation (mAHP amplitude at one minute prior to stimulation: 5.8±0.5 mV, n=18, mAHP amplitude six minutes post stimulation: 5.4±0.5 mV, n=18, $p>0.05$; Wilcoxon matched-pairs signed-ranks test; Fig. 31E). The significant reduction in mAHP amplitude at six minutes post stimulation is most likely due to rundown of the currents underlying the mAHP. Fig. 31F compares the suppression of sAHP at six minutes post stimulation with the suppression of mAHP. HFS leads to significantly greater

sAHP suppression than mAHP suppression at six minutes following the end of stimulation ($p<0.05$, Mann Whitney test).

6.3.2: The suppression of sAHP by HFS is NMDAR dependent

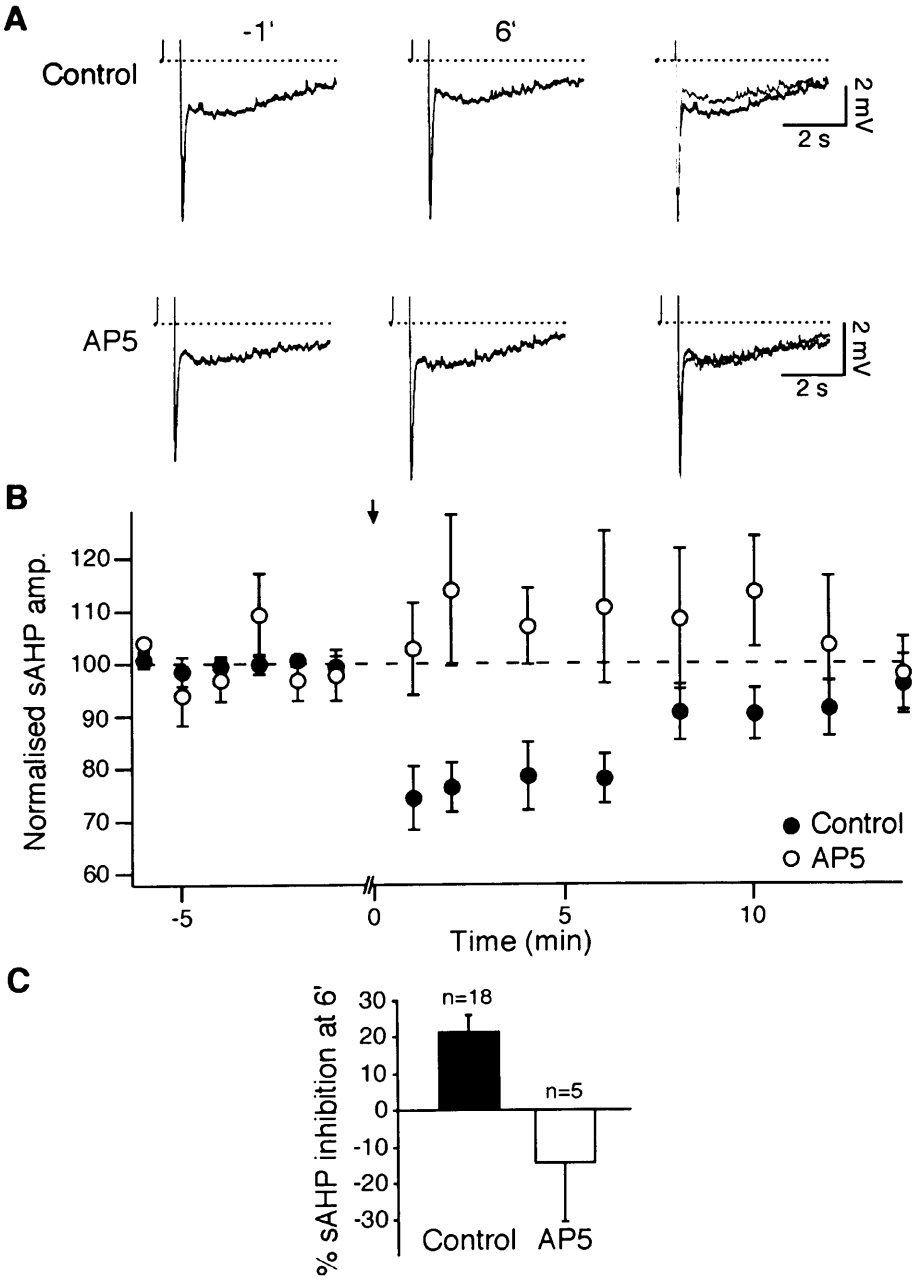

Figure 32: HFS-mediated sAHP suppression is NMDAR dependent

A, Representative traces comparing the sAHP one minute prior (-1') and six minutes post (6') HFS of the Schaffer collaterals in a control cell (upper row) and a cell preincubated with 100 μM AP5 (lower row). AP5 was added in the bath for at least 30 minutes prior to HFS delivery. In the control cell, HFS of the Schaffer collateral pathway results in sAHP suppression that is still visualised at six minutes post stimulation. The sAHP suppression

induced by HFS of the Schaffer collaterals is largely abolished in the presence of AP5 (100 μM).

B, Graph illustrating the time-course of the effect of HFS on sAHP amplitude in control cells (n=14 - 18) and cells treated with AP5 (n=5). There was no significant change in sAHP amplitude after stimulation in the presence of AP5 ($p=0.58$; n=5; repeated measures ANOVA). ***C,*** Bar chart depicting the effect of HFS of the Schaffer collaterals on sAHP amplitude 6 minutes post stimulation in control (n=18) and slices incubated with AP5 (n=5). There was a significant difference between the sAHP suppression 6 minutes post stimulation in AP5 (% sAHP increase at 6': 14.5±16.3 %; n=5) compared to control conditions (% sAHP inhibition at 6': 21.4±4.6 %; n=18; $p<0.005$; unpaired t test).

In order to assess whether the suppression of the sAHP induced by high frequency stimulation of the Schaffer collaterals was NMDAR dependent, experiments were conducted in the presence of the NMDAR blocker AP5 (100 μM). 100 μM AP5 was added to the ACSF at least 30 minutes prior to high frequency synaptic stimulation. In the presence of AP5 the effect of high frequency synaptic stimulation on sAHP was largely abolished (Fig. 32A and B). There was no significant difference in the time course of the sAHP amplitude before and after stimulation as revealed by a one way, repeated measures ANOVA in the presence of AP5 (n=5, $p=0.58$; Fig. 32B). Accordingly, there was no significant difference between the mean amplitude of sAHP one minute prior (mean sAHP amplitude at -1': 1.6±0.5 mV; n=5) and six minutes post stimulation in the presence of AP5 (mean sAHP amplitude at 6': 1.7± 0.5 mV; n=5; $p=0.55$; paired t test). This corresponded to an increase in sAHP amplitude of 14.5± 16.3 % (n=5) (Fig. 32C). The suppression of sAHP induced by synaptic stimulation was significantly reduced in AP5 compared with control conditions for the first six minutes post stimulation (one way ANOVA, $p<0.01$; Fig. 32B). An unpaired t test between the two conditions at six minutes post stimulation revealed that there was significant difference between the sAHP suppression in control conditions (% sAHP suppression: 21.4±4.6%, n=18), and the lack of sAHP suppression in AP5 (% sAHP suppression: -14.5±16.3 %, n=5, $p<0.005$; Fig. 32C). Taken together, these results indicated that high frequency stimulation resulting in sAHP suppression involves the activation of NMDAR.

6.3.3: The suppression of sAHP by HFS is mGluR independent

The sAHP can be inhibited by activation of metabotropic glutamate receptors (mGluR) (Charpak *et al.*, 1990). The mGluR-mediated suppression of sAHP in CA1 pyramidal neurons occurs via activation of type 5 mGluR ($mGluR_5$) and $G\alpha_q$ (Krause *et al.*, 2002), and does not involve PKA (Pedarzani & Storm, 1996a). To test the role of $mGluR_5$ in the suppression of sAHP induced by high frequency synaptic stimulation, experiments were conducted in the presence of 10 μM MPEP hydrochloride, which is a specific antagonist at $mGluR_5$ in hippocampal slices (Mannaioni *et al.*, 2001).

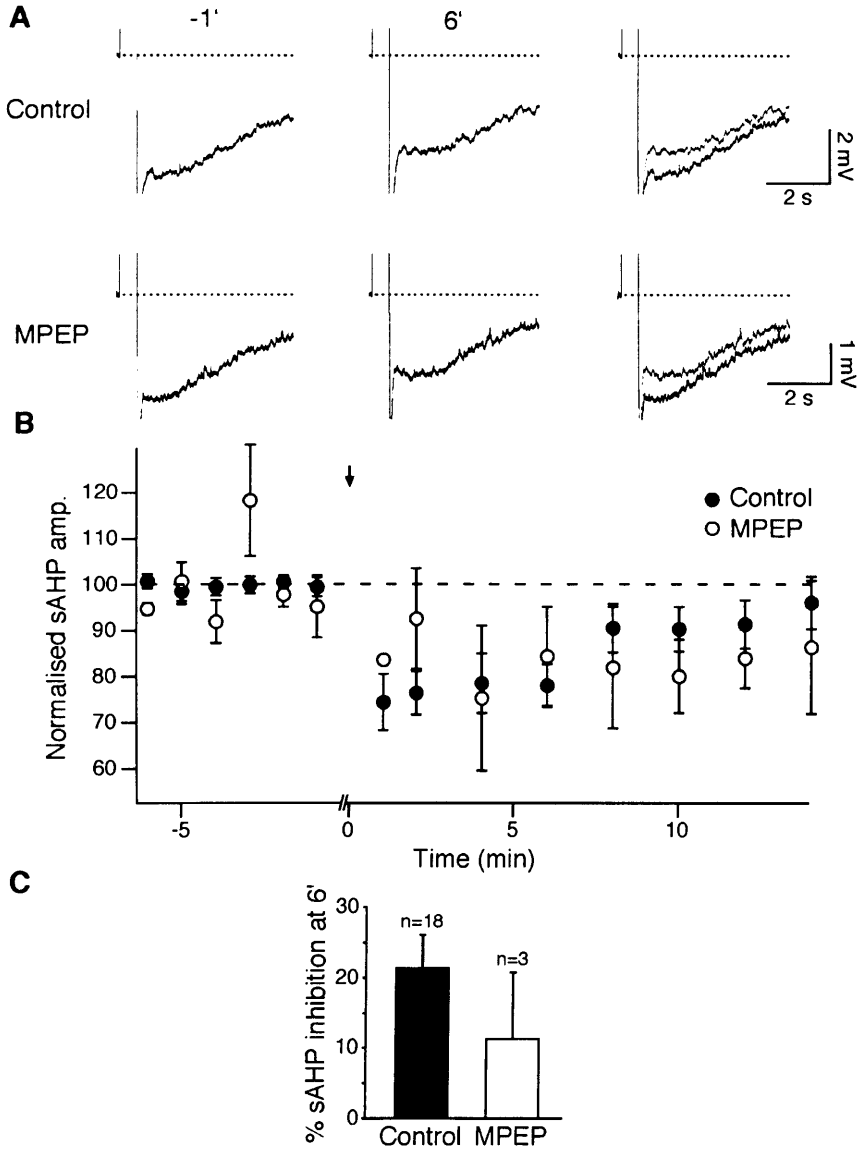

Figure 33: Activation of metobotropic glutamate receptors is not responsible for HFS- induced sAHP suppression

A, The $mGluR_5$ antagonist MPEP hydrochloride (MPEP; 10 μM) was applied to the bath at least thirty minutes prior to HFS delivery to the Schaffer collateral pathway. In slices pre-incubated with MPEP, sAHP suppression was still elicited by HFS.

B, Graph comparing the time-course of sAHP in experiments conducted in the presence of MPEP (n=3) and under control conditions (n=14 - 18). A Friedman test (non parametric ANOVA) revealed that there was no significant effect of HFS of the Schaffer collaterals on sAHP amplitude in the presence of MPEP (n=3; p=0.06).

C, Bar diagram comparing the sAHP suppression at six minutes post stimulation in control conditions (% sAHP inhibition at 6': 21.4±4.6 %; n=18) and in slices pre-incubated with MPEP (% sAHP inhibition at 6': 11.3±9.4 %; n=3). There was no significant difference between the sAHP suppression measured at six minutes post HFS of the Schaffer collaterals in control conditions or slices pre-incubated with MPEP (p=0.41; Mann Whitney test).

Fig. 33 compares the effect of high frequency synaptic stimulation in the presence of 10 μM MPEP and in the control situation. From Fig. 33A it can be seen that the suppression of sAHP induced by synaptic stimulation was intact in the presence of 10 μM MPEP. In a Friedman test, the effect of synaptic stimulation on the amplitude of sAHP in the presence of MPEP was not significant (n=3, p=0.06; Fig. 33B). However, there was no significant difference between the effect of synaptic stimulation on the sAHP in the presence of MPEP or in the control situation six minutes following stimulation (p=0.41; Mann Whitney test; Fig. 33C). These results indicate that the sAHP suppression generated by high frequency synaptic stimulation occurs independently of the activation of $mGluR_5$.

6.3.4: The suppression of sAHP induced by HFS is AC1/AC8 dependent

In order to directly assay whether activation of the Ca^{++} stimulatable ACs, AC1/AC8, by high frequency synaptic stimulation leads to sAHP suppression, we conducted experiments comparing the effect of high frequency stimulation on sAHP in WT and DKO mice (Fig. 34). In WT mice there was a 21.4±4.6 % suppression of the sAHP 6 minutes post stimulation (n=18; Fig. 34A, B and C). In CA1 neurons from DKO mice, the mean sAHP amplitude one minute prior to

stimulation was 1.6±0.3 mV compared with 1.6±0.3 mV six minutes post HFS to the Schaffer collaterals (n=10; p=0.74; paired t test). This indicated that the sAHP suppression was significantly abolished in DKO mice (Fig. 34A, B and C). Fig. 34B compares the time course of change in sAHP in the two groups of animals. In a repeated measures ANOVA, there was no significant change with time in the sAHP amplitude in DKO (n=8, p=0.11) compared with WT cells (n=12, p<0.0001). The results indicate that the suppression of sAHP induced by high frequency synaptic stimulation requires the activation of AC1/AC8.

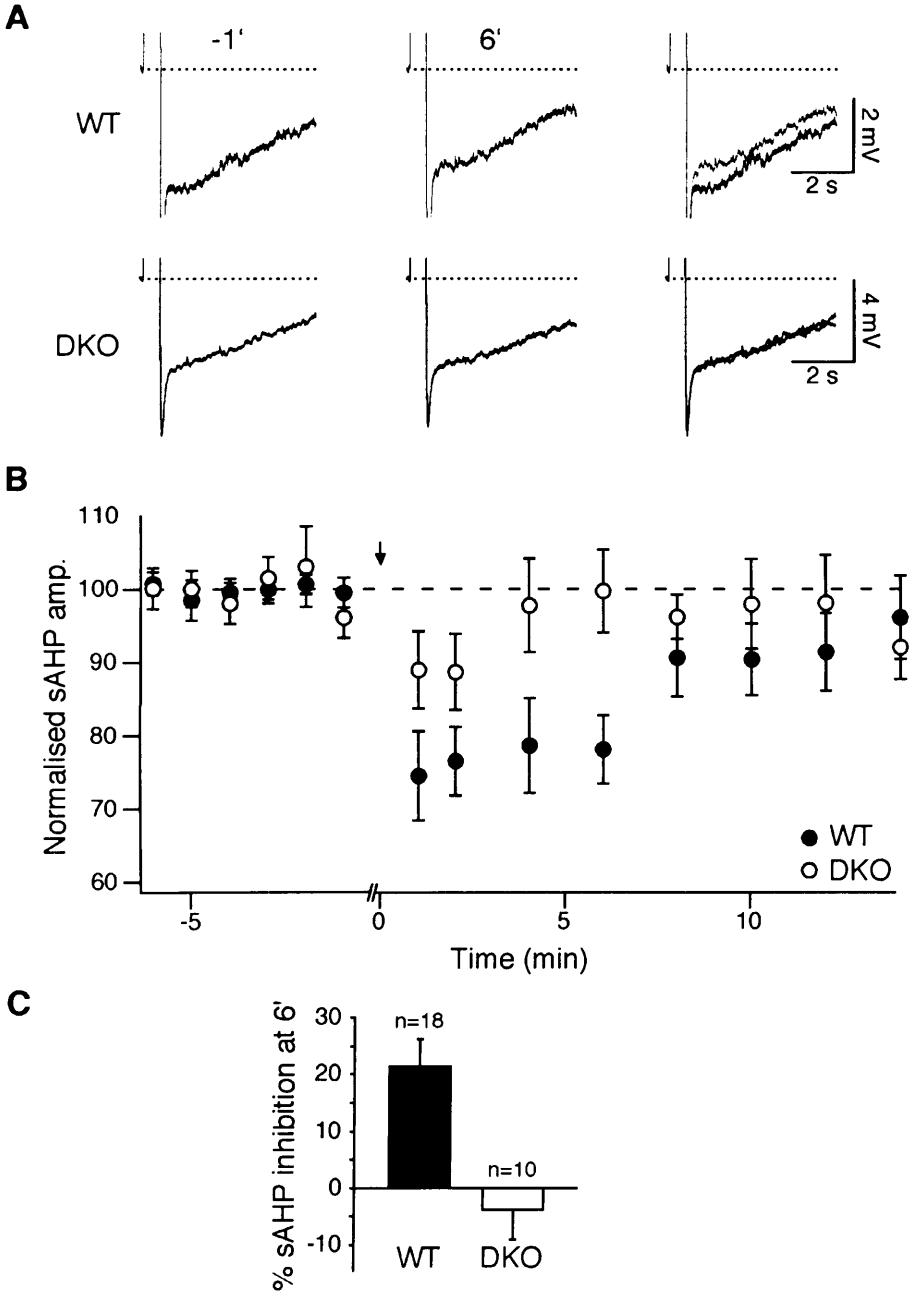

Figure 34: HFS induced sAHP suppression is abolished in AC1/AC8 DKO mice

A, HFS of the Schaffer collaterals induces sAHP suppression in WT mice, as evident 6 minutes after stimulation (upper row). This sAHP suppression is still present 6 minutes after synaptic stimulation. However, in DKO mice the sAHP suppression is largely abolished (lower row).

B, Time-course of sAHP illustrating the significant difference between the effect of HFS of Schaffer collaterals on sAHP in WT (n=14-18) and DKO mice (n=8-10). In WT mice there is significant difference in the sAHP amplitude following HFS (n=12; $p<0.0001$; repeated measures ANOVA), whereas there is no change in sAHP amplitude in slices from DKO mice (n=8; p=0.11; repeated measures ANOVA).

C, Bar diagram showing a significant difference in the sAHP suppression six minutes post stimulation in CA1 neurons from DKO (white bar; n=10) and WT mice (black bar; n=18; $p<0.005$; unpaired t test. Bars are mean, error bars are SEM.

6.3.5: The suppression of sAHP induced by HFS is PKA dependent

In order to test the role of post-synaptic PKA in the suppression of sAHP induced by high frequency synaptic stimulation, we included the PKA inhibitory peptide PKI_{6-22} (1 mM) in the patch pipette solution. To allow adequate perfusion of PKI_{6-22} into the cell, synaptic stimulation was delivered at least 45 minutes after achieving the whole cell configuration, and access resistance was maintained <20 MΩ for the duration of the experiment. As a positive control, 1 μM isoproterenol was routinely applied to the sI_{AHP} recorded in voltage clamp at the end of the experiment in both control cells and cells which had been intracellularly perfused with PKI_{6-22}. Cells displaying no inhibition of the effect of isoproterenol on the sAHP in the presence of PKI_{6-22} were excluded from the analysis, as this was taken as an indication of an insufficient diffusion of the PKA inhibitor. In 7 out of 7 cells recorded in the presence of PKI_{6-22}, application of 1 μM isoproterenol resulted in 23.9±6.3 % inhibition of sI_{AHP} (Fig. 35D). There was significant difference comparing the effect of 1 μM isoproterenol on the sI_{AHP} in the presence and absence of PKI_{6-22} (% inhibition of sI_{AHP} in the absence of PKI_{6-22}: 70.8±5.9, n=3, $p<0.005$; unpaired t test; Fig 35D). These results indicate that in these 7 cells, the effect of PKA was largely inhibited by PKI_{6-22}.

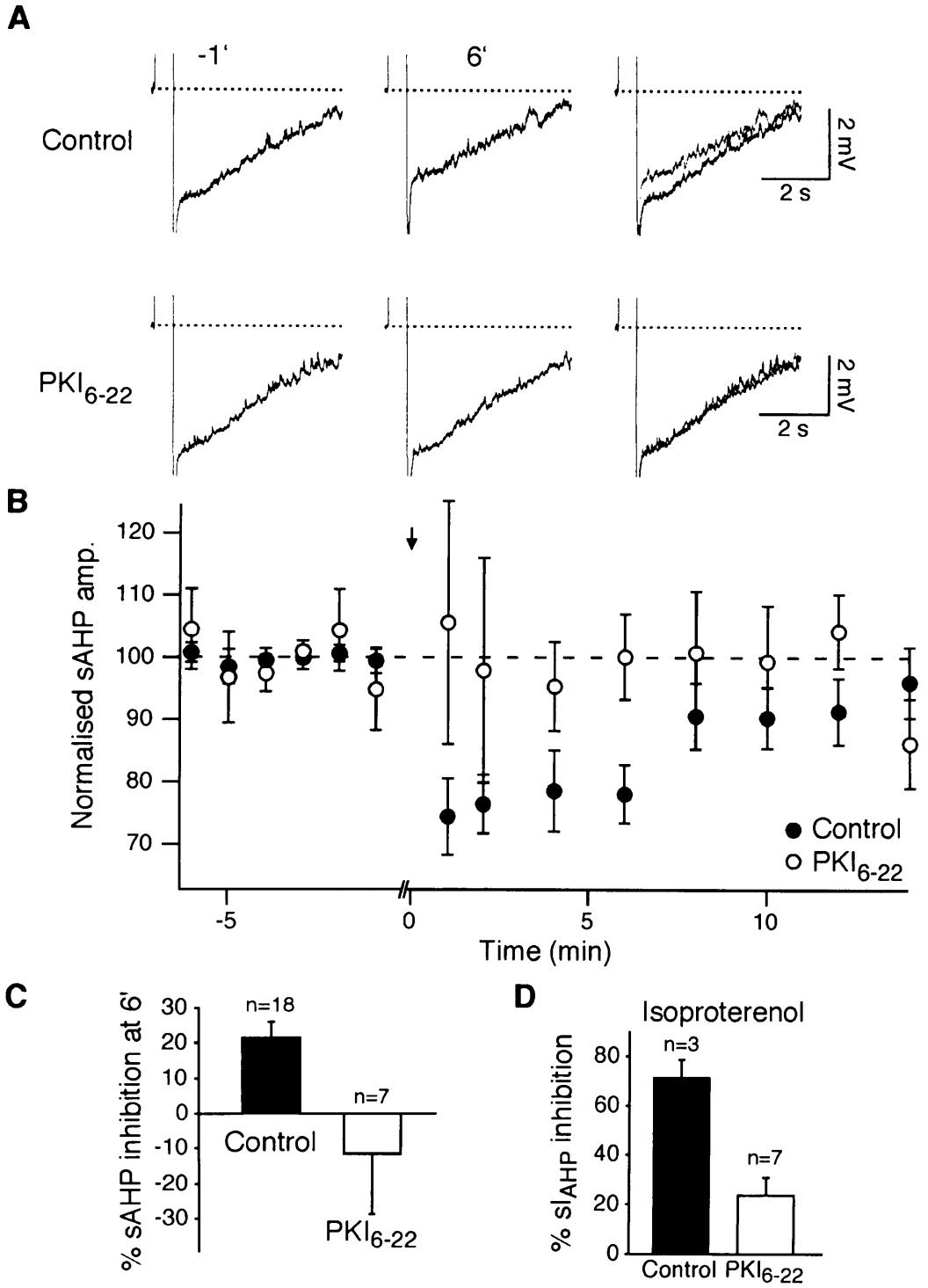

Figure 35: Inhibiting PKA prevents the HFS-induced sAHP suppression

A, PKI_{6-22} is a pseudosubstrate inhibitor of PKA. PKI_{6-22} (1 mM) was included in the recoding pipette solution. In order to ensure adequate diffusion of PKI_{6-22} into the cell, the access resistance was maintained at <20 MΩ for at least 45 minutes prior to HFS of the Schaffer collaterals. Inclusion of PKI_{6-22} in the recording pipette resulted in suppression of the HFS induced effect on sAHP (lower row; compare with upper row).

B, Time-course of sAHP illustrates that delivery of HFS did not result in a significant sAHP suppression in CA1 neurons recorded in the presence of PKI_{6-22} (n=14-18 for controls; n=3-7 for PKI_{6-22}). In a Friedman test (non parametric ANOVA) there was no significant change in sAHP amplitude following HFS of the Schaffer collaterals (n=3; p=0.59).

C, In cells in which PKI_{6-22} was included in the recording pipette, the effect of HFS on sAHP suppression at six minutes post stimulation was abolished (n=7; p=0.78; paired t test). In addition there was a significant difference between the effect of HFS six minutes post stimulation in control (n=18) and PKI_{6-22} dialised cells (n=7; $p<0.05$; Mann Whitney test).

D, In experiments with PKI_{6-22}, 1 μM isoproterenol was routinely applied at the end of the experiments as a positive control for the effectiveness of the PKA inhibition. In control cells, isoproterenol inhibited 70.8±5.9 % of the sAHP (n=3). By contrast, in cells is which PKA was inhibited, isoproterenol achieved only 23.9±6.3 % sAHP inhibition (n=7). The difference in the isoproterenol mediated sAHP inhibition was significant between control and PKI_{6-22} cells ($p<0.005$).

Fig. 35A shows representative traces taken one minute prior and six minutes after stimulation in control and cells recorded in the presence of PKI_{6-22}. From these traces it can be seen that the effect of high frequency synaptic stimulation on the sAHP was largely abolished in the presence of PKI_{6-22}. The effect is quantified in Fig. 35C. In cells recorded in the presence of PKI_{6-22} there was no significant effect of high frequency synaptic stimulation on the sAHP (% sAHP amplitude at six minutes: -111.5±17.4%, n=7, p=0.78, paired t test). The sAHP suppression in the presence of PKI_{6-22} was significantly reduced compared with that in the control situation (% sAHP suppression at six minutes in control: 21.4±4.6, n=18, $p<0.05$; Mann Whitney test; Fig. 35C). A Friedman test (non parametric ANOVA) on the time-course of the sAHP suppression following high frequency synaptic stimulation in the presence of PKI_{6-22} shown in Fig. 35B showed no significance (n=3, p=0.59). These results indicate that the suppression of sAHP induced by high frequency synaptic stimulation requires activation of PKA, and that the locus of the PKA effect is post-synaptic, in agreement with the results obtained by Blitzer et al. (1995) in rat CA1 pyramidal neurons.

6.3.6: An LTP-inducing pairing protocol leads to postsynaptic sAHP suppression

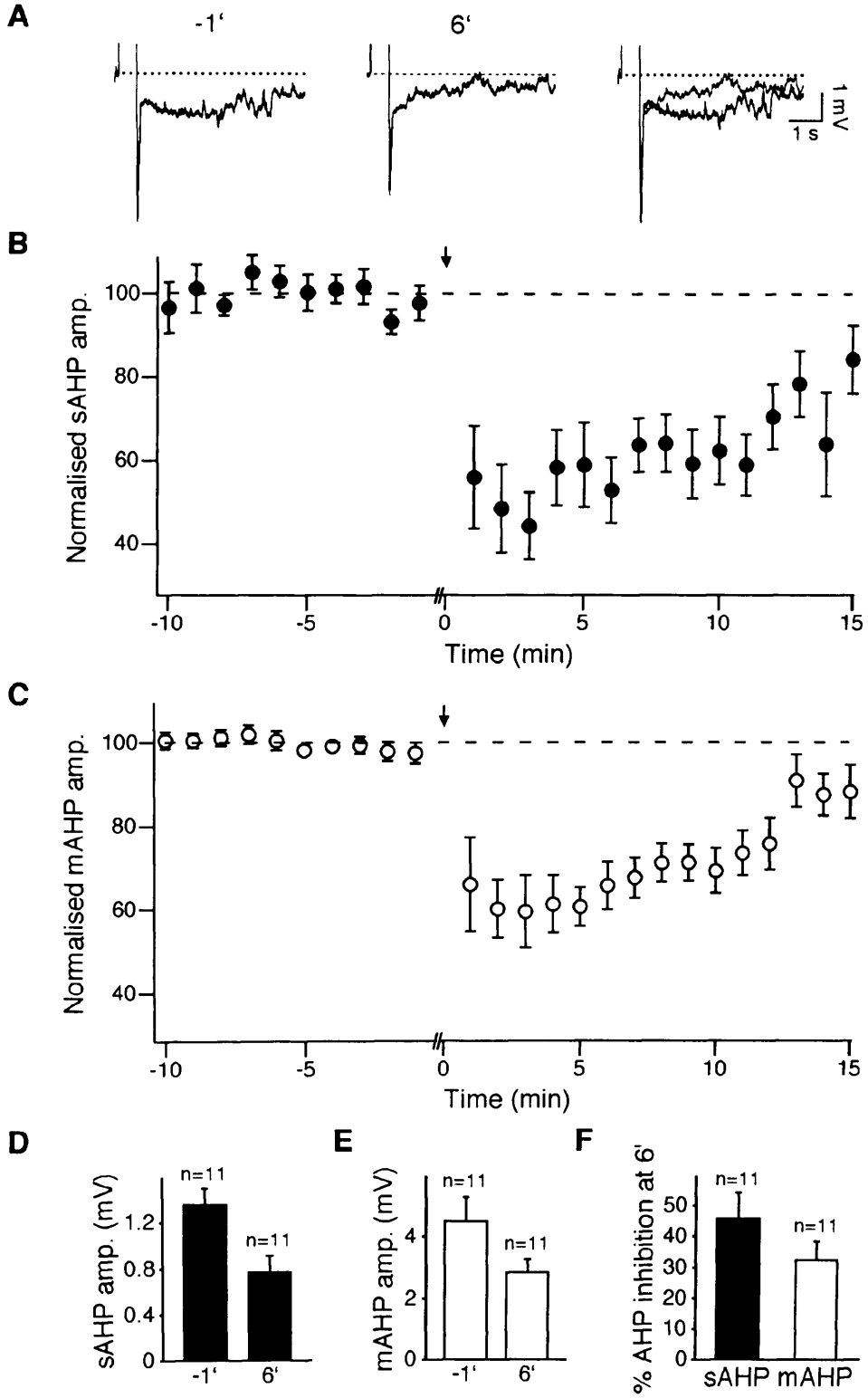

Figure 36: A pairing protocol induces sAHP suppression.

A, Pairing post-synaptic depolarisation with presynaptic stimulation results in sAHP suppression. The stimulus protocol coupled CA1 post synaptic depolarisation to 0 mV with 200 stimuli delivered at 5 Hz to the Schaffer collateral pathway. Experiments were conducted at 30 °C in the presence of 50 μM picrotoxin. Under these conditions, the pairing protocol induced a partial suppression of sAHP. Traces shown are one minute prior to stimulation (-1'; left panel) and 6 minutes after the end of stimulation (6'; middle panel). Each trace is an average of three consecutive sweeps, acquired every 20 seconds.

B, Graph showing the time-course of the change in sAHP amplitude in response to the pairing protocol. Stimulation was delivered as indicated by the arrow. Each point is the mean 4-12 experiments. The error bars are SEM. The data was normalised to the average sAHP amplitude in the last ten minutes of recording before stimulation. The time-course of the change in sAHP amplitude in response to the pairing protocol was significant when a subset of data were analysed using a repeated measures ANOVA ($n=6$, $p<0.0001$).

C, Time-course of the change in mAHP amplitude in response to the pairing protocol. Error bars are SEM. Each point is the mean of 4-12 experiments. Data was normalised to the average mAHP amplitude in the last ten minutes before stimulation. The time-course of the change in mAHP amplitude in response to the pairing protocol was significant when a subset of data were analysed using a repeated measures ANOVA (same cells as in ***B***; $n=6$; $p<0.0001$).

D, A significant sAHP suppression was observed six minutes after stimulus delivery. The mean sAHP amplitude one minute prior to stimulus delivery (-1') was 1.4±0.1 mV ($n=11$) compared with 0.8±0.1 mV ($n=11$) measured six minutes after stimulus delivery (6'; $p<0.0005$; paired t test).

E, The mean mAHP amplitude observed six minutes after stimulus delivery (6'; 4.5±0.7 mV; $n=11$) was significantly different to the mean mAHP amplitude measured one minute before delivery of the pairing protocol (-1'; 2.8±0.4 mV; $n=11$; $p<0.05$; paired t test).

F, Quantification of the AHP suppression measured six minutes after delivery of the pairing protocol. The mean AHP amplitude at six minutes post stimulation was normalised to the mean AHP amplitude one minute prior to stimulus delivery. Mean sAHP inhibition at six minutes post stimulation was 45.8±8.5 % ($n=11$). The mean mAHP suppression was 32.5±5.5 % at six minutes after delivery of the pairing protocol.

The primary aim of this set of experiments was to investigate whether other commonly used LTP-inducing protocols, besides the high frequency stimulation

of Schaffer collaterals, elicit a similar transient reduction of sAHP in the postsynaptic cells. In particular, we tested the hypothesis that an LTP-inducing pairing protocol could elicit sAHP suppression. The pairing protocol consisted of simultaneous post-synaptic depolarisation of CA1 neurons to 0 mV, coupled with low frequency stimulation of the Schaffer collaterals at 5 Hz. Experiments were conducted at 30°C in the presence of 50 μM picrotoxin. Under these conditions, administration of the LTP-inducing pairing protocol also resulted in sAHP reduction (Fig. 36A). The time course of sAHP suppression is shown in Fig. 36B. A repeated-measures ANOVA revealed that the sAHP suppression is significant over time ($n=6$, $p<0.0001$). The effect is quantified in Fig. 36. The sAHP was significantly suppressed six minutes after, when compared to one minute prior to stimulation (% sAHP suppression six minutes post stimulation: 45.8±8.5%, $n=11$; $p<0.0005$; paired t test; Fig. 36D, F).

In a subset of cells, we investigated whether there was a change in input resistance immediately after stimulation, compared with immediately prior to stimulation. In a paired t test, there was no significant change in input resistance over the delivery of the LTP pairing protocol (mean input resistance before stimulation: 115.0±8.5 MΩ; mean input resistance after stimulation: 105.2±14.2 MΩ, $n=3$, $p=0.27$).

Figure 36C shows the transient change in mAHP amplitude following delivery of the pairing protocol. The mean mAHP amplitude one minute prior to stimulus delivery was 2.8±0.4 mV ($n=11$; Fig. 36E). Delivery of the pairing protocol resulted in significant mAHP suppression (% mAHP suppression six minutes post stimulus delivery: 32.5±5.5 %; $n=11$; $p<0.05$; paired t test; Fig. 36D, F).

6.3.7: sAHP suppression by an LTP-inducing pairing protocol is NMDAR dependent

The aim of this part of the study was to test whether the LTP-inducing pairing protocol elicits a transient inhibition of sAHP by the same signal transduction pathway as high frequency synaptic stimulation. In order to determine whether the sAHP suppression elicited by the LTP-inducing pairing protocol is dependent on activation of NMDAR, experiments were conducted in the presence of the NMDAR blocker AP5 (100 μM). Slices were bathed in 100 μM AP5 at least 30

minutes prior to stimulation. Fig. 37 compares the effect of the LTP-inducing pairing protocol in the presence of 100 μM AP5 and in the control situation.

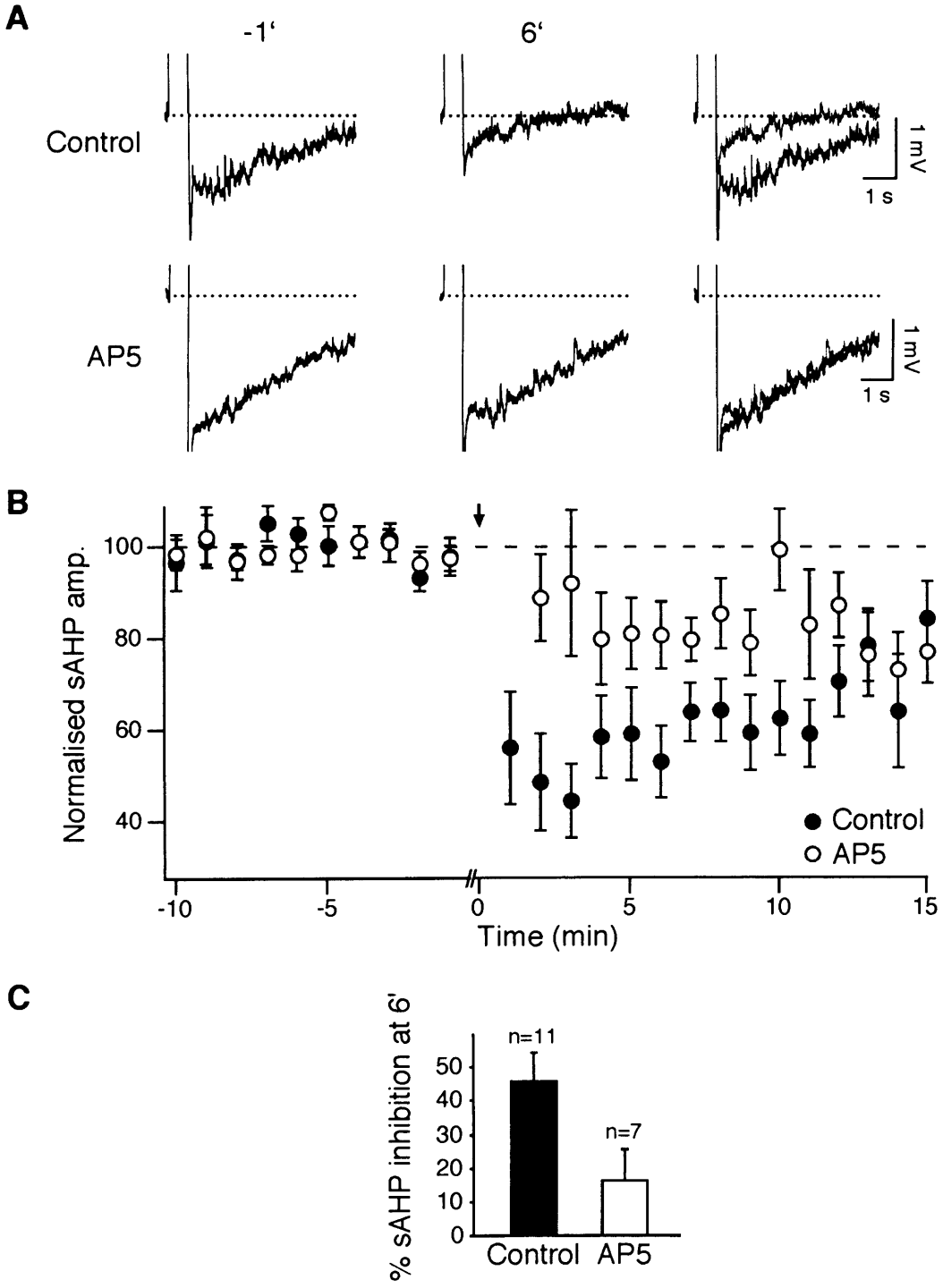

Figure 37: The pairing protocol induced sAHP suppression is NMDAR-dependent

A, Addition of 100 μM AP5 thirty minutes prior to delivery of the pairing protocol suppressed the stimulation induced effect on the sAHP in CA1 neurons. The sAHP suppression can be seen in the control situation (upper row), whereas when AP5 is present in the bath, the sAHP suppression is largely abolished (lower row).

B, Graph comparing the effect of the pairing protocol on sAHP amplitude over time in the presence and absence of AP5 (n=4-12 in control; n=3-7 in AP5). In a subset of cells, there is no significant change in sAHP amplitude with delivery of the pairing protocol when AP5 is present (n=3, p=0.69; Friedman test).
C, Bar diagram illustrating the effect of the pairing protocol on sAHP amplitude six minutes after delivery of stimulation in the presence and absence of AP5. Data was normalised to the sAHP amplitude one minute prior to delivery of the pairing protocol. There was no significant change in sAHP amplitude six minutes after delivery of the pairing protocol in the presence of AP5 (% sAHP inhibition: 16.5±9.0 %; n=7; p=0.12; paired t test). There was a significant difference between the sAHP suppression elicited by the pairing protocol six minutes following stimulation in control (% sAHP suppression: 45.8±8.5 %, n=11) compared with in the presence of AP5 ($p<0.05$; unpaired t test).

When AP5 was present in the bath, the effect of the LTP-inducing pairing protocol on sAHP was largely abolished (Friedman test; n=3; $p>0.69$; Fig. 37A and B). In 100 μM AP5 there was no significant difference comparing the mean sAHP amplitude in the first minute prior to stimulation (1.5±0.2 mV; n=7) to six minutes after stimulation (mean sAHP amplitude at six minutes post stimulation: 1.3±0.2 mV, n=7; p=0.12; paired t test). Fig. 37C shows the sAHP suppression elicited by the pairing protocol six minutes following stimulus delivery in the presence and absence of AP5. The sAHP suppression in the presence of AP5 (16.5±9.0 %; n=7) was significantly different from the sAHP suppression elicited in control CA1 neurons (45.8±8.5 %; n=7; $p<0.05$; unpaired t test). These results indicate that the sAHP suppression elicited by an LTP pairing protocol is largely dependent on the activation of NMDAR.

6.3.8: sAHP suppression by an LTP-inducing pairing protocol requires Ca^{++} stimulatable ACs

The signal transduction cascade leading to the reduction of sAHP in CA1 neurons triggered by high frequency synaptic stimulation of the Schaffer collaterals involved the activation of NMDAR, AC1/AC8, and PKA. After showing that the sAHP inhibition caused by the LTP-inducing pairing protocol requires NMDAR

activation, the next logical step is to test whether AC1/AC8 are important for the suppression of sAHP by this stimulation protocol, in analogy to what we observed for the high frequency stimulation protocol. To test this hypothesis, we compared the effect of the LTP-inducing pairing protocol on sAHP in WT and DKO mice.

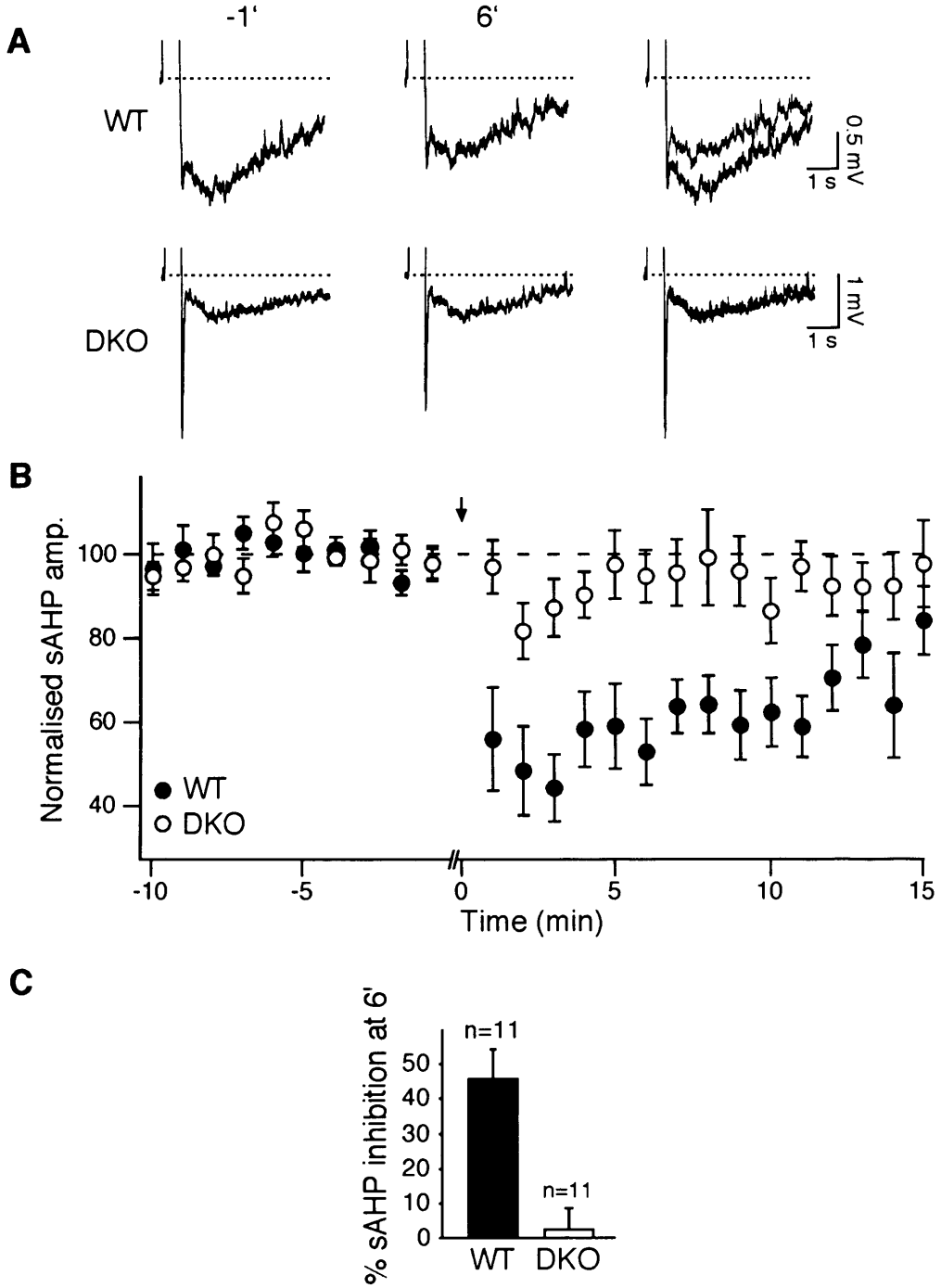

Figure 38: Activation of Ca^{++} stimulatable ACs mediates the suppression of sAHP by the pairing protocol

A, Representative traces taken from a WT and a DKO CA1 neuron one minute before (-1') and six minutes after (6') delivery of the pairing protocol. The pairing protocol-induced sAHP suppression is abolished in the DKO at six minutes post stimulus (lower row).

B, Graph comparing the sAHP suppression over time in WT (n=4-12) and DKO (n=3-11) cells. There is no significant change induced by the pairing protocol in DKO animals in a subset of cells (n=6, p=0.41; repeated measures ANOVA).

C, Bar diagram showing that the sAHP is not significantly suppressed six minutes in DKO cells (% sAHP inhibition in DKO CA1 neurons: 2.5±5.9 %, n=11; p=0.54; paired t test). The sAHP amplitude at six minutes was normalised to the sAHP amplitude one minute prior to delivery of the pairing protocol. When the sAHP suppression at six minutes is compared across the groups of animals, there is a significant difference between the two groups of animals ($p<0.0005$; unpaired t test).

The sAHP suppression elicited by the LTP-inducing pairing protocol was largely abolished in DKO mice. This is illustrated in Fig. 38A. The effect is quantified in Fig. 38C, where the sAHP suppression at six minutes after stimulation is compared in DKO and WT mice. In WT mice there was a 45.8±8.5 % suppression of sAHP (n=11), while this was 2.5±5.9 % in DKO mice (n=11; $p<0.0005$; unpaired t test; Fig. 38C). In accordance with this result, the effect of the LTP-inducing pairing protocol on the sAHP amplitude was not significant in a one-way repeated-measures ANOVA (n=6, p=0.41; Fig. 38B).

In addition, there was no significant difference between the sAHP amplitude measured one minute prior to stimulation and six minutes post stimulation in DKO mice (sAHP amplitude at one minute prior to stimulation: 1.1±0.1 mV; n=11; sAHP amplitude six minutes post stimulation: 1.1±0.1 mV; n=11; p=0.54; paired t test). In conclusion, these results indicate that the LTP-inducing pairing protocol causes a transient reduction in sAHP by activating AC1/AC8 in CA1 pyramidal neurons.

6.4.0: Discussion

The primary aim of this section of experiments was to investigate the possible involvement of the Ca^{++} stimulatable ACs in the glutamatergic modulation of sAHP in CA1 pyramidal neurons invoked by synaptic stimulation of the Schaffer collateral pathway. Consistent with previous experiments (Blitzer *et al.*, 1995), HFS led to partial suppression of the sAHP in an NMDAR- and PKA-dependent manner. The effect of HFS on the sAHP was absent in slices from DKO mice, indicating that activation of Ca^{++} stimulatable ACs mediated this effect. Additionally, an LTP-inducing pairing protocol was shown to elicit sAHP suppression dependent on the activation of NMDAR and the expression of Ca^{++} stimulatable ACs.

6.4.1: HFS: glutamate receptors responsible for the inhibition of sAHP

The sAHP is inhibited by the activation of mGluRs (Charpak *et al.*, 1990), specifically of type 5 ($mGluR_5$) in CA1 pyramidal neurons (Mannaioni *et al.*, 2001). The signal transduction cascade mediating the $mGluR_5$ effect has been shown to involve $G\alpha_q$ (Krause *et al.*, 2002) and is independent of activation of PKA (Pedarzani & Storm, 1996a). Three lines of experimental evidence presented in this study converge on the idea that the sAHP suppression induced in CA1 pyramidal neurons by high frequency synaptic stimulation of the Schaffer collateral pathway is independent of activation of $mGluR_5$ and dependent on activation of NMDAR. Firstly, HFS induced sAHP suppression in slices bathed in 10 μM MPEP hydrochloride, which has been shown to be sufficient to inhibit $mGluR_5$ in hippocampal cells (Mannaioni *et al.*, 2001). Secondly, HFS in slices bathed in 100 μM AP5, an NMDAR antagonist, did not induce sAHP suppression. This is consistent with the fact that the HFS paradigm is commonly used to elicit NMDAR-dependent LTP of the CA3-CA1 synapses (Bliss & Collingridge, 1993). Thirdly, the suppression of sAHP, induced by HFS, was found to be dependent on the activation of PKA, as it was abolished when the PKA inhibitor PKI_{6-22} was included in the intracellular milieu. In summary, based on our evidence we can

conclude that the suppression of sAHP induced in CA1 neurons by HFS of the Schaffer collateral pathway is NMDAR-dependent and independent of activation of $mGluR_5$.

6.4.2: Postsynaptic PKA is responsible for sAHP suppression

It has previously been reported that PKA is involved in the sAHP suppression induced in CA1 pyramidal neurons by HFS of the Schaffer collaterals (Blitzer *et al.*, 1995). However, those experiments were conducted by inclusion of the PKA inhibitor Rp-cAMPS in the recording pipette. Rp-cAMPS is membrane permeant, and therefore its possible diffusion out of the CA1 neurons and into the glutamatergic presynaptic terminals cannot be strictly excluded, together with a potential presynaptic role for PKA activation. The experiments presented in this thesis address this issue through the use of PKI_{6-22}. PKI_{6-22} is a membrane-impermeable, pseudosubstrate inhibitor of PKA that acts by binding to the substrate recognition site of the PKA catalytic subunit (Cheng *et al.*, 1986). Therefore, the intracellular application of PKI_{6-22} to the postsynaptic cell through the patch pipette specifically targets a postsynaptic locus of PKA action. Additionally, the specific nature of the interaction between PKI_{6-22} and PKA unequivocally demonstrates the role of PKA activation in the modulation of sAHP. The results presented in this thesis therefore confirm and extend the findings reported by Blitzer et al. (1995), showing that the postsynaptic activation of PKA in CA1 pyramidal neurons by the high frequency stimulation of the Schaffer collaterals is an essential step in the pathway leading to the inhibition of sAHP.

6.4.3: Time-course of the effect of HFS on sAHP

HFS of the Schaffer collaterals resulted in a transient sAHP suppression in CA1 neurons, which returned to baseline within 15 minutes. Evidence supporting an involvement of the cAMP-PKA signal transduction cascade and the time course of sAHP suppression following high frequency stimulation of the Schaffer collaterals is further strengthened by biochemical experiments conducted in the 1990s. In particular, it was shown that the concentration of cAMP within CA1

rises immediately after the induction of LTP by 100 Hz stimulation of the Schaffer collateral pathway and returns to baseline over 10-20 minutes (Chetkovich & Sweatt, 1993). PKA was shown to be transiently activated by the same stimulation protocol between 2 and 10 minutes after delivery of the LTP-inducing stimuli (Roberson & Sweatt, 1996). Therefore, the time course of both the rise in cAMP concentration and activation of PKA is consistent with their role in suppressing the sAHP in response to high frequency stimulation.

6.4.4: Activation of PKA by an LTP pairing protocol

The high frequency synaptic stimulation paradigm described above comprised 1 second-long trains of stimuli delivered at 100 Hz. This is a typical experimental paradigm used for the induction of LTP and known to activate NMDA receptors (Bliss & Collingridge, 1993). In 1961, Kandel showed that cat CA3 pyramidal cells spontaneously fire short bursts of action potentials with the underlying depolarisation lasting up to 100 msec (Kandel & Spencer, 1961). However, bursts of action potentials as long as 1 second in duration have not been reported. Therefore, the physiological relevance of the sAHP suppression induced by high frequency synaptic stimulation is questionable. In order to address this issue, a protocol that paired postsynaptic depolarisation with pre-synaptic low frequency stimulation within the range of the hippocampal theta rhythm, previously used for the induction of LTP (Otmakhov & Lisman, 2002), was tested. In the experiments presented in this thesis (Fig. 37), this protocol induced a robust, transient sAHP suppression in an NMDAR-dependent manner. Otmakhova et al. (2000) used two different PKA inhibitors to show that a similar pairing protocol leads to the activation of PKA during the induction of early phase LTP. Therefore, it is probable that the sAHP suppression elicited by delivery of the pairing protocol reflects a transient rise in cAMP and activation of PKA.

6.4.5: Does activation of "h" channels explain the suppression of sAHP by synaptic stimulation?

This study has shown an involvement of AC1/AC8 in the suppression of the sAHP elicited by two stimulation paradigms: HFS and an LTP-inducing pairing

protocol. The activation of AC1/AC8 would lead to generation of cAMP. cAMP has been demonstrated to cause a depolarising shift in the activation curve of I_h by a direct effect of cAMP on the underlying HCN channel (DiFrancesco & Tortora, 1991; Santoro *et al.*, 1998). I_h is a slowly developing inward current, activated by hyperpolarisation (Halliwell & Adams, 1982). In CA1 pyramidal neurons, the activation of I_h occurs at around -50 mV at the soma (Maccaferri *et al.*, 1993) compared to at more hyperpolarised potentials (~-60 mV) in the dendrites (Magee, 1998). The current is much larger in the dendrites than at the soma (Magee, 1998). This indicates that the density of the underlying HCN channels is much higher in the dendrites. Therefore the increase in cAMP concentration at the dendrites through the synaptic stimulation paradigms used in this study could lead to activation of I_h at more depolarised potentials. Therefore, the cAMP dependent activation of a slowly developing inward current could counteract the outward current that underlies sAHP. This would result in the generation of a sAHP of reduced amplitude.

Increased activation of I_h would lead to an increase in membrane conductance that would be recorded as a decrease in input resistance. However, delivery of either HFS or the LTP-inducing pairing protocol did not result in a significant change in input resistance. The HCN channels that underlie I_h are directly gated by cAMP, independently of the activation of PKA (Santoro *et al.*, 1998). In this study, sAHP suppression elicited by high frequency synaptic stimulation was abolished in the presence of the PKA inhibitor PKI_{6-22}. Therefore, the sAHP suppression elicited by high frequency stimulation is not attributable to an increase in I_h. Additionally, if activation of I_h by cAMP was indirectly responsible for the sAHP suppression elicited by the synaptic stimulation protocols used in this study, a concomitant noticeable increase in mAHP would be expected. Application of the HCN channel blocker ZD7288 has been shown to inhibit the mAHP elicited at -80 mV (Gu *et al.*, 2005), indicating that I_h contributes to the mAHP-line waveform measured at this membrane potential. A shift in the activation curve of HCN channels caused by generation of cAMP would increase their contribution to the mAHP. However, delivery of the LTP pairing protocol and HFS resulted in a transient

decrease in the recorded mAHP. Therefore, it is concluded that sAHP suppression elicited by synaptic stimulation is not due to cAMP dependent activation of I_h.

6.4.6: Functional implications of the modulation of sAHP by repetitive synaptic stimulation on EPSPs, temporal summation and LTP induction

Activity dependent modifications of synaptic efficacy are thought to underlie learning and memory (Bliss & Collingridge, 1993). The sAHP regulates synaptic efficacy by modulating the EPSP waveform, and thereby affecting temporal EPSP summation and the threshold for LTP induction (Fuenzalida *et al.*, 2007). Potentiation of the sAHP, through its repetitive activation, was shown to lead to a decrease in synaptic efficacy (Borde *et al.*, 1995; Borde *et al.*, 1999). This dampening of synaptic excitation was demonstrated to be due to the decrease in input resistance and concomitant membrane hyperpolarisation elicited by potentiation of sAHP (Borde *et al.*, 1999). The effect of the sAHP on the EPSP waveform has been shown in different ways. In particular, Lancaster et al. (2001) showed that (i) EPSPs were sufficient to trigger a sAHP, even in the absence of action potentials; (ii) deactivating sI_{AHP} by photolysis of BAPTA derivatives led to a slowing of the time course of decay of the EPSP (Lancaster *et al.*, 2001) and (iii) the sAHP, triggered by action potentials or subthreshold EPSPs, reduced the overall synaptic response area following trains of stimuli, indicating that the sAHP functioned to reduce temporal summation (Lancaster *et al.*, 2001). Consistent with this study, Sah and Bekkers (1996) demonstrated that the concomitant activation of the sAHP by depolarising current injections led to EPSPs with smaller amplitude and faster decay than when the sAHP was not activated. This study was extended to demonstrate that the sAHP selectively shunts NMDA mediated EPSPs (Fernandez de Sevilla *et al.*, 2007), whilst Ca^{++} influx through NMDAR is sufficient to activate sI_{AHP} (Borde *et al.*, 1999).

These observations suggest a pathway whereby synaptic activity leads to the generation of EPSPs, in turn activating the sAHP. Subsequent EPSPs triggered during the sAHP would have a smaller amplitude and a shorter decay time constant. Therefore, the sAHP, besides causing a reduction in postsynaptic

excitability, would reduce temporal summation, resulting in a lower probability of LTP induction and/or reduced LTP magnitude, if LTP is induced. However, the results presented in this thesis show that repetitive synaptic stimulation, either at high frequency or at low frequency coupled with simultaneous postsynaptic depolarisation, leads to a temporary suppression of the sAHP via activation of NMDAR, AC1/AC8 and PKA. This could potentially offset the effect of the sAHP on EPSPs, temporal summation and LTP threshold and/or magnitude, providing the postsynaptic neuron with a mechanism that favours the induction of LTP, increases the magnitude of LTP, or the temporal window of LTP induction. The temporary nature of the suppression of the sAHP (~ 15 minutes) would prevent hyperexcitability.

Chapter 7: General Discussion

7.1: Possible co-localisation of D1 receptors and NMDA receptors

In summary, in this study we have shown a role for the Ca^{++} stimulatable ACs in the suppression of sAHP, induced by specific patterns of synaptic stimulation leading to the activation of NMDA receptors. The results also indicate a possible involvement for AC1/AC8 in the dopamine-mediated inhibition of sI_{AHP}. There has been a growing body of literature on the relationship between the D1 dopamine receptor (D1R) and NMDAR at the postsynaptic level (reviewed by Missale *et al.*, 2006). In particular, the NMDAR NR1 and NR2A subunits have been shown to coimmunoprecipitate with the D1 dopamine receptor; this, together with other biochemical and imaging evidence (Lee *et al.*, 2002; Fiorentini *et al.*, 2003), suggest a physical interaction between the D1R and NMDAR. In the striatum, a model has been proposed that allosteric modulation of NMDAR by glutamate leads to the "trapping" of previously freely diffusible D1 receptors in spines (Scott *et al.*, 2006) indicating that, at least in the striatum the D1R and NMDAR can be positioned in the same sub-cellular location. Evidence for similar spinal trapping of D1 receptors by NMDAR in the hippocampus is lacking, however, the principle that the NMDAR and D1R are co-localised may indicate that they couple to the same AC in a signalling domain. Mockett et al. (2004) have shown that, in the hippocampal CA1 region, NMDAR and D1R activation produces a synergistic increase in cAMP suggesting a functional interaction between the NMDAR, D1 receptor and AC1/AC8. As previously discussed, the receptor subtype likely to be responsible for the inhibition of the sAHP by dopamine is the D1 subtype. Therefore it is likely that the modulation of the sAHP by dopamine and activation of NMDAR is transduced by the activation of AC1/AC8 because the NMDAR and D1 receptor are co-localised. This hypothesis should be tested in future experiments.

7.2: The role of the cAMP signalling cascade in learning and memory

The role of the cAMP signalling cascade in learning and memory was first demonstrated in *Drosophila*. Characterization of the learning mutants *amnesiac, dunce, rutabaga and DCO* revealed defects in the cAMP signalling pathway. For example, the gene mutated in the aforementioned *Drosophila* mutant *amnesiac* encodes an adenylyl cyclase activating peptide (Feany & Quinn, 1995). And the genes mutated in the *Drosophila* mutants *dunce, rutabaga,* and *DCO,* encode a cAMP phosphodiesterase (Chen *et al.*, 1986), a Ca^{++} stimulatable AC (Livingstone *et al.*, 1984) and a cAMP-dependent protein kinase (Foster *et al.*, 1984), respectively.

Evidence for the involvement of the Ca^{++} stimulatable AC in learning and memory in vertebrates has been studied through the generation of knockout mice. In the hippocampus there are two forms of long-term plasticity that are dependent on the activation of AC1/AC8. Mossy fibre LTP is dependent on presynaptic Ca^{++}, cAMP and PKA. Single knockouts of AC1 (Villacres *et al.*, 1998) and AC8 (Wang *et al.*, 2003) both show deficits in mossy fibre LTP, a phenotype that can be rescued by administration of the AC activator forskolin (Villacres *et al.*, 1998). LTP at the Schaffer collateral-CA1 synapse is dependent on the activation of NMDAR and post synaptic Ca^{++}. DKO mice lacking both AC1 and AC8 show a complete loss of long lasting LTP with normal presynaptic function (Wong *et al.*, 1999). Consistent with the role of Ca^{++} stimulatable ACs in hippocampal long-term plasticity, the DKO mice showed a robust long-term memory deficit in passive avoidance behavioural tests. The deficit was significant when tested at 30 min, 24 hr, and 8 days post training. However, the DKO mice displayed normal passive avoidance at 5 mins post training, indicating that learning and short-term memory were intact (Wong *et al.*, 1999).

There are several lines of evidence that implicate PACAP in learning and memory. PACAP has been shown to increase Schaffer collateral NMDA dependent excitatory post-synaptic currents and miniature NMDA dependent excitatory post synaptic currents in cultured hippocampal neurons (Macdonald *et al.*, 2005). This indicates that PACAP enhances NMDAR function. Ca^{++} entry

through the NMDAR is thought to be crucial for the generation of LTP of the Schaffer collateral pathway. LTP is also associated with an increase in NMDAR function (Bliss & Collingridge, 1993). Therefore it could be predicted that PACAP might facilitate the induction of LTP in the Schaffer Collateral Pathway. Consistent with this prediction, it has been reported that PACAP application increased the amplitude of field EPSPs in the CA1 region of the hippocampus (Roberto & Brunelli, 2000). Further evidence for the role of PACAP in learning and memory comes from studies of mice deficient in either PACAP or the PAC-1-R. Although LTP at the Schaffer collateral synapse has not been studied in these mice, LTP at the perforant pathway-granule cell synapse in the dentate gyrus has been the focus of investigation. LTP at the perforant pathway-granule cell synapse is similar to that in the Schaffer collateral pathway in that it requires Ca^{++} influx through post synaptic NMDAR for LTP expression (Bliss & Collingridge, 1993). PAC-1-R are expressed in the granule cells of the dentate gyrus (Shioda *et al.*, 1997). Additionally, application of a high concentration of PACAP in vitro induces a long lasting facilitation of excitatory transmission in the dentate gyrus (Kondo *et al.*, 1997). In mutant mice, that express a reduced number of PAC-1-R or a PACAP protein levels, threshold LTP was impaired in the dentate gyrus *in vivo* (Matsuyama *et al.*, 2003). Consistent with the role for LTP in learning and memory (Bliss & Collingridge, 1993), PAC-1-R deficient mice show a deficit in contextual fear conditioning, a hippocampal-dependent associative learning paradigm (Otto *et al.*, 2001a).

This study has investigated the modulation of the sI_{AHP}/sAHP by two components implicated in the cAMP pathway, namely the Ca^{++} stimulatable ACs and PACAP, an AC-activating peptide. Both components of the cAMP pathway were shown to lead to, or be involved in, the suppression the sI_{AHP}/sAHP. This may indicate a role for the sAHP in learning and memory.

7.3: A role for the AHP currents in learning

The mAHP and the sAHP have been shown to be modulated by experience in the hippocampus. Trace eye blink conditioning (trace EBC) is a hippocampal dependent task, because it is impaired in rabbits that have undergone

hippocampectomy (Moyer *et al.*, 1990). Trace EBC is associated with a reduction in the post burst AHP (Disterhoft *et al.*, 1986). In CA1 pyramidal cells, there is a transient reduction in the post burst AHP and associated spike frequency adaptation after trace EBC learning (Moyer *et al.*, 1996). This reduction in post burst AHP is only observed in neurons from animals that acquire the EBC (Disterhoft *et al.*, 1988). Furthermore, once the AHP suppression is induced, the sAHP remains reduced in amplitude after application of TTX and TEA (Coulter *et al.*, 1989). This indicates that the sAHP reduction is due to a change in the intrinsic properties of the post-synaptic neuron and not due to changes in synaptic transmission. In another hippocampal dependent task, the spatial water maze (Morris *et al.*, 1982), rodents that acquired the task displayed a reduced AHP in dorsal CA1 pyramidal neurons (Oh *et al.*, 2003). Spatial water maze learning has been shown to specifically involve the dorsal hippocampus (Moser *et al.*, 1993). Voltage clamp recording demonstrated that both the I_{AHP} and sI_{AHP} were suppressed by spatial learning (Oh *et al.*, 2003). Finally, recordings from hippocampal CA1 neurons during odour discrimination tasks showed that neurons from trained rats had a reduced post burst sAHP and adaptation (Zelcer *et al.*, 2006). Additionally enhanced neuronal excitability (reduced post burst AHP), resulting from prior training in the odour discrimination task, facilitated learning of a novel hippocampal dependent rule-learning task (Zelcer *et al.*, 2006). In conclusion, the AHP has been demonstrated to decrease in amplitude with learning in the CA1 region of the hippocampus, and this reduction in the sAHP can facilitate learning of another task.

The sAHP increases in amplitude in an age dependent manner (Wu *et al.*, 2002). Furthermore, it has been shown that there is an age-related impairment in trace EBC. This was implied for two reasons; (i) over 50 % of aging animals fail to meet the learning criteria on the trace EBC task (Thompson *et al.*, 1996) and (ii) those aging animals that learnt the trace EBC task needed more trials compared to younger animals (Thompson *et al.*, 1996). This illustrates the old adage that learning becomes harder with age. The link between AHP amplitude and learning is further strengthened by studies in aged animals in the spatial water maze. Tombaugh et al. (2005) found that aged rats with smaller AHPs learned the

location of the hidden platform whereas those with a large post-burst AHP were unable to do so. This inverse relationship between AHP amplitude and learning has also been demonstrated for young animals (Oh *et al.*, 2003). These results indicate that learning is associated with a reduced sAHP.

This study and others have demonstrated that delivery of electrophysiological paradigms to CA1 pyramidal cells, which have been used to elicit synaptic plasticity, results in a partial and transient suppression of sAHP and mAHP. Furthermore, pharmacological manipulations that have been shown to suppress sI_{AHP} have also been demonstrated to facilitate the induction of synaptic plasticity (Blitzer *et al.*, 1995). As previously discussed, the blockade of SK channels by apamin, facilitates the induction of LTP (Behnisch & Reymann, 1998; Norris *et al.*, 1998; Foster, 1999). The monoaminergic neurotransmitters: dopamine (Otmakhova & Lisman, 1996), noradrenaline (Thomas *et al.*, 1996), and serotonin, also facilitate the induction of LTP at the Schaffer collateral pathway by a cAMP dependent mechanism (Frey *et al.*, 1993). Taken together the evidence indicates that negative modulation of AHP currents promotes learning in the CA1 region of the hippocampus. More direct evidence for the involvement of sAHP in learning processes will be hopefully obtained in the near future when specific pharmacological tools targeting the sAHP channels will be developed, or the sAHP channels will be identified, allowing the generation of sAHP-deficient animal models. Although given the powerful role of sAHP in controlling neuronal excitability, there may be foreseeable problems associated with studying learning processes in a sAHP channel knock out mouse which could be predicted to be profoundly epileptic.

Bibliography

Abel T, Nguyen PV, Barad M, Deuel TA, Kandel ER & Bourtchouladze R. (1997). Genetic demonstration of a role for PKA in the late phase of LTP and in hippocampus-based long-term memory. *Cell* **88,** 615-626.

Aldenhoff JB, Gruol DL, Rivier J, Vale W & Siggins GR. (1983). Corticotropin releasing factor decreases postburst hyperpolarizations and excites hippocampal neurons. *Science* **221,** 875-877.

Alessi DR, Cuenda A, Cohen P, Dudley DT & Saltiel AR. (1995). PD 098059 is a specific inhibitor of the activation of mitogen-activated protein kinase kinase in vitro and in vivo. *J Biol Chem* **270,** 27489-27494.

Alford S, Frenguelli BG, Schofield JG & Collingridge GL. (1993). Characterization of Ca2+ signals induced in hippocampal CA1 neurones by the synaptic activation of NMDA receptors. *J Physiol* **469,** 693-716.

Alger BE & Nicoll RA. (1980). Epileptiform burst afterhyperolarization: calcium-dependent potassium potential in hippocampal CA1 pyramidal cells. *Science* **210,** 1122-1124.

Andersen P. (2007). *The hippocampus book.* Oxford University Press, Oxford ; New York.

Andrade R. (1998). Regulation of membrane excitability in the central nervous system by serotonin receptor subtypes. *Ann N Y Acad Sci* **861,** 190-203.

Andrade R & Chaput Y. (1991). 5-Hydroxytryptamine4-like receptors mediate the slow excitatory response to serotonin in the rat hippocampus. *J Pharmacol Exp Ther* **257,** 930-937.

Andrade R, Malenka RC & Nicoll RA. (1986). A G protein couples serotonin and GABAB receptors to the same channels in hippocampus. *Science* **234,** 1261-1265.

Andrade R & Nicoll RA. (1987). Pharmacologically distinct actions of serotonin on single pyramidal neurones of the rat hippocampus recorded in vitro. *J Physiol* **394,** 99-124.

Aoki K, Zubkov AY, Parent AD & Zhang JH. (2000). Mechanism of ATP-induced [Ca(2+)](i) mobilization in rat basilar smooth muscle cells. *Stroke* **31,** 1377-1384; discussion 1384-1375.

Baker LP, Nielsen MD, Impey S, Hacker BM, Poser SW, Chan MY & Storm DR. (1999). Regulation and immunohistochemical localization of betagamma-

stimulated adenylyl cyclases in mouse hippocampus. *J Neurosci* **19,** 180-192.

Baker LP, Nielsen MD, Impey S, Metcalf MA, Poser SW, Chan G, Obrietan K, Hamblin MW & Storm DR. (1998). Stimulation of type 1 and type 8 Ca2+/calmodulin-sensitive adenylyl cyclases by the Gs-coupled 5-hydroxytryptamine subtype 5-HT7A receptor. *J Biol Chem* **273,** 17469-17476.

Beaudet MM, Parsons RL, Braas KM & May V. (2000). Mechanisms mediating pituitary adenylate cyclase-activating polypeptide depolarization of rat sympathetic neurons. *J Neurosci* **20,** 7353-7361.

Behnisch T & Reymann KG. (1998). Inhibition of apamin-sensitive calcium dependent potassium channels facilitate the induction of long-term potentiation in the CA1 region of rat hippocampus in vitro. *Neurosci Lett* **253,** 91-94.

Bekkers JM. (2000). Distribution of slow AHP channels on hippocampal CA1 pyramidal neurons. *J Neurophysiol* **83,** 1756-1759.

Benardo LS & Prince DA. (1982a). Cholinergic excitation of mammalian hippocampal pyramidal cells. *Brain Res* **249,** 315-331.

Benardo LS & Prince DA. (1982b). Dopamine action on hippocampal pyramidal cells. *J Neurosci* **2,** 415-423.

Benton DC, Monaghan AS, Hosseini R, Bahia PK, Haylett DG & Moss GW. (2003). Small conductance Ca2+-activated K+ channels formed by the expression of rat SK1 and SK2 genes in HEK 293 cells. *J Physiol* **553,** 13-19.

Bergson C, Mrzljak L, Smiley JF, Pappy M, Levenson R & Goldman-Rakic PS. (1995). Regional, cellular, and subcellular variations in the distribution of D1 and D5 dopamine receptors in primate brain. *J Neurosci* **15,** 7821-7836.

Bickmeyer U, Heine M, Manzke T & Richter DW. (2002). Differential modulation of I(h) by 5-HT receptors in mouse CA1 hippocampal neurons. *Eur J Neurosci* **16,** 209-218.

Blanton MG, Lo Turco JJ & Kriegstein AR. (1989). Whole cell recording from neurons in slices of reptilian and mammalian cerebral cortex. *J Neurosci Methods* **30,** 203-210.

Bliss TV & Collingridge GL. (1993). A synaptic model of memory: long-term potentiation in the hippocampus. *Nature* **361,** 31-39.

Blitzer RD, Wong T, Nouranifar R, Iyengar R & Landau EM. (1995). Postsynaptic cAMP pathway gates early LTP in hippocampal CA1 region. *Neuron* **15,** 1403-1414.

Bond CT, Herson PS, Strassmaier T, Hammond R, Stackman R, Maylie J & Adelman JP. (2004). Small conductance Ca2+-activated K+ channel knock-out mice reveal the identity of calcium-dependent afterhyperpolarization currents. *J Neurosci* **24,** 5301-5306.

Borde M, Bonansco C & Buno W. (1999). The activity-dependent potentiation of the slow Ca2+-activated K+ current regulates synaptic efficacy in rat CA1 pyramidal neurons. *Pflugers Arch* **437,** 261-266.

Borde M, Bonansco C, Fernandez de Sevilla D, Le Ray D & Buno W. (2000). Voltage-clamp analysis of the potentiation of the slow Ca2+-activated K+ current in hippocampal pyramidal neurons. *Hippocampus* **10,** 198-206.

Borde M, Cazalets JR & Buno W. (1995). Activity-dependent response depression in rat hippocampal CA1 pyramidal neurons in vitro. *J Neurophysiol* **74,** 1714-1729.

Botelho LH, Rothermel JD, Coombs RV & Jastorff B. (1988). cAMP analog antagonists of cAMP action. *Methods Enzymol* **159,** 159-172.

Braas KM, May V, Harakall SA, Hardwick JC & Parsons RL. (1998). Pituitary adenylate cyclase-activating polypeptide expression and modulation of neuronal excitability in guinea pig cardiac ganglia. *J Neurosci* **18,** 9766-9779.

Brewster AL, Chen Y, Bender RA, Yeh A, Shigemoto R & Baram TZ. (2007). Quantitative analysis and subcellular distribution of mRNA and protein expression of the hyperpolarization-activated cyclic nucleotide-gated channels throughout development in rat hippocampus. *Cereb Cortex* **17,** 702-712.

Cai X, Wei DS, Gallagher SE, Bagal A, Mei YA, Kao JP, Thompson SM & Tang CM. (2007). Hyperexcitability of distal dendrites in hippocampal pyramidal cells after chronic partial deafferentation. *J Neurosci* **27,** 59-68.

Cali JJ, Zwaagstra JC, Mons N, Cooper DM & Krupinski J. (1994). Type VIII adenylyl cyclase. A Ca2+/calmodulin-stimulated enzyme expressed in discrete regions of rat brain. *J Biol Chem* **269,** 12190-12195.

Campbell RM & Scanes CG. (1992). Evolution of the growth hormone-releasing factor (GRF) family of peptides. *Growth Regul* **2,** 175-191.

Cantrell AR, Smith RD, Goldin AL, Scheuer T & Catterall WA. (1997). Dopaminergic modulation of sodium current in hippocampal neurons via

cAMP-dependent phosphorylation of specific sites in the sodium channel alpha subunit. *J Neurosci* **17,** 7330-7338.

Charpak S, Gahwiler BH, Do KQ & Knopfel T. (1990). Potassium conductances in hippocampal neurons blocked by excitatory amino-acid transmitters. *Nature* **347,** 765-767.

Chartrel N, Tonon MC, Vaudry H & Conlon JM. (1991). Primary structure of frog pituitary adenylate cyclase-activating polypeptide (PACAP) and effects of ovine PACAP on frog pituitary. *Endocrinology* **129,** 3367-3371.

Chen CN, Denome S & Davis RL. (1986). Molecular analysis of cDNA clones and the corresponding genomic coding sequences of the Drosophila dunce+ gene, the structural gene for cAMP phosphodiesterase. *Proc Natl Acad Sci U S A* **83,** 9313-9317.

Cheng HC, Kemp BE, Pearson RB, Smith AJ, Misconi L, Van Patten SM & Walsh DA. (1986). A potent synthetic peptide inhibitor of the cAMP-dependent protein kinase. *J Biol Chem* **261,** 989-992.

Chetkovich DM, Gray R, Johnston D & Sweatt JD. (1991). N-methyl-D-aspartate receptor activation increases cAMP levels and voltage-gated Ca2+ channel activity in area CA1 of hippocampus. *Proc Natl Acad Sci U S A* **88,** 6467-6471.

Chetkovich DM & Sweatt JD. (1993). nMDA receptor activation increases cyclic AMP in area CA1 of the hippocampus via calcium/calmodulin stimulation of adenylyl cyclase. *J Neurochem* **61,** 1933-1942.

Choi EJ, Wong ST, Hinds TR & Storm DR. (1992). Calcium and muscarinic agonist stimulation of type I adenylylcyclase in whole cells. *J Biol Chem* **267,** 12440-12442.

Cliffe IA, Brightwell CI, Fletcher A, Forster EA, Mansell HL, Reilly Y, Routledge C & White AC. (1993). (S)-N-tert-butyl-3-(4-(2-methoxyphenyl)-piperazin-1-yl)-2-phenylpropanamid e [(S)-WAY-100135]: a selective antagonist at presynaptic and postsynaptic 5-HT1A receptors. *J Med Chem* **36,** 1509-1510.

Cole AE & Nicoll RA. (1983). Acetylcholine mediates a slow synaptic potential in hippocampal pyramidal cells. *Science* **221,** 1299-1301.

Cole AE & Nicoll RA. (1984). The pharmacology of cholinergic excitatory responses in hippocampal pyramidal cells. *Brain Res* **305,** 283-290.

Colino A & Halliwell JV. (1987). Differential modulation of three separate K-conductances in hippocampal CA1 neurons by serotonin. *Nature* **328,** 73-77.

Collingridge GL, Kehl SJ & McLennan H. (1983a). Excitatory amino acids in synaptic transmission in the Schaffer collateral-commissural pathway of the rat hippocampus. *J Physiol* **334,** 33-46.

Collingridge GL, Kehl SJ & McLennan H. (1983b). The antagonism of amino acid-induced excitations of rat hippocampal CA1 neurones in vitro. *J Physiol* **334,** 19-31.

Constanti A & Sim JA. (1987). Calcium-dependent potassium conductance in guinea-pig olfactory cortex neurones in vitro. *J Physiol* **387,** 173-194.

Conti AC, Maas JW, Jr., Muglia LM, Dave BA, Vogt SK, Tran TT, Rayhel EJ & Muglia LJ. (2007). Distinct regional and subcellular localization of adenylyl cyclases type 1 and 8 in mouse brain. *Neuroscience* **146,** 713-729.

Coulter DA, Lo Turco JJ, Kubota M, Disterhoft JF, Moore JW & Alkon DL. (1989). Classical conditioning reduces amplitude and duration of calcium-dependent afterhyperpolarization in rabbit hippocampal pyramidal cells. *J Neurophysiol* **61,** 971-981.

Davare MA, Avdonin V, Hall DD, Peden EM, Burette A, Weinberg RJ, Horne MC, Hoshi T & Hell JW. (2001). A beta2 adrenergic receptor signaling complex assembled with the Ca2+ channel Cav1.2. *Science* **293,** 98-101.

Davare MA, Horne MC & Hell JW. (2000). Protein phosphatase 2A is associated with class C L-type calcium channels (Cav1.2) and antagonizes channel phosphorylation by cAMP-dependent protein kinase. *J Biol Chem* **275,** 39710-39717.

Davies SP, Reddy H, Caivano M & Cohen P. (2000). Specificity and mechanism of action of some commonly used protein kinase inhibitors. *Biochem J* **351,** 95-105.

de Rooij J, Zwartkruis FJ, Verheijen MH, Cool RH, Nijman SM, Wittinghofer A & Bos JL. (1998). Epac is a Rap1 guanine-nucleotide-exchange factor directly activated by cyclic AMP. *Nature* **396,** 474-477.

Descarries L & Mechawar N. (2000). Ultrastructural evidence for diffuse transmission by monoamine and acetylcholine neurons of the central nervous system. *Prog Brain Res* **125,** 27-47.

Deschaux O & Bizot JC. (2005). Apamin produces selective improvements of learning in rats. *Neurosci Lett* **386,** 5-8.

Di Mauro M, Cavallaro S & Ciranna L. (2003). Pituitary adenylate cyclase-activating polypeptide modifies the electrical activity of CA1 hippocampal neurons in the rat. *Neurosci Lett* **337,** 97-100.

Dickson L, Aramori I, McCulloch J, Sharkey J & Finlayson K. (2006). A systematic comparison of intracellular cyclic AMP and calcium signalling highlights complexities in human VPAC/PAC receptor pharmacology. *Neuropharmacology* **51,** 1086-1098.

DiFrancesco D & Tortora P. (1991). Direct activation of cardiac pacemaker channels by intracellular cyclic AMP. *Nature* **351,** 145-147.

Disterhoft JF, Coulter DA & Alkon DL. (1986). Conditioning-specific membrane changes of rabbit hippocampal neurons measured in vitro. *Proc Natl Acad Sci U S A* **83,** 2733-2737.

Disterhoft JF, Golden DT, Read HL, Coulter DA & Alkon DL. (1988). AHP reductions in rabbit hippocampal neurons during conditioning correlate with acquisition of the learned response. *Brain Res* **462,** 118-125.

Dudai Y & Zvi S. (1984). Adenylate cyclase in the Drosophila memory mutant rutabaga displays an altered Ca2+ sensitivity. *Neurosci Lett* **47,** 119-124.

Dudai Y & Zvi S. (1985). Multiple defects in the activity of adenylate cyclase from the Drosophila memory mutant rutabaga. *J Neurochem* **45,** 355-364.

Duffy SN & Nguyen PV. (2003). Postsynaptic application of a peptide inhibitor of cAMP-dependent protein kinase blocks expression of long-lasting synaptic potentiation in hippocampal neurons. *J Neurosci* **23,** 1142-1150.

Eyers PA, Craxton M, Morrice N, Cohen P & Goedert M. (1998). Conversion of SB 203580-insensitive MAP kinase family members to drug-sensitive forms by a single amino-acid substitution. *Chem Biol* **5,** 321-328.

Fagan KA, Mahey R & Cooper DM. (1996). Functional co-localization of transfected Ca(2+)-stimulable adenylyl cyclases with capacitative Ca2+ entry sites. *J Biol Chem* **271,** 12438-12444.

Favata MF, Horiuchi KY, Manos EJ, Daulerio AJ, Stradley DA, Feeser WS, Van Dyk DE, Pitts WJ, Earl RA, Hobbs F, Copeland RA, Magolda RL, Scherle PA & Trzaskos JM. (1998). Identification of a novel inhibitor of mitogen-activated protein kinase kinase. *J Biol Chem* **273,** 18623-18632.

Feany MB & Quinn WG. (1995). A neuropeptide gene defined by the Drosophila memory mutant amnesiac. *Science* **268,** 869-873.

Fernandez de Sevilla D, Fuenzalida M, Porto Pazos AB & Buno W. (2007). Selective shunting of the NMDA EPSP component by the slow

afterhyperpolarization in rat CA1 pyramidal neurons. *J Neurophysiol* **97,** 3242-3255.

Fiorentini C, Gardoni F, Spano P, Di Luca M & Missale C. (2003). Regulation of dopamine D1 receptor trafficking and desensitization by oligomerization with glutamate N-methyl-D-aspartate receptors. *J Biol Chem* **278,** 20196-20202.

Flynn GE, Johnson JP, Jr. & Zagotta WN. (2001). Cyclic nucleotide-gated channels: shedding light on the opening of a channel pore. *Nat Rev Neurosci* **2,** 643-651.

Foehring RC. (1996). Serotonin modulates N- and P-type calcium currents in neocortical pyramidal neurons via a membrane-delimited pathway. *J Neurophysiol* **75,** 648-659.

Foster JL, Guttman JJ, Hall LM & Rosen OM. (1984). Drosophila cAMP-dependent protein kinase. *J Biol Chem* **259,** 13049-13055.

Foster TC. (1999). Involvement of hippocampal synaptic plasticity in age-related memory decline. *Brain Res Brain Res Rev* **30,** 236-249.

Fremeau RT, Jr., Duncan GE, Fornaretto MG, Dearry A, Gingrich JA, Breese GR & Caron MG. (1991). Localization of D1 dopamine receptor mRNA in brain supports a role in cognitive, affective, and neuroendocrine aspects of dopaminergic neurotransmission. *Proc Natl Acad Sci U S A* **88,** 3772-3776.

Frey U, Huang YY & Kandel ER. (1993). Effects of cAMP simulate a late stage of LTP in hippocampal CA1 neurons. *Science* **260,** 1661-1664.

Fuenzalida M, Fernandez de Sevilla D & Buno W. (2007). Changes of the EPSP waveform regulate the temporal window for spike-timing-dependent plasticity. *J Neurosci* **27,** 11940-11948.

Gasbarri A, Sulli A & Packard MG. (1997). The dopaminergic mesencephalic projections to the hippocampal formation in the rat. *Prog Neuropsychopharmacol Biol Psychiatry* **21,** 1-22.

Gereau RWt & Conn PJ. (1994). Presynaptic enhancement of excitatory synaptic transmission by beta-adrenergic receptor activation. *J Neurophysiol* **72,** 1438-1442.

Gerlach AC, Maylie J & Adelman JP. (2004). Activation kinetics of the slow afterhyperpolarization in hippocampal CA1 neurons. *Pflugers Arch* **448,** 187-196.

Gould MC & Stephano JL. (2000). Inactivation of Ca(2+) action potential channels by the MEK inhibitor PD98059. *Exp Cell Res* **260,** 175-179.

Grabauskas G, Lancaster B, O'Connor V & Wheal HV. (2007). Protein kinase signalling requirements for metabotropic action of kainate receptors in rat CA1 pyramidal neurones. *J Physiol* **579,** 363-373.

Gray R & Johnston D. (1987). Noradrenaline and beta-adrenoceptor agonists increase activity of voltage-dependent calcium channels in hippocampal neurons. *Nature* **327,** 620-622.

Gu N, Vervaeke K, Hu H & Storm JF. (2005). Kv7/KCNQ/M and HCN/h, but not KCa2/SK channels, contribute to the somatic medium after-hyperpolarization and excitability control in CA1 hippocampal pyramidal cells. *J Physiol* **566,** 689-715.

Gu N, Vervaeke K & Storm JF. (2007). BK potassium channels facilitate high-frequency firing and cause early spike frequency adaptation in rat CA1 hippocampal pyramidal cells. *J Physiol* **580,** 859-882.

Gupta RC, Neumann J, Watanabe AM, Lesch M & Sabbah HN. (1996). Evidence for presence and hormonal regulation of protein phosphatase inhibitor-1 in ventricular cardiomyocyte. *Am J Physiol* **270,** H1159-1164.

Gustafson EL, Durkin MM, Bard JA, Zgombick J & Branchek TA. (1996). A receptor autoradiographic and in situ hybridization analysis of the distribution of the 5-ht7 receptor in rat brain. *Br J Pharmacol* **117,** 657-666.

Haas HL & Gahwiler BH. (1992). Vasoactive intestinal polypeptide modulates neuronal excitability in hippocampal slices of the rat. *Neuroscience* **47,** 273-277.

Haas HL & Konnerth A. (1983). Histamine and noradrenaline decrease calcium-activated potassium conductance in hippocampal pyramidal cells. *Nature* **302,** 432-434.

Hadley JK, Noda M, Selyanko AA, Wood IC, Abogadie FC & Brown DA. (2000). Differential tetraethylammonium sensitivity of KCNQ1-4 potassium channels. *Br J Pharmacol* **129,** 413-415.

Halliwell JV & Adams PR. (1982). Voltage-clamp analysis of muscarinic excitation in hippocampal neurons. *Brain Res* **250,** 71-92.

Hannibal J. (2002). Pituitary adenylate cyclase-activating peptide in the rat central nervous system: an immunohistochemical and in situ hybridization study. *J Comp Neurol* **453,** 389-417.

Hanoune J & Defer N. (2001). Regulation and role of adenylyl cyclase isoforms. *Annu Rev Pharmacol Toxicol* **41,** 145-174.

Hashimoto H, Nogi H, Mori K, Ohishi H, Shigemoto R, Yamamoto K, Matsuda T, Mizuno N, Nagata S & Baba A. (1996). Distribution of the mRNA for a pituitary adenylate cyclase-activating polypeptide receptor in the rat brain: an in situ hybridization study. *J Comp Neurol* **371,** 567-577.

Haug T & Storm JF. (2000). Protein kinase A mediates the modulation of the slow Ca(2+)-dependent K(+) current, I(sAHP), by the neuropeptides CRF, VIP, and CGRP in hippocampal pyramidal neurons. *J Neurophysiol* **83,** 2071-2079.

Helmchen F, Imoto K & Sakmann B. (1996). Ca2+ buffering and action potential-evoked Ca2+ signaling in dendrites of pyramidal neurons. *Biophys J* **70,** 1069-1081.

Hensler JG. (2006). Serotonergic modulation of the limbic system. *Neurosci Biobehav Rev* **30,** 203-214.

Hirschberg B, Maylie J, Adelman JP & Marrion NV. (1998). Gating of recombinant small-conductance Ca-activated K+ channels by calcium. *J Gen Physiol* **111,** 565-581.

Hoffman DA & Johnston D. (1999). Neuromodulation of dendritic action potentials. *J Neurophysiol* **81,** 408-411.

Hotson JR & Prince DA. (1980). A calcium-activated hyperpolarization follows repetitive firing in hippocampal neurons. *J Neurophysiol* **43,** 409-419.

Ishihara T, Shigemoto R, Mori K, Takahashi K & Nagata S. (1992). Functional expression and tissue distribution of a novel receptor for vasoactive intestinal polypeptide. *Neuron* **8,** 811-819.

Ishii TM, Maylie J & Adelman JP. (1997). Determinants of apamin and d-tubocurarine block in SK potassium channels. *J Biol Chem* **272,** 23195-23200.

Ji H & Shepard PD. (2006). SK Ca2+-activated K+ channel ligands alter the firing pattern of dopamine-containing neurons in vivo. *Neuroscience* **140,** 623-633.

Kaczorowski CC, Disterhoft J & Spruston N. (2007). Stability and plasticity of intrinsic membrane properties in hippocampal CA1 pyramidal neurons: effects of internal anions. *J Physiol* **578,** 799-818.

Kandel ER & Spencer WA. (1961). Electrophysiology of hippocampal neurons. II. After-potentials and repetitive firing. *J Neurophysiol* **24,** 243-259.

Katsuki H, Izumi Y & Zorumski CF. (1997). Noradrenergic regulation of synaptic plasticity in the hippocampal CA1 region. *J Neurophysiol* **77,** 3013-3020.

Kawasaki H, Springett GM, Mochizuki N, Toki S, Nakaya M, Matsuda M, Housman DE & Graybiel AM. (1998). A family of cAMP-binding proteins that directly activate Rap1. *Science* **282,** 2275-2279.

Kebabian JW & Calne DB. (1979). Multiple receptors for dopamine. *Nature* **277,** 93-96.

Keen JE, Khawaled R, Farrens DL, Neelands T, Rivard A, Bond CT, Janowsky A, Fakler B, Adelman JP & Maylie J. (1999). Domains responsible for constitutive and Ca(2+)-dependent interactions between calmodulin and small conductance Ca(2+)-activated potassium channels. *J Neurosci* **19,** 8830-8838.

Khan ZU, Gutierrez A, Martin R, Penafiel A, Rivera A & De La Calle A. (1998). Differential regional and cellular distribution of dopamine D2-like receptors: an immunocytochemical study of subtype-specific antibodies in rat and human brain. *J Comp Neurol* **402,** 353-371.

Khan ZU, Gutierrez A, Martin R, Penafiel A, Rivera A & de la Calle A. (2000). Dopamine D5 receptors of rat and human brain. *Neuroscience* **100,** 689-699.

Kim JJ & Fanselow MS. (1992). Modality-specific retrograde amnesia of fear. *Science* **256,** 675-677.

Kimura C, Ohkubo S, Ogi K, Hosoya M, Itoh Y, Onda H, Miyata A, Jiang L, Dahl RR, Stibbs HH & et al. (1990). A novel peptide which stimulates adenylate cyclase: molecular cloning and characterization of the ovine and human cDNAs. *Biochem Biophys Res Commun* **166,** 81-89.

Kimura K, Sela S, Bouvier C, Grandy DK & Sidhu A. (1995). Differential coupling of D1 and D5 dopamine receptors to guanine nucleotide binding proteins in transfected GH4C1 rat somatomammotrophic cells. *J Neurochem* **64,** 2118-2124.

Knopfel T, Vranesic I, Gahwiler BH & Brown DA. (1990). Muscarinic and beta-adrenergic depression of the slow Ca2(+)-activated potassium conductance in hippocampal CA3 pyramidal cells is not mediated by a reduction of depolarization-induced cytosolic Ca2+ transients. *Proc Natl Acad Sci U S A* **87,** 4083-4087.

Kohler M, Hirschberg B, Bond CT, Kinzie JM, Marrion NV, Maylie J & Adelman JP. (1996). Small-conductance, calcium-activated potassium channels from mammalian brain. *Science* **273,** 1709-1714.

Kondo T, Tominaga T, Ichikawa M & Iijima T. (1997). Differential alteration of hippocampal synaptic strength induced by pituitary adenylate cyclase activating polypeptide-38 (PACAP-38). *Neurosci Lett* **221,** 189-192.

Koyama T, Nakajima Y, Fujii T & Kawashima K. (1999). Enhancement of cortical and hippocampal cholinergic neurotransmission through 5-HT1A receptor-mediated pathways by BAY x 3702 in freely moving rats. *Neurosci Lett* **265,** 33-36.

Kramar EA, Lin B, Lin CY, Arai AC, Gall CM & Lynch G. (2004). A novel mechanism for the facilitation of theta-induced long-term potentiation by brain-derived neurotrophic factor. *J Neurosci* **24,** 5151-5161.

Krause M, Offermanns S, Stocker M & Pedarzani P. (2002). Functional specificity of G alpha q and G alpha 11 in the cholinergic and glutamatergic modulation of potassium currents and excitability in hippocampal neurons. *J Neurosci* **22,** 666-673.

Lagaud GJ, Lam E, Lui A, van Breemen C & Laher I. (1999). Nonspecific inhibition of myogenic tone by PD98059, a MEK1 inhibitor, in rat middle cerebral arteries. *Biochem Biophys Res Commun* **257,** 523-527.

Lam HC, Takahashi K, Ghatei MA, Kanse SM, Polak JM & Bloom SR. (1990). Binding sites of a novel neuropeptide pituitary-adenylate-cyclase-activating polypeptide in the rat brain and lung. *Eur J Biochem* **193,** 725-729.

Lancaster B & Adams PR. (1986). Calcium-dependent current generating the afterhyperpolarization of hippocampal neurons. *J Neurophysiol* **55,** 1268-1282.

Lancaster B, Hu H, Ramakers GM & Storm JF. (2001). Interaction between synaptic excitation and slow afterhyperpolarization current in rat hippocampal pyramidal cells. *J Physiol* **536,** 809-823.

Lancaster B & Nicoll RA. (1987). Properties of two calcium-activated hyperpolarizations in rat hippocampal neurones. *J Physiol* **389,** 187-203.

Lancaster B & Zucker RS. (1994). Photolytic manipulation of Ca2+ and the time course of slow, Ca(2+)-activated K+ current in rat hippocampal neurones. *J Physiol* **475,** 229-239.

Lee FJ, Xue S, Pei L, Vukusic B, Chery N, Wang Y, Wang YT, Niznik HB, Yu XM & Liu F. (2002). Dual regulation of NMDA receptor functions by direct protein-protein interactions with the dopamine D1 receptor. *Cell* **111,** 219-230.

Lee SH, Park J, Che Y, Han PL & Lee JK. (2000). Constitutive activity and differential localization of p38alpha and p38beta MAPKs in adult mouse brain. *J Neurosci Res* **60,** 623-631.

Lerner EA, Ribeiro JM, Nelson RJ & Lerner MR. (1991). Isolation of maxadilan, a potent vasodilatory peptide from the salivary glands of the sand fly Lutzomyia longipalpis. *J Biol Chem* **266,** 11234-11236.

Lima PA & Marrion NV. (2007). Mechanisms underlying activation of the slow AHP in rat hippocampal neurons. *Brain Res* **1150,** 74-82.

Livingstone MS, Sziber PP & Quinn WG. (1984). Loss of calcium/calmodulin responsiveness in adenylate cyclase of rutabaga, a Drosophila learning mutant. *Cell* **37,** 205-215.

Llano I, Marty A, Armstrong CM & Konnerth A. (1991). Synaptic- and agonist-induced excitatory currents of Purkinje cells in rat cerebellar slices. *J Physiol* **434,** 183-213.

Logothetis DE, Kurachi Y, Galper J, Neer EJ & Clapham DE. (1987). The beta gamma subunits of GTP-binding proteins activate the muscarinic K+ channel in heart. *Nature* **325,** 321-326.

Lopes da Silva FH, Witter MP, Boeijinga PH & Lohman AH. (1990). Anatomic organization and physiology of the limbic cortex. *Physiol Rev* **70,** 453-511.

Luscher C, Jan LY, Stoffel M, Malenka RC & Nicoll RA. (1997). G protein-coupled inwardly rectifying K+ channels (GIRKs) mediate postsynaptic but not presynaptic transmitter actions in hippocampal neurons. *Neuron* **19,** 687-695.

Maccaferri G, Mangoni M, Lazzari A & DiFrancesco D. (1993). Properties of the hyperpolarization-activated current in rat hippocampal CA1 pyramidal cells. *J Neurophysiol* **69,** 2129-2136.

Macdonald DS, Weerapura M, Beazely MA, Martin L, Czerwinski W, Roder JC, Orser BA & MacDonald JF. (2005). Modulation of NMDA receptors by pituitary adenylate cyclase activating peptide in CA1 neurons requires G alpha q, protein kinase C, and activation of Src. *J Neurosci* **25,** 11374-11384.

Madison DV & Nicoll RA. (1982). Noradrenaline blocks accommodation of pyramidal cell discharge in the hippocampus. *Nature* **299,** 636-638.

Madison DV & Nicoll RA. (1984). Control of the repetitive discharge of rat CA 1 pyramidal neurones in vitro. *J Physiol* **354,** 319-331.

Madison DV & Nicoll RA. (1986a). Actions of noradrenaline recorded intracellularly in rat hippocampal CA1 pyramidal neurones, in vitro. *J Physiol* **372,** 221-244.

Madison DV & Nicoll RA. (1986b). Cyclic adenosine 3',5'-monophosphate mediates beta-receptor actions of noradrenaline in rat hippocampal pyramidal cells. *J Physiol* **372,** 245-259.

Magee JC. (1998). Dendritic hyperpolarization-activated currents modify the integrative properties of hippocampal CA1 pyramidal neurons. *J Neurosci* **18,** 7613-7624.

Malenka RC & Nicoll RA. (1986). Dopamine decreases the calcium-activated afterhyperpolarization in hippocampal CA1 pyramidal cells. *Brain Res* **379,** 210-215.

Malinow R, Otmakhov N, Blum KI & Lisman J. (1994). Visualizing hippocampal synaptic function by optical detection of Ca2+ entry through the N-methyl-D-aspartate channel. *Proc Natl Acad Sci U S A* **91,** 8170-8174.

Mamounas LA, Mullen CA, O'Hearn E & Molliver ME. (1991). Dual serotoninergic projections to forebrain in the rat: morphologically distinct 5-HT axon terminals exhibit differential vulnerability to neurotoxic amphetamine derivatives. *J Comp Neurol* **314,** 558-586.

Mannaioni G, Marino MJ, Valenti O, Traynelis SF & Conn PJ. (2001). Metabotropic glutamate receptors 1 and 5 differentially regulate CA1 pyramidal cell function. *J Neurosci* **21,** 5925-5934.

Masuo Y, Ohtaki T, Masuda Y, Tsuda M & Fujino M. (1992). Binding sites for pituitary adenylate cyclase activating polypeptide (PACAP): comparison with vasoactive intestinal polypeptide (VIP) binding site localization in rat brain sections. *Brain Res* **575,** 113-123.

Matsuoka I, Suzuki Y, Defer N, Nakanishi H & Hanoune J. (1997). Differential expression of type I, II, and V adenylyl cyclase gene in the postnatal developing rat brain. *J Neurochem* **68,** 498-506.

Matsuyama S, Matsumoto A, Hashimoto H, Shintani N & Baba A. (2003). Impaired long-term potentiation in vivo in the dentate gyrus of pituitary adenylate cyclase-activating polypeptide (PACAP) or PACAP type 1 receptor-mutant mice. *Neuroreport* **14,** 2095-2098.

Mei YA, Vaudry D, Basille M, Castel H, Fournier A, Vaudry H & Gonzalez BJ. (2004). PACAP inhibits delayed rectifier potassium current via a cAMP/PKA transduction pathway: evidence for the involvement of I k in the anti-apoptotic action of PACAP. *Eur J Neurosci* **19,** 1446-1458.

Meyer JJ, Allen DD & Yokel RA. (1996). Hippocampal acetylcholine increases during eyeblink conditioning in the rabbit. *Physiol Behav* **60,** 1199-1203.

Missale C, Fiorentini C, Busi C, Collo G & Spano PF. (2006). The NMDA/D1 receptor complex as a new target in drug development. *Curr Top Med Chem* **6,** 801-808.

Mockett BG, Brooks WM, Tate WP & Abraham WC. (2004). Dopamine D1/D5 receptor activation fails to initiate an activity-independent late-phase LTP in rat hippocampus. *Brain Res* **1021,** 92-100.

Mongeau R, Blier P & de Montigny C. (1997). The serotonergic and noradrenergic systems of the hippocampus: their interactions and the effects of antidepressant treatments. *Brain Res Brain Res Rev* **23,** 145-195.

Mons N, Harry A, Dubourg P, Premont RT, Iyengar R & Cooper DM. (1995). Immunohistochemical localization of adenylyl cyclase in rat brain indicates a highly selective concentration at synapses. *Proc Natl Acad Sci U S A* **92,** 8473-8477.

Moro O & Lerner EA. (1997). Maxadilan, the vasodilator from sand flies, is a specific pituitary adenylate cyclase activating peptide type I receptor agonist. *J Biol Chem* **272,** 966-970.

Moro O, Tajima M & Lerner EA. (1996). Receptors for the vasodilator maxadilan are expressed on selected neural crest and smooth muscle-derived cells. *Insect Biochem Mol Biol* **26,** 1019-1025.

Moro O, Wakita K, Ohnuma M, Denda S, Lerner EA & Tajima M. (1999). Functional characterization of structural alterations in the sequence of the vasodilatory peptide maxadilan yields a pituitary adenylate cyclase-activating peptide type 1 receptor-specific antagonist. *J Biol Chem* **274,** 23103-23110.

Morris RG, Garrud P, Rawlins JN & O'Keefe J. (1982). Place navigation impaired in rats with hippocampal lesions. *Nature* **297,** 681-683.

Moser E, Moser MB & Andersen P. (1993). Spatial learning impairment parallels the magnitude of dorsal hippocampal lesions, but is hardly present following ventral lesions. *J Neurosci* **13,** 3916-3925.

Moser EI & Paulsen O. (2001). New excitement in cognitive space: between place cells and spatial memory. *Curr Opin Neurobiol* **11,** 745-751.

Moyer JR, Jr., Deyo RA & Disterhoft JF. (1990). Hippocampectomy disrupts trace eye-blink conditioning in rabbits. *Behav Neurosci* **104,** 243-252.

Moyer JR, Jr., Thompson LT & Disterhoft JF. (1996). Trace eyeblink conditioning increases CA1 excitability in a transient and learning-specific manner. *J Neurosci* **16,** 5536-5546.

Muglia LM, Schaefer ML, Vogt SK, Gurtner G, Imamura A & Muglia LJ. (1999). The 5'-flanking region of the mouse adenylyl cyclase type VIII gene imparts tissue-specific expression in transgenic mice. *J Neurosci* **19,** 2051-2058.

Muller W & Connor JA. (1991). Dendritic spines as individual neuronal compartments for synaptic Ca2+ responses. *Nature* **354,** 73-76.

Murchison CF, Zhang XY, Zhang WP, Ouyang M, Lee A & Thomas SA. (2004). A distinct role for norepinephrine in memory retrieval. *Cell* **117,** 131-143.

Nair SG & Gudelsky GA. (2004). Activation of 5-HT2 receptors enhances the release of acetylcholine in the prefrontal cortex and hippocampus of the rat. *Synapse* **53,** 202-207.

Neves G, Cooke SF & Bliss TV. (2008). Synaptic plasticity, memory and the hippocampus: a neural network approach to causality. *Nat Rev Neurosci* **9,** 65-75.

Ngo-Anh TJ, Bloodgood BL, Lin M, Sabatini BL, Maylie J & Adelman JP. (2005). SK channels and NMDA receptors form a Ca2+-mediated feedback loop in dendritic spines. *Nat Neurosci* **8,** 642-649.

Nicol X, Muzerelle A, Bachy I, Ravary A & Gaspar P. (2005). Spatiotemporal localization of the calcium-stimulated adenylate cyclases, AC1 and AC8, during mouse brain development. *J Comp Neurol* **486,** 281-294.

Nielsen MD, Chan GC, Poser SW & Storm DR. (1996). Differential regulation of type I and type VIII Ca2+-stimulated adenylyl cyclases by Gi-coupled receptors in vivo. *J Biol Chem* **271,** 33308-33316.

Nolting A, Ferraro T, D'Hoedt D & Stocker M. (2007). An amino acid outside the pore region influences apamin sensitivity in small conductance Ca2+-activated K+ channels. *J Biol Chem* **282,** 3478-3486.

Norris CM, Halpain S & Foster TC. (1998). Reversal of age-related alterations in synaptic plasticity by blockade of L-type Ca2+ channels. *J Neurosci* **18,** 3171-3179.

Oh MM, Kuo AG, Wu WW, Sametsky EA & Disterhoft JF. (2003). Watermaze learning enhances excitability of CA1 pyramidal neurons. *J Neurophysiol* **90,** 2171-2179.

Otmakhov N & Lisman JE. (2002). Postsynaptic application of a cAMP analogue reverses long-term potentiation in hippocampal CA1 pyramidal neurons. *J Neurophysiol* **87,** 3018-3032.

Otmakhova NA & Lisman JE. (1996). D1/D5 dopamine receptor activation increases the magnitude of early long-term potentiation at CA1 hippocampal synapses. *J Neurosci* **16,** 7478-7486.

Otmakhova NA, Otmakhov N, Mortenson LH & Lisman JE. (2000). Inhibition of the cAMP pathway decreases early long-term potentiation at CA1 hippocampal synapses. *J Neurosci* **20,** 4446-4451.

Otto C, Kovalchuk Y, Wolfer DP, Gass P, Martin M, Zuschratter W, Grone HJ, Kellendonk C, Tronche F, Maldonado R, Lipp HP, Konnerth A & Schutz G. (2001a). Impairment of mossy fiber long-term potentiation and associative learning in pituitary adenylate cyclase activating polypeptide type I receptor-deficient mice. *J Neurosci* **21,** 5520-5527.

Otto C, Martin M, Wolfer DP, Lipp HP, Maldonado R & Schutz G. (2001b). Altered emotional behavior in PACAP-type-I-receptor-deficient mice. *Brain Res Mol Brain Res* **92,** 78-84.

Paxinos G. (1995). *The rat nervous system.* Academic Press, San Diego.

Pedarzani P, Krause M, Haug T, Storm JF & Stuhmer W. (1998). Modulation of the Ca2+-activated K+ current sIAHP by a phosphatase-kinase balance under basal conditions in rat CA1 pyramidal neurons. *J Neurophysiol* **79,** 3252-3256.

Pedarzani P, McCutcheon JE, Rogge G, Jensen BS, Christophersen P, Hougaard C, Strobaek D & Stocker M. (2005). Specific enhancement of SK channel activity selectively potentiates the afterhyperpolarizing current I(AHP) and modulates the firing properties of hippocampal pyramidal neurons. *J Biol Chem* **280,** 41404-41411.

Pedarzani P, Mosbacher J, Rivard A, Cingolani LA, Oliver D, Stocker M, Adelman JP & Fakler B. (2001). Control of electrical activity in central neurons by modulating the gating of small conductance Ca2+-activated K+ channels. *J Biol Chem* **276,** 9762-9769.

Pedarzani P & Storm JF. (1993). PKA mediates the effects of monoamine transmitters on the K+ current underlying the slow spike frequency adaptation in hippocampal neurons. *Neuron* **11,** 1023-1035.

Pedarzani P & Storm JF. (1995a). Dopamine modulates the slow Ca(2+)-activated K+ current IAHP via cyclic AMP-dependent protein kinase in hippocampal neurons. *J Neurophysiol* **74,** 2749-2753.

Pedarzani P & Storm JF. (1995b). Protein kinase A-independent modulation of ion channels in the brain by cyclic AMP. *Proc Natl Acad Sci U S A* **92,** 11716-11720.

Pedarzani P & Storm JF. (1996a). Evidence that Ca/calmodulin-dependent protein kinase mediates the modulation of the Ca2+-dependent K+ current, IAHP, by acetylcholine, but not by glutamate, in hippocampal neurons. *Pflugers Arch* **431,** 723-728.

Pedarzani P & Storm JF. (1996b). Interaction between alpha- and beta-adrenergic receptor agonists modulating the slow Ca(2+)-activated K+ current IAHP in hippocampal neurons. *Eur J Neurosci* **8,** 2098-2110.

Perkel DJ, Petrozzino JJ, Nicoll RA & Connor JA. (1993). The role of Ca2+ entry via synaptically activated NMDA receptors in the induction of long-term potentiation. *Neuron* **11,** 817-823.

Rehmann H, Schwede F, Doskeland SO, Wittinghofer A & Bos JL. (2003). Ligand-mediated activation of the cAMP-responsive guanine nucleotide exchange factor Epac. *J Biol Chem* **278,** 38548-38556.

Ren Y, Barnwell LF, Alexander JC, Lubin FD, Adelman JP, Pfaffinger PJ, Schrader LA & Anderson AE. (2006). Regulation of surface localization of the small conductance Ca2+-activated potassium channel, Sk2, through direct phosphorylation by cAMP-dependent protein kinase. *J Biol Chem* **281,** 11769-11779.

Rishal I, Porozov Y, Yakubovich D, Varon D & Dascal N. (2005). Gbetagamma-dependent and Gbetagamma-independent basal activity of G protein-activated K+ channels. *J Biol Chem* **280,** 16685-16694.

Roberson ED & Sweatt JD. (1996). Transient activation of cyclic AMP-dependent protein kinase during hippocampal long-term potentiation. *J Biol Chem* **271,** 30436-30441.

Roberto M & Brunelli M. (2000). PACAP-38 enhances excitatory synaptic transmission in the rat hippocampal CA1 region. *Learn Mem* **7,** 303-311.

Rouse ST, Edmunds SM, Yi H, Gilmor ML & Levey AI. (2000a). Localization of M(2) muscarinic acetylcholine receptor protein in cholinergic and non-cholinergic terminals in rat hippocampus. *Neurosci Lett* **284,** 182-186.

Rouse ST, Hamilton SE, Potter LT, Nathanson NM & Conn PJ. (2000b). Muscarinic-induced modulation of potassium conductances is unchanged in mouse hippocampal pyramidal cells that lack functional M1 receptors. *Neurosci Lett* **278,** 61-64.

Routledge C. (1996). Development of 5-HT1A receptor antagonists. *Behav Brain Res* **73,** 153-156.

Ruat M, Traiffort E, Leurs R, Tardivel-Lacombe J, Diaz J, Arrang JM & Schwartz JC. (1993). Molecular cloning, characterization, and localization of a high-affinity serotonin receptor (5-HT7) activating cAMP formation. *Proc Natl Acad Sci U S A* **90,** 8547-8551.

Sah P & Bekkers JM. (1996). Apical dendritic location of slow afterhyperpolarization current in hippocampal pyramidal neurons: implications for the integration of long-term potentiation. *J Neurosci* **16,** 4537-4542.

Sah P & Clements JD. (1999). Photolytic manipulation of [Ca2+]i reveals slow kinetics of potassium channels underlying the afterhyperpolarization in hippocampal pyramidal neurons. *J Neurosci* **19,** 3657-3664.

Sah P & Faber ES. (2002). Channels underlying neuronal calcium-activated potassium currents. *Prog Neurobiol* **66,** 345-353.

Sailer CA, Hu H, Kaufmann WA, Trieb M, Schwarzer C, Storm JF & Knaus HG. (2002). Regional differences in distribution and functional expression of small-conductance Ca2+-activated K+ channels in rat brain. *J Neurosci* **22,** 9698-9707.

Sakai Y, Hashimoto H, Shintani N, Tomimoto S, Tanaka K, Ichibori A, Hirose M & Baba A. (2001). Involvement of p38 MAP kinase pathway in the synergistic activation of PACAP mRNA expression by NGF and PACAP in PC12h cells. *Biochem Biophys Res Commun* **285,** 656-661.

Sandler VM & Ross WN. (1999). Serotonin modulates spike backpropagation and associated [Ca2+]i changes in the apical dendrites of hippocampal CA1 pyramidal neurons. *J Neurophysiol* **81,** 216-224.

Santoro B, Liu DT, Yao H, Bartsch D, Kandel ER, Siegelbaum SA & Tibbs GR. (1998). Identification of a gene encoding a hyperpolarization-activated pacemaker channel of brain. *Cell* **93,** 717-729.

Saxena M, Williams S, Brockdorff J, Gilman J & Mustelin T. (1999a). Inhibition of T cell signaling by mitogen-activated protein kinase-targeted hematopoietic tyrosine phosphatase (HePTP). *J Biol Chem* **274,** 11693-11700.

Saxena M, Williams S, Tasken K & Mustelin T. (1999b). Crosstalk between cAMP-dependent kinase and MAP kinase through a protein tyrosine phosphatase. *Nat Cell Biol* **1,** 305-311.

Schiller J, Helmchen F & Sakmann B. (1995). Spatial profile of dendritic calcium transients evoked by action potentials in rat neocortical pyramidal neurones. *J Physiol* **487 (Pt 3),** 583-600.

Schumacher MA, Crum M & Miller MC. (2004). Crystal structures of apocalmodulin and an apocalmodulin/SK potassium channel gating domain complex. *Structure* **12,** 849-860.

Schumacher MA, Rivard AF, Bachinger HP & Adelman JP. (2001). Structure of the gating domain of a Ca2+-activated K+ channel complexed with Ca2+/calmodulin. *Nature* **410,** 1120-1124.

Schwartzkroin PA & Stafstrom CE. (1980). Effects of EGTA on the calcium-activated afterhyperpolarization in hippocampal CA3 pyramidal cells. *Science* **210,** 1125-1126.

Scott L, Zelenin S, Malmersjo S, Kowalewski JM, Markus EZ, Nairn AC, Greengard P, Brismar H & Aperia A. (2006). Allosteric changes of the NMDA receptor trap diffusible dopamine 1 receptors in spines. *Proc Natl Acad Sci U S A* **103,** 762-767.

Shah M & Haylett DG. (2000). The pharmacology of hSK1 Ca2+-activated K+ channels expressed in mammalian cell lines. *Br J Pharmacol* **129,** 627-630.

Shah MM, Javadzadeh-Tabatabaie M, Benton DC, Ganellin CR & Haylett DG. (2006). Enhancement of hippocampal pyramidal cell excitability by the novel selective slow-afterhyperpolarization channel blocker 3-(triphenylmethylaminomethyl)pyridine (UCL2077). *Mol Pharmacol* **70,** 1494-1502.

Shao LR, Halvorsrud R, Borg-Graham L & Storm JF. (1999). The role of BK-type Ca2+-dependent K+ channels in spike broadening during repetitive firing in rat hippocampal pyramidal cells. *J Physiol* **521 Pt 1,** 135-146.

Shapiro ML & Eichenbaum H. (1999). Hippocampus as a memory map: synaptic plasticity and memory encoding by hippocampal neurons. *Hippocampus* **9,** 365-384.

Shi GX, Rehmann H & Andres DA. (2006). A novel cyclic AMP-dependent Epac-Rit signaling pathway contributes to PACAP38-mediated neuronal differentiation. *Mol Cell Biol* **26,** 9136-9147.

Shioda S, Shuto Y, Somogyvari-Vigh A, Legradi G, Onda H, Coy DH, Nakajo S & Arimura A. (1997). Localization and gene expression of the receptor for pituitary adenylate cyclase-activating polypeptide in the rat brain. *Neurosci Res* **28,** 345-354.

Spengler D, Waeber C, Pantaloni C, Holsboer F, Bockaert J, Seeburg PH & Journot L. (1993). Differential signal transduction by five splice variants of the PACAP receptor. *Nature* **365,** 170-175.

Spruston N, Jaffe DB, Williams SH & Johnston D. (1993). Voltage- and space-clamp errors associated with the measurement of electrotonically remote synaptic events. *J Neurophysiol* **70,** 781-802.

Squire LR, Stark CE & Clark RE. (2004). The medial temporal lobe. *Annu Rev Neurosci* **27,** 279-306.

Stackman RW, Hammond RS, Linardatos E, Gerlach A, Maylie J, Adelman JP & Tzounopoulos T. (2002). Small conductance Ca2+-activated K+ channels modulate synaptic plasticity and memory encoding. *J Neurosci* **22,** 10163-10171.

Ster J, De Bock F, Guerineau NC, Janossy A, Barrere-Lemaire S, Bos JL, Bockaert J & Fagni L. (2007). Exchange protein activated by cAMP (Epac) mediates cAMP activation of p38 MAPK and modulation of Ca2+-dependent K+ channels in cerebellar neurons. *Proc Natl Acad Sci U S A* **104,** 2519-2524.

Stocker M. (2004). Ca(2+)-activated K+ channels: molecular determinants and function of the SK family. *Nat Rev Neurosci* **5,** 758-770.

Stocker M, Hirzel K, D'Hoedt D & Pedarzani P. (2004). Matching molecules to function: neuronal Ca2+-activated K+ channels and afterhyperpolarizations. *Toxicon* **43,** 933-949.

Stocker M, Krause M & Pedarzani P. (1999). An apamin-sensitive Ca2+-activated K+ current in hippocampal pyramidal neurons. *Proc Natl Acad Sci U S A* **96,** 4662-4667.

Stocker M & Pedarzani P. (2000). Differential distribution of three Ca(2+)-activated K(+) channel subunits, SK1, SK2, and SK3, in the adult rat central nervous system. *Mol Cell Neurosci* **15,** 476-493.

Storm JF. (1987). Action potential repolarization and a fast after-hyperpolarization in rat hippocampal pyramidal cells. *J Physiol* **385,** 733-759.

Storm JF. (1989). An after-hyperpolarization of medium duration in rat hippocampal pyramidal cells. *J Physiol* **409,** 171-190.

Storm JF. (1990). Potassium currents in hippocampal pyramidal cells. *Prog Brain Res* **83,** 161-187.

Strobaek D, Hougaard C, Johansen TH, Sorensen US, Nielsen EO, Nielsen KS, Taylor RD, Pedarzani P & Christophersen P. (2006). Inhibitory gating modulation of small conductance Ca2+-activated K+ channels by the synthetic compound (R)-N-(benzimidazol-2-yl)-1,2,3,4-tetrahydro-1-naphtylamine (NS8593) reduces afterhyperpolarizing current in hippocampal CA1 neurons. *Mol Pharmacol* **70,** 1771-1782.

Strobaek D, Jorgensen TD, Christophersen P, Ahring PK & Olesen SP. (2000). Pharmacological characterization of small-conductance Ca(2+)-activated K(+) channels stably expressed in HEK 293 cells. *Br J Pharmacol* **129,** 991-999.

Strobaek D, Teuber L, Jorgensen TD, Ahring PK, Kjaer K, Hansen RS, Olesen SP, Christophersen P & Skaaning-Jensen B. (2004). Activation of human IK and SK Ca2+ -activated K+ channels by NS309 (6,7-dichloro-1H-indole-2,3-dione 3-oxime). *Biochim Biophys Acta* **1665,** 1-5.

Strong PN. (1990). Potassium channel toxins. *Pharmacol Ther* **46,** 137-162.

Sun QQ, Prince DA & Huguenard JR. (2003). Vasoactive intestinal polypeptide and pituitary adenylate cyclase-activating polypeptide activate hyperpolarization-activated cationic current and depolarize thalamocortical neurons in vitro. *J Neurosci* **23,** 2751-2758.

Tatsuno I, Yada T, Vigh S, Hidaka H & Arimura A. (1992). Pituitary adenylate cyclase activating polypeptide and vasoactive intestinal peptide increase cytosolic free calcium concentration in cultured rat hippocampal neurons. *Endocrinology* **131,** 73-81.

Taylor RD. (2003). Effect of the neuropeptide PACAP on the slow calcium-activated potassium current sIAHP in hippocampal neurons. In *Department of Physiology*, pp. 45. University College London, London.

Thomas DR, Middlemiss DN, Taylor SG, Nelson P & Brown AM. (1999). 5-CT stimulation of adenylyl cyclase activity in guinea-pig hippocampus: evidence for involvement of 5-HT7 and 5-HT1A receptors. *Br J Pharmacol* **128,** 158-164.

Thomas MJ, Moody TD, Makhinson M & O'Dell TJ. (1996). Activity-dependent beta-adrenergic modulation of low frequency stimulation induced LTP in the hippocampal CA1 region. *Neuron* **17,** 475-482.

Thompson LT, Moyer JR, Jr. & Disterhoft JF. (1996). Trace eyeblink conditioning in rabbits demonstrates heterogeneity of learning ability both between and within age groups. *Neurobiol Aging* **17,** 619-629.

Tiberi M, Jarvie KR, Silvia C, Falardeau P, Gingrich JA, Godinot N, Bertrand L, Yang-Feng TL, Fremeau RT, Jr. & Caron MG. (1991). Cloning, molecular

characterization, and chromosomal assignment of a gene encoding a second D1 dopamine receptor subtype: differential expression pattern in rat brain compared with the D1A receptor. *Proc Natl Acad Sci U S A* **88,** 7491-7495.

Tokarski K, Zahorodna A, Bobula B & Hess G. (2003). 5-HT7 receptors increase the excitability of rat hippocampal CA1 pyramidal neurons. *Brain Res* **993,** 230-234.

Tombaugh GC, Rowe WB & Rose GM. (2005). The slow afterhyperpolarization in hippocampal CA1 neurons covaries with spatial learning ability in aged Fisher 344 rats. *J Neurosci* **25,** 2609-2616.

Tompkins JD, Hardwick JC, Locknar SA, Merriam LA & Parsons RL. (2006). Ca2+ influx, but not Ca2+ release from internal stores, is required for the PACAP-induced increase in excitability in guinea pig intracardiac neurons. *J Neurophysiol* **95,** 2134-2142.

Torres GE, Holt IL & Andrade R. (1994). Antagonists of 5-HT4 receptor-mediated responses in adult hippocampal neurons. *J Pharmacol Exp Ther* **271,** 255-261.

Traub RD, Wong RK, Miles R & Michelson H. (1991). A model of a CA3 hippocampal pyramidal neuron incorporating voltage-clamp data on intrinsic conductances. *J Neurophysiol* **66,** 635-650.

van der Staay FJ, Fanelli RJ, Blokland A & Schmidt BH. (1999). Behavioral effects of apamin, a selective inhibitor of the SK(Ca)-channel, in mice and rats. *Neurosci Biobehav Rev* **23,** 1087-1110.

Vaudry D, Gonzalez BJ, Basille M, Yon L, Fournier A & Vaudry H. (2000). Pituitary adenylate cyclase-activating polypeptide and its receptors: from structure to functions. *Pharmacol Rev* **52,** 269-324.

Vilaro MT, Cortes R, Gerald C, Branchek TA, Palacios JM & Mengod G. (1996). Localization of 5-HT4 receptor mRNA in rat brain by in situ hybridization histochemistry. *Brain Res Mol Brain Res* **43,** 356-360.

Villacres EC, Wong ST, Chavkin C & Storm DR. (1998). Type I adenylyl cyclase mutant mice have impaired mossy fiber long-term potentiation. *J Neurosci* **18,** 3186-3194.

Villacres EC, Wu Z, Hua W, Nielsen MD, Watters JJ, Yan C, Beavo J & Storm DR. (1995). Developmentally expressed Ca(2+)-sensitive adenylyl cyclase activity is disrupted in the brains of type I adenylyl cyclase mutant mice. *J Biol Chem* **270,** 14352-14357.

Visel A, Alvarez-Bolado G, Thaller C & Eichele G. (2006). Comprehensive analysis of the expression patterns of the adenylate cyclase gene family in the developing and adult mouse brain. *J Comp Neurol* **496,** 684-697.

Waddell S, Armstrong JD, Kitamoto T, Kaiser K & Quinn WG. (2000). The amnesiac gene product is expressed in two neurons in the Drosophila brain that are critical for memory. *Cell* **103,** 805-813.

Wainger BJ, DeGennaro M, Santoro B, Siegelbaum SA & Tibbs GR. (2001). Molecular mechanism of cAMP modulation of HCN pacemaker channels. *Nature* **411,** 805-810.

Wang H, Pineda VV, Chan GC, Wong ST, Muglia LJ & Storm DR. (2003). Type 8 adenylyl cyclase is targeted to excitatory synapses and required for mossy fiber long-term potentiation. *J Neurosci* **23,** 9710-9718.

Willoughby D & Cooper DM. (2007). Organization and Ca2+ regulation of adenylyl cyclases in cAMP microdomains. *Physiol Rev* **87,** 965-1010.

Wong ST, Athos J, Figueroa XA, Pineda VV, Schaefer ML, Chavkin CC, Muglia LJ & Storm DR. (1999). Calcium-stimulated adenylyl cyclase activity is critical for hippocampus-dependent long-term memory and late phase LTP. *Neuron* **23,** 787-798.

Wright DE, Seroogy KB, Lundgren KH, Davis BM & Jennes L. (1995). Comparative localization of serotonin1A, 1C, and 2 receptor subtype mRNAs in rat brain. *J Comp Neurol* **351,** 357-373.

Wu WW, Oh MM & Disterhoft JF. (2002). Age-related biophysical alterations of hippocampal pyramidal neurons: implications for learning and memory. *Ageing Res Rev* **1,** 181-207.

Wu ZL, Thomas SA, Villacres EC, Xia Z, Simmons ML, Chavkin C, Palmiter RD & Storm DR. (1995). Altered behavior and long-term potentiation in type I adenylyl cyclase mutant mice. *Proc Natl Acad Sci U S A* **92,** 220-224.

Xia XM, Fakler B, Rivard A, Wayman G, Johnson-Pais T, Keen JE, Ishii T, Hirschberg B, Bond CT, Lutsenko S, Maylie J & Adelman JP. (1998). Mechanism of calcium gating in small-conductance calcium-activated potassium channels. *Nature* **395,** 503-507.

Xia ZG, Refsdal CD, Merchant KM, Dorsa DM & Storm DR. (1991). Distribution of mRNA for the calmodulin-sensitive adenylate cyclase in rat brain: expression in areas associated with learning and memory. *Neuron* **6,** 431-443.

Yang SN. (2000). Sustained enhancement of AMPA receptor- and NMDA receptor-mediated currents induced by dopamine D1/D5 receptor

activation in the hippocampus: an essential role of postsynaptic Ca2+. *Hippocampus* **10,** 57-63.

Yao L, Arolfo MP, Dohrman DP, Jiang Z, Fan P, Fuchs S, Janak PH, Gordon AS & Diamond I. (2002). betagamma Dimers mediate synergy of dopamine D2 and adenosine A2 receptor-stimulated PKA signaling and regulate ethanol consumption. *Cell* **109,** 733-743.

Zbicz KL & Weight FF. (1985). Transient voltage and calcium-dependent outward currents in hippocampal CA3 pyramidal neurons. *J Neurophysiol* **53,** 1038-1058.

Zelcer I, Cohen H, Richter-Levin G, Lebiosn T, Grossberger T & Barkai E. (2006). A cellular correlate of learning-induced metaplasticity in the hippocampus. *Cereb Cortex* **16,** 460-468.

Zhang L, Weiner JL, Valiante TA, Velumian AA, Watson PL, Jahromi SS, Schertzer S, Pennefather P & Carlen PL. (1994). Whole-cell recording of the Ca(2+)-dependent slow afterhyperpolarization in hippocampal neurones: effects of internally applied anions. *Pflugers Arch* **426,** 247-253.

Zheng M, Zhang SJ, Zhu WZ, Ziman B, Kobilka BK & Xiao RP. (2000). beta 2-adrenergic receptor-induced p38 MAPK activation is mediated by protein kinase A rather than by Gi or gbeta gamma in adult mouse cardiomyocytes. *J Biol Chem* **275,** 40635-40640.

Zhong Y. (1995). Mediation of PACAP-like neuropeptide transmission by coactivation of Ras/Raf and cAMP signal transduction pathways in Drosophila. *Nature* **375,** 588-592.